IDENTIFICATION OF NOVEL TARGET GENES FOR THE PLASTICITY-RELATED TRANSCRIPTION FACTOR ZIF268

Donna M. McDade

A thesis presented for the degree of PhD

Division of Neuroscience and Biomedical Systems

Institute of Biomedical and Life Sciences

University of Glasgow

G12 8QQ

April 2007

Abstract

Activity based alterations in synaptic connectivity are thought to underlie the processes involved in learning and memory. Measurable changes in neuronal activation by long-term potentiation (LTP) are widely investigated as a possible cellular correlate of this phenomenon, as it can be induced quickly to elicit long-lasting modifications. These long-term changes in the activity of neuronal circuits are sustained by an altered pattern of gene expression and protein synthesis. The inducible transcription factor zif268 has been implicated in almost all models of neuronal plasticity. Downstream targets of zif268 are widely believed to contribute to the duration and stabilisation of NMDA receptor dependent LTP which, in turn, can be linked to various models of learning and memory. However, these downstream targets are only just starting to receive attention.

By utilising a wide range of contemporary neuroscience techniques covering molecular & cell biology approaches, this thesis proposes two known proteins, gephyrin and ubiquilin, as well as a novel gene (urma), as potential downstream targets of zif268. Both gephyrin and ubiquilin are associated with $GABA_A$ receptors at inhibitory synapses. Gephyrin is thought to cluster and anchor $GABA_A$ receptors at postsynaptic sites whilst ubiquilin is reported to regulate receptor surface expression. We found that gephyrin mRNA and protein expression levels were downregulated in response to increased levels of zif268 by transient transfection in PC-12 cells and NMDA stimulation in primary cultured cortical neurones. In addition, ubiquilin mRNA and protein levels were also downregulated within the same experimental paradigms, implying that both gephyrin and ubiquilin are downstream transcriptional targets of this plasticity-related gene.

A previously reported microarray experiment (James *et al.* 2005) contained 144 ESTs significantly affected by the transient transfection of zif268 in PC-12 cells compared to control. Bioinformatic analyses of these tags revealed interesting genomic areas pertaining to little published information. After further investigation, EST AI169020 revealed a novel transcript that was downregulated in response to NMDA treatment of primary cortical neurones. Additional data mining suggests

that urma may be a rarely expressed transcription factor. Basal levels of urma mRNA were also decreased in the zif268 knockout mouse, as were ubiquilin mRNA levels.

Zif268 is a regulatory immediate early gene, activating or suppressing downstream targets that play a role in the duration and stabilisation of LTP. These results indicate that gephyrin and ubiquilin are potential mediators of NMDA receptor-dependent plasticity, by modifying inhibitory-signalling. In addition, zif268 may actively suppress a novel plasticity-related transcription factor, urma. These findings may underlie important processes in learning and memory.

Contents

List of Tables

List of Figures

Chapter 1

Chapter 3

Chapter 4

Chapter 5

Chapter 6

Chapter 7

Acknowledgements

First and foremost I'd like to thank my supervisor, Professor Brian J Morris for all his help, support and encouragement over the past 3 and a half years.

For a great time in the lab, I thank Dr. Allan James for all his help and invaluable advice with everything molecular & Dr. Anne-Marie Conway for her protein expertise. To Dr Kara McNair and Dr Susan Cochran, thank you for keeping me sane and listening to my drivel.

To my mum and dad, I love you heaps and piles and hope this makes you proud. Granny & Pappy, thank you for your constant belief in me. Dyan & Damian, cheers for the beers. To Mollie and Neve, thank you for always making me smile and Danny, Jill & Nicole, thanks for the visits and moral support. In addition, I have to mention Jeni & Ian Percival for your encouragement (and financial backing) whilst providing many a fun-packed, wine-filled weekend.

Last, but by no means least, Craig. This is for you.

Author's Declaration

I declare that the work in this thesis is entirely my own, with the exception of the results presented in figures 7.2 and 7.9, which were produced in collaboration with Dr. Allan James.

Signature …….

Donna M. McDade

This work has not been presented in part or alone for any other degree course. Some of the work contained herein has been published in part: a list follows.

1. **McDade, D.M.**, Conway, A.M., James, A.B., & Morris, B.J., (2005) Evidence that Gephyrin and Ubiquilin are Novel Target Genes of the Plasticity-related Transcription Factor Zif268. *British Neuroscience Association Meeting*, Brighton. Abstr., vol 18, P25

2. **McDade, D.M** Conway, A.M., James, A.B., & Morris, B.J., (2005) Identification of gephyrin and ubiquilin as novel target genes for the plasticity - related transcription factor zif268. *Society for Neuroscience*, Washington DC. Abstract Viewer/Itinerary Planner, Program No. 497.18.

3. **McDade, D.M.,** Conway, A.M., James, A.B., & Morris, B.J., (2006) Gephyrin and Ubiquilin are Novel Target Genes of the Plasticity-related Transcription Factor Zif268. *Scottish Neuroscience Group*, University of Strathclyde.

Abbreviations

AA	arachidonic acid
aCSF	artificial cerebrospinal fluid
AD	Alzheimer's disease
ADP	adenosine diphosphate
AMPA	alpha-amino-3-hydroxy-5-methyl-4-isoxazolepropionic acid
AMPAR	AMPA receptor
ANCOVA	analysis of co-variance
ANOVA	analysis of variance
APV	D(-)-2-amino-5-phosphonovaleric acid
APP	amyloid precursor protein
ATP	adenosine triphosphate
β-ME	β-mercaptoethanol
BSA	bovine serum albumin
Ca^{2+}	calcium
CA	cornu ammonis
CAMK	calcium/calmodulin dependent protein kinase
cAMP	cyclic adenosine 3',5'-monophosphate
CAT	chloramphemiol acetyl transferase
CBP	CREB binding protein
cGMP	cyclic guanosine monophosphate
CNS	central nervous system
CRE	cyclic-AMP-responsive element
CREB	cyclic-AMP response element binding
DAN	differential screening-selected gene abbarrative in neuroblastoma
DEPC	diethylpyrocarbonate
Dlc	dynein light chain
Egr	early growth response
ELISA	enzyme-linked immunosorbent Assay
EPSP	excitatory postsynaptic potential
ERK	extracellular-signal related kinase
EST	expressed sequence tag

GABA	γ-aminobutyric acid
$GABA_AR$	γ-aminobutyric acid type A receptor
GABARAP	$GABA_AR$-associated protein
GAP	GTPase-activating protein
GAPDH	glyceraldehyde-3-phosphate dehydrogenase
GDP	guanosine diphosphate
GEF	guanyl nucleotide exchange factors
GFP	green fluorescent protein
GluR	glutamate receptor
GlyR	glycine receptor
GPCRs	G-protein coupled receptors
GTP	guanosine triphosphate
HD	Huntington's disease
IEG	immediate early gene
ISH	*in situ* hybridisation
K^+	potassium
LTD	long-term depression
LTP	long-term potentiation
MAPK	mitogen-activated protein kinase
MEK	MAPK/ERK kinase
Mena/VASP	(mammalian enabled)/vasodilator-stimulated phosphoprotein
mEPSC	miniature excitatory postsynaptic current
Mg^{2+}	magnesium
MoCo	molybdenum cofactor
mTOR	mammalian target of rapamycin
MTP	microtitre plate
Na^+	sodium
NMDA	n-methyl-D-aspartate
NMDAR	NMDA receptor
PBS	phosphate buffered saline
PC-12	pheochromocytoma cell line
PD	Parkinson's disease
PDI	protein-disulfide isomerase
pERK	phosphorylated ERK
PKA	cAMP-dependent protein kinase
PKC	protein kinase C

PKG	cGMP-dependent kinase
PNMT	phenylethanolamine N-methyltransferase
polyQ	polyglutamine
PP1	protein phosphatase type-1
PP2a	protein phosphatase type-2a
PSD	postsynaptic density
PVDF	polyvinyldifluoride
RER	rough endoplasmic reticulum
RIPA	radioimmunoprecipitation
RT	room temperature
SOC	Super Optimal Catabolite repression
SRE	serum response elements
t-ERK	total ERK
T-TBS	tris-tween buffered saline
TH	tyrosine hydroxylase
UIM	ubiquitin interacting motif
XTT	tetrazolium salt
Zif268	Zinc finger binding protein clone 268

Chapter 1

General Introduction

1.1 Introduction

This thesis identifies 3 novel target genes of the plasticity related immediate early gene zif268: gephyrin, ubiquilin and the novel gene, urma. Zif268 is implicated in many different forms of neuronal plasticity. Long-term potentiation (LTP) is a type of synaptic plasticity thought to be the cellular mechanism of memory formation. Like memory, synaptic plasticity can occur in short-term and long-lasting forms. Downstream targets of zif268 are widely believed to contribute to the duration and stabilisation of LTP and, therefore, to learning and memory. These downstream targets of zif268 are only just starting to receive attention; a description follows in the text.

Long-term changes in the activity of neuronal circuits are sustained by an altered pattern of gene expression and protein synthesis. The importance of protein degradation is starting to emerge as an area of intense research, and therefore I will briefly introduce the proteasome (a protein complex that digests proteins marked for degradation) and its proposed involvement in LTP. Intriguingly, zif268 was recently linked to the neuroproteasome, a subject that will be addressed.

In addition, I will introduce two $GABA_A$ receptor ($GABA_AR$) associated proteins: ubiquilin, which regulates cell surface expression, and gephyrin, a scaffolding protein thought to cluster and anchor $GABA_ARs$ at the postsynaptic membrane.

1.1.1 Neuronal Plasticity

Neuronal plasticity is a term used to describe the many and varied changes that occur within the brain as a result of internal and external stimuli i.e. development, injury and/or learning and memory. These phenomena can lead to changes in the structure and function of synapses, neurones and neural networks.

Animal models of neuronal plasticity include neuronal development in the visual cortex after light stimulation (Wiesel & Hubel 1963), spatial learning in the hippocampus (Bliss & Lomo 1973), long-term habituation in *Aplysia* (Dale *et al.* 1988), fear conditioning in the amygdala (Rogan *et al.* 1997), olfactory memory formation in the olfactory bulb (Matsuoka *et al.* 1997), procedural memory in the striatum and cerebellum (Karachot *et al.* 2001) and eyeblink conditioning in the cerebellum (Kishimoto *et al.* 2001).

1.1.2 Long Term Potentiation

LTP is widely believed to be a form of plasticity involved in learning and memory, thus providing an important key to understanding the cellular and molecular mechanisms that underlie memory formation and storage. Long-lasting, activity-dependent changes in the weight or strength of synaptic communication could constitute a basic mechanism underlying the brain translating experiences into memories (Walton *et al.* 1999).

The most investigated form of synaptic plasticity – a measurable change in synaptic connections, is LTP. It can be induced within fractions of seconds using short bursts of tetanic high frequency electrical stimulation to the connection between two neurones, eliciting modifications that can last for periods of weeks or even months. This results in a semi-permanent trace of the past activation of the synapse. Ultimately, upon induction of LTP and appropriate activation of specific neurones, it is generally believed that synapses can be strengthened by the production and persistence of long-term changes in the activity of neuronal circuits, developing and incorporating into a memory network.

In 1894, Santiago Ramon y Cajal proposed that learning was not due to new cell growth, but to a strengthening of connections between existing neurones. This was further elaborated by Hebb's Postulate (1949), which describes how the connection from pre-synaptic neurone A to post-synaptic neurone B can be modified. He proposed that such a mechanism could stabilise the specific neuronal activity patterns in the brain, stating that:

> "When an axon of cell A is near enough to excite cell B and repeatedly or persistently takes part in firing it, some growth process or metabolic change takes place in one or both cells such that A's efficiency, as one of the cells firing B, is increased."

Several rules must be adhered to for successful LTP induction: a) Co-operativity: the existence of an intensity threshold for induction, b) Associativity: a weak input can be potentiated if active at the same time as a strong stimulus, c) Input Specificity: if an input is not active at the time of the tetanus, it will not share the potentiation (Bliss & Collingridge 1993).

There are distinct phases of LTP in which the early phases seem to be controlled by second messengers and kinases, which modify existing proteins and lasts for

approximately 1 to 3 hours. The late phases of LTP depend on immediate early gene initiation of gene transcription and new protein synthesis, which starts after approximately 4 hours and can be maintained for weeks *in vivo* (Morris 2004).

1.1.2.1 The hippocampus

The hippocampal formation is found within the limbic system and comprises the entorhinal cortex, subiculum, dentate gyrus and the hippocampus proper. The hippocampus itself is separated into 4 regions cornu ammonis (CA) 1, CA2, CA3 and CA4 (Lorente de No 1934) (see figure 1.1).

The perforant pathway is the major afferent projection into the hippocampus and originates from different layers of the entorhinal cortex. It consists of a lateral and medial component: the lateral path begins in layers III and V and travels to the subiculum and the pyramidal cells of the CA1, whilst the medial section begins in layers II and IV and travels to the granule cells of the dentate gyrus and pyramidal cells of the CA3.

Within the hippocampal formation, as a simplification, the major projections are the mossy fibre pathway and the Schaffer collateral pathway. The mossy fibres link the granule cells of the dentate gyrus to the CA3 pyramidal neurones and the Schaffer collateral pathway projects from the CA3 to the CA1 cells. In addition there are a myriad of other minor pathways that interlink all the regions of the hippocampal formation, although the CA3 neurones only innervate the CA1 neurones (reviewed in Amarel & Witter, 1989).

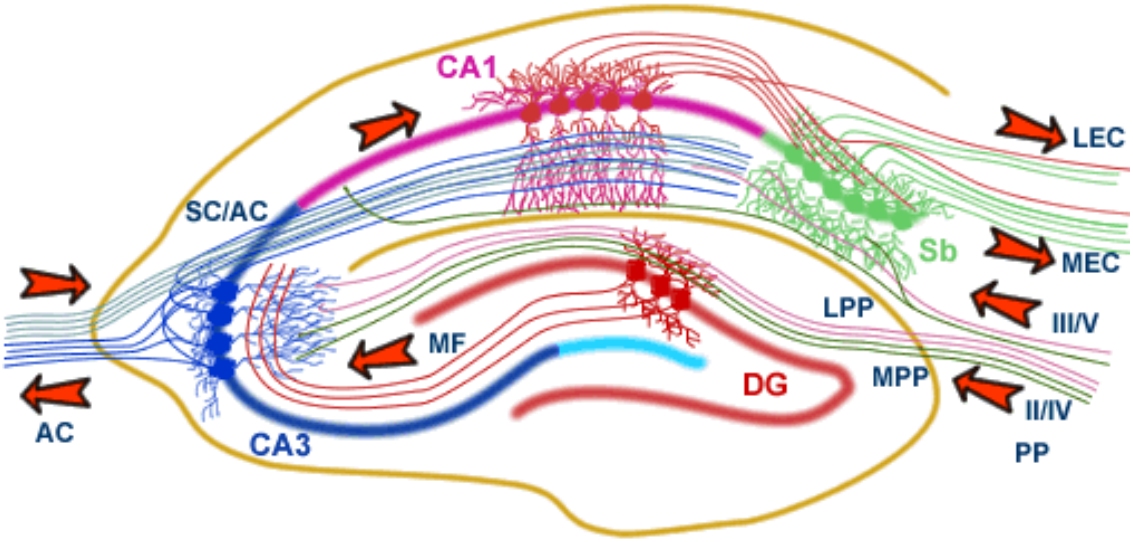

Figure 1.1: Diagram of the hippocampal formation. The entorhinal cortex layers II/IV gives rise to the medial perforant path (MPP) which extends to the dentate gyrus (DG) and CA3. The mossy fibres (MF) also send information from the DG to CA3. CA3 innervates CA1 via the Schaffer Collateral Pathway (SC) and to the CA1 region of the contralateral hippocampus via the Associational Commissural Pathway (AC). The lateral perforant path travels to the subiculum (Sb) and CA1. CA1 innervates the subiculum which, in turn, return to the lateral (LEC) and medial (MEC) entorhinal cortex. Taken from http://www.bris.ac.uk/Depts/Synaptic/info/pathway/hippocampal.htm

In accordance with Hebb's Postulate, Bliss & Lomo (1973) elicited long-lasting strong responses in postsynaptic granule cells of rabbits after tetanic stimulation of the presynaptic fibres of the perforant pathway. It can be generated in a variety of brain regions, but the induction of LTP within the perforant path of the hippocampus shows a clear relationship with endogenous learning and memory (Bliss & Collingridge 1993). Memory deficits can be observed using electrophysiological procedures to saturate LTP within the hippocampal formation before learning, in a manner that prevents the capacity for further synaptic changes during learning (Barnes *et al.* 1994). It can be produced throughout the limbic forebrain with few exceptions, however, pathways within the hippocampus show significantly greater LTP effects compared with pathways outwith the hippocampal formation (Racine *et al.* 1983).

In addition to hippocampal LTP, other structures within the brain that can display LTP include the striatum, amygdala, cerebellum and cerebral cortex (Salin *et al.* 1996; Charpier & Deniau 1997; Rogan *et al.* 1997).

1.1.3 Long Term Depression

Another form of synaptic plasticity is long term depression (LTD). This phenomenon can present itself in two separate forms: *de novo* LTD and depotentiation. Depotentiation has the capability to reverse the effects of LTP at synapses after low frequency stimulation within the hippocampus (Barrionuevo *et al.* 1980). *De novo* LTD may contribute to memory formation and consists of a use-dependent weakening of synaptic conductivity (reviewed in Linden & Connor 1995). LTD at the excitatory synapse between parallel fibres and Purkinje cells in the cerebellum has been attributed to the acquisition of classically conditioned eye-blink responses (Ekerot & Kano 1985).

The induction of LTD can occur with high frequency and prolonged low frequency stimulation, depending on the brain region. Area CA1 of the hippocampus requires low frequency stimulation over long periods of time for the induction of LTD (Dudek & Bear 1992). In contrast, high frequency stimulation can induce LTD in the cerebellar cortex, neocortex, striatum and nucleus accumbens (Artola & Singer 1993). LTP and LTD can be activated using similar stimulation parameters but LTP requires a stronger depolarisation and greater increase in Ca^{2+} concentration than LTD (Artola *et al.* 1990).

LTD typically requires the NMDA receptor, although this is not essential (Mulkey & Malenka 1992; Anwyl 2006). In contrast to LTP, LTD can occur at inactive synapses (anti-Hebbian or heterosynaptic LTD) as well as active synapses (Hebbian or homosynaptic LTD), and is generally regarded as the 'inverse' of LTP (Bolshakov & Siegelbaum 1994; Bear & Abraham 1996; Oliet *et al.* 1997).

1.1.4 NMDA Receptor-dependent LTP

LTP-inducing stimuli progressively depolarise the postsynaptic cell by releasing glutamate from the presynaptic cell. A magnesium ion gates the calcium-permeable glutamate-activated N-methyl-D-aspartate (NMDA)-type receptor (Nowak *et al.* 1984), necessitating a voltage-dependent activation. Therefore, the NMDA receptor (NMDAR) contributes little to basal postsynaptic responses during low frequency synaptic transmission at most glutamatergic synapses. However, once glutamate has evoked a large excitatory postsynaptic potential (EPSP), via activation of another glutamate receptor subtype, the α-amino-3-hydroxy-5-methyl-4-isoxazole propionic acid (AMPA) receptor (AMPAR), the depolarisation of the

postsynaptic cell by an influx of Na^+ and K^+ (McLennan 1983) is sufficient to relieve the magnesium ion from the NMDAR channel. Activation of the NMDAR therefore may only occur once the cell is sufficiently depolarised and glutamate has bound, allowing Ca^{2+} to enter the cell (Mayer & Westbrook 1987). The flood of Ca^{2+} through the receptor channel increases the intracellular Ca^{2+} concentration giving the necessary signal for LTP induction (Harvey & Collingridge 1992). As well as entering the cell via NMDAR, calcium also enters through voltage gated calcium channels and is released from intracellular stores.

1.1.4.1 NMDAR-dependent LTP and the hippocampus

The NMDAR is assembled from a combination of subunits designated NR_1 and $NR_{2A–D}$. NR_1, the essential receptor subunit of the NMDAR, has eight alternative splice variants that have different expression patterns within the human brain (Rigby *et al.* 1996). In the cerebral cortex and the hippocampus, NMDARs are assembled from NR_1, NR_{2A}, and NR_{2B} subunits (Conti *et al.* 1997; Kaczmarek *et al.* 1997). NR3 subunits are also likely to be present, at least at some developmental stages. The hippocampus is one of the most NMDAR dense regions of the brain. The Schaffer collateral/CA1 synapses and the perforant path/dentate gyrus synapses comprise two major hippocampal pathways involved in NMDA-dependent LTP. NMDAR-dependent plasticity in the CA3-CA1 region of the hippocampus is the most intensively studied connection for synaptic plasticity. Rat *in vivo* and *in vitro* studies have implicated NMDAR as a necessary factor for LTP induction and maintenance in the CA1 region of the hippocampus (Harris *et al.* 1984; Wigstrom & Gustafsson 1986; Collingridge *et al.* 1988). Specific NMDAR antagonists completely block the generation of associative LTP, but minimally effect basal synaptic transmission (Teyler 1987; Collingridge *et al.* 1983). In addition, transgenic mice overexpressing the NR2B subunit of the NMDAR were shown to have enhanced LTP in the hippocampus, and superior learning performances in several tasks when compared to wildtypes (Tang *et al.* 1999).

LTP requires a postsynaptic calcium increase, and the rise of NMDAR-dependent intracellular calcium seems to be the critical trigger. Increases in the uptake and retention of Ca^{2+} after tetanic stimulation in the hippocampus have been demonstrated (Baimbridge & Miller 1981; Kuhnt *et al.* 1985). In addition, increasing the extracellular concentration of Ca^{2+} can increase LTP in the CA1 region of the rat hippocampus (Mulkeen *et al.* 1988), whilst decreasing levels

surrounding rat hippocampal slices prevents LTP (Dunwiddie & Lynch 1979). LTP induction can be blocked by EGTA, which binds free calcium ions (Lynch *et al.* 1983), and anti-S-100, a calcium binding protein, prevents LTP in the CA1 of the hippocampus (Lewis & Teylor 1986). In contrast, directly raising the amount of postsynaptic calcium by photolysis of caged calcium can increase LTP (Malenka *et al.* 1988). It is unknown whether an increase in calcium alone is sufficient to trigger LTP or whether additional factors are required, probably provided by additional synaptic activity.

1.1.5 LTP in the Cerebral Cortex

Memories of sensory experiences are thought to form within the areas that process the sensory information, and therefore any synaptic neurone activated within the sensory cortices of the cerebral cortex would be permanently modified by that sensory event (Bear 1996). In support of this, it has been found that neurones within the primary auditory cortex display altered responses once an auditory discrimination task has been learnt (Weinberger & Diamond 1987; Edeline *et al.* 1993), and neurones of the inferior temporal cortex display altered responses after face recognition tasks in primates (Rolls *et al.* 1989).

The neocortex is the major site for storage of nonspatial declarative memory (i.e. it stores memories of facts and events that do not require spatial information). Using the same high frequency stimulation that induces LTP in the CA1 region of the hippocampus, stimulation of neocortical layer IV induces LTP in neocortical layer III in mouse, rat and cat visual cortex and rat somatosensory cortex (Kirkwood *et al.* 1993; Castro-Alamancos *et al.* 1995). LTP has also been induced in the human inferotemporal cortex, a region thought to accommodate visual memories (Chen *et al.* 1996). Critical factors for these types of cortical LTP are the levels of NMDAR activation and availability (Markram *et al.* 1995).

1.1.6 LTP in the Striatum

Specific forms of associative learning and reward produce long-term changes in synaptic efficiency within the striatum (Reynolds *et al.* 2001; Schultz 2002). In this area, dopamine mainly acts on D1 receptors, found on dynorphin and substance P containing spiny neurones that project to the substantia nigra, and D2 receptors, found on enkephalin containing spiny neurones that project to the globus pallidus (Le Moine *et al.* 1990; Gerfen *et al.* 1991; Levey *et al.* 1993). These neurons are

of equal number and comprise approximately 90% of the total number of striatal neurones (Gerfen & Young 1988; Kawaguchi *et al.* 1990).

D2 receptors, found presynaptically, inhibit the release of glutamate from corticostriatal synapses (Maura *et al.* 1988; Bamford *et al.* 2004), activation of D2 receptors attenuates NMDA responses in the striatum (Cepeda *et al.* 1993) and inhibits calcium currents in isolated spiny striatal neurones (Surmeier *et al.* 1996). High frequency stimulation of the striatum unpredictably induces both LTP and LTD *in vivo* (Charpier & Deniau 1997; Reynolds & Wickens 2000; Reynolds *et al.* 2001) and *in vitro* (Akopian *et al.* 2000; Partridge *et al.* 2000). However, after chronic haloperidol administration, which blocks D2 receptors, high frequency stimulation of corticostriatal fibres invariably induces LTP, which is blocked by MK-801 (Centonze *et al.* 2004). Tetanic stimulation of cortical fibres projecting to the striatum in D2 receptor-null mice produces LTP which is blocked by the addition of D(-)-2-amino-5-phosphonoaleric acid (APV - an NMDAR antagonist that competitively inhibits the receptor binding site), suggesting a regulatory function for D2 receptors on synaptic plasticity expressed in striatal areas (Calabresi *et al.* 1997).

1.1.7 Cellular Cascades involved in LTP

Once AMPARs have sufficiently depolarised the cell and released the voltage-dependent Mg^{2+} block in the NMDAR, the resultant Ca^{2+} influx is probably restricted to the vicinity of the activated spines (Regehr & Tank 1990; Sabatini *et al.* 2002).

A key component of LTP seems to be calcium-calmodulin-dependent protein kinase II (CaMKII) (Madison *et al.* 1991; Lisman 1994) which is activated by Ca^{2+} bound to calmodulin. CaMKII, an oligomeric protein consisting of 10-12 subunits, is a major constituent of the postsynaptic density (PSD), and is therefore found in high concentrations close to the glutamate receptors that mediate synaptic transmission (Malenka *et al.* 1989). Upon activation, it can translocate to synapses (Strack *et al.* 1997; Shen & Meyer 1999) and bind to NMDARs (Leonard *et al.* 1999). CaMKII is able to undergo long term modification, resulting in a calcium influx by binding to the region around serine 1303 in the cytoplasmic domain of the NMDAR NR2B subunit (Leonard *et al.* 1999; Strack *et al.* 2000; Bayer *et al.* 2001). This locks CaMKII in an activated state that cannot be

reversed by phosphatases (Bayer *et al.* 2001), leading to the generation of Ca^{2+}-independent activity, which increases after LTP induction. Transgenic mice in which threonine 286 has been mutated to alanine have normal basal synaptic transmission, but do not exhibit LTP (Giese *et al.* 1998). Persistently active CaMKII can mimic LTP (Pettit *et al.* 1994; Lledo *et al.* 1995), inhibitors of CaMKII prevent the induction of LTP (Malinow *et al.* 1989) tetanic stimulation of CA1 increases CaMKII activity (Miyamoto & Fukunaga 1996) and APV blocks LTP-associated CaMKII autophosphorylation (Fukunaga *et al.* 1996), indicating a key role for CaMKII in the early phases of LTP. Behaviourally, mice with no alpha subunit of CaMKII display a deficit in learning (Silva *et al.* 1992), and mice with a point mutation at threonine 286 show no spatial learning in the Morris water maze (a spatial learning task) (Giese *et al.* 1998).

The critical substrates of CaMKII within LTP are poorly understood. One known substrate of CaMKII however, is the AMPAR. AMPARs are tetrameric receptors, comprised of 2 subunits selected from GluR1–GluR4; these receptors allow Na^+ to enter the cell, and play a major role in glutamate-induced membrane depolarization (Doble 1995). After NMDA stimulation and calcium influx in cultured hippocampal cells, CaMKII autophosphorylates at threonine 286 and anchors to the NMDAR (Tan *et al.* 1994), phosphorylating AMPAR in the CA1 region after the induction of LTP in this area (Barria *et al.* 1997b) and phosphorylates the GluR1 AMPAR at Ser831 in HEK293 cells (Barria *et al.* 1997a; Mammen *et al.* 1997). It may also assemble insertion slots for newly delivered AMPARs (Lisman *et al.* 2002). GluR1 knockout mice show normal basal synaptic transmission however, associative LTP is absent in region CA1 (Zamanillo *et al.* 1999). Phosphorylation of AMPAR results in potentiation of whole cell AMPAR mediated currents due to an increase in single channel conductance of existing receptors, or by recruiting new high-conductance-state AMPARs (Derkach *et al.* 1999).

CaMKIV is also transiently upregulated after LTP-inducing stimuli. It is phosphorylated by CaMK kinase and acts on cyclic AMP-responsive element-binding protein (CREB) at serine 133 which, in turn, leads to the expression of c-Fos protein. During LTP in the rat CA1, CREB and c-Fos expressions are increased; an effect that can be inhibited with the use of CaMK inhibitors (Kasahara *et al.* 2001).

CaMKII can activate the calcium-dependent adenylyl cyclase (Chetkovich & Sweatt 1993), which leads to local increases in cAMP, a possible downstream mediator of NMDA-dependent LTP (Chetkovich *et al.* 1991). Deficits in hippocampal LTP and memory tests can be found in mutant mice lacking adenylyl cyclase (Wu *et al.* 1995), and the early phase of LTP has been shown to rely on postsynaptic levels of cAMP (Blitzer *et al.* 1995).

cAMP-dependent protein kinase, also known as protein kinase A (PKA) phosphorylates inhibitor-1, an endogenous protein phosphatase inhibitor, indirectly boosting CaMKII activity (Blitzer *et al.* 1998). Like CaMK, PKA can phosphorylate CREB at serine 133 in response to elevated levels of cAMP (Gonzalez & Montminy 1989), and inhibition of PKA blocks the expression of LTP (Frey *et al.* 1993; Matthies & Reymann 1993). The timecourse of PKA actions in LTP seem rather controversial as the PKA inhibitor, H89, suppresses early phase LTP (Otmakhova *et al.* 2000), whereas Frey *et al.* (1993) found that inhibition of PKA specifically blocked late phase LTP. Transgenic mice with a mutation in the regulatory subunit of PKA display a marked reduction of late phase LTP in area CA1 with concomitant deficiencies in spatial memory and contextual fear (Abel *et al.* 1997).

PKC has also been implicated in LTP through the use of transgenic mice. PKC gamma-mutant mice have a reduced capability for LTP in the hippocampus and display mild deficits in learning tasks (Abeliovich *et al.* 1993a, b). In addition, reduced levels of PKC in the hippocampus decrease performance in the Morris water maze, effectively linking PKC and spatial memory (Wehner *et al.* 1990). Specific inhibitors of PKC decrease the potentiation of synaptic responses and can reduce the proportion of PKC associated with the membrane (Wang & Feng 1992; Reymann *et al.* 1988). Again, there is controversy over the timings of LTP disruption with the use of differing PKC inhibitors and results suggest that it may be involved in both the early and late phases (Wang & Feng 1992). Injecting PKC into the pyramidal cells of the CA1 elicits long lasting enhancement of synaptic transmission in a manner similar to LTP (Hu *et al.* 1987), and PKC seems to target many proteins with proposed LTP involvement. One such protein, F1 (also known as B-50 and GAP-43) shows increased phosphorylation in the hippocampus immediately after, 1 hour after and even 3 days after the induction of LTP as well as after a spatial learning task (Lovinger *et al.* 1986); effects that are blocked by APV (Linden *et al.* 1988).

NMDAR activation, and the ensuing increase in intracellular calcium, causes an increase in activity of guanyl nucleotide exchange factors (GEFs), catalysing the exchange of GDP for GTP on low molecular weight GTPases such as Ras. At the same time, the activity of the GTPase-activating proteins (GAPs), which aid the hydrolysis of GTP to GDP, is decreased. The increase and corresponding decrease in activity of the GEFs and GAPs subsequently leads to an overall increase in Ras activity. In addition, the activated kinases CaMK and PKC can both phosphorylate Ras. KO mice deficient in Ras-GRF1 (Ras-guanine-nucleotide releasing factor 1) show a loss of LTP in the amygdala (Brambilla *et al.* 1997), and Ras activation is necessary for delivering AMPARs to the synapse during NMDAR-dependent LTP in the hippocampus (Zhu *et al.* 2002).

Ras can activate the tyrosine kinase src, which may participate in LTP induction by enhancing NMDA receptor function (Lu *et al.* 1998). Src activity is increased by LTP induction, and blocking src prevents LTP within the CA1 of the hippocampus (Lu *et al.* 1998). However, O'Dell *et al.* (1992) found that mutations in the src gene did not affect the induction or maintenance of LTP. Ras also activates Raf, a serine/threonine protein kinase that phosphorylates the enzyme MAPK/ERK kinase (MEK). Inhibition of MEK prevents hyperphosphorylation of extracellular signal-regulated kinase (ERK) (also known as mitogen-activated protein kinases (MAPK)), blocks LTP induction in the hippocampus (English & Sweatt 1997), and impairs the learning and memory of animals in spatial learning, fear conditioning and conditioned taste aversion (Atkins *et al.* 1998; Selcher *et al.* 1999; Schafe *et al.* 2000). In addition, LTP-induced increases in AMPAR transmission via CaMKII are also disrupted by MEK inhibition, linking ERK activation and CaMKII activity (Zhu *et al.* 2002).

The ERK isoforms -1 and -2 (ERK1 and ERK2), are widely expressed in the mammalian nervous system (Boulton *et al.* 1991; Fiore *et al.* 1993a), have been localised in neurones to the nucleus, cytoplasm and dendrites (Patterson *et al.* 2001; Yuan *et al.* 2002), and are activated by glutamatergic signalling (Fiore *et al.* 1993b; Xia *et al.* 1996). LTP-inducing high frequency stimulation of the hippocampus activates ERK (English & Sweatt 1996), as does LTP in the dentate gyrus (Coogan *et al.* 1999), amygdala (Schafe *et al.* 2000) and cortex (Di Cristo *et al.* 2001). However, the specific function of ERK in LTP remains unknown.

The induction of LTP in the dentate gyrus *in vivo* causes phosphorylation and nuclear translocation of ERK (Davis *et al.* 2000; Patterson *et al.* 2001), which then activates two sets of kinases – ribosomal protein S6 kinases (RSKs) and mitogen- and stress-activated kinases (MSKs). With reference to area CA1 of the hippocampus, evidence suggests the cAMP-responsive element-binding protein (CREB) kinase, Rsk2, is critical for the maintenance of LTP within this area (Guzowski & McGaugh 1997; Bourtchuladze *et al.* 1994). PKA and CaMKIV phosphorylate the transcription factor CREB at serine 133 (Dash *et al.* 1991; Deak *et al.* 1998) leading to the activation of several IEGs by binding to the CRE sites present in their promoter regions and, ultimately, regulating gene transcription. In contrast, CaMKII can phosphorylate CREB at serine 142 which reduces CREB-mediated transcription (Matthews *et al.* 1994; Wu *et al.* 2001). LTP induction increases CREB phosphorylation (Bito *et al.* 1996) and transcription regulation requires the maintenance of CREB phosphorylation at serine 133, which has been attributed to Rsk2 via ERK (Hardingham *et al.* 2001; Wu *et al.* 2001). However, Rsk2 targeted deletion does not seem to alter CREB phosphorylation (Sassone-Corsi *et al.* 1999; Bruning *et al.* 2000). More recently, Msk1, rather than Rsk2, has been linked to CREB phosphorylation in neurones (Arthur *et al.* 2004; Rakhit *et al.* 2005). Evidence from *Aplysia*, *Drosophila*, mice and rats demonstrates that region-specific cAMP-responsive transcription mediated by CREB is crucial in the establishment of long term, but not short-term, memory (Kaang *et al.* 1993; Yin *et al.* 1994; Bourtchuladze *et al.* 1994; Lamprecht *et al.* 1997; Yin & Tully 1996). In addition, MEK inhibitors block CREB targeted gene transcription after LTP induction and fear dependent learning (Impey *et al.* 1998; Athos *et al.* 2002), and in CREB deficient mice, LTP induction decreases more rapidly than in control mice (Bourtchuladze *et al.* 1994).

1.1.8 LTP Maintenance

The stimulation of cell-surface receptors (e.g. NMDA receptors), and subsequent activation of cytoplasmic second-messenger systems, eventually results in an early wave of immediate early gene transcription. The expression of these genes at the mRNA level rises markedly and transiently in the cell shortly after stimulation and in the absence of *de novo* protein synthesis. Once translated, these inducible transcription factors re-enter the nucleus and regulate the expression of ‘late response genes’. Therefore the molecular changes in

neurones during transient memory formation that subsequently alter transcription are important in the conversion of short-term to long-term memory.

Evidence suggests that all models of neuronal plasticity comprise 3 sequential LTP phases. Phase 1 is dependent on existing protein modification and can last for the initial 2 hours after an LTP-inducing stimulus. This phase is unaffected by transcriptional and translational inhibition. Phase 2 is dependent on increased mRNA translation, subsequently synthesising new protein, and is present between 2 and 8 hours after the initial stimulus. Phase 3 is the most sustained phase of LTP and is dependent on increased gene transcription, as well as further protein and mRNA synthesis, allowing specific synapses to alter the efficiency of their transmission in order to become more effective (Morris 2004). These distinct temporal phases can be seen experimentally in each of the major hippocampal excitatory synaptic pathways (Huang *et al.* 1996) and stable LTP, lasting for months, has been obtained for both medial and lateral perforant path synapses (Abraham *et al.* 2002).

Pharmacological inhibition of activity-induced translation, and the speedy synthesis of *de novo* marker and reporter proteins in response to LTP, have determined that long-lasting forms of LTP require protein synthesis (Stanton and Sarvey 1984; Deadwyler *et al.* 1987; Frey *et al.* 1988; Mochida *et al.* 2001). RNA synthesis inhibitors impair late phase LTP in the CA1 *in vitro* and in the dentate gyrus *in vivo* (Frey *et al.* 1996), and protein (and RNA) synthesis inhibitors impair long term memory formation whilst keeping short term memory intact (Squire *et al.* 1980; Davis & Squire 1984). Thus, protein synthesis is important for the mechanisms of memory consolidation to occur.

The most problematic issues regarding LTP maintenance are the localisation of definitive synaptic modifications providing the foundation for enhanced transmission and the understanding of the mechanisms by which these modifications are made persistent. Alterations observed include an increase in the amount of transmitter released, implying the necessity for a retrograde messenger (Dolphin *et al.* 1982), an increase in the density of glutamate receptors (Lynch *et al.* 1982), an increase in size of dendritic spines (Fifkova & Van Harreveld 1977) ,and an increase in protein synthesis (Duffy *et al.* 1981). Altered glutamate transporter levels have also been suggested to contribute to LTP and memory (Levenson *et al.* 2002; Shen & Linden 2005).

Synaptic plasticity relies on input and synapse specificity, so localisation of protein products for modifications and stabilisation in synaptic strength is an inherent need. There are several schools of thought that attempt to explain how alterations in transcription lead to synapse specific modifications. A definitive model has not been elucidated however, theories include the specific targeting of RNAs and proteins from the nucleus to activated synapses; the existence of a virtual conveyer belt that delivers proteins throughout the cell, but only increases synaptic strength in those synapses activated and 'tagged'; or the ability of synapses to translate their own mRNAs locally (Goelet *et al.* 1986; Sossin 1996; Schuman 1997; Frey & Morris 1998).

mRNA can be translated at synapses, as indicated by the presence of golgi elements, rough endoplasmic reticulum, polyribosomes, translation factors and large populations of mRNAs within dendrites and dendritic spines (Job & Eberwine 2001; Bradshaw *et al.* 2003; Inamura *et al.* 2003). Glutamate receptor agonists induce the synthesis of new proteins in isolated dendrites and synaptoneurosomes (Weiler *et al.* 1997; Bagni *et al.* 2000; Yin *et al.* 2002). LTP induction causes polyribosomes to move from dendritic shafts into spines (Ostroff *et al.* 2002), allowing local protein synthesis and translation in synaptic plasticity. An hour after LTP-inducing high frequency stimulation (HFS), the total number of ribosomes, polysomes, and number of membrane bound ribosomes increase significantly in hippocampal CA1 pyramidal neurones (Wenzel *et al.* 1993). In addition, local application of a protein synthesis inhibitor only impairs LTP in those local dendrites rather than dendrites found further down the cell in Schaffer-commissural synapses on CA1 pyramidal neurones in the murine hippocampus (Bradshaw *et al*. 2003). MEK inhibitors effect LTP within 20 to 30 minutes following high frequency stimulation, and therefore ERK is probably unable to translocate to the nucleus, activate transcription and translation, then send the new gene product to potentiated synapses in such a short space of time (Ohno *et al.* 2001; Rosenblum et al. 2002; Selcher *et al.* 2003). However, separating apical dendrites from their cell bodies allows the induction of LTP that lasts for approximately 3 hours, compared to 8-10 hours in intact slices. This suggests that protein synthesis in isolated dendrites is sufficient for the early expression of translation dependent LTP but mRNA transcription in the soma is required for longer lasting potentiation (Frey *et al.* 1989).

1.1.9 The Immediate Early Gene Zif268

Zinc finger binding protein clone 268 (zif268) (Christy *et al.* 1988), also known as Krox24 (Lemaire *et al.* 1988, Lemaire *et al.* 1990), nerve growth factor-induced gene A (NGFI-A) (Milbrandt 1987), early growth response gene-1 (Egr-1) (Sukhatme *et al.* 1988), tetradecanoyl phorbol acetate-induced sequence 8 (TIS8) (Lim *et al.* 1987), and ZENK (an acronym of zif268, egr-1, NGFI-A, Krox24), is an immediate early gene (IEG) that encodes an 82 and an 88kDa regulatory protein (depending on the initiator sequence) (Lemaire *et al.* 1990). The gene is present in the mammalian genome as a single copy gene located on mouse chromosome 18, and belongs to a multi-gene family of closely related transcription factors, the Egr proteins.

As the name implies, zif268 is a zinc finger protein; it contains 3 zinc fingers in the DNA binding domain that allow the protein to control directly the transcription of other genes (Christy & Nathans 1989; Swirnoff & Milbrandt 1995). There is a high homology in the 3 zinc finger sequences in all members of the Egr family suggesting that the proteins may bind to the same consensus sequence of 5'-GCG(G/T)GGGCG-3' (Christy & Nathans 1989; Cao *et al.* 1993; Swirnoff & Milbrandt 1995) found in the promoter regions of downstream target genes. The other members of the Egr family are Egr-2, also known as Krox 20, Egr-3, also known as PILOT, and Egr-4, also known as NGFI-C and pAT133 (Joseph *et al.* 1988; Crosby *et al.* 1991; Patwardhan *et al.* 1991; Mages *et al.* 1993). Zif268 protein has a modular organisation; there are distinct areas for DNA binding, and the activation or repression of transcription. As befits a transcription factor, the zif268 protein has a nuclear localisation within the neurone, due to a bipartite signal in the DNA-binding domain, which is located in either the second or third zinc finger (Gashler *et al.* 1993). In addition to the DNA binding site, zif268 contains an activation domain that has not been fully characterised and an inhibitory domain located between the two. This allows zif268 expression to be regulated by binding of the transcriptional co-factor proteins NGFI-A binding proteins 1 and 2 (NAB1 and NAB2) which interact with the inhibitory domain (Russo *et al.* 1995; Svaren *et al.* 1996). Both NAB1 and NAB2 block the biological activity of zif268 (Russo *et al.* 1995; Svaren *et al.* 1996; Thiel *et al.* 2000), and interestingly, zif268 has been shown to control the expression of NAB2, allowing for autoregulation via a negative feedback loop (Ehrengruber *et al.* 2000). Zif268 is known to interact directly with other transcription factors/modulators; binding to

CREB-binding proteins (Ramirez *et al.* 1997), NFκB (Chapman & Perkins 2000), NFAT (Decker *et al.* 2003) or C/EBP (Zhang *et al.* 2003) can all modify the transcriptional actions of zif268, suggesting that zif268 can exert a variety of effects depending on which other transcription factors are active at that time.

In, or adjacent to, the promoter region of the zif268 gene are several different regulatory sites, including cyclic-AMP-responsive element (CRE) sites, serum response element (SRE) sites, activator protein 1 like motifs (AP-1), AP-2 like binding sequences, specificity protein 1 element (Sp1) -like motifs, and, in humans, an Egr/Zif268 response element (ERE) (Tsai-Morris *et al.* 1988; Christy & Nathans 1989; Sakamoto *et al.* 1991; Alexandropoulos *et al.* 1992b; Schwachtgen *et al.* 2000). This abundance of regulatory sites allows several different signalling pathways and kinases to induce and modulate zif268, including Elk-1 binding to the SRE sites, CREB binding to the CRE sites and the Fos-Jun dimerised protein binding to the AP-1 site. In addition, its own family members can bind to the ERE site and, for enhanced autoregulation, zif268 itself can also bind.

During development, zif268 is expressed in the endothelial system, thymus, muscle, cartilage, bone and parts of the central and peripheral nervous system (McMahon *et al.* 1990; Watson and Milbrandt 1990). In the rat brain, basal constitutive expression of zif268 mRNA is found in many areas including the primary visual cortex, entorhinal cortex, olfactory cortex, neocortex, and several subcortical regions including the hippocampus and striatum. In the neocortex, zif268 is mainly expressed in layers IV and VI, and in the hippocampus it is expressed at its highest levels in CA1, to a lesser extent in CA2-CA4 and is virtually absent in the dentate gyrus (Schlingensiepen *et al.* 1991). Protein expressions display a very similar pattern to that of mRNA (Beckmann & Wilce 1997).

Zif268 was initially identified as a nerve growth factor response gene product in rat PC-12 cells, and an immediate-early serum and growth factor response gene product in mouse fibroblasts, before similar genes were identified in other species (Sukhatme *et al.* 1988; Milbrandt 1987; Christy *et al.* 1988; Suggs *et al.* 1990; Lau & Nathans 1987).

1.1.10 Zif268 activation in Long Term Potentiation

As an inducible transcription factor, zif268 can be activated by a variety of pharmacological and physiological stimuli including growth factors, neurotransmitters, depolarization, peptides, nitric oxide, ischaemia, seizures, neurodegeneration, apoptosis and cellular stress (reviewed in Hughes & Dragunow 1995; Beckmann & Wilce 1997; Herdegen & Leah 1998). Immediate early genes are rapidly and transiently activated after LTP induction, and therefore possibly constitute an early genomic response for triggering the mechanisms underlying persistent cell modification. An important biological function of these modifications in neurones may be to underlie the maintenance or stabilisation of neuronal plasticity and the formation of long-term memories. With reference to LTP, it has been shown that glutamate, as well as synthetic agonists targeted to specific types of glutamate receptors, are effective in activating zif268 (Condorelli *et al.* 1994). The administration of NMDA and kainate to the cerebral cortex and hippocampus of rats *in vivo* effectively increases zif268 activity (Beckmann *et al.* 1997). The resultant increase in Ca^{2+} within the cytosol can also induce zif268 expression (Murphy *et al.* 1991; Ghosh *et al.* 1994).

Ras can be activated by the protein tyrosine kinase Src in response to an increase in intracellular calcium within PC-12 cells. Src activation, which triggers the formation of an Shc/Grb2 complex (an adaptor protein/growth-factor-receptor binding protein 2), leads to Ras activation in PC-12 cells (Rusanescu *et al.* 1995), which, in turn, activates Raf and further downstream, ERK and zif268 (Qureshi *et al.* 1991; Alexandropoulos *et al.* 1992a). Raf activates MAPK/ERK kinase (MEK) by phosphorylation which, in turn, phosphorylates the serine/threonine kinases ERK1 and ERK2, leading to their activation, and ultimately the modification of many different types of proteins, including transcription factors, like CREB. *In vivo* stimulation of the glutamatergic corticostriatal pathway induces a transient activation of ERK, which is spatially coincident with the onset of zif268 expression in the lateral striatum (Sgambato *et al.* 1998). Infusion of MEK inhibitors prior to LTP can prevent (Davis *et al.* 2000), or attenuate (Rosenblum *et al.* 2002), transcription of zif268 in the dentate gyrus. However, zif268 activation in dentate granule cells by LTP induction of the perforant pathway did not produce a concurrent increase in the level of phosphorylated CREB in one study (Walton *et al.* 1999) and CREB mutant mice display normal constitutive levels of zif268

(Blendy *et al.* 1995). This may suggest that CREB activity is not the major determinant of zif268 expression in hippocampal neurones.

Another possible activator of zif268, Elk-1, binds to the SRE in upstream regulatory regions of IEGs (Wasylyk *et al.* 1998) and is activated simultaneously with ERK, CREB, and zif268 induction *in vivo* (Sgambato *et al.* 1998). Elk-1 is activated by ERK and the c-Jun N-terminal protein kinase (JNK), leading to enhanced DNA-binding activity (Treisman 1995; Whitmarsh *et al.* 1995). LTP induction in the dentate gyrus leads to the phosphorylation of ERK, Elk-1 and CREB and the transcriptional activation of zif268, whilst MEK inhibitors prevent the cascade, resulting in rapidly decaying LTP (Davis *et al.* 2000). This points towards two parallel and possibly co-operating signalling pathways. It remains unknown whether zif268 regulation is dictated by CRE or SRE-mediated transcription, although the contradictory CREB evidence coupled with the presence of 6 SRE sites compared to 2 CRE sites strongly suggests zif268 is controlled by SRE via MAPK-mediated Elk-1 activation. A simplified schematic representation of zif268 induction during LTP is presented in figure 1.2.

1.1.11 Zif268 and Long Term Depression

LTD is a synaptic mechanism of neuronal plasticity that involves a long-lasting decrease in synaptic efficiency following synaptic stimulation. LTD can be induced by similar stimulus conditions, can persist as long as LTP (Abraham et al. 1994), and can be blocked by inhibitors of transcription and translation. Behaviourally, spontaneous recovery of conditioned fear is associated with sustained prefrontal LTD (Herry & Garcia 2002, 2003). Zif268 mRNA is upregulated after LTD induction at CA3/CA1 synapses (Lindecke *et al.* 2006), and increased protein levels correlate strongly with the persistence of heterosynaptic LTD in the perforant path (Abraham *et al.* 1994). Therefore, zif268 induction may be a key factor in inhibitory (LTD) as well as excitatory (LTP) learning paradigms (Herry & Mons 2004).

1.1.12 Zif268 & synaptic plasticity in the dentate gyrus

Zif268 is a regulatory IEG, activating (or suppressing) downstream target genes that presumably play a role in the duration and stabilisation of LTP, in particular the production of LTP phase III. The induction of long-lasting LTP in the dentate gyrus of awake rats consistently increases the expression of zif268 (Cole *et al.*

1989; Wisden *et al.* 1990), but, in contrast, continuous low frequency stimulation does not (Cole *et al.* 1989; Richardson *et al.* 1992; Worley *et al.* 1993). Tetanic stimulation of the perforant path, inducing LTP at dentate gyrus synapses, results in ipsilateral upregulation of zif268 mRNA which is more prevalent in the dorsal than the ventral hippocampus (Cole *et al.* 1989; Richardson *et al.* 1992; Abraham *et al.* 1993; Williams *et al.* 2000). The threshold for inducing zif268 expression is similar to the threshold intensity necessary to induce LTP phase III, but not phases I or II (Abraham *et al.* 1993; Worley *et al*. 1993).

Zif268 upregulation correlates with the persistence of LTP rather than magnitude of induction (Richardson *et al.* 1992) and, after LTP induction, zif268 DNA binding activity to its response element rapidly increases in an NMDAR-dependent manner (Williams *et al*. 2000). Conversely, blocking the induction of LTP by stimulation of the inhibitory commissural input to the dentate gyrus during perforant path tetanization blocks the LTP-associated increase in zif268 expression, as does NMDAR antagonism (Cole *et al*. 1989; Wisden *et al*. 1990; Worley *et al.* 1993; Salin *et al.* 2002).

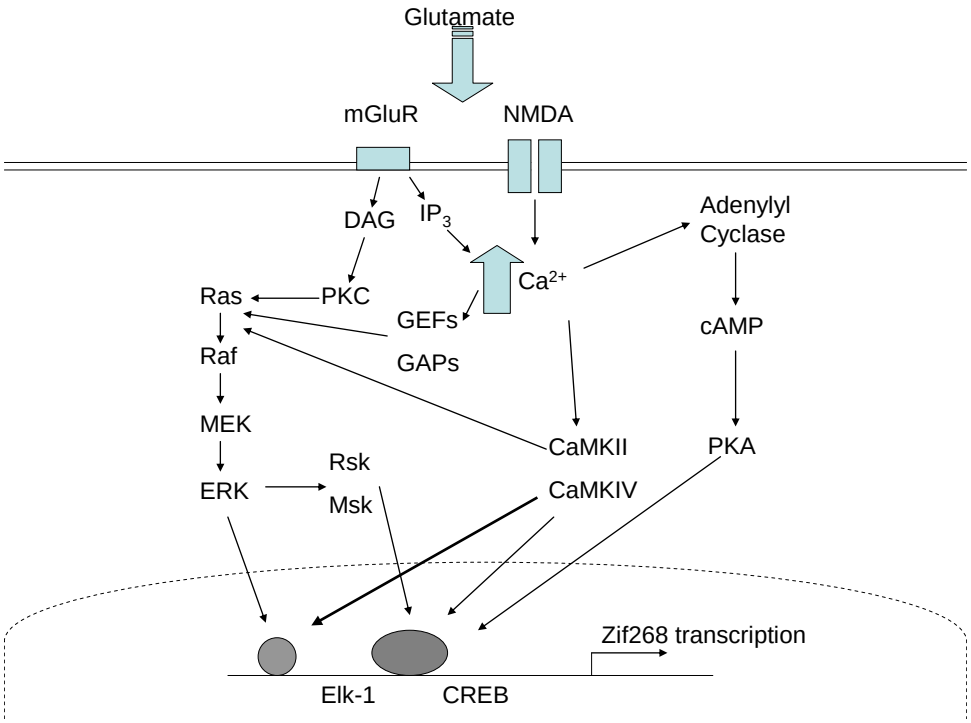

Figure 1.2: A simplified schematic representation of zif268 activation during LTP. The release of glutamate into the synaptic gap between neurones activates glutamate receptors and, in NMDAR-dependent LTP, the NMDA receptor. This leads to several signal transduction cascades that ultimately activate zif268.

After perforant pathway tetanization, zif268 mRNA levels in the dentate gyrus peak with a 6 to 9 fold increase after around 20 minutes, but return to base-line within 2 hours (Cole *et al.* 1989; Wisden *et al.* 1990). Zif268 immunoreactivity peaks around 2 hours and returns to baseline after 8 hours. This timecourse is too prolonged for the initial stages of LTP, which peaks within a couple of minutes following tetanization (Richardson *et al.* 1992), but is consistent with zif268 target genes contributing to phase III of LTP.

1.1.13 Zif268 and neuronal plasticity throughout the brain

Evidence pertaining to zif268's involvement in LTP within other areas of the brain suggests that it is not vital for all types of plasticity in all brain regions. There are very few publications regarding zif268 activation coupled with LTP induction in regions other than the perforant path-granule cell synapse. Zif268 mRNA is upregulated in the primary visual cortex after tetanic stimulation of the dorsolateral geniculate nucleus (Heynen & Bear 2001), and in the insular cortex after stimulation of the basolateral amygdala, although this was also induced by low frequency stimulation and was apparent throughout the entire cortex (Jones *et al.* 1999). Zif268 induction in the CA1 pyramidal cells of the rat hippocampus after LTP has been reported (Roberts *et al.* 1996) although, French *et al.* (2001) detected no changes in zif268 in the CA1 pyramidal cells of the hippocampus after induction of LTP by high-frequency stimulation of the commissural projection in freely moving rats, even though the LTP detected lasted for 5 days. However, they did show zif268 could be modulated in response to electroconvulsive shock and their detection assay was rather insensitive (Prof. B. J. Morris, personal communication) so the negative result after LTP induction should be viewed with caution. Overall therefore, zif268 may be region-specific and not LTP-specific in some systems, although zif268 induction in learning has been relatively widespread.

1.1.14 Zif268 regulation during learning

A rapid increase in zif268 expression has been associated with some, but not all, forms of learning and long-term memory in many different species. In the macaque monkey, visual paired associative learning increases zif268 protein in the anterior temporal lobe, a finding that was not repeated in a simple visual discrimination task or in other IEG products (Okuno & Miyashita 1996; Tokuyama

et al. 2002). Zif268 is also rapidly regulated during associative learning in other species, such as song learning in birds (Mello *et al.* 1992), whereby the upregulation is induced when song birds hear their own conspecies songs. In addition, when a song is presented with a shock, there is a greater increase of zif268 in the caudomedial auditory telencephalon compared to the delivery of a song or a shock by themselves (Jarvis *et al.* 1995). This implies a learning-related aspect to the zif268 induction.

Within rats, associated learning tasks (Malkani & Rosen 2000) and spatial learning tasks (Fordyce *et al.* 1994) have displayed increases in zif268 expression. After 20 minutes training to locate the platform within a water maze, zif268 is upregulated in the hippocampus (Guzowski *et al.* 2001). However, after extended spatial learning over several days, no overexpression of zif268 can be located, providing further evidence for the rapid and transient nature of zif268 activation (Richter-Levin & Segal 1988; Wisden *et al.* 1990). C57 mice have a genetically-defined higher basal level of zif268 compared to the DBA strain of mouse, and the C57 mice perform better in the water maze task than the DBA mice (Fordyce & Wehner 1993). Animals housed in an enriched environment, which improves cognitive function (Hebb 1949), display a significant increase in zif268 mRNA in the CA3 and CA4 areas of the hippocampus compared to those raised in isolation. In addition, these animals performed better in a spatial learning task compared to controls (Toscano *et al.* 2006). Induction of zif268 within the acquisition phase of two-way avoidance training has been demonstrated with a marked accumulation of zif268 occurring within the hippocampus and visual cortex (Nikolaev *et al.* 1992).

Learning-related increases in zif268 expression have also been seen in the accessory olfactory bulb of female mice in response to pheromone signals and putative pheromonal constituents (Brennan *et al.* 1992; Brennan *et al.* 1999), and in the hippocampus after active avoidance learning (Nikolaev *et al.* 1992) or brightness discrimination (Grimm & Tischmeyer 1997). In addition, zif268 expression is elevated in the nucleus of the solitary tract, the parabrachial nucleus, the hypothalamic paraventricular nucleus and the central nucleus of the amygdala in animals trained in conditioned taste aversion (Lamprecht & Dudai 1995).

Fear conditioning is rapidly acquired and has been shown to rely on the amygdala for the memory of fear, with the additional requirement of the hippocampus for

contextual conditioning (Kim & Fanselow 1992; Maren & Fanselow 1996; Rogan & LeDoux 1996; Frankland *et al.* 1998). Contradictory results regarding the involvement of zif268 within the experimental paradigm of associating footshock with a tone or particular environment have been published. Malkani & Rosen (2000), and Hall *et al.* (2000) both report an increase in zif268 mRNA in area CA1 of the hippocampus following contextual fear conditioning in both controls and experimental groups, indicating that the result is not learning specific and merely due to novelty. In the amygdala however, Malkani & Rosen (2000) noted an increase of zif268 in the lateral nucleus of the amygdala specifically in response to learning. Hall *et al.* (2000) on the other hand, also noted a similar increase in the control group exposed to the training chamber relative to naïve controls. In addition, a retention test 24 hours after learning reportedly produced no change in zif268 levels in the CA1 or amygdala in the experiment by Malkani & Rosen (2000) but did produce an increase in these areas in the experiment by Hall *et al.* (2001). Therefore, with regard to contextual fear learning, one group state that zif268 is involved in learning, but not retrieval (Malkani & Rosen 2000), and the other concludes that zif268 is involved in retrieval, but not learning (Hall *et al.* 2000). However, the latter group noted zif268 may also be involved in retrieval in the nucleus accumbens and cingulate cortex (Thomas *et al.* 2002). Following on from their earlier work, Malkani & Rosen (2001) administered APV, an NMDA receptor antagonist known to block the acquisition of fear conditioning (Kim *et al.* 1991; Maren & Fanselow 1996; Lee & Kim 1998), and discovered that it also stopped the learning-induced increase in zif268 expression found by them in the lateral nucleus of the amygdala. Lee *et al.* (2004) reported that zif268 was not required for memory consolidation in hippocampus-dependent contextual fear conditioning, but essential for reconsolidation (whereby a recalled memory is reinforced to become permanent). Further studies are required to elucidate the exact role of zif268 in this particular mode of learning.

Zif268 is also activated in simpler forms of learning. *In vitro,* classical conditioning of the brainstem in turtles increases zif268 protein, which can be reversed with the application of APV, illustrating a dependency for NMDARs (Mokin & Keifer 2006).

1.1.15 The effects of zif268 gene targeted deletion

Topilko *et al.* (1997) generated mutant zif268 null mice by inserting the lacZ gene upstream of the initiation codon, with an additional frameshift mutation upstream of

the DNA binding domain, ensuring that zif268 was neither transcribed nor translated. The pups were born normally and capable of survival to adulthood, but both male and female mice homozygous for mutation had a reduced body size and were sterile. Analysis of tissues and organs revealed numerous deficits in the anterior pituitary and reproductive system.

Comparing zif268 -/- mutant mice to wildtype littermates after induction of LTP in the dentate gyrus displays a comparable potentiation for 50 – 60 minutes after tetanisation. However, measuring 24 and 48 hours after tetanus demonstrates that late LTP in the homozygous and heterozygous mutants decayed back to basal levels within 24 hours after induction. This demonstrates the necessity of activation of zif268 in the stabilisation of long-term LTP in the dentate gyrus (Jones *et al.* 2001).

Behavioural analysis performed on zif268 -/- mutant mice has shown a strong deficiency in long-term memory formation tested on a variety of behavioural tasks, including olfactory discrimination, novel object recognition, conditioned taste aversion and the Morris water maze. This effect was not exhibited during normal short-term retention evaluations, namely spatial behaviour in a T maze, object recognition and social transmission of food preference (Jones *et al.* 2001). These data show that the deficits encountered in zif268 knockout mice are not specific to a particular task, but to a general deficit in the consolidation of memories.

1.1.16 Downstream targets of zif268

The gene products of zif268 can act as nuclear transcription factors to regulate the transcription of target genes. Translation of both newly transcribed and pre-existing mRNAs occurs within hours of LTP induction and plays an important role in maintaining LTP. Up until 2005 and the publication by James *et al.* (2005), very few genes had been suggested as possible CNS targets for LTP-induced regulation by zif268.

Synapsin I and synapsin II gene transcription is activated by an increase in zif268 (Thiel *et al.* 1994; Petersohn *et al.* 1995). In particular, the gene encoding synapsin I is found to be upregulated in the dentate gyrus granule cells after LTP (Hicks *et al.* 1997). Synapsin is a protein of the exocytotic machinery, so this

regulation of a pre-synaptic protein downstream of zif268 activation suggests the propagation of plasticity through neural networks.

Tyrosine Hydroxylase (TH), the enzyme involved in the biosynthesis of the catecholamines, was recently shown to contain an Egr-1 motif in its promoter region (Papanikolaou & Sabban 1999). Transiently transfecting zif268 into PC-12 cells is sufficient to drive the proximal rat TH promoter as measured by the increased activity of the CAT reporter gene (Papanikolaou & Sabban 2000). Phenylethanolamine N-methyltransferase (PNMT) catalyses the conversion of noradrenaline to adrenaline and has two potential ERE sites. PNMT gene expression is enhanced when RS1 cells are transiently transfected with zif268 (Ebert *et al.* 1994) or administered with phorbol 12-myristate 13-acetate (PMA), which stimulates endogenous zif268 (Morita *et al.* 1995). However, PNMT has not been observed to change in models of learning behaviour. Other specific target genes of zif268 include adenosine deaminase (Ackerman *et al.* 1991), acetylcholine esterase (Li *et al.* 1993), the α-myosin heavy chain (Gupta *et al.* 1991) and the cdk5-regulator, p35 (Harada *et al.* 2001).

In 2005, James *et al.* published a microarray experiment that identified 153 differentially expressed known genes as neuronal targets of zif268, the vast majority of which were significantly downregulated. These included neurotransmitters and modulators, receptors, signalling genes, pre-synaptic elements and genes involved in synapse formation, the proteasome, the major histocompatability complex, the immune response, vesicle trafficking, the cytoskeleton, translation, chromaffin cell function and metabolic processes. Rigorous statistical analysis revealed that only 8 of these genes were likely to be false positives. A random selection of candidate genes was verified in two CNS plasticity models *in vitro* and *in vivo,* as representative authentication of the cell line results.

It seems that zif268 may be an activator or suppressor of transcription depending on the context in which the data is gathered. James *et al.* (2005) found that the pattern of altered gene expression was different in differing areas of the brain, namely the hippocampus and the striatum. In addition, TH was downregulated in the PC-12 cells, but has been reported as upregulated (Papanikolaou & Sabban 2000) and indeed downregulated in other reports (Maharjan *et al.* 2005). Also, PDGF-A is suppressed by zif268 in NIH3T3 cells, but enhanced in HEK293 cells

(Wang *et al.* 1999). Most strikingly, in a single cell type – prostate carcinoma cells – zif268 mediates increased transcription of CREB-binding protein (CBP) after one stimulus (serum) and reduced CBP transcription after another stimulus (UV) (Yu *et al.* 2004). The ability of zif268 to act as either a transcriptional activator or repressor may therefore depend on factors such as its phosphorylation state and interaction with other transcription factors.

Within the many known genes identified by the microarray experiment as downstream targets of zif268 were gephyrin and ubiquilin (James *et al.* 2005). Gephyrin displayed a negative fold change of 1.36 and ubiquilin showed a negative fold change of 1.57. These proteins are interesting as they have both been associated with the $GABA_AR$, an inhibitory ligand-gated chloride channel.

1.1.17 The $GABA_AR$

Whilst glutamate is the major excitatory neurotransmitter in the brain, gamma-aminobutyric acid (GABA) is the major inhibitory neurotransmitter. There are 3 GABA receptor subtypes: A, B and C. $GABA_A$ and $GABA_C$ are ionotropic receptors, allowing Cl^- ions to enter the cell, resulting in hyperpolarisation and a reduction in cell excitability. On the other hand, $GABA_B$ is a metabotropic-type receptor, allowing K^+ to enter and reducing presynaptic levels of Ca^{2+} after activation of the associated G-protein.

$GABA_ARs$ are ligand gated inhibitory receptors that are distributed throughout the CNS. They are arranged in a pentameric stoichiometry with subunits recruited from a range of 21 (currently known) different subunits (α_{1-6}, β_{1-4}, γ_{1-4}, δ, ε, π, θ and ρ_{1-3}) (Bonnert *et al.* 1999; Whiting 1999; Burt 2003). The $\alpha1\beta2/3\gamma2$ combination is the predominantly expressed receptor isoform (Fritschy & Mohler 1995) and $2\alpha:2\beta:1\gamma$ is the most likely ratio (Chang *et al.* 1996; Tretter *et al.* 1997; Farrar *et al.* 1999). Gephyrin and the $\gamma2$ subunit are required for the clustering of $GABA_ARs$ at postsynaptic sites (Essrich *et al.* 1998), gephyrin may bind to the $\beta3$ subunit (Kirsch *et al.* 1995), and can be co-localised with the $\alpha1$, $\alpha2$, $\alpha3$, $\beta3$ and $\gamma2$ subunits in rat brain and dissociated cultures (Sassoe-Pognetto *et al.* 2000; Danglot *et al.* 2003). Ubiquilin binds to the $\alpha1$, $\alpha2$, $\alpha3$, $\alpha6$, $\beta1$, $\beta2$ and $\beta3$ subunits of the $GABA_AR$ (Bedford *et al.* 2001).

Synaptically localised $GABA_A$Rs allow phasic GABA-mediated transmission, which is produced by 0.3mM GABA within the synaptic cleft for less than 1 millisecond (Mody *et al.* 1994; Cherubini & Conti 2001; Nusser *et al.* 2001). Once activated, $GABA_A$Rs produce inhibitory postsynaptic potentials (IPSPs), the magnitude of which is determined by the number, and properties, of the receptors present, and the concentration and duration of GABA release. In addition to phasic activation is tonic neurotransmission, produced by continuous activation of extrasynaptic receptors by micro-molar GABA levels, spilt from the synaptic cleft and always present in the extracellular space (Scanziani 2000; Semyanov *et al*. 2004; Mody & Pearce 2004). Tonic inhibition may play a crucial role in regulating neuronal excitability by setting the threshold for action potential generation (Petrini *et al.* 2004).

1.1.18 Gephyrin

Gephyrin is widely expressed throughout the mammalian CNS (Prior *et al.* 1992; Kirsch *et al.* 1993), binds to polymerised tubulin (Kirsch *et al.* 1991), and is co-purified with the inhibitory glycine receptor (Langosch *et al.* 1992). Its association with microtubules may aid the development of a subsynaptic lattice, or scaffold, below the plasma membrane anchoring receptors at the cytoplasmic face of the cell membrane, by binding directly, or possibly indirectly, to the cytoplasmic loops of receptor subunits (Kneussel *et al.* 1999b; Meier *et al.* 2001). The synaptic anchoring of inhibitory receptors was established by antisense oligonucleotide depletion (Kirsch *et al*. 1993; Essrich *et al.* 1998), and gene knockout in mice (Feng *et al.* 1998; Kneussel *et al.* 1999a), which prevented the localisation of GlyRs and $GABA_A$Rs to the synapse. The role of gephyrin in GlyR clustering will be dealt with in more depth in chapter 4.

1.1.19 Gephyrin and the Cytoskeleton

The postsynaptic density (PSD) lines the cytoplasmic face of the cell membrane and comprises microtubules, neurofilaments and their associated proteins. At the PSD of inhibitory synapses, gephyrin interacts with components of the cytoskeleton, and is thought to connect the cytoplasmic domain of glycine receptor and $GABA_A$R polypeptides to 2 cytoskeletal systems, the microtubules (tubulin) and microfilaments (actin; via profilin).

An intact microtubular cytoskeleton seems to be essential for the stabilisation of postsynaptic gephyrin clusters. Gephyrin clusters are enriched with G-actin (actin monomers) but there is no direct association between the two (Giesemann *et al.* 2003), and gephyrin puncta are aligned with filamentous actin (F-actin) in dendrites, and are localised to inhibitory synapses (Bausen *et al.* 2006). Mena (mammalian enabled)/VASP (vasodilator-stimulated phosphoprotein), the f-actin uncapping protein (Bear *et al.* 2002), directly interacts with G-actin (Walders-Harbeck *et al.* 2002) and profilin (Reinhard *et al.* 1992; Reinhard *et al.* 1995; Gertler *et al.* 1996), an actin monomer binding protein that stimulates actin polymerization by increasing ADP/ATP exchange (Sohn & Goldschmidt-Clermont 1994). Therefore, Mena/VASP can recruit profilin/actin monomer complexes to actin filaments in order to allow further filament generation (Huttelmaier *et al.* 1999; Bear *et al.* 2002). Actin microfilaments are thought to control the inhibitory receptor density at postsynaptic sites. Mena/VASP was found to precipitate and co-localise with gephyrin (Giesemann *et al.* 2003), and gephyrin also binds with profilin (Mammoto *et al.* 1998). Both gephyrin and profilin colocalise and physically interact at inhibitory synapses in cultured neuronal cells and spinal cord sections (Giesemann *et al.* 2003). Cultured spinal cord neurones treated with cytochalasin D (a drug that severs the actin cytoskeleton) show a reduction in postsynaptic gephyrin cluster size with an increase in packing density, whilst demecolcine (which disrupts microtubules) decreases the density of postsynaptic gephyrin clusters, increasing the cluster size (Kirsch & Betz 1995). In addition, the lateral mobility of the inhibitory GlyR is restricted at postsynaptic sites by an interaction with the microtubules, and demecolcine decreases GlyR immunoreactivity apposed to presynaptic terminals (Kirsch & Betz 1995). However, depolymerisation of microtubules has no effect on the distribution pattern of $GABA_A$Rs; they remain intact and maintain a synaptic localisation in mature hippocampal cultures (Allison *et al.* 2000), suggesting that some mechanism other than microtubules is required to anchor gephyrin and $GABA_A$R at inhibitory synapses after synaptogenesis. In addition, in HEK293 cells, intracellular gephyrin clusters do not appear to interact with, or depend on, actin filaments (Bausen *et al.* 2006).

Gephyrin binds to dynein light chain-1 and –2 (Dlc-1 and –2) as determined by yeast dihybrid screening and biochemical assays. Dlc-1 and –2 are components of microtubule motor proteins, and seem to interact with gephyrin whilst co-localised at some inhibitory synapses, possibly suggesting a role in retrograde

gephyrin transport (Fuhrmann *et al.* 2002). The subcellular localisation of gephyrin at the synapse may therefore depend on motor proteins. In addition, disrupting microtubules with nocodazole or dynamitin, a dynein transport inhibitor, interferes with gephyrin's transport by dynein intermediate and heavy chains (Maas *et al.* 2006).

The Rho family small G proteins regulate various actin cytoskeleton-dependent cell functions including cell shape change, cell motility and cytokinesis. Collybistin (from Greek κολλυβιστομι: to exchange) is predominantly a brain specific GEF for small GTPases of the Rho/Rac-family thought to constitute an essential component of the signalling machinery that directs gephyrin to the developing postsynaptic membrane (Kins *et al.* 2000). The splice variants I and II were detected as binding partners of the C-terminal domain of gephyrin by yeast dihybrid screening of newborn rat brain. Collybistin I was redistributed to gephyrin-rich cytoplasmic aggregates when co-transfected into HEK293 cells. Collybistin II was able to induce submembrane gephyrin microaggregates, which recruited β subunit containing GlyRs (Kins et al. 2000). In addition, a mutation in exon 2 of the human collybistin gene results in hyperekplexia and epilepsy, possibly due to the misdirected localisation of gephyrin and associated GlyR and $GABA_A$Rs. Therefore, collybistin could be a key protein for the postsynaptic localisation of gephyrin (Harvey *et al.* 2004).

1.1.20 Gephyrin and GABARAP

$GABA_A$R-associated protein (GABARAP) has a tubulin-binding motif (Wang *et al.* 1999; Wang & Olsen 2000), and colocalises with $GABA_A$R in cultured cortical neurones (Wang *et al.* 1999), specifically binding its N-terminal domain to the $GABA_A$R γ2 subunit. In addition GABARAP binds to gephyrin; however, in cultured neurones of gephyrin deficient mice, no difference is seen in GABARAP puncta localisations compared to wildtypes (Kneussel *et al.* 2000). GABARAP is not localised at inhibitory postsynaptic sites but is found in intracellular compartments, particularly concentrated at the ends of the Golgi stacks where transport vesicles bud and fuse (Kittler *et al.* 2001). Therefore, it could interact with $GABA_A$R subunits, and gephyrin before they reach the synapse and ultimately play a role in receptor trafficking. In addition, binding of the GABARAP C-terminus to tubulin, and the N-terminus to $GABA_A$R, suggests a role in linking the receptor to the microtubules, presumably to deliver it to the plasma membrane. Further

evidence has shown that overexpression of GABARAP in hippocampal neurones increases $GABA_A$Rs at the cell surface (Leil *et al.* 2004). However, GABARAP knockout mice show no differences in the number or synaptic distribution of $GABA_A$Rs containing γ2 subunits at gephyrin positive postsynaptic sites compared to wildtypes, suggesting that it may not be essential for trafficking or synaptic localisation after all (O'Sullivan *et al.* 2005).

1.1.21 Gephyrin and the $GABA_A$ Receptor

Gephyrin was originally linked to glycine receptors alone, however, it is found in brain regions known to contain little or no evidence of glycinergic synapses (Malosio *et al.* 1991; Kirsch *et al.* 1993). Gephyrin immunoreactivity can be found in GABAergic synapses in cultured hippocampal (Craig *et al.* 1996), and cortical neurones (Essrich *et al*. 1998), as well as in areas such as the retina, olfactory bulb and spinal cord (Todd *et al.* 1996; Sassoe-Pognetto & Wassle 1997; Giustetto *et al.* 1998). All presently available data, including gene depletion and knockout experiments, strongly indicates that gephyrin is associated with and essential for clustering of not only glycine receptors but specific $GABA_A$R subtypes (Essrich *et al.* 1998; Betz 1998; Feng *et al.* 1998; Kneussel *et al.* 1999a). However, biochemical evidence for a direct association of $GABA_A$Rs subunits and gephyrin has not been demonstrated (Meyer *et al.* 1995), leading to the notion of a hypothesised linker protein that mediates the association of gephyrin with $GABA_A$Rs. Gephyrin is concentrated in the postsynaptic membrane at many inhibitory synapses, and is proposed to mediate clustering and/or synaptic anchoring of $GABA_A$R through indirect binding to the β3 subunit (Kirsch *et al.* 1995). It has also been shown that gephyrin is essential for the postsynaptic clustering of $GABA_A$Rs containing α1 or α2 and γ2 subunits (Essrich *et al.* 1998; Kneussel *et al.* 1999a; Kneussel *et al.* 2001; Levi *et al.* 2004).

There is evidence that infers some interdependence for the synaptic localisation of gephyrin and specific subtypes of the $GABA_A$R. Gephyrin antisense oligonucleotide treatment of cultured cortical and cultured hippocampal neurones displays a reduction in punctate synaptic staining for $GABA_A$R α2 and γ2 subunits. In addition, the generation of mice with a targeted loss of the $GABA_A$R γ2 subunit resulted in a loss of postsynaptic gephyrin and $GABA_A$R clusters (Essrich *et al.* 1998; Schweizer *et al.* 2003). This can be reversed by the transgenic overexpression of the γ3 subunit (Baer *et al.* 1999), presumably due to similar

regions within the subunit sequences. Danglot *et al.* (2003) observed a decrease in the number of gephyrin clusters that did not contain $GABA_AR$ $\gamma2$ subunits during maturation in hippocampal neurones. Gephyrin deficient mice also display a total loss of postsynaptic clusters of $GABA_AR$ $\gamma2$ and $\alpha2$ subunits in cultured hippocampal neurones (Kneussel *et al*. 1999a), providing further evidence that suggests these subunits are essential for clustering. However, Levi *et al.* (2004) utilised gephyrin -/- mice to assess the GABAergic phenotype of cultured hippocampal neurones and observed surface synaptic clusters of $\alpha1$, $\alpha2$ and $\gamma2$ subunits in gephyrin deficient neurones. In spinal cord, $GABA_AR$ $\alpha3$, $\beta2/3$, $\gamma2$ subunit receptor clustering has been described, in an impaired manner, in gephyrin knockout mice (Kneussel *et al.* 2001) suggesting that this clustering might be independent of gephyrin. It is likely that there are probably gephyrin-dependent and -independent mechanisms for $GABA_AR$ clustering.

Surface labelling by immunohistochemistry of gephyrin knockout mice indicates that gephyrin contributes in part to clustering, but not surface insertion or stabilisation, of $GABA_AR$ $\alpha2$ and $\gamma2$ subunits (Levi *et al.* 2004). Danglot *et al.* (2003) argue that gephyrin is more involved in synaptic stabilisation rather than cluster formation; they found that $GABA_AR$ $\gamma2$ subunit clusters were observed in all hippocampal neurones before 10DIV, even when gephyrin clusters were only detected in a few neurones.

The gephyrin gene is highly mosaic (Prior *et al.* 1992) increasing the likelihood of splice variant generation which may go some way to explain the receptor selectivity on postsynaptic gephyrin.

1.1.22 $GABA_A$ receptor trafficking

Receptor ion channels, specialised for chemotransmission between neurones, are highly concentrated at postsynaptic densities apposed to the appropriate presynaptic nerve terminals. $GABA_AR$ density and localisation at the postsynaptic cell membrane determines neuronal excitability and can be affected by many factors, including neuronal activity. The trafficking of receptors at inhibitory synaptic sites is an important feature of neuronal plasticity. During periods of neuronal plasticity and development, the numbers of $GABA_ARs$ is subject to large alterations (Fritschy & Brunig 2003). Insulin can increase the number of $GABA_AR$ at the cell surface, whilst brain derived neurotrophic factor (BDNF) decreases the

synaptic number (Wan *et al.* 1997; Brunig *et al.* 2001). $GABA_A$Rs are subject to continuous turnover: quick recovery and reinsertion of $GABA_A$Rs that have been endocytosed or have been synthesised *de novo* and stored intracellularly allows the rapid adaptation of neural excitability (Luscher & Keller 2001). Figure 1.3 displays a simplified diagram of $GABA_A$R trafficking and targeting at the synapse.

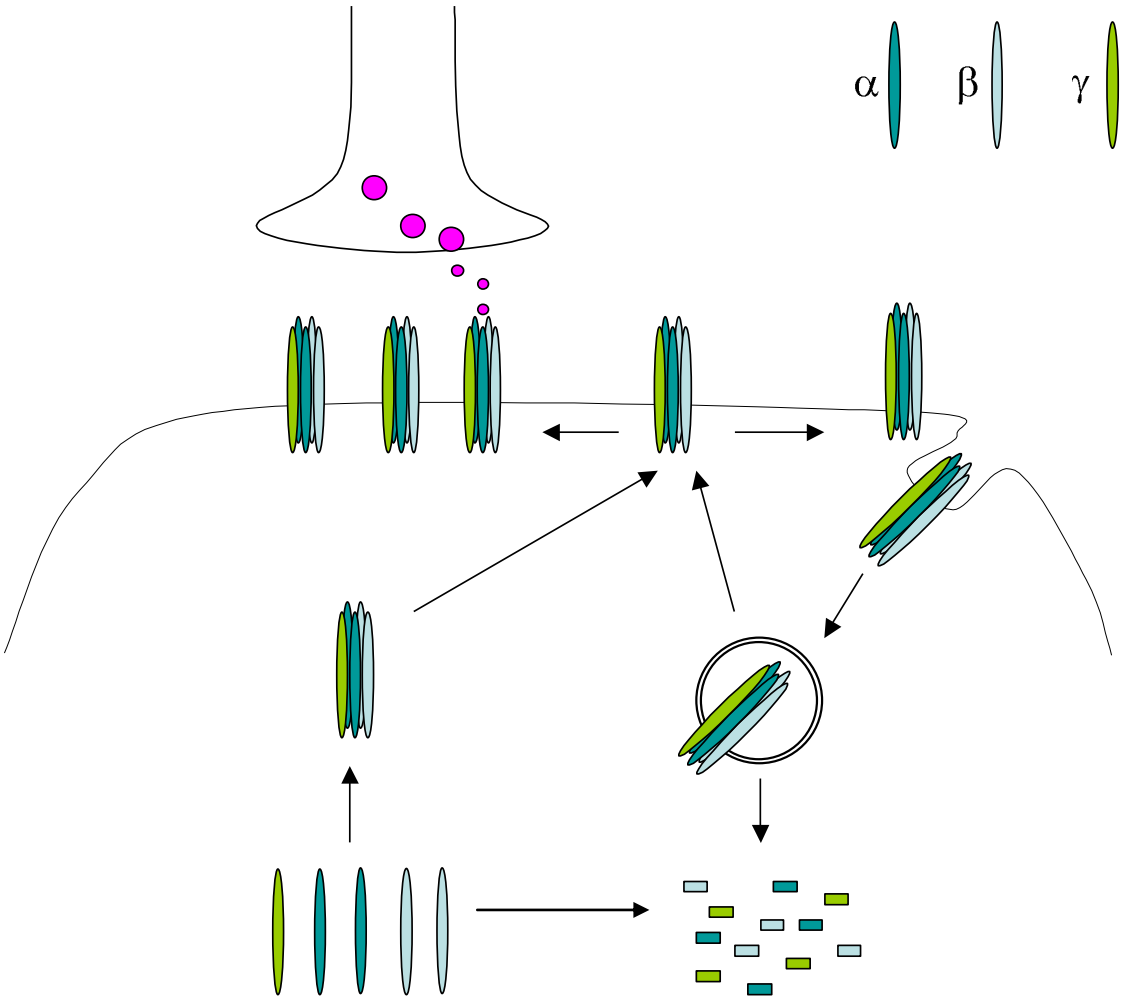

Figure 1.3: A simplified diagram of $GABA_A$ receptor trafficking and targeting at the synapse. Subunits of the $GABA_A$ receptor are synthesised in the endoplasmic reticulum and assembled into heteropentameric structures, predominantly from α, β and γ subunits, most likely with the ratio of 2α:2β:1γ. Assembled receptors are then targeted by the Golgi apparatus to the plasma membrane, whilst unassembled subunits are degraded. Receptors at the cell surface are localised to the synapse, or are targeted to clathrin coated pits and removed from the membrane by endocytosis. Receptors within the endosomes can be either recycled to the cell surface or degraded by the proteasome. Diagram adapted from Barnes (2000).

$GABA_A$R assembly occurs in the endoplasmic reticulum (ER), and an investigation within HEK293 cells revealed that receptors require the α1 and β2 subunits for ER exit and cell surface expression, with the aid of chaperone proteins (Connolly *et al.* 1996b). The β subunit can also determine the route to the surface (Connolly *et al.* 1996a). In cerebellar granule cells, the γ2 subunit confers synaptic localisation,

whilst the δ subunit targets extrasynaptic sites (Jones *et al.* 1997; Brickley *et al.* 1999; Sassoe-Pognetto *et al.* 2000). It is suggested that synaptic targeting of $GABA_AR$ relies on gephyrin as well (Essrich *et al*. 1998). Some of the subunits also undergo alternate splicing, generating additional heterogeneity (Burt & Kamatchi 1991). For instance, the short γ2 subunit (γ2S) is able to reach the plasma membrane when expressed alone, but the long form (γ2L), which differs by 8 amino acids, remains in the ER (Connolly *et al.* 1999a). Either splice variant, when expressed with α1 and β2, is necessary for receptor endocytosis (Connolly *et al.* 1999b).

Once a $GABA_AR$ has reached the synaptic membrane, and remained for the requisite amount of time, the receptor may be mono-ubiquitinated, and those composed of α/β or α/β/γ subunits are recruited to clathrin coated pits and internalised by dynamin dependent constitutive endocytosis (Chapell *et al.* 1998; Connolly *et al.* 1999a; Connolly *et al.* 1999b; Ghansah & Weiss 2001; van Rijnsoever *et al.* 2005). The β and γ $GABA_AR$ subunits interact with the α and β adaptins; components of the AP2 complex that recruits proteins into the clathrin pits (Marsh & McMahon 1999; Kittler *et al.* 2000). Once internalised, $GABA_AR$ are located to a subsynaptic intracellular pool that stains positively for gephyrin (van Rijnsoever *et al.* 2005). Approximately 70% of receptors are then recycled to the cell surface, and the remainder are degraded (Connolly *et al.* 1999b; Kittler *et al.* 2004), a fate that may be decided by ubiquilin (Bedford *et al.* 2001). The constant cycling of receptors between the cell membrane and internal structures has been shown by blocking endocytosis; after 20 to 40 minutes the mIPSC amplitude increases by 50-100% (Kittler *et al.* 2000), and the formation of intracellular receptor clusters is impaired (van Rijnsoever *et al.* 2005). In addition, blocking the interaction between the AP2 complex and the β $GABA_AR$ subunit confers an increased cellular response to the application of GABA (Herring *et al.* 2003).

In addition to impaired receptor localisation in gephyrin knockout mice compared to wildtype, an increased accumulation of intracellular $GABA_AR$ immunoreactive microclusters is observed, suggesting an enhanced receptor internalisation in the absence of gephyrin, and hence a defect in intracellular trafficking (Kneussel *et al*. 1999a).

1.1.23 The ubiquitin-proteasome pathway

Ubiquitin is a small 76 amino acid protein that exists in cells singly or covalently conjugated to other proteins. It may act as a sorting signal in early endosomes to target receptors and proteins for degradation by the lysosomal and proteasomal pathways.

The ubiquitin proteasome system is the major non-lysosomal pathway in eukaryotes for cellular protein degradation. A poly-ubiquitin chain formed from ubiquitin monomers is covalently attached to proteins targeted for destruction. The ubiquitylation process involves E1 (Ub-activating enzyme), E2 (Ub-conjugating enzyme), and E3 (Ub-ligase) enzymes (Hershko & Ciechanover 1998; Voges *et al.* 1999; Glickman & Ciechanover 2002). Ubiquitin is ATP-dependently activated by E1 forming a thioester bond between a cysteine residue and ubiquitin's C-terminal. Ubiquitin is then conjugated to E2 which binds to E3 with the target protein. Ubiquitin is attached from its c-terminus glycine to the protein, or previous ubiquitin, through the ε-amino group of a lysine residue (most commonly K48 of ubiquitin if creating a chain). Proteins can also be ubiquitylated on the α-amino group of the N-terminal residue (Glickman & Ciechanover 2002). E2 and E3 then lengthen the ubiquitin chain, sometimes with the help of E4, an accessory factor (Koegl *et al.* 1999). These multi-ubiquitin tagged substrates are recognised and delivered to the 2.5 MDa proteasome holoenzyme, the 26S proteasome.

The ubiquitin-26S proteasome degrades target proteins ATP-dependently into short polypeptides and recycled ubiquitin. It is comprised of a 20S core chamber with a 19S regulatory cap, which can assemble at each end. Poly-ubiquitylated proteins are first recognised by an interaction with the 19S regulatory complex, which then appears to unfold them and guide them through the 20S catalytic core for degradation (Glickman & Ciechanover 2002).

The 19S regulatory particle is comprised of approximately 18 subunits, and forms two structures, a lid and a base. Within the base are six homologous ATPases (Rpt1-6) which are probably responsible for protein unfolding and guidance through 20S, via a gated channel (Groll *et al.* 1997; Braun *et al.* 1999; Horwich *et al.* 1999). The base also contains three non-ATPases, Rpn1/S2, Rpn2/S1 and Rpn10/S5a (where nomenclature is yeast/human). Rpn10 serves to stabilise the

lid and base, and is the only known subunit that binds tightly to poly-ubiquitin chains, but not mono-ubiquitin (Deveraux *et al.* 1995; Takeuchi *et al.* 1999; Wilkinson *et al.* 2000). However, Rpn1 and 2 may be additional polyubiquitin or UBL binding sites (Davy *et al.* 2001; Saeki *et al.* 2002). The lid seems to be important for effective ubiquitinated protein degradation, although its purpose is unclear (Glickman *et al.* 1998), and consists of a further eight non-ATPases, Rpn3, -5, -6, -7, -8, -9, -11 and -12.

The 20S core particle comprises two structural α protein rings, which surround two catalytic β protein rings. The α subunits interact with the ATPases found in the 19S base, effectively attaching the two 26S particles together (Davy *et al.* 2001; Fu *et al.* 2001). The β subunits contain the proteolytic active sites with each β ring containing a post-glutamyl site, a tryptic site and importantly, a chymotryptic site. The chymotryptic site plays a key role as blocking the catalytic activity of this protein can block all of the proteasomal activity (Kisselev *et al.* 1999).

The multiple conjugating enzymes regulate the number of ubiquitin molecules conjugated to a target protein (Ciechanover & Schwartz 1998) however; at least 4 isopeptide-bonded ubiquitins are needed for recognition by 26S (Thrower *et al.* 2000). Additional cellular regulation can be exerted by the removal of ubiquitins by deconjugating proteins (D'Andrea & Pellman 1998). Conjugation of less than 4 isopeptide-bonded ubiquitins can be referred to as mono-ubiquitination, which is a reversible post-translational modification that may play a role in receptor endocytosis at the plasma membrane (Hicke & Dunn 2003).

Many, but not all of the known functions of ubiquitin conjugation involve the targeted degradation of the modified protein, which in turn can control many processes like cell cycle progression, development and apoptosis. Covalently attached ubiquitin to proteins can also be used as a post-translational modification that can be identified by downstream protein receptors/interactors in non-degradation cellular processes, for example, DNA repair, transcription, signal transduction and sorting of receptors (Hershko & Ciechanover 1998).

There is also a non-ubiquitin proteasomal pathway that will not be dealt with in this thesis.

1.1.24 Ubiquilin is an Ubiquitin-like protein

A highly conserved feature between ubiquilin and its homologous proteins (dealt with in more detail in chapter 5) is the inclusion of the ubiquitin-like (UBL) domain at the N-terminal and ubiquitin-associated (UBA) domain positioned at the C-terminal. Both the UBA and UBL domains have been implicated in the targeting and degradation of proteins by the ubiquitin-proteasome pathways.

UBA domains are commonly occurring sequence motifs, present in one or two copies in some members of the ubiquitination pathway including ubiquitin conjugating enzymes, ubiquitin-carrier proteins and ubiquitin carboxy-terminal hydrolases. They are also present in UV excision repair proteins, DNA repair enzymes, signal transduction proteins and certain protein kinases (Hofmann & Bucher 1996). Fifteen of the 40 core residues within the domain are highly conserved, suggesting they are critical in determining the overall structure (Hershko & Ciechanover 1998). In ubiquilin, the UBA domain serves to bind poly ubiquitin chains *in vitro* suggesting that it blocks ubiquitin chain elongation *in vivo* (Massey *et al.* 2004).

UBL proteins are designated either Type 1 or Type 2. Type 1 UBL proteins can be covalently linked to target proteins in the same way as ubiquitin and may be implicated in post-transcriptional modifications. Type 2 UBL proteins are not ligated to other proteins, and are not fully understood (Hershko & Ciechanover 1998). However, they may be involved in ubiquitin dependent proteolysis due to interactions with the proteasome (see below). Ubiquilin is a type 2 UBL protein (Ko *et al.* 2002).

1.1.25 Ubiquilin and the proteasome pathway

There is much speculation that ubiquilin is involved in the ubiquitin-proteasome pathway. Kleijnen *et al.* (2000) were the first to show direct evidence that ubiquilin associates with both proteasomes and ubiquitin ligases in large complexes. Ubiquilin was found to complex with E6AP, a human E3 ligase, and the 20S catalytic core of the proteasome. This interaction with the proteasome was via the UBL domain of ubiquilin. In addition, overexpression of ubiquilin increased the protein levels of p53, a substrate of E6AP, and IκBα, a substrate of another E3

type ligase, βTRCP. Ubiquilin overexpression had no effect on ubiquitin-independent proteasome substrates however.

Ko *et al.* (2004) demonstrated that the UBA of ubiquilin interacts with poly-ubiquitin chains as overexpression of ubiquilin led to increased accumulation of large poly-ubiquitin chains, compared to a mutant lacking a C-terminus. They also found that the N-terminus UBL interacted with the 19S subunits Rpn3, Rpn10a and Rpn10e, but not Rpn1 or -2. Dsk2 (a yeast homologue of ubiquilin) also binds to polyubiquitylated substrates through the UBA domain of the C-terminus, and to subunits of the 19S and 20S particles of the proteasome through the N-terminus (Funakoshi *et al.* 2002).

1.1.26 Ubiquilin, the Proteasome and $GABA_A$Rs

Ubiquitination of neural surface receptors is generally regarded as a cellular signal for endocytosis of these proteins, allowing for rapid downregulation of receptors at the plasma membrane. Altering the number of $GABA_A$Rs present at postsynaptic sites would effectively alter the response to GABA. Therefore, constant receptor insertion into the plasma membrane would maintain the overall cell surface receptor number. Dynamin dependent constitutive endocytic removal of $GABA_A$Rs at synapses via clathrin coated pits requires the γ2 subunit of $GABA_A$RS and the linker protein AP2 (Connolly *et al.* 1999a; Kittler *et al*. 2000). However, membrane trafficking to replenish the synapse with either recycled or newly synthesised receptors at the membrane is poorly understood, and in the case of $GABA_A$Rs it is unknown whether ubiquitination is a necessary requirement.

Bedford *et al.* (2001) used a series of experiments to isolate ubiquilin, a novel binding partner of the majority of $GABA_A$R α and β subunits, the most commonly expressed $GABA_A$R subunits in the CNS. They located ubiquilin to intracellular compartments including the golgi apparatus and clathrin-coated pits. Utilising ELISA, they monitored the effect of introducing a synthetic peptide, which would compete for ubiquilin binding with the $GABA_A$Rs. This decreased the number of receptors at the cell surface without effecting receptor internalisation. Conversely, overexpression of ubiquilin dramatically increased the number of receptors located on the cell surface. The same effect was witnessed after treatment with a proteasome inhibitor in A293 cells expressing either α1 or β3 subunits. Ubiquilin therefore could enable insertion of $GABA_A$Rs into the synaptic membrane and

increase the half-life of receptor subunits. These findings could implicate the ubiquitin proteasome pathway as a modulator of synaptic function and plasticity.

1.1.27 Long Term Potentiation and the Proteasome

In different brain regions, the subunit composition of the proteasome varies (Noda *et al.* 2000; Ding & Keller 2001) with the pyramidal neurones of the cerebral cortex and hippocampus showing the highest proteasome levels (Mengual *et al.* 1996). In hippocampal neurones, proteins of the proteasome complex are localised in the dendrites near synapses, whilst displaying a higher density in the soma (Ehlers 2003; Rezvani *et al.* 2003; Bingol & Schuman 2006) which, circumstantially, implicates the proteasome in synaptic signalling. Indeed, an emerging concept is that the regulated degradation of proteins by the ubiquitin proteasome pathway is an important modulator of synaptic function and plasticity. However, the precise role of the proteasome in synaptic plasticity requires elucidation as published reports point to both a facilitatory and suppressive function.

In the ubiquitin-dependent proteasome pathway, once a target protein has been ubiquitinated, it is delivered to the proteasome. However, recent evidence has shown an interaction of proteasomes with proteins physically proximal to degradation targets, suggesting that the proteasome moves towards the target protein (Glickman & Raveh 2005). A persistent redistribution of proteasomes from dendritic shafts to functionally active spines, minutes after synaptic stimulation by KCl, has been observed (Bingol & Schuman 2006). APV blocked KCl-induced movements of 19S and 20S, indicating that NMDAR activation is required. NMDA perfusion into a localised site revealed a spatially restricted increase in proteasomal activity, which led to an increase in protein degradation. The long-lasting effects suggest the involvement of the actin cytoskeleton, which was found to be associated with 50% of the proteasomes in dendrites. In addition, proteasomes have been reported to associate with the cytoplasmic tails of receptor complexes (Ferrell *et al.* 2000), suggesting a capacity for rapid remodelling of membrane-associated receptor complexes and for local and persistent remodelling of spines through on-site coordinated synthesis and degradation of proteins (Burbea *et al.* 2002; Ehlers 2003; Colledge *et al.* 2003; Juo & Kaplan 2004; Yi & Ehlers 2005).

The late phase of most, if not all, forms of synaptic plasticity is dependent on enhanced protein synthesis (Morris 2004), and complementary to this, protein degradation has emerged as a mechanism to control synaptic protein composition (Colledge *et al.* 2003). Proteasome inhibitors lead to deficits in LTP and attenuate learning and memory (Jiang *et al.* 1998; Chain *et al.* 1999; Foley *et al.* 2000), whereas compromised proteasome function has been linked to aging and memory impairment in humans (Keller *et al.* 2000). Karpova *et al*. (2006) found that the use of Cbz-leu-leu-leucinal (MG132), a cell permeable peptide aldehyde proteasome inhibitor, blocked late phase LTP by reducing the magnitude of fEPSP slope potentiation, suggesting that late LTP specifically depends on proteasome activity. In addition, induction of LTP dramatically accelerates the degradation of proteins in the presence of anisomycin, which blocks translational activity, compared to a non-LTP control. This effect was reduced in the presence of MG132. Using time-lapse imaging, Karpova *et al*. (2006) were able to show that proteasome mediated protein degradation was induced very quickly after tetanization of the Schaffer collateral CA1 synapses, consistent with the idea that fast proteasome-mediated degradation of scaffolding proteins occurs soon after tetanization. In cultured hippocampal neurones, internalisation of the glutamate receptors GluR1 and GluR2, induced by AMPA, requires protein degradation via the proteasome system (Colledge *et al.* 2003; Patrick *et al.* 2003). The proteasome system effects PKA and MAPK-dependent signalling pathways in the sensory neurone synapses of *Aplysia* (Chain *et al.* 1999).

In contrast to the above evidence, published reports have shown that inhibition of proteasome activity facilitates various forms of plasticity; it augments neurite outgrowth, increases presynaptic neurotransmitter release and enhances postsynaptic glutamate receptor sensitivity, (Obin *et al.* 1999; Speese *et al.* 2003; Zhao *et al.* 2003) suggesting that the proteasome suppresses plasticity. There seems to be no explanation for this discrepancy at present.

1.1.28 Regulation of the neuronal proteasome by zif268

The link between the proteasome and LTP has recently been strengthened further by the finding that zif268 regulates some component genes of the neuronal proteasome. James *et al.* (2006) monitored proteasome activity in zif268 transfected PC-12 cells, and found a significant decrease over time when compared to cells transfected with an N-terminal deletion mutant of zif268 as a

control. The truncated (control) form of zif268 is efficiently translocated to the nucleus, but does not bind to the Egr DNA recognition site. The zif268 mutant displays an inhibitory effect on wildtype zif268-dependent gene transcription through an unknown mechanism (Gosslar *et al.* 1999).

James *et al.* (2006) also found that proteasome activity was significantly elevated in zif268 knockout mice compared to control mice. In particular they investigated psmb9, an inducible proteolytic β subunit of the 20S core and psme2, an interferon-induced subunit of the 19S regulator; transcriptional expression of which increases proteasome activity in the immunoproteasome (Harris *et al.* 2001; Cascio *et al.* 2002). In addition, they also looked at SGK, a proteasomal kinase that protects synaptic glutamate receptors from proteasomal degradation (Boehmer *et al.* 2003; Boehmer *et al.* 2004; Schniepp *et al.* 2004), and Tap1, a subunit of the proteasome-associated antigen peptide transporter (Tap) complex, whose targeted deletion contributes to deficits in synaptic plasticity in mice (Huh *et al.* 2000). In a series of experiments, they determined that mRNA levels of all 4 genes were downregulated in PC-12 cells after transfection of zif268, and overexpressed in zif268 knockout mice when compared to wildtype controls. In addition they found that the promoter activities of psmb9, Tap1 and SGK were suppressed in zif268 transfected PC-12 cells, and that all 3 genes were affected in an *in vivo* model of synaptic plasticity: dopamine antagonist-induced plasticity in the striatum via haloperidol administration. Interestingly, it was discovered that striatal zif268 induction was associated with downregulated psmb9 and Tap1 but upregulated SGK.

These findings are the first to uncover the important role of zif268 in regulating the neuroproteasome and open an exciting and novel area of research.

1.2 Study Aims & Objectives

The main aims of this study were as follows:

- To upregulate zif268 in physiologically relevant conditions in order to investigate the induction of genes in response to cellular activation.

- To extend the findings of James *et al.* (2005) and verify two of the known genes identified as downstream targets of zif268: gephyrin and ubiquilin.

- To data mine the ESTs identified in the microarray experiment performed by James *et al.* (2005) to highlight areas of interest within the genome that have not yet been fully characterised.

- To perform any necessary experimentation required to confirm suspected unknown transcripts that may to be regulated by zif268.

- To theorise the downstream effects of LTP within the whole cell by monitoring the cellular actions of zif268 targets at synapses that are not activated by tetanically-induced glutamate.

Chapter 2

Materials and Methods

2.1 Bioinformatics

A selection of putative zif268 target EST (expressed sequence tag) genes were characterised using various bioinformatic tools. In order to do this, EST nucleotide sequences were retrieved using the National Center for Biotechnology Information database (NCBI, Bethesda, MD, USA; http://www.ncbi.nlm.nih.gov/), and similarity searches of the sequences with the R*attus norvegicus* genome were carried out using BLAST (Basic Local Alignment Tool) at Ensembl (www.ensembl.org). A 3-phase approach was used to catalogue and annotate these cDNA fragments. Firstly, a search was performed for any known gene located at the same chromosomal point. Any EST not in the vicinity of an Ensembl known annotated gene, but within approximately 4kb to an Ensembl predicted or genscan gene (Burge & Karlin 1997) and/or several other ESTs was put forward for further investigation. In the second phase, the relationship(s) of the gene predictions were examined using the orthologous sequences. If a gene prediction had been derived from hypothetical data, and not from any known genes of any organism, it suggested that any findings in this area would be novel. Thirdly, any area that was related to mental retardation in the comparable chromosomal area in *Homo sapiens* was of particular interest. This approach gleaned 4 ESTs for further experimental study (using the PC-12 cell line and verifying in primary cortical neurones): AA998964, AI169020, AI112362 and AI176839.

2.2 Cell Culture Preparation

2.2.1 Primary dissociated cortical cell cultures

All cell culture reagents were purchased from Invitrogen PLC, Paisley, UK unless otherwise stated. Pregnant Wistar rats (300-400 g, gestation day 17-18 (E17-E18)) were euthanized with an intraperitoneal injection of sodium pentobarbitone (Euthatal, Vericore Ltd., Dundee, UK) (1300 mg/kg). Embryos were removed by Caesarean section; decapitated and placed in ice-cold Minimum Essential Media (MEM) supplemented with 5 μg/mL penicillin-streptomycin. Brains were separated from the crania and the cortex removed, minced and washed three times in ice-cold MEM. Thereafter, the cortical tissue was dissociated in 5 mLs of a 2.5% trypsin solution for 30 minutes at 37^{o}C (in a 5% CO_2 incubator). The trypsin was inactivated by the addition of 5 mls foetal bovine serum (FBS), and the tissue washed, pelleted (500*g* for 2 minutes at 4°C) and mechanically dissociated by

trituration (through a sterile pasteur pipette) three times in ice-cold MEM. The resulting dissociated neurones were re-suspended in Dulbecco's Modified Eagle's Media (DMEM, containing GlutaMAX™ I and 4500 mg/L D-Glucose (supplemented with 20% FBS and 5 μg/mL penicillin-streptomycin)) and seeded onto 6-well plates (Corning, Fisher Scientific, Loughborough, UK) or 8-well multichamber slides (Nunc, Fisher Scientific, Loughborough, UK), which had been previously coated with poly-D-lysine (4 μg/mL) (Sigma-Aldrich, Dorset, UK) and mouse laminin (6 μg/μL). The neurones were incubated at 37°C in 5% CO_2 for up to 48 hours, after which they were incubated in 2 mLs per well of Neurobasal™ media containing penicillin-streptomycin (5 μg/mL) and 20% B27 serum-free supplement at 37°C in 5% CO_2. The Neurobasal™ media was partially changed every 2 - 3 days until the primary cortical cultures were used for further study. A residual 500 μL of media was left covering the cells during media changes in order to minimise cellular stress.

2.2.2 PC-12 Cell Line

The PC-12 rat pheochromocytoma cell line (CRL-1721™, American Type Culture Collection, VA, USA) was cultured in DMEM (containing GlutaMAX™ I and 4500 mg/L D-Glucose) supplemented with 10% heat-inactivated FBS and 5 μg/mL penicillin-streptomycin (Invitrogen, Paisley, UK). Cells were maintained in a 75 cm^2 cell culture flask at 37°C in 5% CO_2, and passaged every 7 days using trypsin-EDTA (0.25% trypsin, 1 mM EDTA) (Invitrogen, Paisley, UK).

2.3 In Vitro Culture Treatments

2.3.1 NMDA Stimulation Time-course

Primary cortical neurones were utilised at varying times *in vitro* depending on the assay. For western blotting and RT-PCR procedures, primary neurone cultures were harvested at 7-10 DIV. For immunocytochemistry, although technically very challenging, cells were used at 21 DIV. At this developmental stage (21 DIV), the majority of gephyrin clusters are synaptic and a large proportion of these are associated with $GABA_A$Rs (Danglot *et al.* 2003). The neurones were seeded in either 8-well multichamber slides or 6-well plates and were treated with either 100 μM N-methyl-D-aspartate (NMDA) in 20 mM KCl (added as 20 μL of a 10 mM NMDA in 2 M solution of KCl) dissolved in distilled water or a distilled water vehicle

for differing time periods. The time-course involved cell stimulation for 3 hours, 6 hours or 24 hours. Treatment and control cells were always processed in parallel from a single culture. Neurones were either fixed with formaldehyde (Fluka, Sigma-Aldrich, Dorset, UK) for immunofluorescence (see section 2.5), RNA extracted for RT-PCR (see section 2.4), or protein extracted for Western blotting (see section 2.6).

2.3.2 Transient Transfection

PC-12 cells, 72 hours after passage and seeded in either 6-well plates or 8-well multichamber slides, were pre-incubated for 2 hours in DMEM (containing GlutaMAX™ I and 4500mg/L D-Glucose) supplemented with 10% heat-inactivated FBS and 50 ng/mL NGF-7S (Sigma-Aldrich, Dorset, UK). This facilitated the differentiation of the cells into a neuronal-like cell type (Greene & Tischler 1976). The murine zif268 cDNA expression vectors, pzif268 and ptrzif268, have been described previously (James *et al.* 2005). Both plasmids are based on the pCMV5 (Genbank accession number AF239249) plasmid vector. pzif268 expressed full length zif268, whereas ptrZif268 is an N-terminally deleted (ΔN3-372) version of zif268. Separately, 2 μg of endotoxin-free pzif268 plasmid or 2 μg of ptrzif268 DNA was added to PC-12 cells or primary cortical neurones when seeded in 6-well plates. In 8-well multichamber slides, 0.5 μg of the plasmid vectors was added. Cells were transiently transfected using the cationic lipid reagent Lipofectamine™ 2000 (Invitrogen, Paisley, UK) (2 μl per 1 μg of DNA). The required amounts of DNA and Lipofectamine™ 2000 were separately diluted in Opti-MEM® with GlutaMAX™ (Invitrogen, Paisley, UK) for 5 minutes at room temperature (RT). The diluted DNA and diluted Lipofectamine™ 2000 were then mixed together and incubated at RT for 20 minutes before addition to the wells. The transfection efficiencies of primary neurones with Lipofectamine 2000 is reported at 20-30% (Dalby *et al*. 2004) and for PC-12 cells is 85% (http://www.invitrogen.com/Content/SFS/ProductNotes/F_Lipofectamine%202000b-040923-RD-MKT-TL-HL050602.pdf). PC-12 cells also received 2 μM of the adenyl cyclase activator, forskolin, before all cells were incubated for 48 hours at 37^{o}C in 5% CO_2. James *et al.* (2005) discovered that forskolin was required in order for zif268 to transactivate target gene transcription in PC-12 cells. Neurones were either fixed for immunofluorescence (see section 2.5), RNA extracted for RT-PCR (see section 2.4) or protein extracted for Western blotting (see section 2.6).

2.4 Reverse Transcriptase Polymerase Chain Reaction

2.4.1 RNA Extraction

The protocol for animal tissues in the RNeasy® Mini Kit (Qiagen, Crawley, UK) was utilised, and directions followed as per manufacturer's instructions. For cultured neuronal (7-10 DIV) or PC-12 cells, the cell media was removed thoroughly from plated cells by washing with ice cold 0.1 M phosphate buffered saline (PBS) (Sigma-Aldrich, Dorset, UK), before covering with 600 μl of lysing buffer RLT (containing β-Mercaptoethanol (β-ME)). Cells were immediately scraped into a BioPulveriser Tube, containing Lysing Matrix D, and homogenised using the Hybaid Ryboliser (Thermo Electron Corporation, Cheshire, UK).

For whole tissue (see section 2.8.2, page 81), 30 mg of an adult female Wistar rat brain was removed, mechanically disrupted with a mortar and pestle containing 600 μl buffer RLT (containing β-ME), then placed in a BioPulveriser Tube, containing Lysing Matrix D tube and homogenised using the Hybaid Ryboliser.

For either preparation the resultant mixture was carefully removed, placed in a clean Eppendorf and 600 μl of 70% ethanol added and mixed. Samples were loaded onto RNeasy mini columns and centrifuged for 15 seconds at 9,000 *g* in a 5804 R centrifuge (Eppendorf, Cambridge, UK). This was followed by the addition of 700μl Buffer RW1, spun for 15 seconds at 9,000 *g*, then two times 500μl Buffer RPE (containing ethanol) was added, the first centrifuged for 15 seconds and the second for 2 minutes. Elution was performed by placing the column in a fresh eppendorf with the addition of 30 μl RNase-free water added to the membrane and the column spun for 1 minute at 9,000 *g*. Samples were either then stored at –20°C or used immediately to synthesise first strand cDNA.

2.4.2 First Strand cDNA Synthesis

First strand cDNA synthesis from total RNA was performed using the Superscript™ First-Strand Synthesis System for RT-PCR (Invitrogen, Paisley, UK). Firstly, RNA samples were quantified using the RNA/DNA calculator GeneQuant (Pharmacia Biotech, Amersham, Buckinghamshire, UK). cDNA was synthesised from 1 μg or 500 ng of total RNA from PC-12 cells or primary neurones respectively. RNA was placed in a DNase, RNase-free eppendorf tube with 1 μL

10 mM dNTP (Deoxynucleotide-triphosphate) mix, 1 μL random hexamers (50 ng/μL) and DEPC-treated water up to 10 μL. Each sample was incubated at 65°C for 5 minutes and placed on ice. Then, 2 μL 10x RT (Reverse Transciptase) buffer, 4 μL 25 mM Mg_2Cl_2, 2 μL 0.1 M DTT (Dithiothreitol) and 1 μL RnaseOUT™ Recombinant RNase Inhibitor was prepared, vortexed, added to each sample and controls and mixed thoroughly. All samples and controls were incubated at 25°C for 2 minutes before the addition of 1 μL SuperScript™ II RT (50 U/μL) to each tube. All tubes were mixed and incubated at 25°C for 10 minutes, 42°C for 50 minutes followed by 15 minutes at 72°C, then placed on ice. After the addition of 1 μL RNase H to each tube to degrade residual RNA, all samples were incubated at 37°C for 20 minutes. The resultant 20 μL cDNA sample was then diluted with 80 μL DNase-free water.

2.4.3 Amplification of Target DNA

As an initial step, PCR tubes and equipment were UV irradiated for a minimum of 10 minutes, denaturing any DNA present and therefore removing any possible contaminants. Each tube was then filled with 18 μL ultrapure water, 5 μL 5x PCR buffer (500 μL 10x PCR Buffer [containing Tris·Cl, KCl, $(NH_4)_2SO_4$,15 mM $MgCl_2$; pH 8.7 (Qiagen, Crawley, UK), 10 μL each of 100 mM dATP, dTTP, dGTP, dCTP (Promega, Southampton, UK) and 460 μL ultrapure water], 1.25 μL 20 μM appropriate primer (see table 2.5; section 2.11), 0.25 μL HotStarTaq™ (5 U/μL) (Qiagen, Crawley, UK) and 0.5 μL cDNA. GAPDH was used as a steady state control for normalisation. The PCR program employed involved an initial Taq activating step of 95°C for 15 minutes, followed by cycles of 94°C for 45 seconds (DNA denaturing), 60°C for 45 seconds (annealing of the primers to complementary DNA), and extension at 72°C for 1 minute. The number of cycles was empirically determined for each DNA sequence of interest (detailed within table 2.6; section 2.11, page 89).

2.4.4 Gel Electrophoresis & Analysis

After the addition of 5 μL Blue/Orange 6x Loading Buffer (Promega, Southampton, UK), samples were electrophoresed on 1.5% agarose (Roche Diagnostics, Sussex, UK) gels prepared with 0.5xTBE buffer (Invitrogen, Paisley, UK) and 1 μL GelStar® Nucleic Acid Gel Stain (Cambrex, Berkshire, UK) per 10 mL gel.

Samples were typically electrophoresed at 100 V for 1 hour. Images were captured with a GelCam, attached to a GH10 0.8x electrophoresis hood (BioRad, Hertfordshire, UK), or examined and processed using a MCID image analysis system (MCID 5, Canada). In this paradigm we adjusted for variances by employing ANCOVA (analysis of co-variance), with GAPDH pixel intensity as the co-variate. This statistical procedure is capable of measuring and removing the effects of pre-existing individual differences in samples, for example different efficiencies of mRNA extraction, cDNA synthesis and treatment.

2.5 Immunocytochemistry

2.5.1 Fixation & Staining

Primary cortical cultured neurones, 21 DIV, were fixed using 4% formaldehyde (Fluka, Sigma-Aldrich, Dorset, UK) in 0.1 M PBS (see section 2.12.3) for 20 minutes at 4^{o}C. After three washes with 0.1 M PBS, blocking serum (0.1 M PBS with 15% normal goat serum (Vector, Peterborough, UK)) was added to the cells for one hour at RT. The blocking serum was removed, whereupon cells were immersed in a solution of 0.1 M PBS and 0.5% Triton-X100 (Sigma-Aldrich, Dorset, UK) containing 3% normal goat serum and either 1:100 mouse anti-Gephyrin (Cat. No. 610585, BD Biosciences, Oxford, UK), 1:100 rabbit anti-Ubiquilin (Cat. No. 662052, Calbiochem, Merck Biosciences, Nottingham, UK), 1:100 mouse anti-$GABA_A$ receptor β-chain (Cat. No. MAB341, Merck Biosciences, Nottingham, UK) or 1:200 rabbit anti-$GABA_A$ receptor γ2 (Cat. No. AGA-005, Alomone Labs Ltd., Jerusalem, Israel) over night at 4^{o}C.

After washing the cells three times with 0.1M PBS, neurones were incubated for 60 minutes at RT in the dark with either Alexa 594 goat anti-mouse or goat anti-rabbit (Cat. No. A11032 and A11037 respectively, Molecular Probes, Invitrogen, Paisley, UK) diluted 1:100 with 0.1M PBS containing 5% normal goat serum. Following a further three washes with 0.1M PBS, the slides were left until almost dry before being preserved using the ProLong Antifade Kit (Molecular Probes, Invitrogen, Paisley, UK), which is specifically designed to protect fluorescence for long periods of time. 1 mL of component B (mounting medium) is added to a vial of component A (antifade reagent), mixed carefully and applied to the slide with the coverslip placed on top. Once the mounting medium had dried overnight the coverslip was sealed with nail varnish and the slides stored at -20^{o}C.

2.5.2 Confocal Microscopy, Image Analysis and Statistics

A Bio-Rad MRC 1024 confocal microscope (Bio-Rad, Hertfordshire, UK) mounted on a Nikon microscope (Nikon, Surrey, UK), utilising LaserSharp 2000 software (Bio-Rad, Hertfordshire, UK), for image viewing was used to capture images. The parameters for each set of images were uniform for the protein stained. Immunofluorescence was captured with a x40 oil immersion objective, box size 1024 x 1024, x2.0 digitally zoomed, z-stack images with steps of 0.5-1.0µm and Kalman N=4. Gephyrin and $GABA_A$ receptors were detected with the red laser power at 30, while ubiquilin was detected with a red laser power of 3 due to the intensity of staining. All images were stacked using Confocal Assistant version 4.02 (Freeware, Build 101, Todd Clark Brelje, University of Minnesota, USA), and analysed using Image J (Freeware, 1.34s, National Institute of Health, USA). All results were analysed 'blind', without knowledge of the sample treatment. The threshold for each individual z-stack was assessed, and set when background was at a minimum with diffuse staining throughout the cell. Each neurite was then isolated and the particles counted, mean intensity of punctate staining determined, and the punctate and neurite areas measured. Cell body puncta were not included in case results were skewed due to target protein variablilities in this area compared to neurites.

2.6 Western Blot

2.6.1 Sample Preparation

Adherent PC-12 or primary cortical cultured cells (7-10 DIV) were initially washed with ice-cold 0.1 M PBS, then lysed with ice-cold RIPA buffer (see section 2.12.1), scraped into clean eppendorf tubes and agitated on ice for 15 minutes. Cell extracts were centrifuged at 11,700 *g* for 15 minutes at 4^{o}C, and the supernatants stored at -20^{o}C.

2.6.2 Assessment of Total Protein Content

The Bradford (Bio-Rad) Protein Assay (Bradford 1976) was employed to determine the total protein concentration of each sample. Duplicate standard solutions were created from a stock solution of 2.0 mg/mL BSA (see table 2.1) in order to create a standard curve.

Cortical neurone and PC-12 samples, defrosted and kept on ice, were mixed thoroughly before 10 μL was removed and diluted with de-ionised water 1:100 and 1:200 respectively. Differing dilutions were used for the different cell types as PC-12 cells were generally twice as confluent as the primary neurones. Two aliquots of 400 μL of either sample were then placed in a clean eppendorf tube. Bio-Rad Protein Assay Dye Reagent Concentrate (Bio-Rad, Hertfordshire, UK) was allowed to reach room temperature then diluted 1:1 with de-ionised water. 200 μL of the dye solution was added to each sample, mixed thoroughly, and allowed to incubate at room temperature for 5 minutes. After vortexing again, 200 μL of each duplicate standard and sample was pipetted into a 96 well plate, the absorbance read at 595 nm on an Opsys MR photometer (Dynex Technologies, West Sussex, UK), and protein concentration calculated by linear regression using Revelation™ QuickLINK software v4.03 (Dynex Technologies, West Sussex, UK). A successful assay was determined by a straight-line generated from the standard solutions (where $r^2 \geq 0.99$), variations between the sample and standard duplicates was less than 20%, and all sample protein determinations fell within the set 0.0 - 2.0 mg/mL concentrations (i.e. protein concentration determination by extrapolated data was repeated). All samples were then normalised, by dilution with lysis buffer, to the lowest registered protein concentration before continuing with further experimentation, or storing at -20^{o}C.

Tube	BSA Volume (μL)	De-ionised Water Volume (μL)	Final Concentration (mg/mL)
A	0	400	0.00
B	50	350	0.25
C	100	300	0.50
D	200	200	1.00
E	300	100	1.50
F	400	0	2.00

Table 2.1 Protein Standards for the Bradford (Bio-Rad) Protein Assay

2.6.3 NuPAGE® Bis-Tris Electrophoresis

Instructions were followed as per the NuPAGE® Electrophoresis System instruction booklet (Invitrogen, Paisley, UK). Each normalised sample was deforested on ice and prepared using 65 μL normalised protein, 25 μL NuPAGE® LDS Sample Buffer and 10μl NuPAGE® Reducing Agent (0.5 M DTT) and heated

to 70^{o}C for 10 minutes. After loading 10 μL of Full Range Rainbow recombinant protein molecular weight marker (RPN 800, Amersham Biosciences, Buckinghamshire, UK), equal amounts of total protein (20 μL maximum) were loaded onto NuPAGE® pre-cast 4-12% Bis-Tris polyacrylamide gels housed in an XCell *Sure*Lock™ Mini-Cell (Invitrogen, Paisley, UK). The gel was submerged in 1x SDS NuPAGE® MOPS Running Buffer with 0.25% NuPAGE® Antioxidant within the inner buffer chamber (all NuPAGE® products, Invitrogen, Paisley, UK). The samples were then electrophoresed at 200 V using a PowerPac Basic™ power supply (Bio-Rad, Hertfordshire, UK) for 45 minutes if the protein of interest was less than 50 kDa, or 1 hour if the protein was more than 50 kDa.

2.6.4 NuPAGE® Transfer

After electrophoresis, the gel was transferred to an Invitrolon™ PVDF membrane, in a filter paper sandwich (Invitrogen, Paisley, UK). All blotting pads and filter papers were initially soaked in 700mLs of a 1L solution made from 50mLs 20xNuPAGE® Transfer buffer, 100mLs methanol, 1mL NuPAGE® Antioxidant and 850mLs deionised water. The PVDF membrane was placed in methanol before rinsing in the transfer buffer in order to improve antigen binding. Next, the transfer blot was assembled within the cathode core by assembling 3 blotting pads, a filter paper, the gel, the PVDF membrane, a second filter paper and a further 3 blotting pads. After ensuring no air bubbles were present between any of the layers, the anode core was placed on top, the blot module wedged into the XCell II™ Blot Module chamber (Invitrogen, Paisley, UK), and filled with the remaining 300 mLs of transfer buffer. The outer chamber of the module was filled with deionised water and transfer was performed at 30 V using PowerPac Basic™ power supply (Bio-Rad, Hertfordshire, UK) for 45 minutes.

2.6.5 Blot Efficiency Test

A visual inspection of the membrane to ensure the uniformity of transfer, normalisation of proteins and accuracy of gel sample loading, was achieved by submerging the membranes in Ponceau S Solution (Sigma-Aldrich, Dorset, UK) immediately after transfer. After 5 minutes the membrane was agitated in deionised water, and the transferred protein bands visualised and scrutinised. If the bands appeared consistent, specifically within the expected size range of the protein, the membrane was briefly submerged in 0.1 M sodium hydroxide (BDH

Laboratory Supplies, Poole, UK), then placed in clean deionised water for a few minutes until the staining was removed.

2.6.6 Immunodetection

The membranes were blocked in 3% non-fat dried milk powder (Marvel, Premier International Foods (UK) Ltd., Lincolnshire, UK) for 2 hours, and then soaked in the appropriate primary antibody in 1% milk powder in T-TBS (see section 2.11.2 for buffer ingredients). Antibodies used, and their dilutions, were as follows: anti-gephyrin, 1:500 (Cat. No. 610585, BD Biosciences, Oxford, UK), anti-ubiquilin, 1:500 (Cat. No. 662052, Calbiochem, Merck Biosciences, Nottingham, UK), anti-zif268 (Egr-1 (588)), 1:250 (Cat. No. sc-110, Santa Cruz Biotechnology, Calne, UK), rabbit anti-p70 S6 Kinase, 1:500, (Cat. No. 9202L), rabbit anti-p4E-BP1 (Thr37/46), 1:1,000, (Cat. No. 9459L), mouse anti-pERK (p44/42 MAP Kinase; Thr202/Tyr204), 1:2,000, (Cat. No. 5120), rabbit anti-total ERK, 1:2,000 (Cat. No. 9102) and rabbit anti-pCREB (Ser133), 1:250 (Cat. No. 9191), (all from Cell Signalling, Hertfordshire, UK). Membranes were incubated with the antibody at 4°C overnight before washing 3 times for 15 minutes in T-TBS, then placed in the appropriate secondary antibody, either peroxidase-conjugated AffiniPure anti-mouse IgG 1:10,000 or anti-rabbit IgG 1:10,000 (Cat. No. 115-035-166 and 111-035-144 respectively, Jackson Laboratories, Stratech, Suffolk, UK) for 1 hour with agitation at RT. Thereafter, the membrane was washed 3 times for 15 minutes in T-TBS before covering with ECL plus Western Detection System (Amersham Plc, Buckinghamshire, UK) as per the manufacturer's instructions. Briefly, after equilibrating to RT, 100 μL of solution B was added to 4 mLs of solution A and placed on the membrane, protein side up, for 5 minutes at RT with agitation. The exception was the zi268 antibody, which was probed with a goat anti-rabbit, HRP-conjugate 1:10,000, and protein bands visualised with the Visualizer™ Western Blot Detection Kit (both from Upstate Signalling, Hampshire, UK). The manufacturer's instructions were followed, combining Detection Reagent A and Detection Reagent B in a 1:2 ratio, allowing 3 mLs overall. The solution was then allowed to equilibrate to RT before covering the membrane for 5 minutes with agitation.

2.6.7 Imaging

The blot was developed using Hyperfilm™ ECL high performance chemiluminescence film and a HyperProcessor, automatic autoradiography film processor (both Amersham Plc, Buckinghamshire, UK). Photographs of blots were taken using a Panasonic WV-BP500 camera (Berkshire, UK). Film analysis was performed on a Macintosh computer using the public domain NIH Image program (developed at the U.S. National Institutes of Health and available on the Internet at http://rsb.info.nih.gov/nih-image/). All measurements were performed by hand and reported by the NIH program. Each lane density and area was measured three times for an average reading, the background density was subtracted from the lane density, and this value was multiplied by the area of the band. For normalisation, each value was then transformed to a percentage of control.

2.7 Promoter-Reporter Assay

2.7.1 Gephyrin Promoter Primer Design

The sequences for the gephyrin promoter primer pair were designed to target the cDNA sequence of *Rattus norvegicus* provided by NCBI and utilising information provided by Ramming *et al.* (1997). The primers were designed using the sequence of the M. *musculus* gephyrin 5' untranslated region (UTR) (Genbank accession numbers Y10882 and Y10883). The primers were predicted to flank a region of 882 base pairs of the mouse gephyrin UTR. The primer pair sequences 'Gephyrin Promoter Fwd' and 'Gephyrin Promoter Rev' are described in Table 2.5; see section 2.11.

A second set of mouse gephyrin specific primers were designed to amplify, from the product of the first round PCR, the DNA sequence containing recognition sequences for restriction endonucleases subsequently used directionally to clone the gephyrin promoter into pBLCAT3 (a promoter-less CAT vector, Genbank accession number X64409). Inspection of the pBLCAT3 plasmid map revealed adjacent *SalI* and *XbaI* restriction enzyme sites situated within the multiple cloning site (MCS) of the vector. Neither of these restriction sites were predicted to be present within the sequence amplified during the first round of PCR amplification of the gephyrin 5' UTR.

The primer pair sequences, called 'Gephyrin Promoter Fwd SalI' and 'Gephyrin Promoter Rev XbaI', whereby bold letters denote the palindromic 6 base pair recognition sequences for the *SalI* and *XbaI* restriction enzymes, are shown in table 2.5; see section 2.11.

2.7.2 Genomic DNA Isolation

Total DNA was isolated from cultured PC-12 cells, using the DNeasy® Tissue Handbook (Qiagen, Crawley, UK), and the manufacturer's protocol followed. Briefly, PC-12 cells were rinsed in 0.1 M PBS before scraping from the wells in 200 μL of fresh 0.1 M PBS and placing into an eppendorf tube. 200 μL Buffer AL and 20 μL Proteinase K were added to the cell suspensions before mixing thoroughly by vortexing and heating at 70°C for 10 minutes. 200 μL of 96-100% ethanol was then added, and the mixture applied to a DNeasy Mini Spin Column in a collection tube and centrifuged at 7,200 *g* for 1 minute. The flow-through was discarded and 500 μL Buffer AW1 added to the spin column, centrifuged at 7,200 *g* for 1 minute and the flow through discarded again. 500 μL Buffer AW2 was added, and the column centrifuged at 12,600 *g* for 3 minutes, before discarding the flow through. The column was then placed in a clean fresh eppendorf tube and 200 μL Buffer AE added to the membrane to elute the genomic DNA. This was incubated at room temperature for 1 minute before centrifuging for 1 minute at 7,200 *g*.

2.7.3 Polymerase Chain Reaction (PCR)

Two rounds of PCR were performed to prepare the gephyrin promoter for directional cloning into pBLCAT3. In the first round the reaction contained 12.5 μL DNase and RNase-free water, 5 μL 5x PCR buffer, 3 μL of PC-12 genomic DNA, 1 μL of an equimolar mixture of the forward and reverse primers (10 μM of Gephyrin Promoter Fwd & 10 μM Gephyrin Promoter Rev; see table 2.5), 0.5 μL 50x dNTP mix, 2.5 μL GC Melt and 0.5 μL advantage-GC2 polymerase (BD Biosciences, Oxford, UK). The PCR program employed was 94°C for 3 minutes followed by 30 cycles of 94°C for 30 seconds, 68°C for 3 minutes with a final extension of 68°C for 3 minutes. In order to validate the presence of a single amplicon at the predicted size, 5 μL of the PCR reaction was co-electrophoresed on an ethidium bromide stained 0.5x TBE 1% agarose gel with 100 base pair markers (Promega,

Southampton, UK). To remove unincorporated dNTPs and primers the remaining 20 μL of the reaction was PCR purified using Qiagen's PCR Purification Kit (Qiagen, Crawley, UK). Instructions were followed as per the manufacturer's handbook. Briefly, 100 μL of buffer PB was added to the PCR sample mix (5 volumes buffer to 1 volume sample) and the resulting mixture applied to a QIAquick column and centrifuged. All centrifugation steps were carried out at 11,700 *g* for 60 seconds. The flow-through was discarded and the membrane washed with 750 μL Buffer PE, centrifuged and the flow-through discarded. After an additional spin the QIAquick column was placed in a fresh eppendorf tube and the DNA eluted from the column after centrifugation for 1 minute, with 50μl Buffer EB.

The second round of PCR used the same PCR reaction mixture, but contained 3 μL of a dilute amount of the DNA synthesised during the first round of PCR. An estimate of the concentration of template synthesised during the first round of PCR was determined using the DNA/RNA calculator, GeneQuant as previously described. Subsequently, the PCR product was diluted to approximately 1 fg/μL and this solution used as a source of DNA template for a second round of PCR using an equimolar mixture of 10 μM Gephyrin Promoter Fwd *SalI* & 10 μM Gephyrin Promoter Rev *XbaI* primers (as detailed in table 2.5). The PCR programme was repeated, and the resultant PCR product purified using the Qiagen PCR Purification Kit as before. The purified DNA was quantified using GeneQuant as previously described.

2.7.4 Restriction Endonuclease Digestion

Separately, approximately 160 ng of the gephyrin 5'UTR PCR product (the 'insert') and 100 ng of pBLCAT (the 'vector') were digested with the restriction endonucleases *SalI* and *XbaI* (Promega, Southampton, UK). The recognition sites for these enzymes are 5'-GTCGAC-3' and 5'-TCTAGA-3' for *SalI* and *XbaI* respectively. Digests (20 μL) were performed in 1x Buffer D containing approximately 2μg acetylated bovine serum albumin (BSA) (both from Promega, Southampton, UK). Digest mixtures were vortexed before incubating overnight at 37°C, whereupon 4μl of 6x loading dye (Promega, Southampton, UK) was added to each eppendorf tube and mixed. Both the 'insert' and 'vector' digests were electrophoresed on a 1% agarose 0.5x TBE buffer gel with 1 μL GelStar® Nucleic

Acid Gel Stain (Cambrex, Berkshire, UK) per 10 mL gel, for 1 hour at 100 V. The vector and insert products were excised from the gel, placed in the same eppendorf and purified using the QIAquick Gel Extraction Kit (Qiagen, Crawley, UK). Instructions were followed as per the manufacturer's handbook. Three volumes of Buffer QG were added to 1 volume of combined vector and insert gels before incubating at 50ºC for 10 minutes, with periodic vortexing. One gel volume of isopropanol was then added, mixed and the sample placed in a QIAquick column. After centrifuging at 11,700 *g* for 1 minute, 0.5 mL of Buffer QG was added to the column and centrifuged again at 11,700 *g* for 1 minute. The column was washed with 0.75 mLs Buffer PE before centrifugation at 11,700 *g* for 1 minute, the flow through discarded, and the centrifugation repeated. The column was placed in a clean eppendorf tube and the DNA eluted with 50 μL Buffer EB, incubated at room temperature for 1 minute and centrifuged for 1 minute at 11,700 *g*.

2.7.5 Ligation & Transformation

The Quick Ligation™ Kit (New England BioLabs Inc., Hertfordshire, UK) was utilised, and instructions followed from the manufacturer's directions. 10 μL of 2xQuick Ligation Buffer was added to 10 μL of the combined vector and insert DNA sample and vortexed. After the addition of I μL of Quick T4 DNA Ligase the sample was incubated for 5 minutes at room temperature before placing on ice. One Shot® TOP10 Chemically Competent *E.coli* cells (Invitrogen, Paisley, UK), previously stored at –80°C were thawed and 50 μL added to 2 μL of the DNA sample and mixed. The mixture was placed on ice for 30 minutes before heat shock at 42°C for 30 seconds. 250 μL of room temperate S.O.C. media was then added and the mixture incubated for 1 hour at 37°C, shaking at 200 rpm. After spreading 50 μL of the sample on warmed imMedia™ ampicillin agar (Invitrogen, Paisley, UK) for recombinant *E.coli* strains, the plates were incubated overnight at 37°C.

2.7.6 Plasmid Purification

Successful transformation of the *E.coli* cells with the gephyrin promoter was then determined. Plasmid DNA was isolated from transformed TOP10 *E.coli* cells (Invitrogen, Paisley, UK), using QIAprep Miniprep columns and reagents (Qiagen, Crawley, UK). The manufacturer's protocol was followed. Briefly, cells were

pelleted by centrifugation and re-suspended in 250 μL Buffer P1, then 250 μL P2 and inverted 6 times. Buffer N3 (350 μL) was then added, and the tube inverted 6 times gently before centrifuging at 11,700 *g* for 10 minutes. All further centrifugation steps were also carried out at 11,700 *g*. The supernatant was applied to the QIAprep® Spin Column and centrifuged for 60 seconds. The column membrane was then washed with 0.5 mL of Buffer PB and centrifuged for 60 seconds. After the flow through had been discarded, the membrane was washed again using 0.75 mL Buffer PE and centrifuged for 60 seconds. The flow through was discarded and the column centrifuged again to remove any additional wash buffer. The QIAprep® column was then placed in a clean centrifuge tube. To elute the DNA, 50 μL of Buffer EB was pipetted directly onto the membrane, incubated for 1 minute at room temperature and centrifuged for 1 minute. From the resultant plasmid DNA sample, 5 μL was digested with 0.2 μL BSA Acetylated (10 mg/mL), 1 μL *SalI* (10 U/μL), 1 μL *XbaI* (10 U/μl), 2 μL 10x Buffer D (All Promega, Southampton, UK), 10.8 μL ultrapure water and incubated overnight at 37°C. The following day, 20μl of the restriction endonuclease digests were mixed with 4 μL 6x loading buffer (Promega, Southampton, UK) and electrophoresed on a 1% agarose 0.5x TBE buffer gel with 1 μL GelStar® Nucleic Acid Gel Stain (Cambrex, Berkshire, UK) to every 10 mL gel, for 1 hour at 100 V.

2.7.7 Endotoxin-Free Plasmid Purification

Endotoxin-free plasmid preparations were prepared using the EndoFree® Plasmid Maxi Kit (Qiagen, Crawley, UK), and the manufacturer's protocol followed. Briefly, a single *E.coli* colony was used to inoculate a starter culture of 5mL imMedia™ ampicillin broth (Invitrogen, Paisley, UK). After incubation for 8 hours at 37°C shaking at 200 rpm, 0.1 mL of this starter culture was diluted into 100 mL fresh imMedia™ ampicillin broth (Invitrogen, Paisley, UK) and incubated overnight at 37°C vigorous shaking at 200rpm. The next day, the cultures were centrifuged at 4,500 *g* for 10 minutes at 4°C, after which the supernatant was removed and discarded. The bacterial pellet was resuspended in 10 mLs Buffer P1 (containing 100 μg/mL RNase A) and 10 mLs Buffer P2, mixed by inverting 6 times and incubated at room temperature for 5 minutes. The QIAfilter cartridge was assembled and placed in a clean 50 mL tube. After incubation, ice cold Buffer P3 was added to the lysate, inverted 6 times, poured into the cartridge and incubated at room temperature for 10 minutes. After incubation, the plunger was inserted

into the cartridge and the lysate filtered. Buffer ER (2.5 mLs) was then added; the sample inverted 10 times and incubated on ice for 30 minutes. Meanwhile, a QIAGEN-tip 500 was equilibrated with the addition of 10 mLs Buffer QBT, which then passed through the column by gravity. After incubation, the sample was added to the equilibrated column and allowed to pass through by gravity. The QIAGEN-tip was then washed twice with 30 mLs Buffer QC and finally eluted with 15 mLs Buffer QN; all solutions were allowed to filter of their own accord. DNA precipitation was achieved by the addition of 10.5 mLs room temperature isopropanol, which was then mixed and centrifuged immediately at 4,500 *g* for 1 hour at 4°C. The supernatant was discarded and the pelleted DNA washed with 5 mLs of room temperature endotoxin-free 70% ethanol and centrifuged at 4,500 *g* for 30 minutes. The resulting DNA pellet was carefully dried before re-dissolving in 100 μL endotoxin-free Buffer TE. The plasmid DNA concentration was then determined by GeneQuant.

2.7.8 Co-Transfection

PC-12 cells, seeded in 6 well plates, were pre-incubated with 50 ng/mL NGF-7S (Sigma-Aldrich, Dorset, UK) in DMEM (containing GlutaMAX™ I and 4500 mg/L D-Glucose) supplemented with 10% heat-inactivated FBS for 2 hours. The test well then received 3.5 μg of the cloned gephyrin promoter, 2 μg of endotoxin-free pzif268 and 0.2 μg of β-GAL cloned into a pCMV vector. β-GAL was used to correct for variations in transfection efficiencies. Four control wells were also transiently transfected; control 1 received 3.5 μg of the cloned gephyrin promoter, 2 μg of endotoxin-free ptrzif268 and 0.2 μg of β-GAL, control 2 received 3.5 μg of the cloned gephyrin promoter, 2 μg of pCMV5 empty vector and 0.2 μg of β-GAL, control 3 received 3.5 μg of the pBLCAT3 empty vector, 2 μg of endotoxin-free pzif268 and 0.2 μg of β-GAL and finally, control 4 received 3.5 μg of the pBLCAT3 empty vector, 2 μg of pCMV5 empty vector and 0.2 μg of β-GAL. Transfection was achieved using 2 μL of Lipofectamine™ 2000 (Invitrogen, Paisley, UK) per 1 μg DNA, and performed as per the previous description (see section 2.3.2). The experiment was performed in duplicate with only one set of PC-12 cells receiving 2 μM forskolin to determine the different effects with and without the adenyl cyclase activator. All wells were then incubated for 48 hours at 37^{o}C in 5% $CO_{2.}$

2.7.9 CAT & β-GAL Enzyme-Linked Immunosorbant Assay

2.7.9.1 Sample Preparation

Cells were washed 3 times in ice cold PBS before lysing with 1 part Lysis Buffer provided in the CAT & β-GAL ELISA kits (Roche Diagnostics, Sussex, UK) mixed with 4 parts ultra pure water. To allow for co-transfection studies, the lysis buffer provided is optimised for full compatibility between CAT and β-GAL ELISA's. Firstly, 400 μL of the buffer was added to each well and left to stand for 30 minutes at room temperature. Cells were then scraped into an eppendorf tube and centrifuged at 12,600 *g* for 10 minutes at 4°C. A 100 μL aliquot of the supernatant was then removed and transferred to a clean eppendorf for protein determination. The remaining 300 μL was transferred to a separate clean eppendorf tube and snap-frozen on dry ice before storage at -70°C.

2.7.9.2 BCA (Bicinchoninic Acid) Protein Assay

This copper-based assay was used to quantify the total amount of proteins found in each sample. Directions were followed as per manufacturer's instructions (BCA™ Protein Assay Kit, Pierce, Northumberland, UK). The instructions for the microplate procedure with 3 replicates of standards and samples were adhered to. Firstly, protein standards were prepared using the supplied 2.0 mg/mL BSA diluted with the same diluent as the samples; solution 8 of either the CAT or β-GAL ELISA kit (Roche Diagnostics, Sussex, UK) diluted 1 part to 5 parts ultra-pure water. See table 2.2 for the dilution scheme of protein standards used to determine the standard curve.

The BCA™ working reagent (WR) was then prepared using the following equation:

(9 standards + # unknowns) x (3 replicates) x (200μl WR per sample) = total volume WR required

Preparation of WR involved mixing 50 parts of BCA™ Reagent A to 1 part BCA™ Reagent B and vortexing. 25 μL of each standard and pure undiluted sample was pipetted in triplicate into a 96 well plate before the addition of 200 μL of WR to each well. The plate was then mixed thoroughly on a shaker for 30 seconds after which it was incubated at 37°C for 30 minutes, and then allowed to cool to room temperature. The absorbance was then measured at 595 nm with an Opsys MR

photometer (Dynex Technologies, West Sussex, UK), calculated by quadratic regression using Revelation QuickLINK software v4.03 (Dynex Technologies, West Sussex, UK) and all samples normalised.

2.7.9.3 Preparation of CAT & β-GAL Enzyme Standards

All ELISA kit solutions were equilibrated to room temperature before experimentation. CAT and β-GAL enzyme standards were prepared as per the manufacturer's instructions (see table 2.3 and 2.4) before loading 200 μL in duplicate of each standard into the wells of the microtitre plate (MTP) provided. 200 μL of the samples was then added to the CAT ELISA plate. The remaining sample was diluted 1:5 and 200 μL of the diluent added to the β-GAL ELISA plate.

2.7.9.4 ELISA Assay

Both MTP modules were covered and incubated at 37°C for 1 hour after which the solutions were removed and the wells rinsed with washing buffer. The CAT ELISA wells were washed 5 times and the β-GAL wells 3 times for 30 seconds each. 200 μL of a freshly prepared solution of digoxigenin-labelled (DIG) CAT or β-GAL antibody, anti-CAT-DIG (2 μg/mL) or anti-β-GAL-DIG (0.5 μg/mL), was then applied to the respective MTP modules, covered and incubated at 37°C for 1 hour. The modules were washed as before, after which 200 μL of a freshly prepared solution of an antibody to digoxigenin conjugated to peroxidase (POD), anti-DIG-POD (150 mU/mL), was then applied to both MTP modules, before covering and incubation at 37°C for 1 hour. Both MTP modules were then washed again as before. The β-GAL module received 200 μL of the peroxidase substrate ABTS to each well for approximately 5 minutes before being read on an MRX photometer (Dynex Technologies, West Sussex, UK) at 405 nm (reference wavelength 490 nm) linked to Revelation™ software (Dynex Technologies, West Sussex, UK). The CAT module received 200 μL of the peroxidase substrate ABTS including substrate enhancer for approximately 45 minutes with agitation. The CAT ELISA module was then read on the same photometer.

Tube	BSA Volume (μL)	Lysis Buffer Volume (μL)	Final Concentration (μg/mL)
A	300 of stock	0	2000
B	375 of stock	125	1500
C	325 of stock	325	1000
D	175 of tube B	175	750
E	325 of tube C	325	500
F	325 of tube E	325	250
G	325 of tube F	325	125
H	100 of tube G	400	25
I	0	400	0

Table 2.2: Protein Standards for the BCA Protein Assay

Step	CAT Enzyme working dilution (approx. 1 ng/mL)	Sample Buffer	Approx. CAT Enzyme concentration (ng/mL)
0	0	1000 μL	0
1	1000 μL	0	1.0
2	500 μL of Step 1	500 μL	0.5
3	500 μL of Step 2	500 μL	0.25
4	500 μL of Step 3	500 μL	0.125

Table 2.3: Standards for the CAT ELISA, used to produce a calibration curve for the CAT enzyme

Step	β-GAL Stock Solution (approx. 25 ng/mL)	Sample Buffer	Approx. β-GAL enzyme concentration (pg/mL)
0	0	1000 μL	0
1	50 μl	950 μL	1250
2	500 μL of Step 1	500 μL	625
3	500 μL of Step 2	500 μL	312
4	500 μL of Step 3	500 μL	156
5	500 μL of Step 4	500 μL	78

Table 2.4: Standards for the β-GAL ELISA, used to produce a calibration curve for the β-GAL enzyme

2.8 Identification of the Novel Gene related to EST AI169020

2.8.1 Product Verification

Bioinformatically, it was discovered that EST AI169020 could be associated with the predicted transcript ENSRNOT00000012253 (www.ensembl.org), located on chromosome 4 of *Rattus norvegicus*. Therefore, exon-intron boundary spanning primers of this transcript were designed (designated Tr12253; see table 2.5; section 2.11).

Differentiated PC-12 cells cDNA was used in a PCR reaction to validate the Tr12253 Fwd & Tr12253 Rev primers. In addition, the EST AI169020 Fwd primer was combined with the Tr12253 Fwd primer (as they were designed on complementary DNA strands) in order to verify that a single product could be produced. The PCR reaction and PCR programme were performed as previous experiments (see section 2.4.3) with the AI169020 Fwd & AI169020 Rev primers, Tr12253 Fwd & Tr12253 Rev primers or Tr12253 Fwd & EST Ai169020 Fwd primers. Two controls were also performed using 2 of the same sets of primers, but replacing PC-12 cDNA with ultrapure water. Products were then separated on a 1.5% agarose gel as previously described (section 2.4.4).

2.8.2 Product Generation and Sequencing

The next stage involved verifying a single product with the Tr12253 Fwd & EST Ai169020 Fwd primers using adult Wistar rat cerebral cortex. The RNA was extracted as previously described (section 2.4.1) and first strand cDNA synthesis achieved using Superscript™ First-Strand Synthesis System for RT-PCR (Invitrogen, Paisley, UK). After quantifying the total RNA present by GeneQuant, cDNA synthesis was performed using 1 μL Oligo$(dT)_{12\text{-}18}$ (0.5 μg/μL), 1 μL 10 mM dNTP mix and 8 μL (1.37 μg) RNA. The suggested controls were also performed, namely No RT Control (No Superscript™ II RT added in the later stage) and Control RNA (the supplied RNA was used instead of the primary cortical RNA). The sample and controls were incubated at 65°C for 5 minutes and placed on ice. 2 μL 10xRT buffer, 4 μL 25mM Mg_2Cl_2, 2 μL 0.1M DTT and 1 μL RnaseOUT™ Recombinant RNase Inhibitor was then added to the sample and controls, mixed thoroughly and incubated at 42°C for 2 minutes. After the addition of 1 μL of SuperScript™ II RT to the sample and Control RNA, but not to No RT Control, the

tubes were mixed gently and incubated at 42°C for 50 minutes followed by 15 minutes at 72°C, then placed on ice. 1 μL RNase H was added to each tube and all eppendorf tubes incubated at 37°C for 20 minutes. cDNA samples were then quantified using the RNA/DNA calculator GeneQuant instrument.

The sequencing was carried out by Geneservice (Cambridge, UK), who required 10 μL of 20 ng/μL concentration of purified product per reaction and 10 μL of 3.2 pmol/μL primers with a GC content of 50-55% and Tm 55-60°C. To this end, the cDNA sample was diluted 1 in 5 with ultrapure water, and PCR performed with three eppendorf tubes containing 9 μL adult rat cerebral cortical cDNA, 5 μL 5xPCR buffer, 1.25 μL Tr12253 Fwd & EST AI169020 Fwd primers, 0.25 μl HotStar Taq and 9.5 μL dH_2O. In addition, extra PCR reactions were carried out using 9 μL cDNA of the two controls, No RT Control and Control RNA. The PCR programme was as previously described (section 2.4.3; 45 cycles), and the products electrophoresed on a 1.5% agarose as detailed in section 2.4.4. The cDNA of the samples (not controls) were excised from the gel and separately purified using the QIAquick Gel Extraction Kit (Qiagen, Crawley, UK). To ensure the required concentration and quantity of product was reached, 3 of the purified PCR reactions were combined. Primers were designed bioinformatically using Ensembl (www.ensembl.org) utilising the predicted sequence of the novel gene ascertained from EST and predicted gene information, allowing the design of 3 additional primers producing approximately 500 base pair product sizes with approximately 100 base overlaps (see table 2.5 for details).

2.8.3 Novel Gene Cloning

Once the sequence had been determined and returned from Geneservice, it was submitted to two websites predicting initiation codons and protein sequences (http://www.hri.co.jp/atgpr/ and http://ca.expasy.org/tools/dna.html), both of which returned the same data. From this information, new primers were designed to flank the coding region in order to clone the novel gene sequence into the pCR®II-TOPO® vector (Invitrogen, Paisley, UK).

The primer sequences were designed to anneal upstream of the ATG start codon, but not to include the TAG stop codon, in order that any later cloning into tagged vectors would include any tag positioned downstream of the multiple cloning site. Primers amplified a product of 724 bases and are detailed in table 2.5. The PCR

reaction was prepared as previously described (section 2.4.3) with 0.5 μL purified cDNA from Wistar adult rat cortex. The PCR programme (previously described in section 2.4.3; 30 cycles) was followed by sample electrophoresis on a 1% agarose gel (see section 2.4.4) at 100V for 1.5 hours, allowing full separation of bands. The 724 base pair band was then excised and purified using the QIAquick Gel Extraction Kit (Qiagen, Crawley, UK) as described in section 2.7.4.

The TOPO TA Cloning® Version P manual was used to clone the novel gene insert into the pCR®II-TOPO vector. 4 μL of purified PCR product was added to the provided 1 μL Salt Solution and 1 μL TOPO® vector (both Invitrogen, Paisley, UK), mixed gently and incubated at room temperature for 5 minutes, before placing on ice. 2 μL of this reaction was then added to thawed One Shot® TOP10 Chemically Competent *E.Coli* cells (Invitrogen, Paisley, UK), gently mixed and incubated on ice for 30 minutes. After heat shock for 30 seconds at 42°C, 250 μl of room temperate S.O.C. media was added and the mixture incubated for 2 hours at 37°C, shaking at 200 rpm. 75 μL from the transformation was then spread on pre-warmed imMedia™ Kan agar (Invitrogen, Paisley, UK) and incubated overnight at 37°C.

From the resultant transformants, 3 colonies were used to inoculate 5 mLs imMedia™ Kan broth (Invitrogen, Paisley, UK), placed on an orbital shaker at 200 rpm, and incubated overnight at 37°C. The plasmid DNA was then isolated and purified using the QIAprep® Miniprep Handbook for purification of plasmid DNA (Qiagen, Crawley, UK) as before (section 2.7.6). To verify the clones contained the novel gene insert, the plasmid was digested with the endonuclease restriction enzyme *EcoR1*. This involved 5 μL plasmid DNA, 0.2 μL BSA Acetylated (10 mg/mL), 1 μL *EcoR1* (10 U/μL), 2 μL 10x Buffer H (All Promega, Southampton, UK), 11.8 μL ultrapure water incubated overnight at 37°C. The following day, 20 μL of the digests were mixed with 4 μL 6x loading buffer (Promega, Southampton, UK) and electrophoresed on a 1.5% agarose 0.5x TBE buffer gel for 1 hour at 100V, then soaked in 5 μL GelStar® Nucleic Acid Gel Stain (Cambrex, Berkshire, UK) per 50 mL 1x TBE buffer (Invitrogen, Paisley, UK).

2.9 Genotyping

2.9.1 Purification of DNA from rodent tails

Zif268 null mice are sterile, therefore breeding heterozygous zif268 mutant mice (donated by P. Charnay, Paris, France) provided mice with a targeted inactivation of the zif268 gene, as well as additional heterozygotes and wildtypes. The DNeasy® Tissue Handbook provided the protocol for purifying total DNA from rodent tails, and the instructions followed. Approximately 0.5 cm length of mouse-tail, harvested at 4-6 weeks old, was placed in a centrifuge tube and fully covered with 180 μL of Buffer ATL. After the addition of 20 μL proteinase K, tubes were vortexed to mix, and the tails incubated at 55°C on a rocking platform overnight. 400 μL of Buffer AL-ethanol mixture was then added and the sample thoroughly mixed. To bind DNA, the sample was pipetted into a DNeasy Mini spin column with collection tube, centrifuged at 7,200 *g* for 1 minute and the flow-through discarded. To wash the DNeasy membrane and bound DNA, 500 μL of buffer AW1 followed by 500 μL of buffer AW2 were added to the spin column, centrifuging at 7,200 *g* for 1 minute after buffer AW1, and for 3 minutes at 11,700 *g* after AW2. The spin column was placed in a clean eppendorf tube and 200 μL of Buffer AE pipetted directly onto the membrane. After incubation for 1 minute at room temperature, the sample was centrifuged at 7,200 *g* for 1 minute. The elutant containing the DNA was then removed from the eppendorf tube and placed back onto the membrane before centrifuging again.

2.9.2 Polymerase Chain Reaction

Firstly, all equipment was UV irradiated for 30 minutes. Then, to each PCR tube was added: 5 μL 5xPCR mixture, 1.25 μL 100μM mix of zif268 forward and reverse primers including the LacZ forward (as described in Topilko *et al.* (1997), and detailed in table 2.5), 0.25 μL HotStar Taq, 10 μL mouse DNA and 8.5 μL distilled water. The PCR programme consisted of 35 cycles of 1 minute at 94°C, 2 minutes at 55°C and 2 minutes at 72°C. Samples were then separated on a 1.5% agarose gel as previously described (section 2.4.4).

2.10 In Situ Hybridisation

2.10.1 Tissue preparation

In this study, 11 knockouts and 11 wildtypes, matched for age and sex, were selected for experimentation. Five each of the wildtypes and knockouts were treated with 1 mg/kg haloperidol (Sigma-Aldrich, Dorset, UK) (dissolved in 0.5% hydroxypropyl methyl cellulose (HPMC)) (Fisher Scientific, Loughborough, UK) intraperitoneally and 6 of each were treated with the same volume of 0.5% HPMC (vehicle). All animals were humanely killed 6 hours after injection and according to UK Home Office guidelines governing the ethical use of animals. The brains were removed and rapidly frozen on dry ice and stored at -80ºC. 20 μm sections were cut on a cryostat through Bregma 1.00 mm and -0.40 mm, thaw-mounted onto frosted poly-L-lysine-coated slides and air-dried. Sections were fixed in fresh, ice cold 4% paraformaldehyde in 1x PBS for 5 minutes. Following a 3 minute rinse in DEPC-treated PBS, sections were transferred to 70% ethanol for 3 minutes and then stored in 95% ethanol at 4ºC.

2.10.2 Preparation of probes

DNA antisense oligonucleotide probes were designed to be complimentary to the mouse mRNA sequence of enkephalin as haloperidol has been shown to increase enkephalin and zif268 levels in the striatum (Morris *et al.* 1988). The oligonucleotide sequence was:

Enkephalin: TGCATCCTTCTTCATGAAGCCGCCATACCTCTTGGCAAGGATCTC

Homology analysis using BLASTn searches of the databases available through Ensembl (www.ensembl.org) identified no known mouse sequences to which this probe was likely to hybridise other than the desired mRNA sequence. A working stock solution of 0.3 pmol/μL was made using TE buffer, and the concentration of this working solution checked by GeneQuant (Pharmacia Biotech, Amersham, Buckinghamshire, UK) as before. Radioactive probes were made by end-labelling the oligonucleotides (MWG Biotech, Ebersberg, Germany) with [^{35}S]dATP (Perkin Elmer, Buckinghamshire, UK) using terminal deoxynucleotidyl transferase (Roche Diagnostics, Sussex, UK). This involved mixing 2 μL of oligonucleotide with 2 μL 5x TdT Reaction buffer, 0.6 μL 25mM $CoCl_2$, 2 μL DEPC-treated H_2O and 2.5 μL

[^{35}S]dATP to an eppendorf tube, vortexing the solution and adding 2 μL TdT enzyme (800 U/reaction). This was mixed by pipetting and incubated on a heat block for 1 hour at 37ºC, after which 60 μL DEPC-treated H_2O was added. To remove unincorporated nucleotides, the QIAquick Nucleotide Removal Kit (Qiagen, Crawley, UK) was utilised and the instructions followed as per the manufacturer's protocol. Briefly, 467 μL of buffer PN was added to the labelled oligonucleotide eppendorf tube and mixed. The solution was then applied to a provided column and centrifuged at 5,400 *g* for 1 minute before the column was washed with 2 x 500 μL buffer PE (including ethanol), centrifuging for 1 minute at 5,400 *g*, then for 1 minute at 11,700 *g* after the second wash. To elute the probe, the column was placed in an RNAse-free eppendorf tube, 100 μL of buffer added to the column and then centrifuged for 1 minute at 11,700 *g.* The labelled oligonucleotide was then counted on an LSA-2200 Liquid Scintillation Analyser (Perkin Elmer, Buckinghamshire, UK) to ensure a count range of 50,000 dpm/μL to 200,000 dpm/μL, after which 1 μL of 1M DTT (dithiothreitol) was added to preserve the probe from oxidation.

2.10.3 Hybridisation

Slides were removed from ethanol and allowed to air dry for up to 1 hour. 1.5 μL of labelled oligonucleotide and 1.5 μL of 1mM DTT were added to 150μl of hybridisation buffer (see 2.12.5), applied to the slides and covered with Parafilm® "M", laboratory film (American National Can™ Company, IL, USA) avoiding bubbles. The slides were placed in a dish with a towel soaked in 4x SSC (see 2.12.4) for humidity and incubated at 42^{o}C overnight. The next day slides were submerged in 1x SSC for 30 minutes at room temperature followed by 1x SSC at 55^{o}C for 30 minutes with agitation, before washing in 0.1x SSC, followed by 70% ethanol then 100% ethanol. Slides were allowed to air dry for 30 minutes before exposing to BioMax MR Emulsion film (Kodak, London, UK) for approximately 1 week. Films were developed using a HyperProcessor, automatic autoradiography film processor (Amersham Plc, Buckinghamshire, UK).

2.10.4 Imaging

Photographs of sections were taken using a Panasonic WV-BP500 camera (Berkshire, UK). Film analysis was performed on a Macintosh computer using the public domain NIH Image program.

2.11 PCR Primers and Cycle Details

Each primer was designed to be exon-intron boundary spanning, except for GAPDH, in order to preclude genomic amplification from DNA. Primers were also designed to have similar melting temperatures (Tm) of no more than 65°C and a GC (guanine and cytosine) content of approximately 40%-60%. All the primers designed for use within this thesis are detailed in table 2.5.

In order to obtain the maximum amount of information from the log linear phase of the RT-PCR reaction (described in section 2.4), the results from every second cycle number was utilised. Three of the cycles were then used to create a straight line. The novel gene PCR reaction was monitored over 3 consecutive cycles however, as the log linear phase was too short to monitor over 5 cycles. The cycle numbers for each amplicon in each cell type examined are detailed in table 2.6.

Primer Name	Sequence	Orientation
Section 2.4.3		
Ubiquilin Fwd:	5'-CTCGGTCCAGCAGTTCAAAGAGGAAAT-3'	sense
Ubiquilin Rev:	5'-TCCTCCAAGTCCACCTAAACCAAAGGAG-3'	anti-sense
Gephyrin Fwd:	5'-CTTGCTGCAAAGATTCCAGACTCCATC-3'	sense
Gephyrin Rev:	5'-CTCGCCCCATTCCATCTCGGTAAT-3'	anti-sense
EST AI169020 Fwd:	5'-CAAAATGAATTCAAATGACGCAACA-3'	sense
EST AI169020 Rev:	5'-ACTTTGTCGTAAGCTGCTTGGAATG-3'	anti-sense
EST AI176839 Fwd:	5'-CAAGAATAGACCAACACTGGCATCC-3'	sense
EST AI176839 Rev:	5'-GATATTCATTTGCAGATGGCTGGAC-3'	anti-sense
GAPDH Fwd:	5'-CCGCTGATGCCCCCATGTTTGTGAT-3'	sense
GAPDH Rev:	5'-GGCATGTCAGATCCACAACGGATAC-3'	anti-sense
Section 2.7.1		
Gephyrin Promoter Fwd:	5'-GTTCTGCCACCCATGCCGCTT-3'	sense
Gephyrin Promoter Rev:	5'-GATCATTCCCTCGGTCGCCATG-3'	anti-sense
Gephyrin Promoter Fwd SalI:	5'-AT**GTCGAC**GTTCTGCCACCCATG-3'	sense
Gephyrin Promoter Rev XbaI:	5'-GT**TCTAGA**GATCATTCCCTCGGTCGC-3'	anti-sense
Section 2.8		
Tr12253 Fwd:	5'- AGACAATCGCGTGGCCTACATG -3'	sense
Tr12253 Rev:	5'-GCTTTTTATCCTCCTCCTCAGAATCTG-3'	anti-sense
EST Ai169020 Fwd:	5'-CAAAATGAATTCAAATGACGCAACA-3'	sense
Sequence 2:	5'-GGATCCAGATTCAGTTCCTG-3'	sense
Sequence 3:	5'-GCTCTTCACCGCTTTTCTTC-3'	sense
Sequence 4:	5'-TCCGGAGACTTATGGCAATG-3'	sense
Novel Gene Fwd:	5'-AGACAATCGCGTGGCCTACAT-3'	sense
Novel Gene Rev:	5'-CGGCGAGTCTGAGCTTGAACT-3'	anti-sense
Section 2.9		
Krox24 Fwd:	5'-GAGTGTGCCCTCAGTAGCTT-3'	sense
Krox24 Rev:	5'-GGTGCTCATAGGGTTGTTCGCT-3'	anti-sense
LacZ Rev:	5'-AACGACTGTCCTGGCCGTAACC-3'	anti-sense

Table 2.5: Details of all the primers designed for this thesis. The table is split into relevant sections for ease of use and are detailed as described in the text.

Amplicon	Cell Type	Cycle Number
GAPDH	PC-12	24
	Primary Cortical Neurones	22-26
	Adult Cerebral Cortex	25-29
Gephyrin	PC-12	30
	Primary Cortical Neurones	30-34
	Adult Cerebral Cortex	33-37
Ubiquilin	PC-12	25
	Primary Cortical Neurones	28-32
	Adult Cerebral Cortex	31-35
AI176839	PC-12	30
	Primary Cortical Neurones	32-36
AI169020	PC-12	35
Urma	Primary Cortical Neurones	29-31
	Adult Cerebral Cortex	30-34

Table 2.6: Details of PCR cycle numbers monitored for each amplicon in each of the cell types examined.

2.12 Solutions & Buffers

2.12.1 Radioimmunoprecipitation (Ripa) Buffer

	Concentration	Quantity*	Supplier
Trizma Base	0.5 M	60 mg	Sigma-Aldrich, Dorset, UK
NaCl	0.15 M	87.6 mg	BDH, VWR, Poole, UK
Igepal	1%	100 μL	Sigma-Aldrich, Dorset, UK
Triton	0.5%	50 μL	Sigma-Aldrich, Dorset, UK
SDS	0.1%	10 mg	BDH, VWR, Poole, UK
Protease Inhibitor Cocktail		1 tablet	Roche Diagnostics, Sussex, UK

* Dissolved in 10 mLs de-ionised water. Stored at 4°C. pH 7.4

2.12.2 T-TBS

	Concentration	Quantity*	Supplier
NaCl	1 M	58.44 g	BDH, VWR, Poole, UK
Trizma Base	0.1 M	12.1 g	Sigma-Aldrich, Dorset, UK

* Dissolved in 1L de-ionised water. 10x stock solution. pH 7.5. Dilute 100 mLs in 1L de-ionised water then add 0.5mLs Tween-20. Stored at room temperature.

2.12.3 10x PBS

	Concentration	Quantity*	Supplier
NaCl	1.3 M	75.79 g	BDH, VWR, Poole, UK
Na_2HPO_4	70m M	9.93 g	BDH, VWR, Poole, UK
NaH_2PO_4	30m M	4.68 g	BDH, VWR, Poole, UK

* Dissolved in 1L de-ionised water. Filter, DEPC treat and autoclave. Stored at room temperature.

2.12.4 20x SSC

	Concentration	Quantity*	Supplier
NaCl	3 M	175.32 g	BDH, VWR, Poole, UK
Na Citrate	0.3 M	88.23 g	BDH, VWR, Poole, UK

* Dissolved in 1L de-ionised water. Filter, DEPC treat and autoclave. Stored at room temperature.

2.12.5 Hybridisation Buffer

	Concentration	Quantity*	Supplier
Formamide	100%	25 mL	Fluka, Sigma-Aldrich, Dorset, UK
SSC	20x	10 mL	See 2.11.4
Na_3PO_4	0.5 M	2.5 mL	BDH, VWR, Poole, UK
$Na_4P_2O_7$	0.1 M	0.5 mL	BDH, VWR, Poole, UK
Polyadenylic Acid	5 mg/mL	1 mL	Sigma-Aldrich, Dorset, UK
Dextran Sulfate		5 g	Fisher Scientific, Loughborough, UK

* Dissolved in 50mLs DEPC-treated water. Stored at 4°C.

Chapter 3

Induction of LTP-related Proteins in Cultured Cortical Neurones

3.1 Introduction

Under experimental conditions, inducing LTP usually involves the maintenance of brain slices in a constant stream of artificial cerebrospinal fluid (aCSF) with continual oxygen perfusion whilst applying electrical LTP-inducing tetanic stimuli via capillary electrodes along neural pathways or across neuronal membranes. In 2001, a new and simple pharmacological methodology was developed that allowed the chemical induction of NMDAR-dependent LTP within murine cultured primary hippocampal neurones (Lu *et al.* 2001). This involved the selective activation of synaptically located NMDARs, which are physiologically stimulated by glutamate release from presynaptic terminals. This was achieved by applying an extracellular solution, which was similar to aCSF[1] but contained an increased glucose concentration, presumably reflecting the increased glucose requirement of cultured neurones (typical glucose concentrations within culture media are approximately 20-30 mM). Importantly, the extracellular solution contained no Mg^{2+}, which is usually present at approximately 3 mM in aCSF, or at 1 mM for electrophysiological LTP inducing experimental paradigms (within Neurobasal™ culture media, this is 0.38 mM). The extracellular solution did contain glycine, the co-agonist of NMDAR, with the addition of strychnine to block the activation of non-NMDA related glycine receptors, as well as other pharmacological agents (detailed in the methods). This was reported as a significant advance over previous approaches. For example, application of NMDA may not reliably produce LTP, possibly reflecting the activation of extra-synaptic NMDA receptors, which have been linked to LTD (Lu *et al*. 2001).

Spontaneous miniature excitatory postsynaptic currents (mEPSCs) measured from single neurones can represent one or two quanta of transmitter release. An increase in the amplitude of the mEPSCs can be indicative of LTP (Manabe *et al.* 1992; Oliet *et al.* 1996). Lu *et al.* (2001), and subsequently Man *et al.* (2003), found that a three minute application of glycine perfused with the extracellular solution, and then washed out, rapidly increased the amplitude and frequency of mEPSCs. This phenomenon was eliminated when synaptic NMDARs, activated by the spontaneous release of glutamate, were selectively blocked by pre-treating cultures for 10 minutes with MK-801 (an open channel blocker of NMDAR

[1] aCSF contains approximately (mM): NaCl, 120; $NaHCO_3$, 26; KCl, 3; NaH_2PO_4, 1.25; Glucose, 10; $CaCl_2$, 2; and $MgSO_4$, 1-3.

(MacDonald & Nowak 1990; Rosenmund *et al.* 1993)). The subsequent application of glycine for 3 minutes then failed to enhance mEPSCs.

Using the same method, but with an increased exposure to glycine of 15 minutes, Ehlers (2003) looked at changes in the post synaptic density (PSD) and protein turnover within cultured cortical synapses and the effects these had on CREB and ERK phosphorylation (pCREB and pERK respectively). He found that activation of synaptic NMDARs with the application of the extracellular solution, including 200 μM glycine for 15 minutes, induced a 2 to 3 fold increase in induction of both CREB and ERK proteins when analysed by immunoblotting.

ERK is significantly activated after glutamate treatment, NMDA treatment or high frequency stimulation sustained for 3 to 15 minutes and CREB is activated after 5 to 15 minutes (Kurino *et al.* 1995; Iida *et al.* 2001; Liu *et al.* 1999; Sgambato *et al.* 1998). In 2003, Ehlers stimulated cultured rat hippocampal neurones (14 – 30 DIV), for 15 minutes with glycine in order to allow phosphorylation of ERK and CREB, as measured by western blot.

Arachadonic acid (AA) mimetics, such as ETYA, may also chemically induce LTP. LTP inducing tetanic stimulation of the hippocampal CA1 region induces the release of AA via the activation of ionotropic glutamate receptors and can alter synaptic transmission alone by increasing the slope of field excitatory postsynaptic potentials in a manner similar to LTP (Nishizaki *et al*. 1999). In addition, AA has been shown to induce LTP in 0.1mM magnesium (Kato *et al.* 1991) and can increase the amplitude of EPSPs (Ramakers & Storm 2002).

In the series of experiments presented in this chapter, an attempt was made to repeat and optimise the above protocols to permit the induction of LTP within cultured cortical neurones. The basic paradigm involved the application of the extracellular (control) solution and the addition of glycine for 15 minutes, which was subsequently removed and the neurones harvested for immunoblotting to detect phosphorylation levels of CREB and ERK proteins. The ability to produce neurochemical changes characteristic of LTP in cultured neurones would greatly facilitate studies into the mechanisms of late-phase LTP.

3.2 Aims and Objectives

- Optimise the experimental protocol to suit available laboratory conditions.

- Pharmacologically induce LTP in cultured primary cortical neurones.

- Repeat the experiment described in Ehlers (2003) by measuring ERK and CREB phosphorylation levels during pharmacologically induced LTP.

3.3 Method Development

3.3.1 Experiment 1: LTP in culture

3.3.1.1 Control Salt Solution

The following control salt solution was prepared using the description in Lu *et al.* (2001). The solution is composed of, NaCl, KCl, Glucose and $CaCl_2$, which are all present in aCSF. In addition it contains HEPES, a buffer, strychnine, which blocks glycine receptors, bicuculline, a competitive antagonist of GABARs and TTX, which blocks voltage-gated sodium channels.

	Concentration	**Quantity***	**Supplier**
NaCl	140mM	0.4g	BDH, VWR, Poole, UK
$CaCl_2$	1.3mM	65µl[a]	Fisher Scientific, Loughborough, UK
KCl	5mM	750µl[b]	BDH, VWR, Poole, UK
25mM HEPES	25mM	0.3g	Sigma-Aldrich, Dorset, UK
Glucose	33mM	0.3g	Fisher Scientific, Loughborough, UK
Strychnine	1µM	375µl[c]	Fisher Scientific, Loughborough, UK
Bicuculline	20µM	1ml[d]	Tocris, Avonmouth, UK
Tetrodotoxin	0.5µM	7.5µl[e]	Tocris, Avonmouth, UK

* Dissolved in 50mls de-ionised water. Stored at 4°C.

[a] of a 1M stock solution

[b] of a 333.3mM stock solution (2.485g in 100mls de-ionised water)

[c] of a 133µM stock solution (4.45mg in 100mls de-ionised water)

[d] of a 1mM stock solution (25mg bicuculline in 4.9mls de-ionised water, diluted 1:10 with de-ionised water)

[e] of a 3.3mM stock solution

3.3.1.2 Protocol

As Ehlers (2003) used cultured primary cortical neurones at 14-30 DIV, we utilised primary cortical neurones of similar ages (15 - 25 DIV). These were seeded in 3 wells of a 6 well plate and denoted sample 1, 2 or 3. Sample 1 received the control salt solution, sample 2 the LTP test and sample 3 an MK-801 control (figure 3.1). Firstly, the Neurobasal™ media (Invitrogen, Paisley, UK) was removed and replaced with 2 mLs control salt solution (detailed above in section 3.3.1.1) for all samples. Immediately thereafter, 10 µM MK-801 was added to sample 3 and the plate incubated at 37°C in 5% CO_2 for 10 minutes. After this

period, 200 µM glycine was added to the LTP test well (sample 2) and to the MK-801 control (sample 3) and the plate incubated for 15 minutes at 37°C in 5% CO_2. An additional culture plate was simultaneously stimulated and incubated for 2 hours at 37°C in 5% CO_2. Samples were then harvested, the protein normalised and a western blot performed as per the western blotting procedure described in section 2.6 (including ponceau S staining to check for equal levels of total protein).

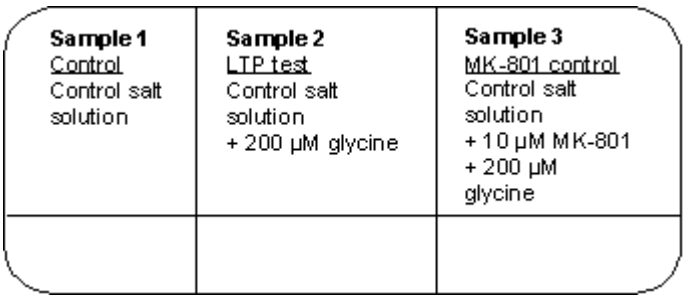

Figure 3.1: Diagram of a stylised 6 well plate illustrating the conditions of LTP in cultured cortical neurone experiments. Each plate contained a control (sample 1), LTP test (sample 2) and MK-801 control (sample 3) wells and the composition of each solution is detailed.

3.3.1.3 Results

In this first experiment, the published materials and methods in Ehlers (2003) provided the protocol. A 15-minute 200 µM glycine stimulation in the presence of the control salt solution (which contained no Mg^{2+}) was followed by a western blot to assess ERK 1/2 (p44/42 MAPK) dual phosphorylation at threonine 202 and tyrosine 204, as an indicator of LTP. In addition, cultured neurones stimulated for 2 hours were assessed for zif268 activation. As can be seen in figure 3.2, there was no significant difference between pERK levels in control and LTP test samples. There did seem to be an increase in pERK protein levels in cells pre-treated for 10 minutes with MK-801, however. Zif268 immunoreactivity was not affected by experimentation (see figure 3.2).

3.3.2 Experiment 2: The effect of phosphatase inhibitor, okadaic acid, on LTP in culture

Okadaic Acid is an inhibitor of protein phosphatase type-1 and type-2a, which de-phosphorylate phosphoproteins (Haystead *et al.* 1989). Protein phosphatases were therefore addressed as possible mediators of the unchanged phosphorylated proteins within this experimental paradigm. The experiment was conducted in the same way as experiment 1 however, 100 nM of the phosphatase inhibitor, okadaic acid (Tocris Cookson Ltd., Avonmouth, UK), was added to each well at the same

time as the control salt solution. The experiment then proceeded as previously detailed.

3.3.2.1 Results

Applying 100 nM okadaic acid to all samples before the addition of 200 µM glycine had no obvious effect on CREB phosphorylation at serine 133 or ERK 1/2 phosphorylation in either controls (sample 1 and 3) or the test well (sample 2) (figure 3.3, n=2).

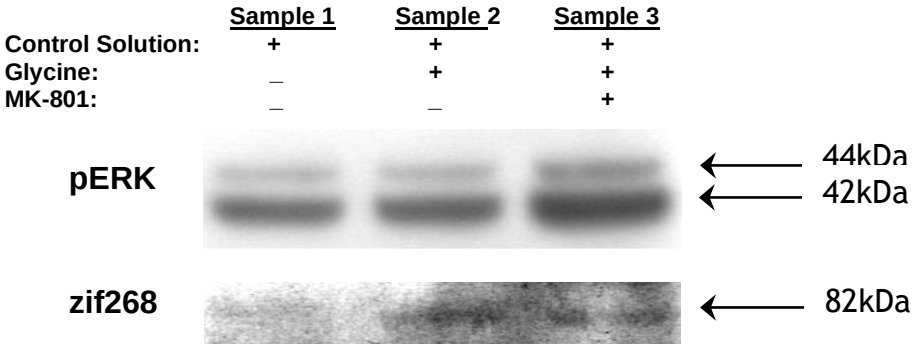

Figure 3.2: Experiment 1 - LTP in culture. Representative western blots of pERK and zif268 immunoreactivity from cultured cortical neurones after sample 3 was pre-incubated with 10 µM MK-801 for 10 minutes followed by the addition of 200 µM glycine to samples 2 & 3 for 15 minutes (for pERK) or 2 hours (for zif268), as described in experiment one. Lanes displayed: Sample 1, control; Sample 2, LTP test; Sample 3, MK-801 control. pERK, n=3, zif268, n=1.

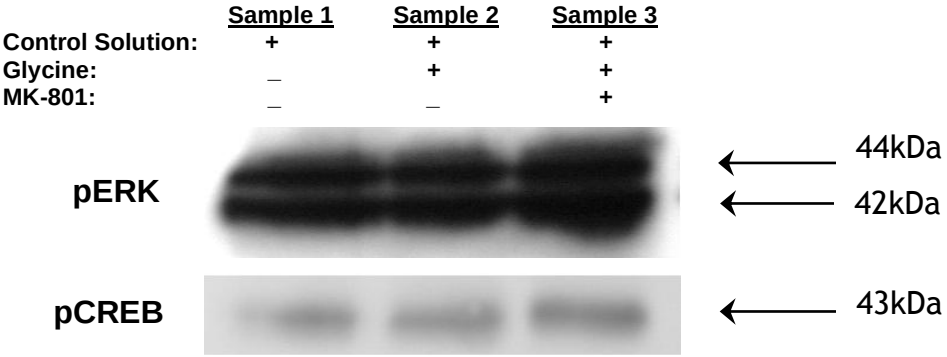

Figure 3.3: Experiment 2 – The effect of okadaic acid. Representative western blots of pERK and pCREB immunoreactivity from cultured cortical neurones after all samples received 100 nM okadaic acid with the control solution. Sample 3 was then pre-incubated with 10 µM MK-801 for 10 minutes followed by the addition of 200 µM glycine to samples 2 & 3 for 15 minutes, as described in experiment 2. Lanes displayed: Sample 1, control; sample 2, LTP test; Sample 3, MK-801 control. n=2.

3.3.3 Experiment 3: The effect of phosphatase inhibitor, cantharidin, on LTP in culture

This experiment was conducted as experiment 1, however, 0.38 mM Mg^{2+} was added to the control well (sample 1) with the addition of the control salt solution.

This served to lower the baseline of LTP-induced protein phosphorylation. All subsequent experiments (i.e. experiments 4 to 10) included 0.38 mM Mg^{2+} in the control (sample 1) well. Cantharidin (Tocris Cookson Ltd., Avonmouth, UK) (2 μM) an inhibitor of protein phosphatase 2a, was also applied to each well (sample 1, 2 and 3). The experiment then proceeded as before, with a 10 minute pre-incubation period of 10 μM MK-801 for sample 3, followed by the addition of 200 μM glycine to the LTP test and MK-801 control for 15 minutes before the samples were harvested for western blotting.

3.3.3.1.1 Results

In this experiment, total ERK (tERK) protein was also probed to confirm the normalisation of ERK protein in all experimental paradigms. Overall, there was no apparent difference between pERK or pCREB protein levels in both controls and the test well (figure 3.4, n=2).

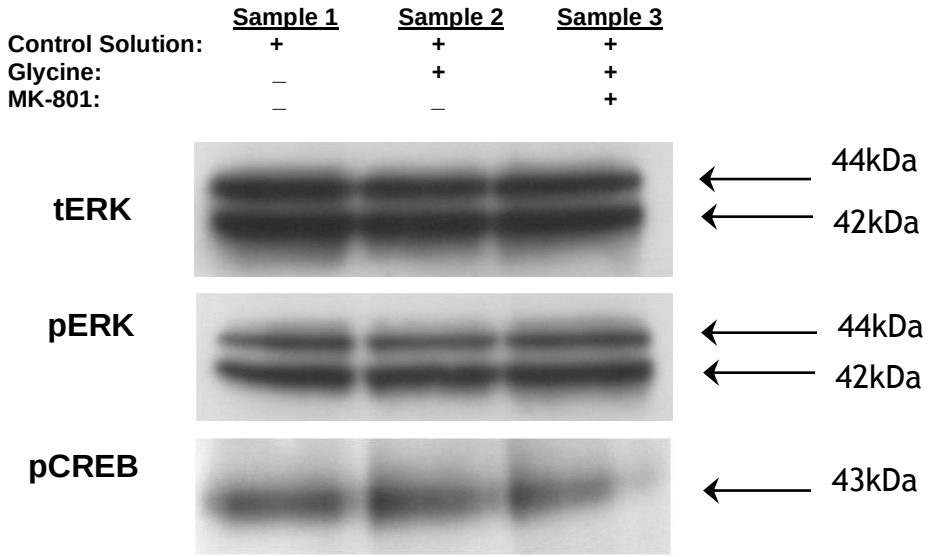

Figure 3.4: Experiment 3 – the effect of cantharidin. Representative western blots of tERK, pERK and pCREB immunoreactivity from cultured cortical neurones after treatment with 2 μM cantharidin with the control solution. Sample 3 was then pre-incubated with 10 μM MK-801 for 10 minutes followed by the addition of 200 μM glycine to samples 2 & 3 for 15 minutes, as described in experiment 3. Lanes displayed: Sample 1, control; Sample 2, LTP test; Sample 3, MK-801 control. n=2.

3.3.4 Experiment 4: The effect of osmolarity on LTP in culture

Osmolarity refers to the total molar concentration of the solutes. Rapid changes in extracellular osmolarity can have profound effects on cell homeostasis. The published data from Invitrogen Plc (Paisley, UK) regarding the Neurobasal™ media, to which was added penicillin-streptomycin (5 μg/mL) and 20% B27 serum-free supplement, allowed the calculation of the overall osmolarity used in neuronal

cells maintenance to be approximately 210 – 250 mosmol^{-1}. The salt solution was 325 – 345 mosmol^{-1} (Lu *et al.* 2001), requiring an adjustment period for the cultured cells in which the osmolarity could be raised and allow the cells to adapt. In order to increase the osmolarity of the media, 100 mM sucrose was added to the cultured primary cortical neurones overnight by removing the Neurobasal™ media from all the samples and replacing it with Neurobasal™ media containing 1.71g sucrose per 50mls media. The next day, the experiment proceeded as per experiment 3, with the control salt solution application occurring immediately before the application of 2 µM cantharidin to all samples.

3.3.4.1 Results

The Neurobasal™ media bathing the neurones was fortified with 100mM sucrose, and the cells incubated at 37^{o}C in 5% CO_2 overnight in order to raise the osmolarity of the extracellular solution. The protein levels of pERK and pCREB remained unchanged in the LTP test well (sample 2) after raising the resting osmolarity of the media before treating with 2 µM cantharidin, when compared to both the control well (sample 1) and MK-801 control (sample 3), as determined by western blotting (figure 3.5, n=2).

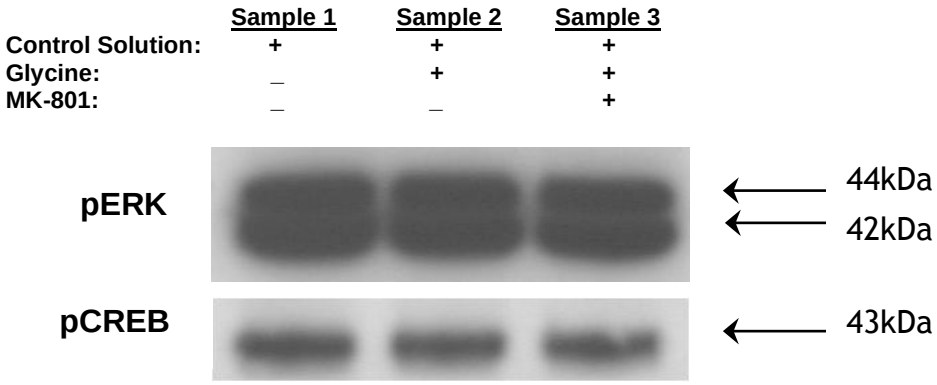

Figure 3.5: Experiment 4 – the effect of osmolarity on LTP in culture. A representative western blot of pERK & pCREB immunoreactivity from cultured cortical neurones after increasing the osmolarity of the media and treating with 2 µM cantharidin and control solution simultaneously. Sample 3 was then pre-incubated with 10 µM MK-801 for 10 minutes followed by the addition of 200 µM glycine to samples 2 & 3 for 15 minutes, as described in experiment 4. Lanes displayed: Sample 1, control; Sample 2, LTP test; Sample 3, MK-801 control**. n=2.**

3.3.5 Experiment 5: The effect of decreasing glycine cell solution bathing time on LTP in culture

On the advice of Professor Mike Ehlers and Dr Mikyoung Park, (Howard Hughes Medical Institute, Duke University), the glycine bathing time was reduced. Therefore, as before, the Neurobasal™ media for all cultured cortical neurones

was fortified with 100 mM sucrose the night prior to experimentation. The next day, all neurones received the control solution and sample 1 also received 0.38 mM Mg^{2+}. Then, 200 µM glycine was applied to samples 2 and 3, with the simultaneous addition of 10 µM MK-801 to sample 3, and cells incubated at 37^{o}C in 5% CO_2 for 3 minutes. After this period, all solutions were removed. Immediately thereafter, fresh control solution was added to all samples. Sample 1 also received 0.38 mM Mg^{2+}, sample 3 received 10 µM MK-801 and the plate was incubated for 12 minutes at 37^{o}C in 5% $CO_{2.}$ Samples were then harvested, the protein normalised and a western blot performed as per the western blotting procedure described in section 2.6.

3.3.5.1 Result

After direct contact with Professor Mike Ehlers and Dr Mikyoung Park, Howard Hughes Medical Institute, Duke University the protocol for inducing LTP was adjusted. The addition of glycine for 3 minutes to the LTP test well had no significant effect on ERK protein phosphorylation compared to controls (see figure 3.6, n=2). CREB phosphorylation did seem to increase in the LTP test well compared to sample 1 control, however there was no obvious difference between the LTP test well and the MK801 control.

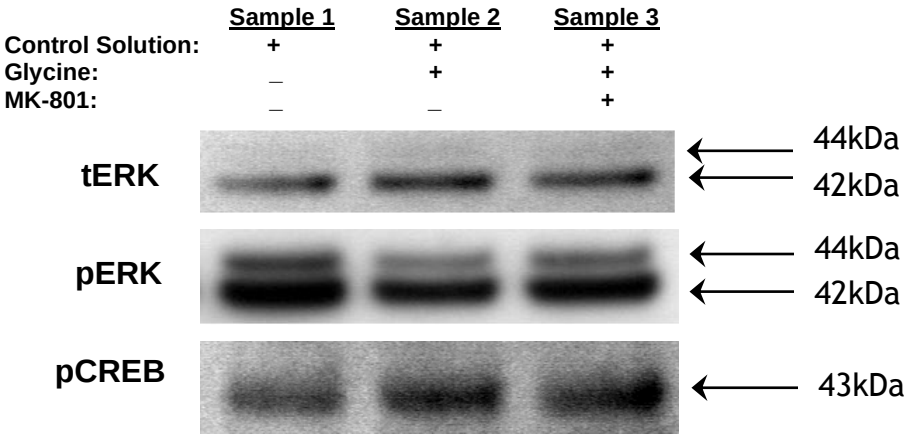

Figure 3.6: Experiment 5 – the effect of decreased glycine cell bathing time. Representative western blots of tERK, pERK and pCREB immunoreactivity from cultured cortical neurones after increasing the osmolarity of the media and treating with control solution in all samples with the addition of 0.38 mM Mg^{2+} to sample 1, 200 µM glycine to samples 2 & 3 and 10 µM MK-801 to sample 3 simultaneously for 3 minutes. This was followed by the removal of all solutions and replacement of fresh control solution to all 3 samples, with the addition of 0.38 mM Mg^{2+} to sample 1 and 10 µM MK-801 to sample 3, as described in experiment 6. Lanes displayed: Sample 1, control; Sample 2, LTP test; Sample 3, MK-801 control**. n=2.**

3.3.6 Experiment 6: The effect of decreased glycine concentration on LTP in culture

High concentrations of glycine could be counteractive to LTP induction (Lu *et al.* 2001) and therefore the effects of a decreased glycine concentration were investigated. This experiment was repeated as per experiment 5 however, only 50 µM glycine was added to sample 2 (LTP test) and sample 3 (MK-801 control) wells for 3 minutes.

3.3.6.1 Result

The addition of 50 µM glycine to the LTP test well and MK-801 control well instead of 200 µM glycine had no effect on the level of activation of ERK protein as measured by dual phosphorylation at threonine 202 and tyrosine 204, as seen in figure 3.7 (n=2). There was also no apparent difference in pERK protein phosphorylation levels between the sample 1 control and the LTP test well (sample 1).

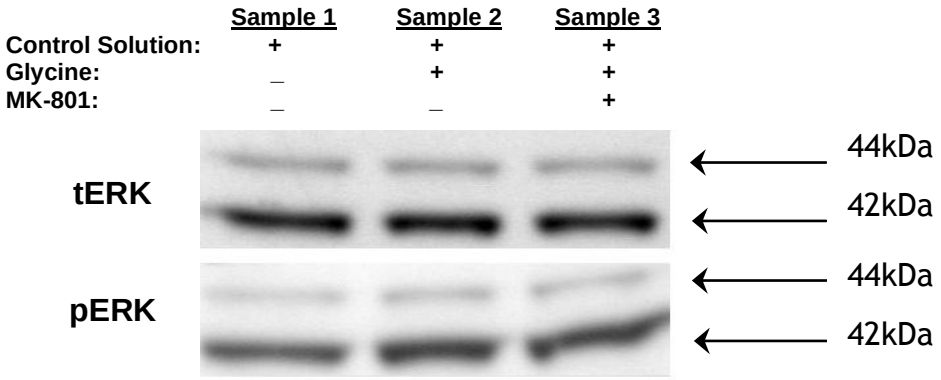

Figure 3.7: Experiment 6 – the effect of decreased glycine concentration. Representative western blots of tERK and pERK immunoreactivity from cultured cortical neurones after increasing the osmolarity of the media and treating with control solution in all samples with the addition of 0.38 mM Mg^{2+} to sample 1, 50 µM glycine to samples 2 & 3 and 10 µM MK-801 to sample 3 simultaneously for 3 minutes. This was followed by the removal of all solutions and replacement of fresh control solution to all 3 samples, with the addition of 0.38 mM Mg^{2+} to sample 1 and 10 µM MK-801 to sample 3, as described in experiment 7. Lanes displayed: Sample 1, control; Sample 2, LTP test; Sample 3, MK-801 control. n=2.

3.3.7 Experiment 7: The effect of decreased glycine concentrations with unchanged cell culture media osmolarity

This was a repeat of experiment 6 using 50 µM glycine however, the Neurobasal™ media remained unchanged and was not fortified with sucrose the night prior to experimentation.

3.3.7.1 Result

In this experiment, the media was not fortified with sucrose to elevate osmolarity in the wells of the cultured cortical neurones. Applying 50 µM glycine for 3 minutes to samples 2 and 3 with the addition of the control solution has slightly decreased the level of phosphorylated ERK protein compared to the sample 1 control and MK-801 sample 3 control (see figure 3.8, n=2).

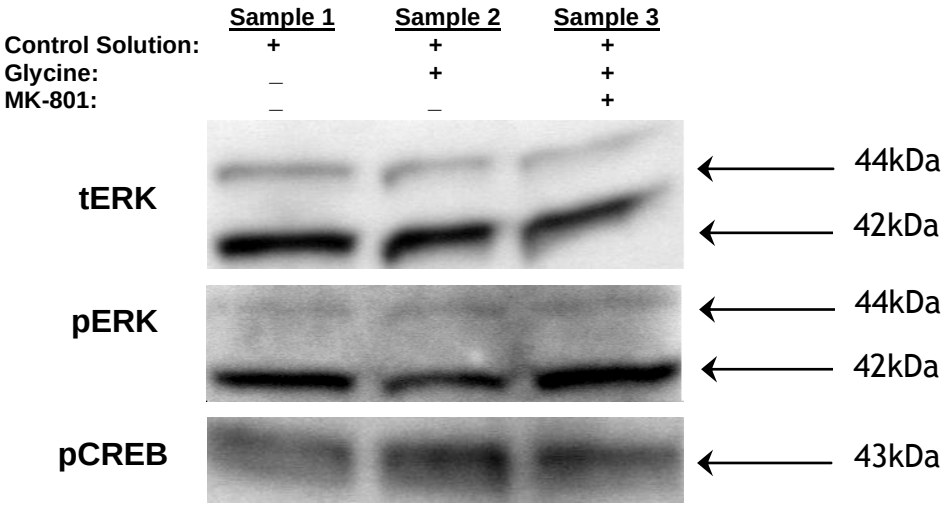

Figure 3.8: Experiment 7 – the effect of decreased glycine concentration with unchanged cell culture media. Representative western blots of tERK, pERK and pCREB immunoreactivity from cultured cortical neurones after treating with control solution in all samples with the addition of 0.38 mM Mg^{2+} to sample 1, 50 µM glycine to samples 2 & 3 and 10 µM MK-801 to sample 3 simultaneously for 3 minutes. This was followed by the removal of all solutions and replacement of fresh control solution to all 3 samples, with the addition of 0.38 mM Mg^{2+} to sample 1 and 10 µM MK-801 to sample 3, as described in experiment 8. Lanes displayed: Sample 1, control; Sample 2, LTP test; Sample 3, MK-801 control. n=2.

3.3.8 Experiment 8: The effect of ETYA on LTP in culture

ETYA is an analogue of AA, which has been implicated in LTP induction. We therefore investigated the effects of ETYA on levels of phospo-ERK protein levels in cultured cortical neurones. Firstly, 100 mM sucrose was added to the cultured primary cortical neurones the night prior to experimentation. The next day, sample 1 received the control salt solution (fortified with 0.38 mM Mg^{2+}), whilst sample 2 and sample 3 received the control salt solution only. Immediately thereafter, 200 µM glycine was added to samples 2 and 3 and 5 µM ETYA (Alexis Biochemicals, Nottingham, UK), an AA analogue, applied to sample 3. The plate was then incubated for 15 minutes at 37^{o}C in 5% CO_2, and the experiment completed as before.

3.3.8.1 Result

The addition of ETYA to sample 3 with the glycine application provided no observable differences between total ERK proteins and phosphorylated ERK proteins in the LTP test wells compared to both the sample 1 control and MK-801 sample 3 control (see figure 3.9, n=2).

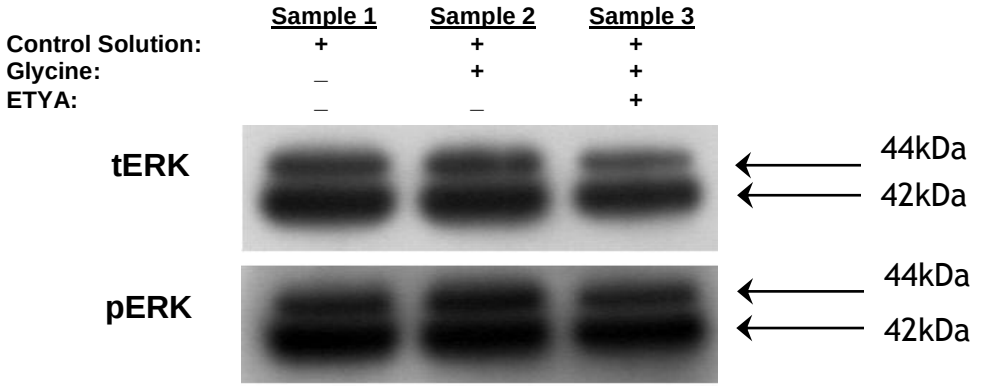

Figure 3.9: Experiment 8 – the effect of ETYA on LTP in culture. A representative western blot of tERK & pERK immunoreactivity from cultured cortical neurones after increasing the osmolarity of the media and treating the cells with the addition of 0.38 mM Mg^{2+} to sample 1, 200 µM glycine to samples 2 & 3 and 5 µM ETYA to sample 3 for 15 minutes, as described in experiment 9. Lanes displayed: Sample 1, control; Sample 2, LTP test; Sample 3, LTP and ETYA test. n=2.

3.3.9 Experiment 9: The effect of a modified salt solution on LTP in culture

A new control solution was prepared which contained the original ingredients (see section 3.3.1.1), with the exception of TTX and bicuculline, in order to maximise any possible LTP-like activity. The night prior to experimentation, the Neurobasal ™ media was fortified with 100 mM sucrose and applied to all the sample wells containing cultured cortical neurones. The next day the new control solution was applied to all samples with the simultaneous addition of 0.38 mM Mg^{2+} to sample 1, 50 µM glycine to samples 2 and 3 and 10 µM MK-801 to sample 3. All samples were then incubated at 37°C in 5% CO_2 for 3 minutes. After this period, the solutions were removed and fresh control solution added to all wells. Sample 1 then received 0.38 mM Mg^{2+}, sample 3 received 10 µM MK-801 and the plate was incubated for 12 minutes at 37°C in 5% CO_2. Samples were harvested, the protein normalised and a western blot performed as per the western blotting procedure described in section 2.6.

3.3.9.1 Result

Removing 0.5 µM TTX and 20 µM Bicuculline from the control solution and stimulating NMDAR with 200 µM glycine for 3 minutes simultaneously did not alter the phosphorylation state of ERK protein when compared to cells treated with the addition of MK-801 or cells that had not been exposed to glycine (see figure 3.10, n=2).

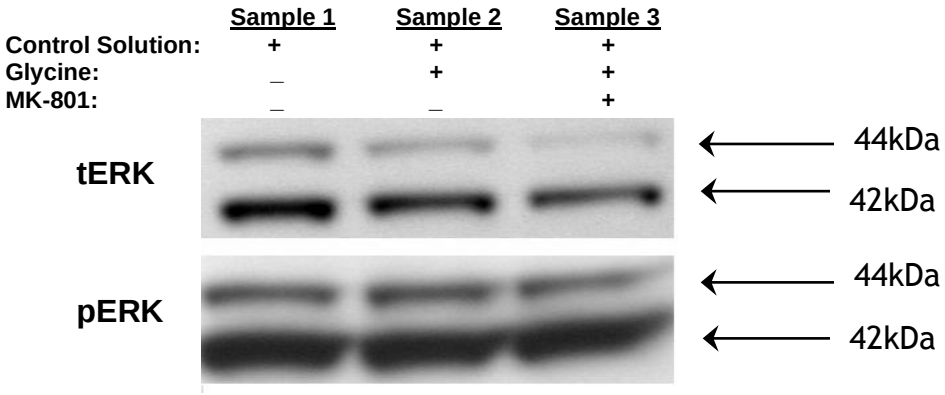

Figure 3.10: Experiment 10 – the effect of removing TTX and bicuculline from the LTP salt solution. Representative western blots of tERK and pERK immunoreactivity from cultured cortical neurones after treating with control solution lacking TTX and Bicuculline in all samples with the addition of 0.38 mM Mg^{2+} to sample 1, 50 µM glycine to samples 2 & 3 and 10 µM MK-801 to sample 3 simultaneously for 3 minutes. This was followed by the removal of all solutions and replacement of fresh control solution lacking TTX and Bicuculline to all 3 samples, with the addition of 0.38 mM Mg^{2+} to sample 1 and 10 µM MK-801 to sample 3, as described in experiment 10. Lanes displayed: Sample 1, control; Sample 2, LTP test; Sample 3, MK-801 control. n=2.

3.3.10 Zif268 is NMDAR dependently upregulated in cultured cortical neurones

In order to upregulate zif268 in a physiologically relevant paradigm, primary cortical neurones (10DIV) were stimulated with 100 µM NMDA. In the first instance, neurones were treated with either (1) vehicle, (2) 100 µM NMDA in 20mM KCl, (3) 10 µM MK-801, or (4) 100 µM NMDA in 20mM KCl and 10 µM MK-801 for 6 hours (see figure 3.11, n=1). Cytosolic proteins were then harvested and a western blot performed to visualise zif268 levels. Basal levels of zif268 protein were not detectable in the vehicle treated sample. After 6 hours, zif268 was not changed in the sample treated with MK-801 alone when compared to vehicle. There was a very small increase in zif268 protein levels in the sample treated with NMDA and MK-801, however, a noticeable increase was detected in the sample treated with 100 µM NMDA in 20mM KCl.

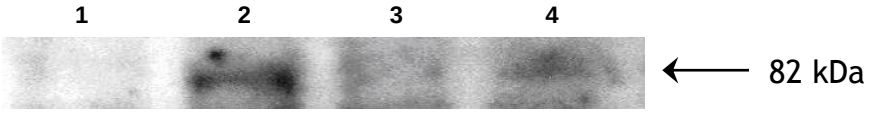

Figure 3.11: Zif268 upregulation after NMDA stimulation. A western blot of zif268 immunoreactivity from cultured cortical neurons (10 DIV) treated for 6 hours with either (1) vehicle, (2) 100 µM NMDA in 20 mM KCl, (3) 10 µM MK-801, or (4) 100 µM NMDA in 20 mM KCl and 10 µM MK-801. n=1.

3.4 Discussion

In these experimental paradigms, the results obtained by others for the induction of LTP in cultured neurones could not be reproduced. Lu *et al.* (2001) used the perfusing solution as a control, which contained the same components as the control solution used in the experiments contained within this thesis (apart from the addition of Mg^{2+} in experiments 4 - 10). In Ehlers (2003), when measuring the phosphorylation of ERK and CREB, the control was the culture media alone (Dr Mikyoung Park, personal communication). We observed no changes in phosphorylation states of ERK or CREB when compared to control in any of the experiments performed. Lu *et al.* (2001) presented evidence that MK-801 pre-treatment could block the induction of LTP within cultured cells however, there were no changes in the activation of ERK or CREB when treated with MK-801, 10 minutes before or at the same time as glycine, compared to the LTP solution alone.

In the first experiment an increase in pERK could only be seen by the addition of MK-801 to the cultured neurones. This could be due to a problem with protein normalisation, as total ERK was not measured providing a measurable basal level of protein within the cells. MK-801 blocks synaptic NMDARs; therefore it is possible to assume that non-synaptic NMDARs could be involved in the increased ERK activation relative to non-MK-801 treated cells. However, both ERK and CREB are shut off by the activation of extrasynaptic NMDAR (Ivanov *et al.* 2006; Hardingham, 2006) and in Ehlers (2001) a separate solution is used to specifically activate these receptors, which includes CNQX (an AMPAR/kainate receptor antagonist), nifedipine (a calcium channel blocker) and 100 µM NMDA.

All the experimental samples were maintained on ice from lysis to denaturation for western blotting. This maintains a low temperature, causing phosphatase inhibition. However, as there were no phosphatase inhibitors in the lysis buffer, we therefore addressed the possible problem of phosphatases by the addition of different compounds in the experimental paradigm. Okadaic acid binds to and inhibits serine/threonine protein phosphatases, allowing the accumulation of phosphorylated substrates (Tachibana *et al.* 1981; Guy *et al.* 1992). Serine/threonine protein phosphatase type 1 (PP1) and protein phosphatase type 2a (PP2a) are the dominant protein phosphatases acting on phosphoproteins (Haystead *et al.* 1989) and PP2a has been implicated in dephosphorylating ERK2

in vivo (Sontag *et al.* 1993). Okadaic acid treatment of PC-12 cells has been shown to cause an increased phosphorylation of ERK (Miyasaka *et al.* 1990), in addition, evidence suggests that CREB can be regulated by PP1 (Hagiwara *et al.* 1992; Alberts *et al.* 1994) and/or PP2 (Wadzinski *et al.* 1993; Wheat *et al.* 1994). Therefore, the addition of okadaic acid to all samples was an attempt to decrease any dephosphorylating actions of the phosphatases present in the cell extracts. However, as the results show, this approach was unsuccessful in allowing us to promote activation of either ERK or CREB in the LTP-inducing cultures when compared to controls.

As a further attempt to address the possible effects of phosphatases acting on CREB and ERK phosphorylation states, cantharidin was added to cultures along with the control solution. This protein phosphatase inhibitor, like okadaic acid, also suppresses the activities of both PP1 and PP2a (Honkanen 1993; Li *et al.* 1993b; Knapp *et al.* 1998). As with previous experiments, the addition of cantharidin did not assist ERK and/or CREB protein phosphorylation in the LTP test samples. Any future experiments would probably benefit from the addition of phosphatase inhibitors in the RIPA buffer, rather than altering the experimental solution.

An increased extracellular osmolarity causes decreases in cell volume and can cause neurotransmitter release (Basarsky *et al.* 1994). Cell shrinkage can lead to changes in cellular functions by concentrating intracellular macromolecules, leading to increased macromolecular activity, and activation of membrane transporters (Parker & Colclasure 1992). It can also lead to protein and glycogen inhibition as well as stimulating glycogenolysis and proteolysis, (whereas cell swelling has the opposite effect) (Haussinger *et al.* 1994). The cellular homeostasis was maintained therefore by increasing the osmolarity of the cell culture media the night prior to experimentation, allowing the cells to adjust to environmental changes outwith the critical experimental time period. Testing cellular responses to the LTP inducing solution with or without sucrose fortification of the cell culture media displayed no differences in ERK or CREB activation when compared to controls.

Professor Mike Ehlers and Dr Mikyoung Park, (Howard Hughes Medical Institute, Duke University) advised that the control solution, glycine and MK-801 should be added to the wells simultaneously, as the addition of the control salt solution without the Mg^{2+} was already activating the synaptic NMDARs during the MK-801

preincubation. They also recommended that the glycine activation should only be for a total of 3 minutes. Incorporating these changes into the experimental procedure produced no differences in the phosphorylation of ERK or CREB between the control, MK-801 control or LTP samples. There is a possibility that the pre-incubation of MK-801 is a necessary step for the effective blocking of NMDAR channels and therefore any further attempts may require the addition of MK-801 to the culture media 10 minutes before the addition of the control solution and glycine.

Applying 200 µM of glycine to cells is a suprasaturating level (Lu *et al.* 2001), and it has been reported that saturating the NMDAR at the synapse will induce glycine-primed endocytosis and therefore leave a lower number of receptors available to engage in LTP (Nong *et al.* 2003; Martina *et al.* 2004). Therefore, we decided to decrease the glycine concentration to 50 µM to look at LTP induction within cultured cells. This had no effect on the phosphorylated proteins involved in the LTP signalling pathway.

ETYA (5,8,11,14-eicosatetraynoic acid) is a polyunsaturated fatty acid analogue of AA and current published results indicate that AA can facilitate LTP induction (Williams *et al.* 1989; Drapeau *et al.* 1990; O'Dell *et al.* 1991). However, application of ETYA at a concentration sufficient to mimic AA actions (Ramakers & Storm 2002) did not elevate pERK or pCREB levels.

The LTP inducing solution (control solution with the addition of glycine) contained strychnine to block glycine receptors. In addition, it contained bicuculline, a competitive antagonist of, primarily, the ionotropic GABA receptors. These would serve to limit inhibitory actions on the cell. HEPES is an organic chemical buffer that maintains physiological pH and TTX selectively blocks voltage-gated sodium channels, therefore blocking the passage of action potentials. TTX was removed from the solution in order to allow the passage of action potentials along the neurones and because of evidence that it could cause a large decrease in the levels of pERK (Chandler *et al.* 2001). Bicuculline was also removed to reduce any excessive activity in control culture wells. This produced no effect on the activation of ERK or CREB after the addition of glycine when compared to the non-glycine control or MK-801 control.

The experiments described in the results section involved the manual removal and application of all solutions. However, in Lu *et al.* (2001) each well was continuously superfused (1 mL/min) from a single barrel of a computer-controlled multibarreled perfusion system, with glycine supplementation applied from an alternate barrel. This small, but significant, alteration could be a major factor in the failure of ERK and CREB phosphorylation. There is a possibility that solutions were not entirely removed, leaving residual unwanted compounds within the wells. If they were indeed completely removed, this would lead to rapid homeostatic changes within the cells, and possibly oxygen and electrolyte starvation between solution changes. In addition, cultured cortical neurones were utilised in this study rather than cultured hippocampal neurones in the literature. However, the mechanisms of synaptic plasticity are believed to show extensive commonalities between the cortex and the hippocampus.

English & Sweatt (1996), investigating the role of ERK in hippocampal LTP, found that p42 ERK, but not p44, is activated in area CA1 after direct activation of PKC and NMDAR, and after LTP inducing high frequency stimulation. We found no evidence to support this within cultured cortical neurones.

Zif268 protein levels were also unchanged by application of the LTP salt solution. Therefore, NMDA stimulation was used to induce zif268 in order to gauge downstream effects. The caveat with this technique is that it causes changes not only to zif268, but also to many other genes, proteins and processes within the cells. Nevertheless, it is a physiologically relevant paradigm and consistent with the NMDAR-dependent LTP involved in synaptic plasticity. In order to show zif268 induction, NMDA in KCl was applied to cultured cells and the results compared with several controls. KCl was used to depolarise the cell in order to relieve the magnesium block within the NMDAR, which activated zif268 as detected by western blot. This effect was attenuated with the addition of MK-801. As additional controls, the effects of the experimental vehicle and MK-801 alone were separately analysed and were found not to induce zif268. Therefore, NMDA activates a profusion of cellular targets, which also includes increasing zif268 expression. In this particular western blot the Visualiser system was used as it seemed to detect low levels of protein more effectively than ECL. The zif268 antibody is directed towards the C-terminal, and has been characterised and referenced for many years (Murphy *et al.* 2004; Thyss *et al.* 2005).

In summary, phosphorylation states of the ERK and CREB proteins did not differ from total ERK amounts or either of the controls suggesting that these proteins were not activated in any paradigms tested. The results suggest that the described protocols, while possibly capable of inducing a short term facilitation of synaptic transmission, may not induce the pattern of change in signalling pathways that are characteristic of LTP in hippocampal or cortical tissue. However, NMDA and KCl treatment of cortical neurones in culture increases pERK levels (Rakhit *et al.* 2005) and pCREB levels (Conway & Morris, unpublished) in an MK-801 sensitive manner. The evidence that zif268 levels are also increased (figure 3.12) suggests that exposure of cultured neurones to NMDA, in the presence of a mild depolarising agent such as 20 mM KCl, produces many of the biochemical changes associated with LTP. NMDA application can induce LTP in the presence of ACPD, an mGluR agonist, which was APV dependent (Fujii *et al.* 2003). In addition, it can potentiate synaptic transmission in the hippocampus (Kauer *et al.* 1988; Broutman & Baudry 2001). Lee et al (2001) found that a 3-minute application of 20 μM NMDA induced LTD in the CA1, which was measured for 1 hour. Broutman & Baudry (2001), describe a 5 minute 50 μM NMDA application initially inducing LTD, which then increases EPSP amplitudes above baseline after 1 hour. Therefore, the duration of NMDA application, and subsequent measurement of activity, may be time sensitive for LTP induction. However, whether or not NMDA/KCl induces LTP, it appears to activate a plasticity-signalling pathway of ERK - CREB - zif268 and hence is of use to study events downstream of zif268 induction.

Chapter 4

Gephyrin as a downstream target of zif268

4.1 Introduction

Gephyrin (Prior *et al.* 1992) was originally identified as a peripheral membrane protein (Schmitt *et al.* 1987) and is a ubiquitously expressed 93 kDa receptor-associated protein. In mouse the gephyrin gene spans 457 kb, containing 30 exons, and is located on chromosome 12D2. In humans it is 668 kb with 27 exons located on chromosome 14q23.3 (Rees *et al.* 2003). The gene encodes a protein containing an N-terminal G-domain, a C-terminal E-domain (which show high similarity to and are therefore named after, the *E.Coli* proteins Mo**g**A and Mo**e**A respectively) and a proline-rich linker region in the centre. The N-terminal domain forms a trimer and the C-terminal forms a dimer leading to the synaptic assembly of a gephyrin hexagonal submembrane lattice, onto which receptors are anchored (Kneussel & Betz 2000; Schwarz et al. 2001; Sola et al. 2001).

4.1.1 Gephyrin Splice Variants

Gephyrin is a highly mosaic gene due to the numerous exons in both mouse and human; many gephyrin gene variants have been identified. Splicing occurs in all three domains with each domain containing at least 3 variable exons. Alternative splicing has been found to affect the functions of gephyrin in mouse, but not human, and is ideal for dealing with the diverse functional demands of this protein.

In mouse there are ten exons that can be spliced out, denoted C1-C7 and C4′-C6′ (Paarmann *et al.* 2006). The C7 cassette contains a stop codon (Sola *et al*. 2004) effectively truncating the protein at the C-terminus, interfering with the interaction of many of gephyrin's binding partners. Nova proteins, neuronal regulators of pre-mRNA splicing, control the C3 cassette in neurones (Ule *et al.* 2003), indicating the possible importance of C3 in the periphery. The inclusion of C5′ may interfere with GlyR anchoring in hippocampal and spinal cord neurones (Meier & Grantyn 2004). Cassette 1 does not produce detectable hybridisation results within rat adult and developing brains (Kirsch et al. 1993), suggesting little or no mRNA signals for this particular exon. This evidence led to the avoidance of cassette 1 when designing *in situ* hybridisation oligonucleotide probes for experimentation within this thesis.

Alternative splicing may be tissue specific suggesting that gephyrin's function may be altered in each case. For example, there are copious quantities of cassette C3

in the liver (Prior *et al.* 1992), whilst C5 seems more abundant in muscle than other tissues (Ramming *et al.* 2000).

4.1.2 Regional & Cellular Distribution of Gephyrin

Gephyrin and its variants are found in peripheral tissues in the heart, muscle, retina, testis, spleen, kidney, lung and liver, as well as in the central nervous system (Hermann *et al.* 2001; Prior *et al.* 1992).

Immunoreactivity of gephyrin in the brain is widely distributed and can largely be found at its most intense in layers III, V and VI of the neocortex. The hippocampal formation shows high levels of immunoreactivity, especially in the granule cell layer of the dentate gyrus. The amygdaloid nuclei show varying amounts, while the thalamic nuclei show high to moderate amounts. It is distributed heterogeneously throughout the medulla and shows intense labelling in the pons (Waldvogel *et al.* 2003).

At a cellular level, gephyrin immunoreactivity is found on the plasma membrane of the soma and dendrites, probably representing postsynaptic sites. Immunoreactivity is also found intracellularly, presumably reflecting the intracellular localisation of recently formed protein, which is en route to receptor membrane sites (Waldvogel *et al.* 2003).

4.1.3 The role of Gephyrin & Glycine Receptors

Gephyrin co-purifies with the mammalian glycine receptors (GlyRs) found in rat spinal cord (Pfeiffer *et al.* 1982; Graham *et al*. 1985). Gephyrin binds via its MoeA domain to an 18-amino-acid amphipathic sequence in the large intracellular loop connecting transmembrane segments 3 and 4 of the GlyR β subunit (Meyer *et al.* 1995; Kneussel *et al.* 1999b). As mentioned in the introduction, gephyrin seems to play a crucial role in the postsynaptic clustering of GlyRs and $GABA_A$Rs, although information regarding the relationship between $GABA_A$Rs and gephyrin can often be contradictory. The role of gephyrin at glycinergic synapses can point towards a possible generalized mechanism for inhibitory receptor accumulation at synapses by gephyrin.

Both GlyRs and $GABA_A$Rs belong to a superfamily of ligand-gated ion channels that share common structural and functional features as well as similar

transmembrane topologies (Moss & Smart 2001; Schrader *et al.* 2004). The GlyR is composed of the α and β subunits, 2 glycosylated integral membrane proteins which have a stoichiometry of either three α to two β subunits (Langosch *et al.* 1988) or two α to three β subunits (Grudzinska *et al.* 2005). Four genes encode the α subunits (GLRA1-4) together with a single β polypeptide gene (GLRB). GlyRs allow the passage of chloride ions through the central pore of the pentameric receptor formed by the M2 α-helical segments of the individual subunits. This hyperpolarizes the cell in mature neurones, thereby preventing action potentials. Glycine is the major inhibitory neurotransmitter in the spinal cord and brainstem.

Gephyrin binds to heteromeric GlyR with high affinity (Kirsch *et al.* 1995), and in cultured spinal neurones anchors and immobilises GlyRs on the subsynaptic cytoskeleton (Kirsch & Betz 1995) suggesting that gephyrin organises the development, localisation and clustering of GlyRs at inhibitory post-synaptic membrane specialisations (Kirsch *et al*. 1996). It has been shown that the loss of gephyrin expression via antisense depletion of primary neurones (Kirsch *et al*. 1993) or by gene knockout in mice (Feng *et al*. 1998), prevents the synaptic clustering of GlyRs. Single expression of GlyR β (but not α) subunits targeted to intracellular gephyrin aggregates in HEK293 cells show that gephyrin binding is mediated by the β subunit (Kirsch *et al.* 1995). In addition, the β subunit is responsible for receptor assembly and channel properties (Kirsch 2006).

During embryonic development, gephyrin accumulates at spinal postsynaptic sites prior to the GlyR (Kirsch *et al.* 1993; Bechade *et al.* 1996), and promotes receptor clustering in an activity dependent manner (Kirsch & Betz 1998). It has been proposed that glycine induces calcium signals, triggering transmitter release in embryonic cultured neurones (Kirsch & Betz 1998). This causes gephyrin to accumulate at the cytoplasmic face of nerve terminal-postsynaptic cell specialisations in spinal cord and other regions of the CNS (Triller *et al.* 1985; Altschuler *et al.* 1986). Gephyrin binds with high affinity to polymerised tubulin (Kirsch *et al.* 1991) and microfilaments (Kirsch & Betz 1995; Giesemann *et al*. 2003) as well as to the GlyR (Meyer *et al* 1995; Kneussel *et al.* 1999). Gephyrin clusters could then trap GlyRs creating a postsynaptic GlyR matrix increasing gephyrin cluster size further, possibly by way of local cytoskeleton reorganisation. Extrasynaptic receptors from non-innervated plasma membrane would then be

removed. Similar information regarding the accumulation of $GABA_A$Rs and gephyrin at postsynaptic specialisations still requires clarification.

In young cultured neurones (early DIV), spontaneous formation of gephyrin-GlyR clusters at non-innervated plasma domains are consistently observed (Kirsch & Betz 1995) (Levi *et al.* 1999). However, these accumulations may precede gephyrin-dependent clustering, creating a two-step process (Meier *et al.* 2000b). In spinal interneurones, newly synthesised GlyRs diffuse in the plasma membrane as stable clusters (Rosenberg *et al.* 2001) and the interaction of GlyR with gephyrin increases its rate of accumulation at synapses. During development, gephyrin is associated with intracellular somatic and dendritic vesicles both *in vitro* and *in vivo* (Colin *et al.* 1996; Colin *et al.* 1998). After partial glycine denervation, gephyrin is detected with vesicles in the area of the golgi apparatus (Seitanidou *et al.* 1992).

Transfecting gephyrin-GFP reveals that many GlyR puncta are co-localised with gephyrin around the nucleus and throughout the cytoplasm in COS-7 cells and 3DIV spinal cord neurones (Hanus *et al.* 2004). This interaction alters the behaviour of intracellular aggregates of gephyrin-GFP-GlyR compared to aggregates of gephyrin-GFP alone. When in the presence of the GlyR binding domain, aggregates are seen to move more rapidly, with a directed movement away from or toward the centre of the cell compared to the gephyrin-GFP aggregates. It was also found that microtubule depolymerisation by 1μM nocodazole dramatically reduced the displacements of gephyrin-GFP aggregates associated with the binding domain, suggesting that they usually travel along the microtubules along the secretory pathway. Movements of gephyrin-GFP aggregates were not affected. Moreover, by using temperature changes to block GlyR in and then release it from the trans-golgi network, it was shown that gephyrin accelerates the accumulation of GlyR and increases the number of receptors at the plasma membrane of the soma, followed by the neurites.

4.1.4 Additional functions of Gephyrin

Homozygous disruption of the murine gephyrin gene is lethal at birth (Feng *et al.* 1998), and autoimmunity to gephyrin has been reported in a patient with Stiff-Man Syndrome (SMS) (Butler *et al.* 2000). In addition, gephyrin knockout mice display a loss of molybdenum coenzyme (MoCo) dependent enzyme activities in liver and

intestine and share the same phenotype as human hereditary hyperekplexia (Johnson *et al.* 1989), a neurological disorder caused by mutations to glycine receptors (Shiang *et al.* 1993; Rees *et al.* 1994; Rees *et al.* 2002) and MoCo deficiency (Reiss *et al.* 2001). Gephyrin catalyses crucial steps in MoCo biosynthesis, specifically in the incorporation of molybdenum, which is important for the activity of different oxidoreductases (Johnson *et al.* 1989) and is a highly conserved process from bacteria to mammals. There are significant sequence similarities between gephyrin and MoCo biosynthesis proteins from bacteria (Nohno *et al.* 1988), invertebrates (Kamdar *et al.* 1994) and plants (Stallmeyer *et al.* 1995). Indeed, transfection of rat gephyrin has been shown to rescue the phenotype of MoCo biosynthesis mutants in E.Coli and plants (Stallmeyer *et al.* 1999). This is a novel non-neuronal catalytic function of gephyrin in intermediary metabolism that is not connected to synaptogenesis, and is a possible explanation for the ubiquitous expression and distinct splice variants of the gephyrin gene in all mammalian tissue (Prior *et al*. 1992).

Gephyrin has also been found to interact with RAFT1, the rapamycin and FKBP12 target protein (Sabatini *et al.* 1999). This could regulate the subsynaptic translational machinery thought to initiate protein synthesis in dendritic subcompartments and will be dealt with in more depth in chapter 6.

Overall there is considerable evidence that gephyrin is widely expressed and has the capacity to form many isoforms with distinct functions. This may enable gephyrin to perform multiple functions in relation to synapse formation and maintenance. As detailed previously, gephyrin is linked to the postsynaptic clustering of GlyRs as well as $GABA_A$Rs and therefore may play a key role in inhibitory neurotransmission. This chapter attempts to expand our knowledge of gephyrin with reference to synaptic plasticity and introduces this scaffolding protein as a novel downstream target of zif268.

4.2 Aims & Objectives

- Identify and verify the presence of gephyrin within the PC-12 cell line.

- Validate the original microarray experiment by transfecting PC-12 cells with full length or truncated zif268 and investigating any changes in gephyrin RNA and protein levels.

- Extend the findings found in PC-12 cells by using primary cortical neurones stimulated with either NMDA or vehicle over 24 hours and investigating gephyrin expression at the RNA and protein levels.

- Look at Gephyrin RNA and protein levels harvested from zif268 knockout and wildtype mice to investigate the effects of genetic manipulation.

- Investigate whether gephyrin mRNA levels are altered after administration of haloperidol, which induces zif268 in striatal neurones, in wildtype mice and in mice with a targeted genetic deletion of zif268.

4.3 Results

4.3.1 PC-12 cells stain positively for gephyrin

Identification of gephyrin expression within the PC-12 cell line was achieved using immunocytochemistry on partially differentiated and undifferentiated cells using a mouse anti-gephyrin antibody. Secondary antibody staining alone was essentially used as a control to illustrate that there is no non-specific staining in cells treated with or untreated with nerve growth factor (figure 4.1 A & B). There is a marked difference in cells probed with anti-gephyrin. In undifferentiated cells, distinct puncta can be seen throughout the cytoplasm (figure 4.1C). Nerve growth factor treated PC-12 cells show a neuronal-like shape with the appearance of processes. Gephyrin immunoreactivity can be seen throughout the cell and processes and displays stronger staining than undifferentiated PC-12 cells (figure 4.1D).

4.3.2 Gephyrin is downregulated in PC-12 cells after transient transfection with zif268

RT-PCR was performed using GAPDH primers and exon-intron spanning primers for gephyrin. Gephyrin RNA was significantly downregulated after transient transfection of 1 µg/mL full-length zif268 cDNA in PC-12 cells pre-treated with 50 ng/mL nerve growth factor when compared to cells transfected with 1 µg/mL of truncated zif268 cDNA ($p<0.05$, one sample t-test, $n=5$; see figure 4.2). Gephyrin displays a decrease of 28% in RNA levels of PC-12 cells transfected with full-length zif268 compared to controls.

Figure 4.3 is a representative blot of a PVDF membrane stained with Ponceau S solution directly after protein transfer and immediately prior to blocking. Uniformity of protein bands allowed the continuation of the western blot.

Gephyrin protein levels display a significant downregulation of 7% in PC-12 cells transiently transfected with full-length zif268 compared to control ($p<0.05$, one-tailed one sample t-test, $n=6$; see figure 4.4 A & B).

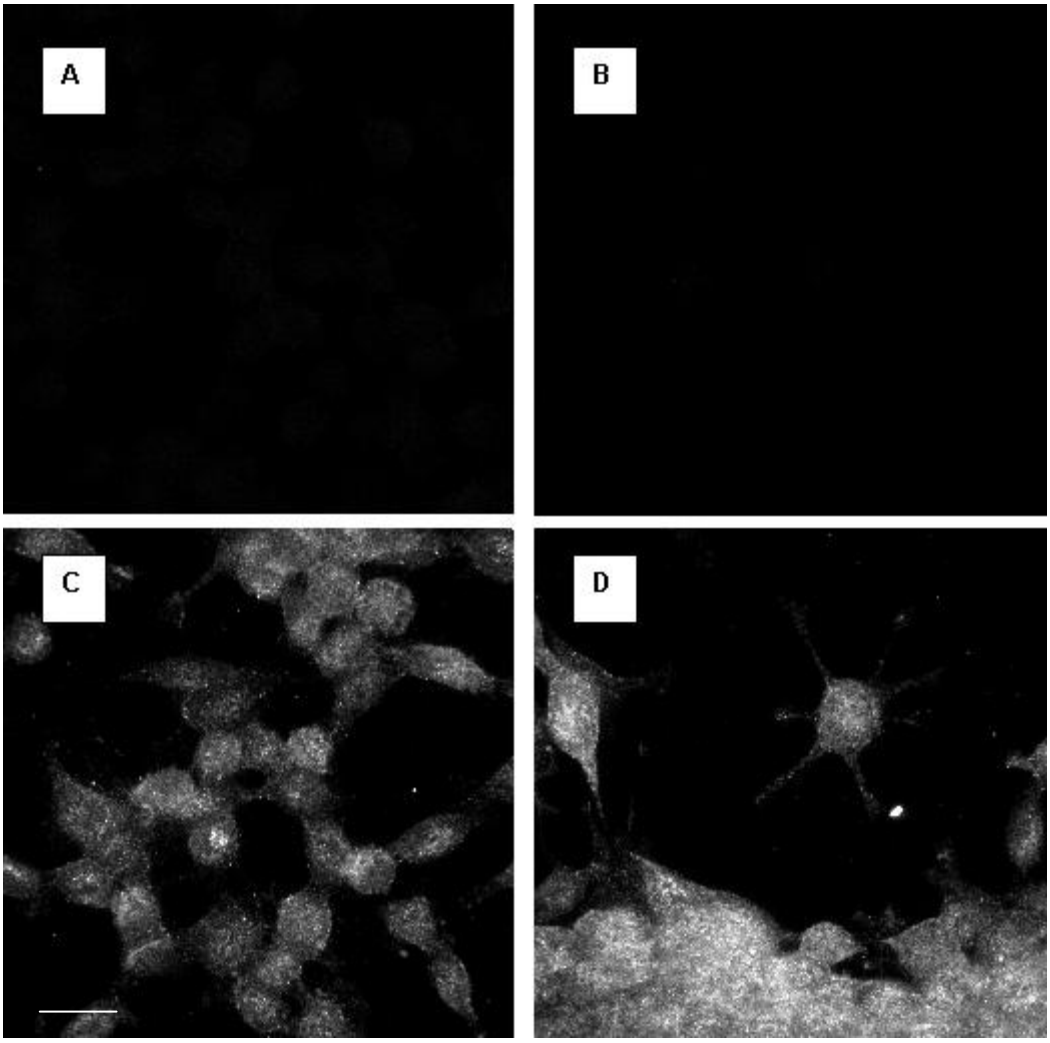

Figure 4.1: Confocal images of gephyrin in PC-12 cells. *A,* undifferentiated PC-12 cells stained only with 1:100 anti-mouse Alexa 594 secondary antibody. *B,* PC-12 cells pre-incubated for 2 hours with 50ng/mL NGF-7S and stained only with anti-mouse Alexa 594 secondary antibody. *C,* undifferentiated PC-12 cells stained with 1:100 anti-gephyrin and 1:100 anti-mouse Alexa 594. D: PC-12 cells pre-incubated for 2 hours with 50ng/mL NGF-7S and stained with 1:100 anti-gephyrin and 1:100 anti-mouse Alexa 594 secondary antibody. Scale bar 15μm.

4.3.3 Gephyrin is time-dependently downregulated in cultured cortical neurones after NMDA treatment

As mentioned in Chapter 2, cultured cortical neurones prepared for western blotting and RT-PCR were 7-10 DIV. Neurones treated immunocytochemically were 21 DIV. It was reasoned that whole cell measures of gephyrin did not require localisation at the synapse, and therefore did not need to be aged for 21 days, which was technically very challenging.

Throughout this thesis, three statistical tests are performed. The one sample t-test is used when comparing treated PC-12 cells to control and analyses the mean value of the sample to a known value, which, in this thesis, is 100% (the control value). In addition, the ANOVA was used when comparing primary neurones treated with NMDA for differing lengths of time. This tests the analysis of variance

between groups and is preferable to performing numerous t-tests. The ANCOVA is utilised when there is a shared covariate (in this case, GAPDH) and a control and treated group. This compares two linear regressions and is a statistical control for the variability found in some reference genes (Bond *et al.* 2002).

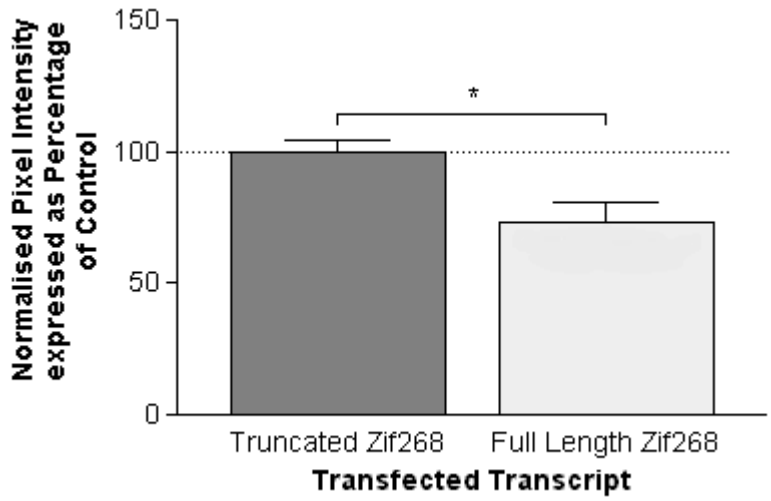

Figure 4.2: The effect of zif268 on gephyrin mRNA levels in PC-12 cells. Graph comparing gephyrin mRNA levels from PC-12 cells transiently transfected with either truncated or full-length zif268, as assessed by signal intensities at a single RT-PCR cycle. Results are presented as gephyrin normalised pixel intensity after normalisation to the corresponding GAPDH. All data expressed as a mean percentage of control (mean signal after expression of truncated zif268) ± SEM, *p<0.05, one sample t-test, n=5.

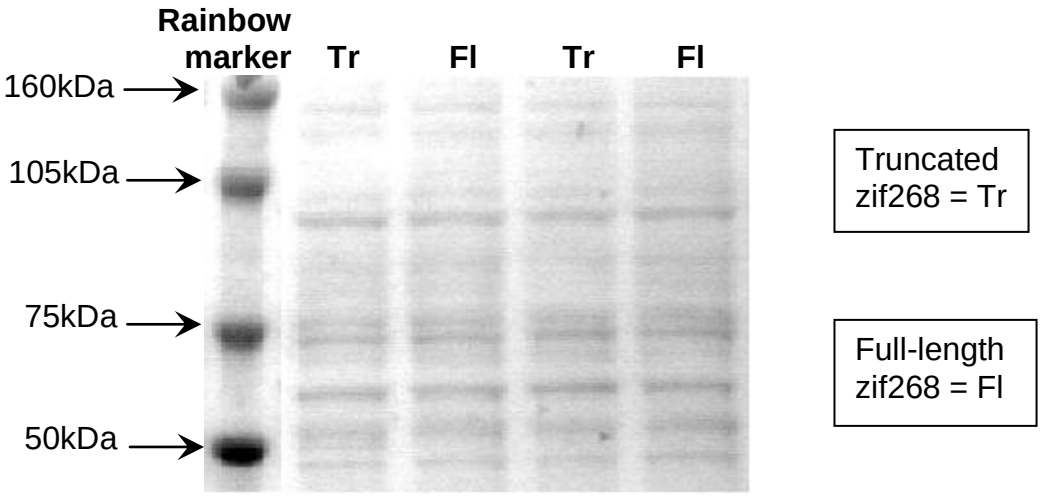

Figure 4.3: Representative image of a western blot of a PVDF membrane stained with Ponceau S solution directly after transfer. This blot contains two lanes of cytosolic lysates from PC-12 cells transiently transfected with truncated zif268 (Tr) and two lanes of cytosolic lysates from PC-12 cells transiently transfected with full-length zif268 (Fl).

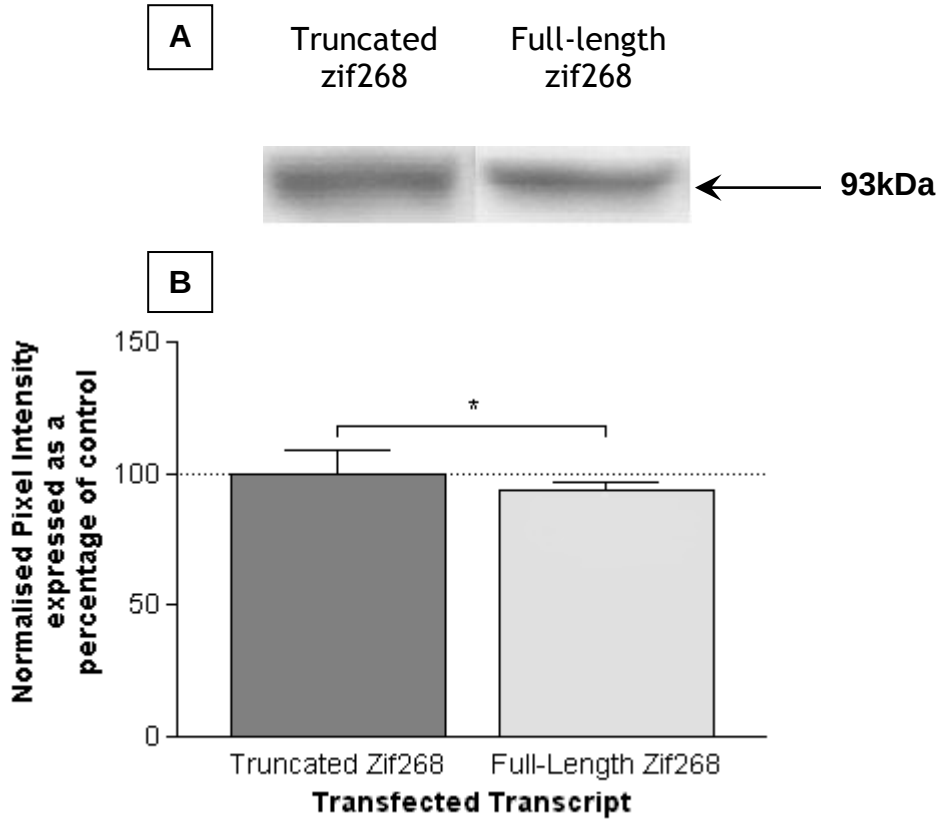

Figure 4.4: The effect of zif268 on gephyrin protein levels in PC-12 cells. *A,* Representative western blot comparing gephyrin immunoreactivity in PC-12 cells transiently transfected with either truncated or full-length zif268. *B,* Graph comparing gephyrin protein levels from PC-12 cells transiently transfected with either truncated or full-length zif268 as determined by western blotting. Results are presented as gephyrin normalised pixel intensity. All data expressed as a mean percentage of control (mean signal after expression of truncated zif268) ± SEM, *p<0.05, one-tailed one sample t-test, n=6.

Gephyrin mRNA harvested from 6 hour NMDA stimulated primary neurones (7-10 DIV) was significantly downregulated in the RT-PCR reaction when compared to neurones treated with vehicle for 6 hours ($p<0.01$, $F(1,16) = 11.69$, ANCOVA, n=4; see figure 4.5). In contrast, at 24 hours gephyrin mRNA was not significantly altered in primary cortical neurones stimulated with NMDA compared to neurones stimulated with vehicle ($p>0.05$, $F(1,15) = 1.84$, n=4; figure 4.6). It can be seen within the graph that the regression lines do not touch and that the 3 datasets (representing information taken at 3 different cycle numbers) are clearly defined. The log values have been used within the statistical analysis as this can decrease the variability found when comparing various arbitrary numbers (pixel intensity), without changing the relationship between the numbers.

Utilising immunocytochemistry, an overall effect of NMDA stimulation was found on gephyrin immunoreactivity when compared to vehicle treated primary cultured cortical neurones ($p<0.01$ $F(1,30) = 15.67$, 3-way ANOVA (factors: time, treatment

and culture), n=6; see figure 4.7). In particular, gephyrin protein levels are downregulated when stimulated for 3 hours with NMDA, displaying 29.83% ± 8.39 less immunoreactivity per square micron compared to vehicle-treated cells ($p<0.05$, Tukeys *post hoc* test). Figure 4.8 shows representative images of neurones stimulated for 3 hours with either with 100 µM NMDA in 20 mM KCl or vehicle. There was no overall effect of time ($p = 0.283$, $F(2,30) = 1.32$) and no interaction between treatment and time ($p = 0.522$, $F(2,30) = 0.67$). For normalisation and resultant statistical analysis, the log value of pixel intensities was used. For graphical representation all values are presented as percentages of control (vehicle treatment).

Gephyrin protein levels determined by western blotting of cultured cortical neurones also show an overall effect of NMDA stimulation when compared to vehicle treated cells ($p<0.01$, $F(1,23) = 28.12$, 3-way ANOVA (factors: culture, time and treatment); see figure 4.9 A & B). Specifically, there was a significant downregulation of gephyrin immunoreactivity of primary cortical neurones stimulated for 3 hours with 100µM NMDA in 20mM KCl showing 37.82% ± 10.19 of immunoreactivity compared to vehicle treated cells ($p<0.01$, Tukeys *post hoc* test). There was also an overall effect of the duration of NMDA stimulation compared to vehicle treated cells and a significant effect of the interaction between treatment and duration of treatment compared to control ($p<0.01$, $F(2, 23) = 5.82$ and $p<0.05$, $F(2,23) = 4.20$ respectively, 3-way ANOVA).

4.3.4 Gephyrin RNA and protein levels are not effected in zif268 knockout mice

Figure 4.10 is a representative DNA genotyping agarose gel of wildtype, heterozygous, and zif268 knockout mice. When genotyped, $zif268^{+/+}$ mice show a wildtype allele of 362 base pairs, $zif268^{+/-}$ display the wildtype allele and a disrupted allele of 520 base pairs, whereas $zif268^{-/-}$ only have the disrupted allele present (Topilko *et al.* 1997).

A comparison of mRNA levels of gephyrin from zif268 knockout and wildtype mice by RT-PCR show no significant differences ($p>0.05$ $F(1,13) = 0.08$, ANCOVA, wildtype, n=3, zif268 knockout, n=4; see figure 4.11). In addition, comparing gephyrin immunoreactivity signal intensities from western blots extracted from

either wildtype or zif268 knockout mice also show no effects of a zif268-targeted deletion (see figure 4.12 A & B).

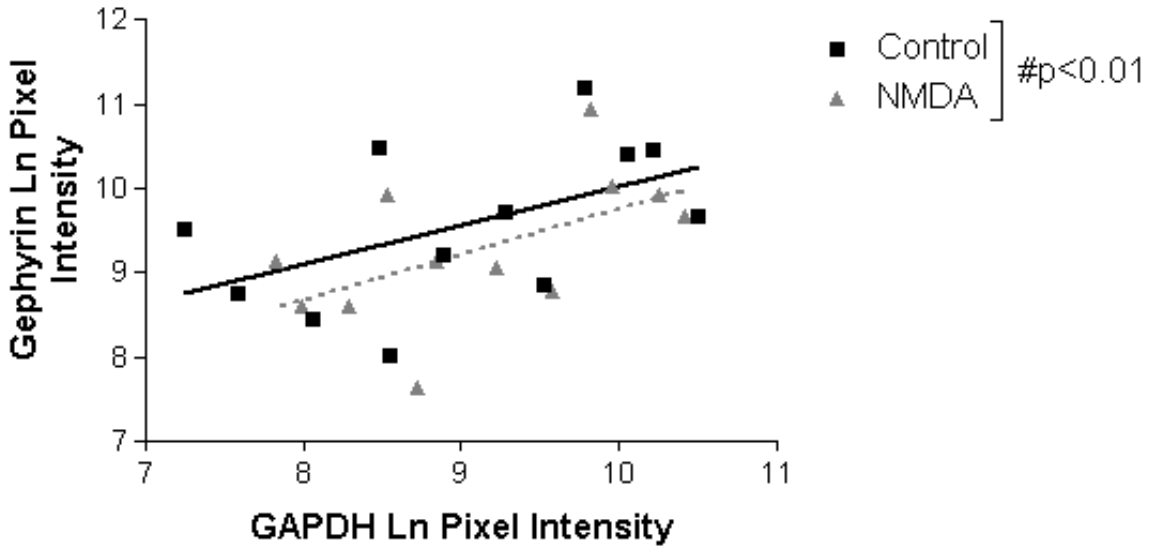

Figure 4.5: The effect of 6 hours NMDA stimulation on gephyrin mRNA in cultured neurones. Graph illustrating gephyrin log pixel intensity as a function of GAPDH log pixel intensity, determined by RT-PCR of primary cultured cortical neurones stimulated for 6h with either 100μM NMDA in 20mM KCl or vehicle. #p<0.01 F(1,16)=11.69, ANCOVA, n=4.

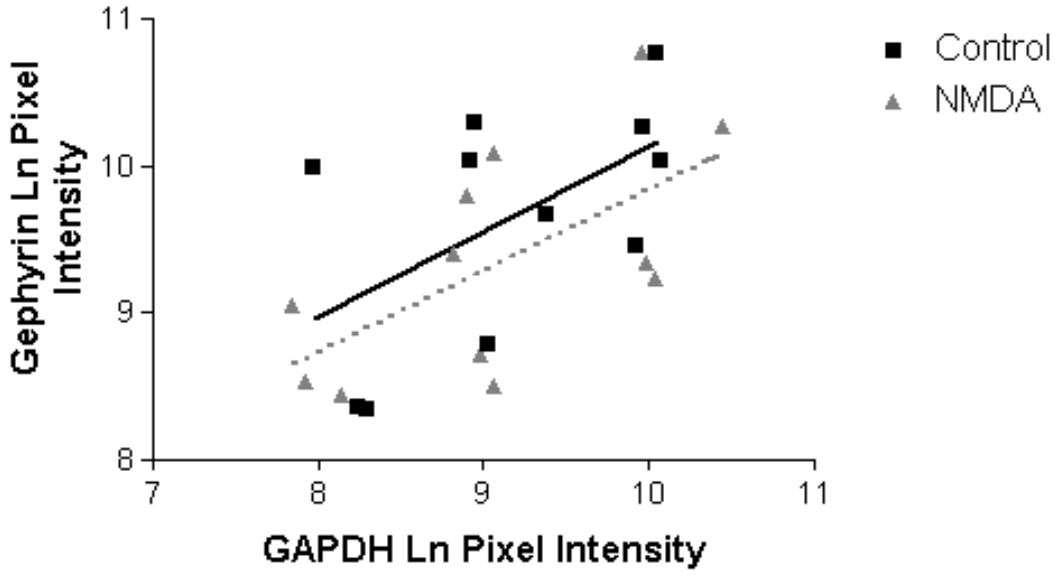

Figure 4.6: The effect of 24 hours NMDA stimulation on gephyrin mRNA in cultured neurones. Graph illustrating gephyrin log pixel intensity as a function of GAPDH log pixel intensity, as determined by RT-PCR of primary cultured cortical neurones stimulated for 24h with either 100μM NMDA in 20mM KCl or vehicle. ANCOVA revealed no significant effect of NMDA treatment, p>0.05, F(1,15) = 1.84, n=4.

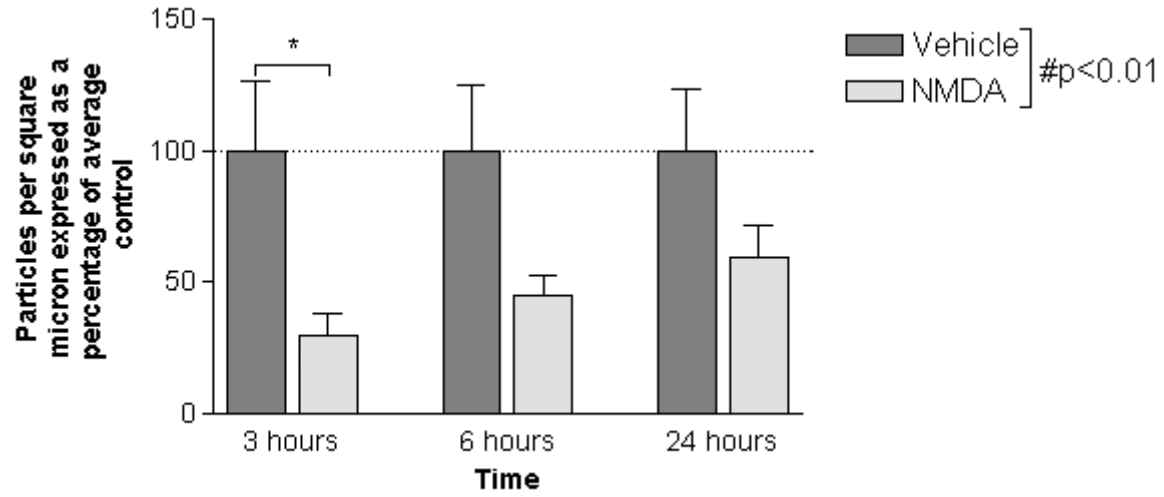

Figure 4.7: The effect of NMDA stimulation on gephyrin protein levels in cultured neurones. Graph illustrating the effect of treatment of 3, 6 or 24 hour stimulation of 100µM NMDA in 20mM KCl or vehicle on gephyrin immunoreactivity of 21 DIV primary cultured cortical neurones as detected by immunocytochemistry. Results are presented as the number of puncta measured per square micron and expressed as a mean percentage of the signal in control (vehicle-treated) cells ± SEM. Effect of NMDA #p<0.01 F(1,30) = 15.67, 3-way ANOVA, *p<0.05, Tukeys *post hoc* test, n=6.

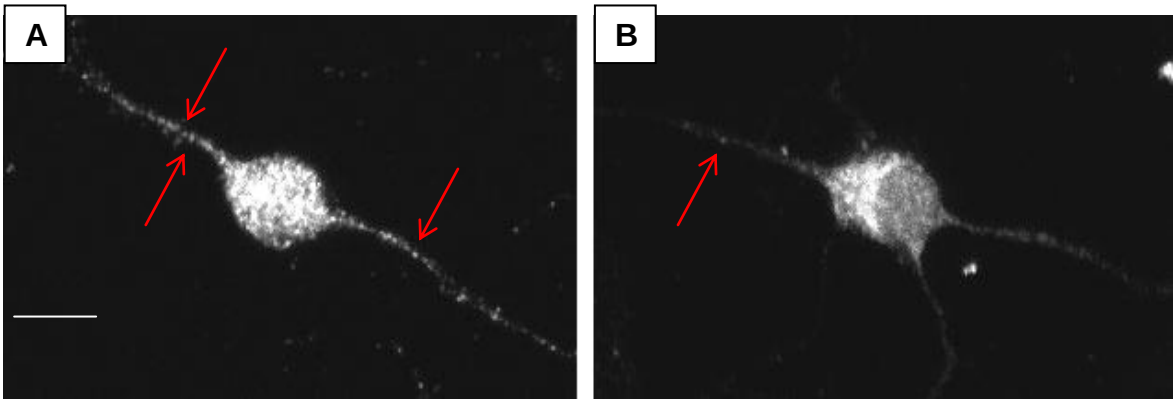

Figure 4.8: Images of gephyrin within cultured neurones after 3 hours NMDA stimulation. Representative primary cultured cortical neurones (21 DIV) treated for 3 hours with vehicle (A) compared to those treated with 100 µM NMDA in 20 mM KCl (B), probed with anti-gephyrin and visualised with a confocal microscope as per the immunocytochemistry protocol. When measuring the number of puncta, the particles present in the cell, visualised within a z-stacked image, were analysed by Image J, before the dendritic measurement area was defined and the number of puncta counted. Scale bar 15 µm.

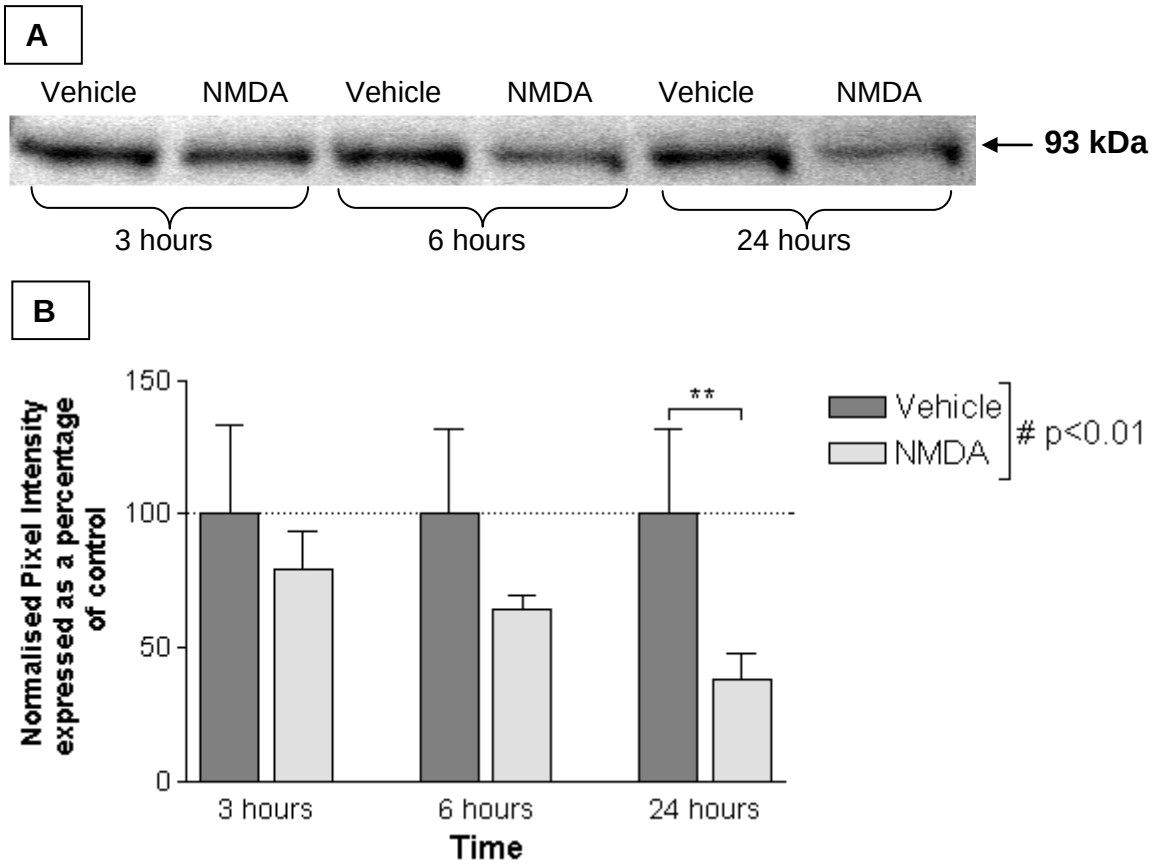

Figure 4.9: The effect of NMDA stimulation on gephyrin protein levels in cultured neurones by western blot. *A,* Representative western blot of cultured cortical neurones stimulated with 100µM NMDA in 2mM KCl or vehicle for either 3, 6 or 24 hours. *B,* Graph comparing gephyrin immunoreactive signal intensities from western blots of primary cortical neurones (7-10 DIV) stimulated for 3, 6 or 24 hours with 100µM NMDA in 20mM KCl or vehicle. Results are presented as normalised pixel intensity and expressed as a mean percentage of control (vehicle treatment) ± SEM. Effect of NMDA #p<0.01, F (1,23) = 28.12, effect of time p<0.01, F(2, 23) = 5.82, interaction of treatment and time p<0.05, F(2,23) = 4.20, effect of culture p<0.01, F(5,23) = 18.58, 3-way ANOVA, **p<0.01, Tukeys *post hoc* test, n=6.

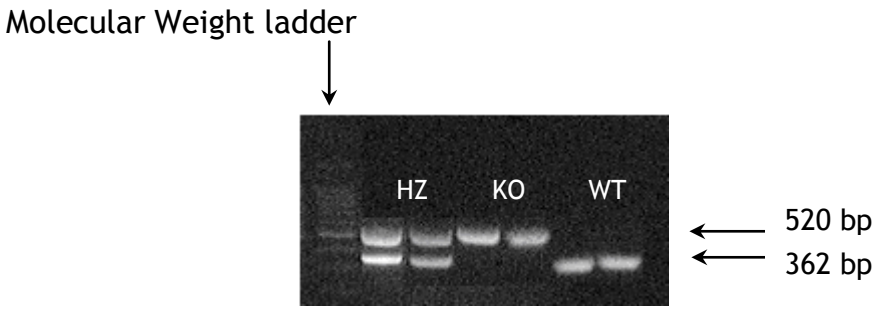

Figure 4.10: Representative image of genotyping results for the zif268 knockout colony. The wildtype allele is a 362 base pair band. The disrupted allele is 520 base pairs long and is found in zif268 knockout mice. Heterozygotes display both a wildtype and a disrupted allele. WT = wildtype, HZ = heterozygote, KO = zif268 knockout mouse.

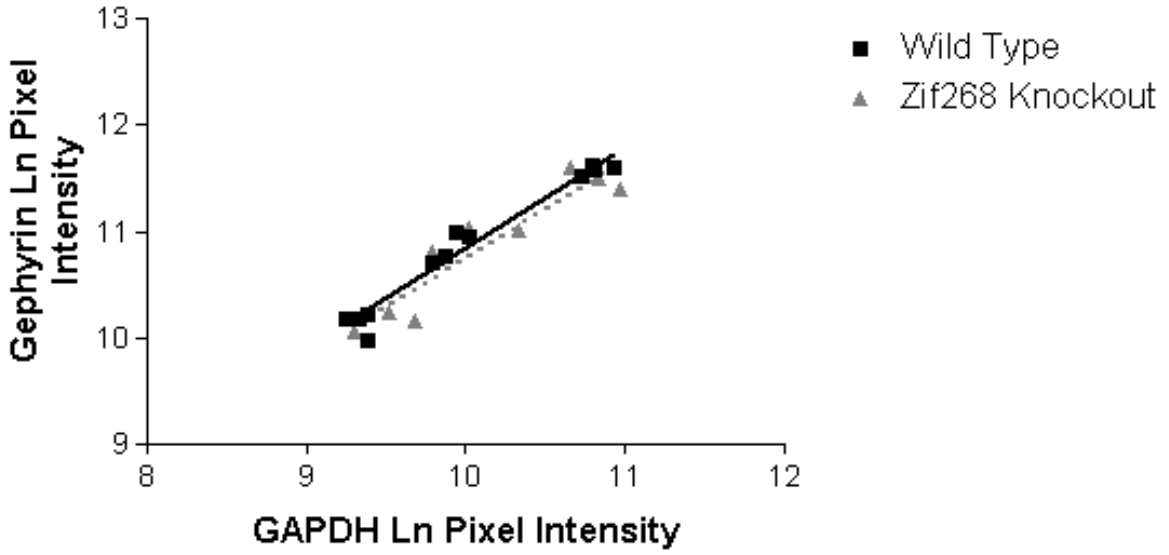

Figure 4.11: The effect of a zif268 targeted deletion on gephyrin mRNA in the adult cortex. Graph illustrating gephyrin log pixel intensity as a function of GAPDH log pixel intensity, as determined by RT-PCR of adult cerebral cortex tissue from either wildtype or zif268 knockout mice. ANCOVA found no significant effect of zif268 targeted gene deletion, $p>0.05$ $F(1,13) = 0.08$. Wildtype, n=3, zif268 knockout, n=4.

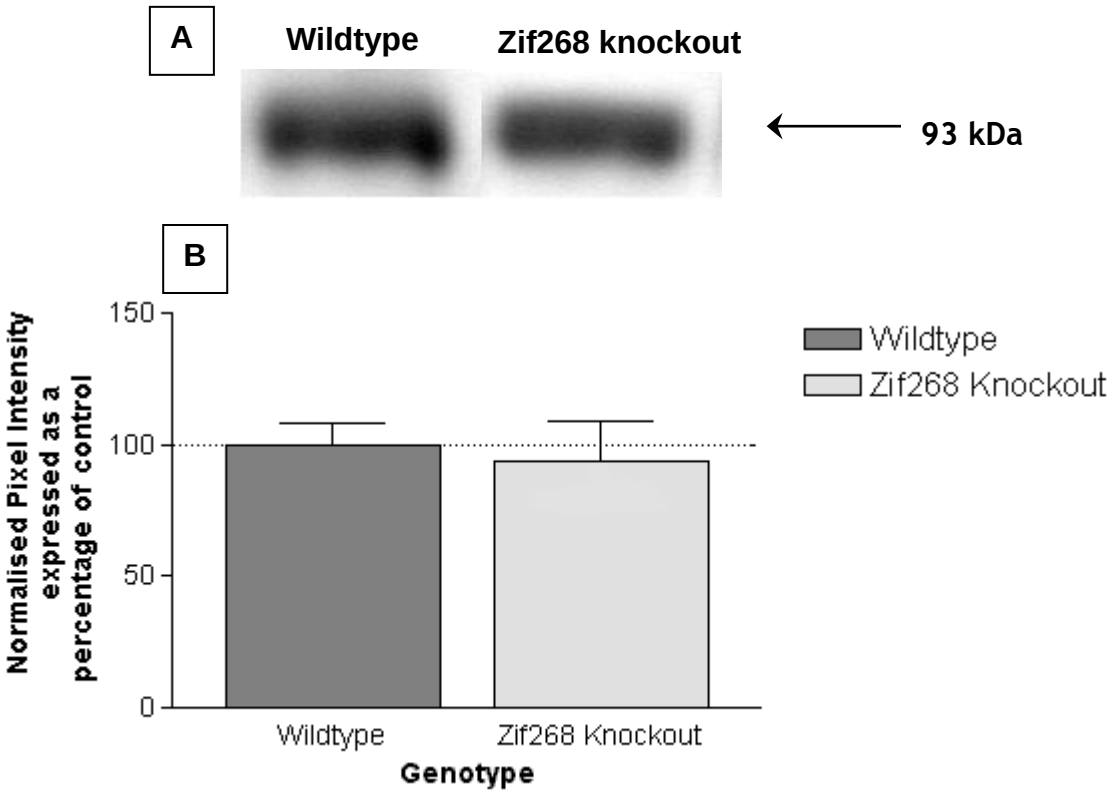

Figure 4.12: The effect of a zif268 targeted deletion on gephyrin protein levels in the adult cortex. A, Representative western blot comparing gephyrin immunoreactivity in adult cortical tissue from wildtype and zif268 knockout mice. *B,* Graph comparing gephyrin immunoreactivity signal intensities from western blots of adult cerebral cortex tissue extracted from either wildtype or zif268 knockout mice. Results are presented as normalised pixel intensity and expressed as a mean percentage of control (wildtype tissue) ± SEM. Wildtype, n=5, zif268 knockout, n=3.

4.3.5 Haloperidol administration to zif268 knockout and wildtype mice effectively induces enkephalin in the striatum

Haloperidol administration *in vivo* increases glutamate release from corticostriatal terminals and produces LTP of corticostriatal transmission (Calabresi et al. 1997; Cepeda et al. 2001) by D2 receptor blockade. This model of CNS plasticity also significantly increases zif268 and enkephalin within the striatum (Morris et al. 1988; Nguyen et al. 1992; Simpson & Morris 1994; Keefe and Gerfen 1995; Cochran et al. 2002). Haloperidol-induced responses within zif268 knockout mice were therefore measured indirectly by way of enkephalin mRNA levels.

Enkephalin mRNA levels in the striatum were determined by ^{35}S *in situ* hybridisation after intraperitoneal administration of 1 mg/kg haloperidol or vehicle in zif268 knockout or wildtype mice. Figure 4.13A shows a representative image of enkephalin upregulation in the striatum. Approximately 6 hours after treatment, no animals showed signs of catalepsy. Enkephalin mRNA was significantly increased by 7% in all mice administered with haloperidol when compared to vehicle treated animals ($p<0.01$, $F(1,17) = 10.70$, 3-way ANOVA (factors: treatment, genotype and sex), haloperidol treated, female n = 4, male n = 6, vehicle treated, female n = 4; male n = 8, see figure 4.13B). There was also a significant effect of sex ($p<0.05$, $F(1,17) = 7.36$, 3-way ANOVA; not shown). There was no effect of genotype on the mRNA levels of enkephalin in the striatum ($p>0.05$, $F(1,17) = 2.33$, 3-way ANOVA).

Gephyrin oligonucleotide ^{35}S and ^{33}P labelling was unfortunately unsuccessful within the time constraints of the PhD. This, therefore, means that the gephyrin mRNA levels of wildtype and zif268 knockout throughout the brain after administration of haloperidol or vehicle will not be presented in this thesis.

4.3.6 Zif268 interacts with the promoter region of the gephyrin gene in PC-12 cells

A promoter reporter assay was performed to investigate the activity of the gephyrin promoter in response to increased zif268 levels. This experiment involved cloning the gephyrin promoter into a vector expressing chloramphemiol acetyl transferase (CAT). The CAT reporter construct was transiently co-transfected into PC-12 cells with plasmid vectors expressing either full length zif268 (pzif268) or a truncated version of zif268 (ptrzif268), allowing us to monitor the transactivity of zif268 acting

on putative cis-binding elements of the gephyrin promoter, thereby influencing gephyrin gene expression. Cells were co-transfected with a β-Gal expression vector to control for any variation in transfection efficiency.

The murine gephyrin promoter (described in Ramming *et al.* (1997)) was used to perform a BLAST search of the *Rattus norvegicus* genome (www.ensembl.com). This had significant similarity to rat gephyrin RNA X66366, which then provided more of the 5' upstream sequence for the gephyrin promoter within rat. Firstly, flanking promoters were designed, and a PCR reaction amplified the targeted gephyrin promoter from genomic DNA. This produced the predicted amplicon of approximately 882 base pairs.

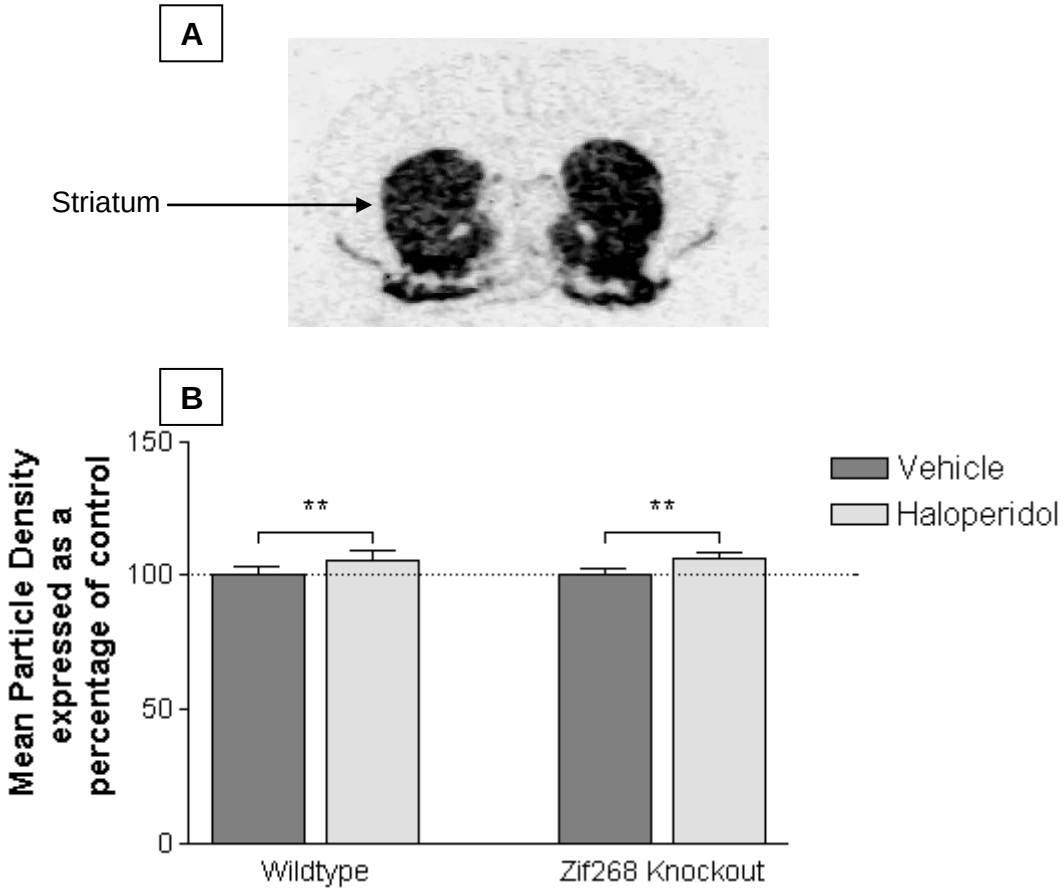

Figure 4.13: The effect of haloperidol on enkephalin mRNA in the striatum of zif268 knockout and wildtype mice. *A*, Localisation of enkephalin mRNA by in situ hybridisation in wildtype mouse brain - coronal section at striatal level. *B,* Graph illustrating the effect of 1 mg/kg haloperidol administration to zif268 knockout and wildtype mice on enkephalin mRNA levels in the striatum compared with vehicle administration as detected by *in situ* hybridisation. Results are expressed as mean pixel intensity ± SEM. Effect of haloperidol treatment **p<0.01, F(1,17) = 10.70, effect of sex p<0.05, F(1,17) = 7.36, 3-way ANOVA. No significant effect was found for genotype p>0.05, F(1,17) = 2.33. Haloperidol, n= 10 (wildtype, n= 5, zif268 knockout n= 5), vehicle, n= 12 (wildtype, n= 6, zif268 knockout, n= 6).

Using the PCR product as a DNA pool for the second round of PCR, primers, containing restriction endonuclease recognition sites, were used to generate DNA strands containing both the gephyrin promoter and digestion sites for future

directional ligation with the vector. pBLCAT3 is a promoter-less vector allowing a synthetically inserted non-native promoter to drive transcription (see figure 4.14). Investigation of the MCS and gephyrin promoter region revealed 2 restriction enzyme recognition sites (*SalI* and *XBaI*) which were present in the MCS but not in the promoter. Primers were therefore designed to bind to the gephyrin promoter region, with the additional 6 base restriction enzyme recognition sites added to the 5' end of each primer, allowing incorporation of the *SalI* site at the 5' end and the *XBaI* site at the 3' end of the promoter during the elongation phase of the PCR reaction (see figure 4.15). The 4.3 kb vector and promoter were then separately digested with the restriction enzymes and electrophoresed to ensure the correct molecular weights were obtained. After ligation, TOP10 cells were transformed with the gephyrin promoter-containing vector and the clones were verified by doubly digesting with the *SalI* and *XbaI* restriction enzymes followed by electrophoresis of the resultant products (see figure 4.16).

PC-12 cells were transiently transfected with the β-GAL expression vector and either the empty vector (pBLCAT3) or the gephyrin promoter-driven pBLCAT3 (pGPHN), and either full-length zif268 (pzif268), truncated zif68 (ptrzif268) or empty vector (pCMV5). The experiment was performed both in the presence and absence of forskolin. All previous transient transfections were conducted in the presence of forskolin after the finding that elevated cAMP, usually present during neuronal plasticity, was required for the modulation of synapsin1 expression by zif268 (James et al. 2004). For the purposes of the promoter reporter assay, transient transfections were performed in the presence and absence of forskolin in order to delineate the necessity of this adenyl cyclase activator for the modulation of gephyrin expression by zif268. The subsequent ELISA results prominently show that β-gal activity is significantly decreased when cells are treated with forskolin ($p<0.01$, one-way ANOVA, see figure 4.17). The following CAT results are therefore presented in their raw form and not normalised to β-gal transfection efficiencies. Results are presented as a percentage of control (empty vector or ptrzif268 as detailed).

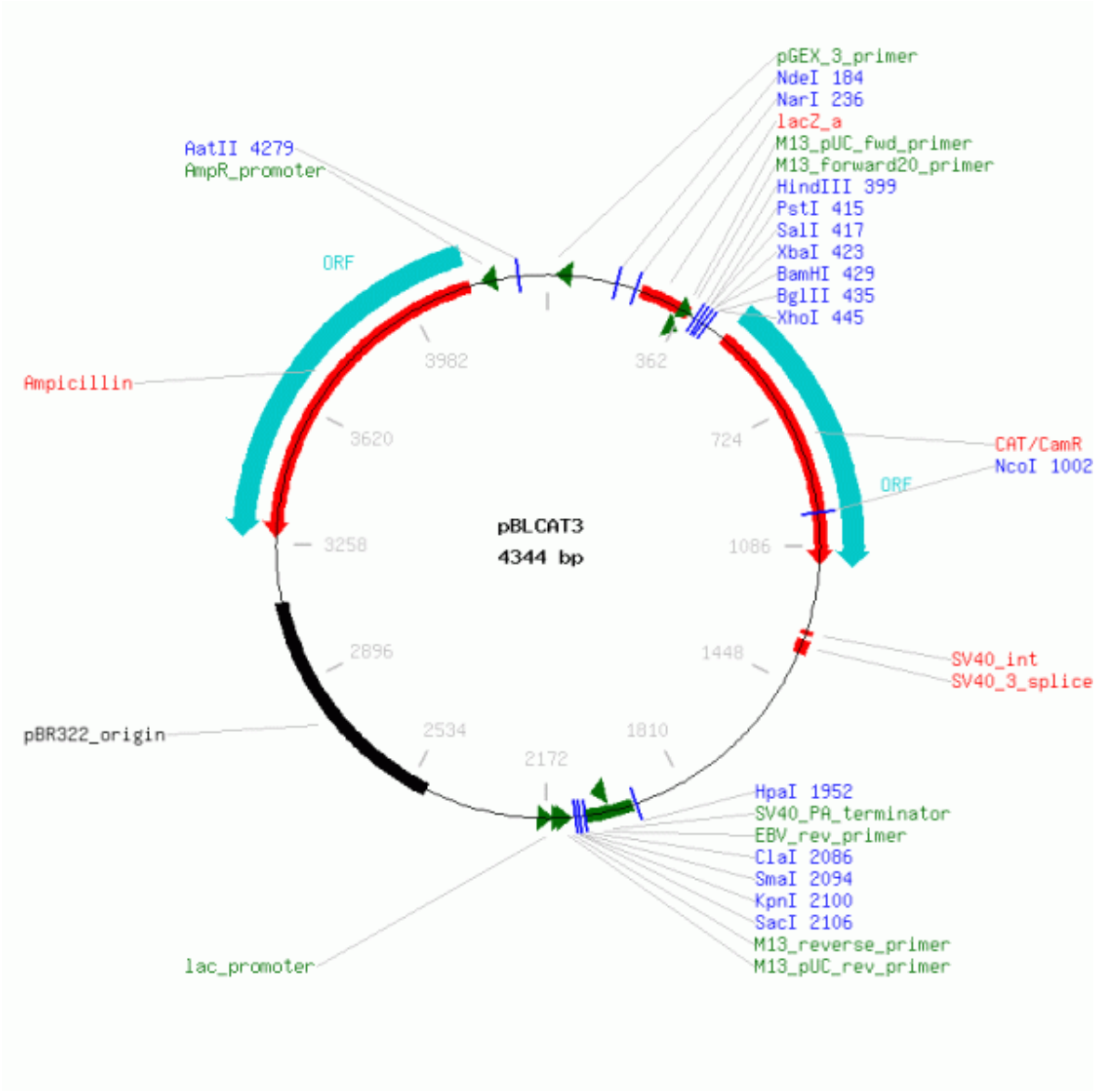

Figure 4.14: A diagram of the promoter-less CAT vector pBLCAT3. In the top right hand corner the MCS is clearly detailed, including the *SalI* and *XbaI* sites which were used directionally to clone the gephyrin promoter into the vector. Taken from http://www.addgene.org/pgvec1?f=d&cmd=genvecmap&vectorid=5260&format=html&mtime=1143220471

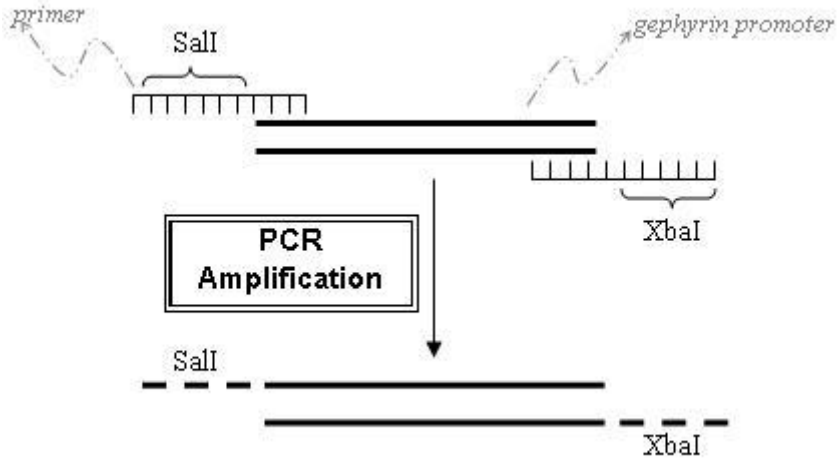

Figure 4.15: Diagram of the double stranded DNA gephyrin promoter with annealed primers designed to each contain restriction enzyme sites at the 5' ends. During the elongation phase of the PCR, DNA polymerase within the reaction will synthesise new strands of DNA incorporating the restriction enzyme sites onto the ends of the newly formed complementary strand.

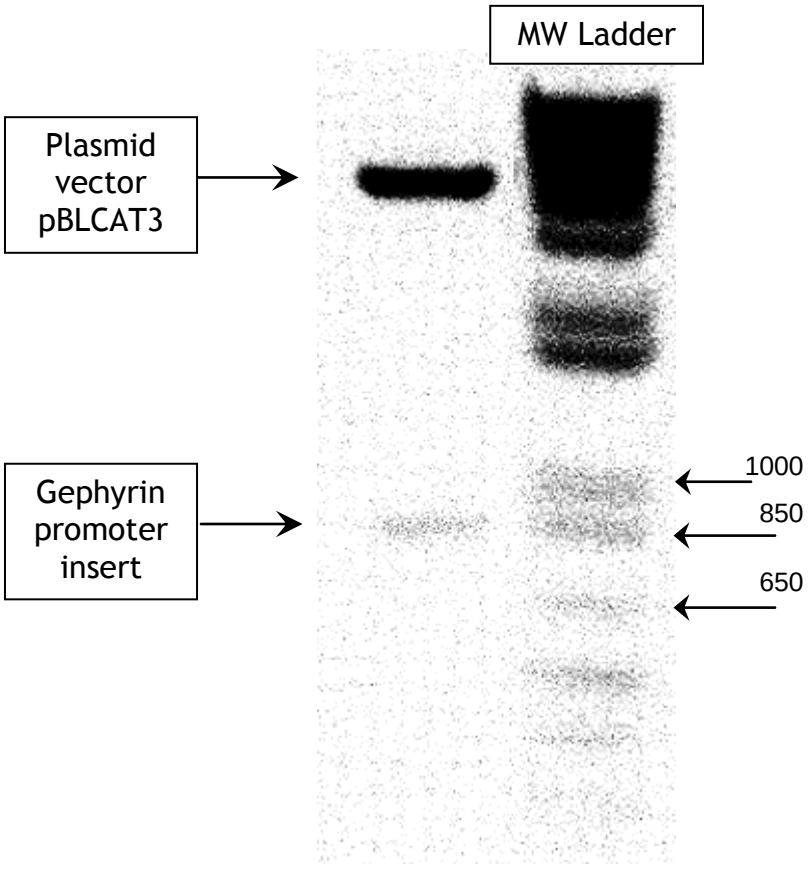

Figure 4.16: An image of an agarose gel containing the gephyrin promoter insert with the pBLCAT3 vector electrophoresed for 1 hour after restriction enzyme digestion with *SalI* and *XbaI*. Numbers denote base pairs. The contrast has been adjusted to reverse the polarity of the image for enhanced visualisation of the molecular weight bands.

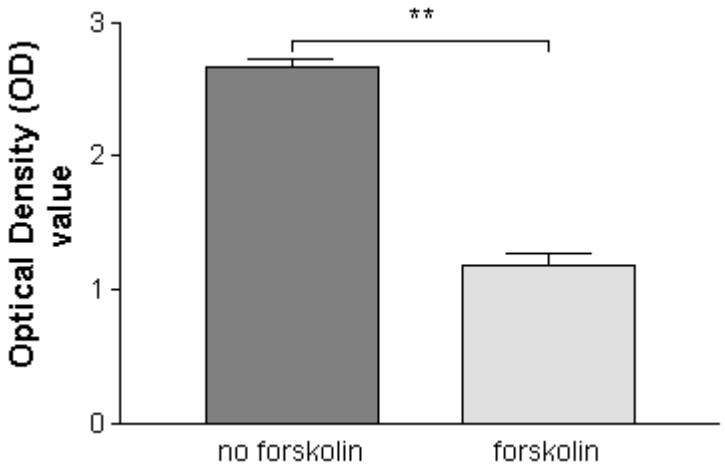

Figure 4.17: The effect of forskolin on β-gal activity. Graph illustrating β-gal activity in PC-12 cells transiently transfected with β-gal in the presence or absence of 2 μM forskolin for 48 hours as detected by ELISA. Results are presented as optical density (OD) values ± SEM. **p<0.01 one-way ANOVA, $F(1, 28) = 174.43$, n=3.

Co-transfecting pzif268 had little effect on pBLCAT3 as measured by CAT activity in the presence of forskolin, compared to the CAT activity of the pBLCAT3 when co-transfected with pCMV5. However, in the absence of forskolin, the ELISA detected a significant decrease in pBLCAT3 CAT activity in cells co-transfected with pzif268 compared to pBLCAT3 activity when co-transfected with pCMV5 (one-sample t-test, $p<0.05$; see figure 4.18) suggesting zif268 action on the CAT empty vector independent of the gephyrin insert. However, expressing pzif268 and pGPHN relative to pzif268 co-transfected with pBLCAT3 revealed a significant suppressive action in the presence of forskolin ($p<0.05$, one sample t-test, n=3, see figure 4.19) suggesting zif268 action on gephyrin. There was no significant effect in the absence of forskolin.

Comparing the effect of pzif268 to ptrzif268 on the gephyrin insert, the effect of pzif268 on pGPHN was not significantly different to the effect of ptrzif268 on pGHPN in the presence of forskolin. In the absence of forskolin, pzif268 significantly decreased pGPHN activity, compared to pGPHN co-transfected with ptrzif268 ($p<0.05$, one sample t-test, n=3, see figure 4.20). Inserting the gephyrin promoter into pBLCAT3 significantly affects the CAT activity as measured by ELISA in the absence of forskolin ($p<0.05$, one sample t-test, n=3; see figure 4.21). A similar tendency was observed in the presence of forskolin, although it did not reach statistical significance.

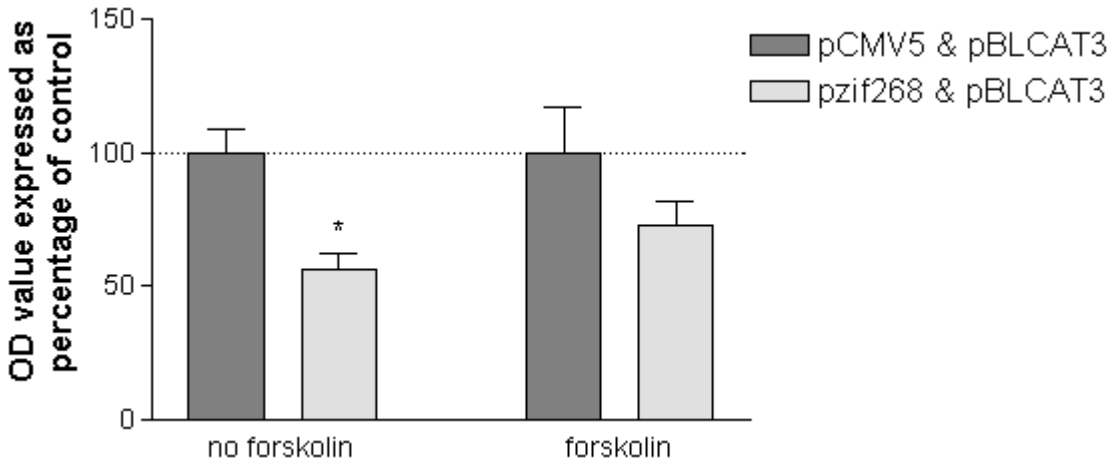

Figure 4.18: The effect of pzif268 on CAT activity. Graph illustrating CAT activity in PC-12 cells transiently co-transfected with pzif268 and pBLCAT3 in the presence or absence of 2 µM forskolin for 48 hours as detected by ELISA. Results are presented as optical density values and expressed as a percentage of the optical density values of corresponding control cells (transiently co-transfected with pCMV5 and pBLCAT3 in the presence or absence of forskolin) ± SEM. *p<0.05, one sample t-test, n=3.

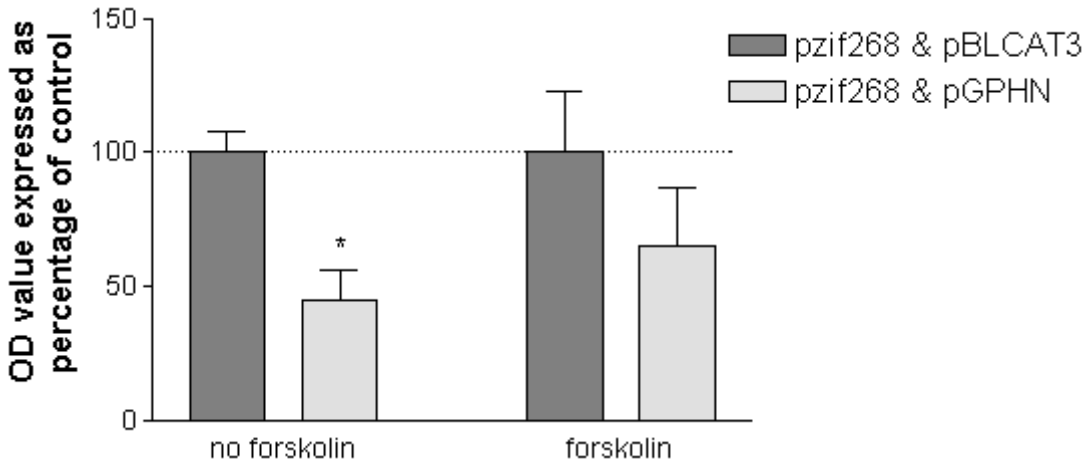

Figure 4.19: Effect of the gephyrin promoter on CAT activity in the presence of zif268. Graph illustrating CAT activity in PC-12 cells transiently co-transfected with pzif268 and pGPHN in the presence and absence of 2 µM forskolin for 48 hours as detected by ELISA. Results are presented as optical density values and expressed as a percentage of the optical density values of corresponding control cells (transiently co-transfected with pzif268 and pBLCAT3 in the presence or absence of forskolin) ± SEM. *p<0.05, one sample t-test, n=3.

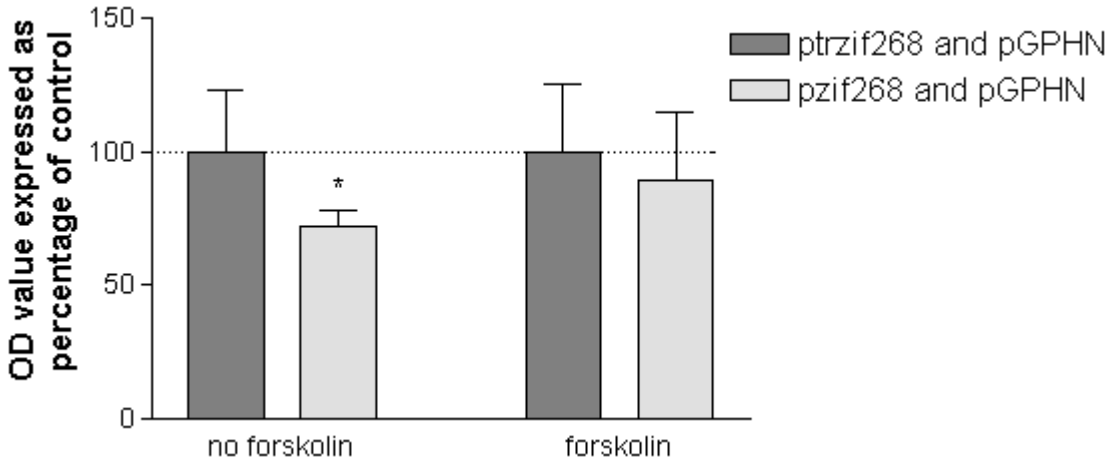

Figure 4.20: The effect of zif268 on the gephyrin promoter. Graph illustrating CAT activity in PC-12 cells transiently co-transfected with pzif268 and pGPHN in the presence and absence of 2 µM forskolin for 48 hours as detected by ELISA. Results are presented as optical density values and expressed as a percentage of the optical density values of corresponding control cells (transiently co-transfected with ptrzif268 and pGPHN in the presence or absence of forskolin) ± SEM. *p<0.05, one sample t-test, n=3.

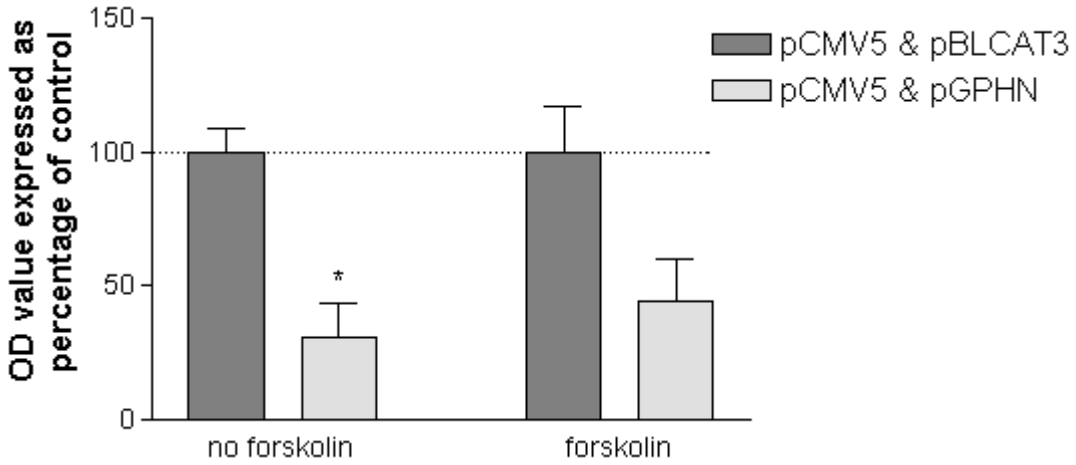

Figure 4.21: The effect of gephyrin on CAT activity. Graph illustrating CAT activity in PC-12 cells transiently co-transfected with pCMV5 and pGPHN in the presence and absence of 2 µM forskolin for 48 hours as detected by ELISA. Results are presented as optical density values and expressed as a percentage of the optical density values of corresponding control cells (transiently co-transfected with pCMV5 and pBLCAT3 in the presence or absence of forskolin) ± SEM. *p<0.05, one sample t-test, n=3.

4.4 Discussion

The data presented in this thesis is the first to implicate gephyrin as a downstream target gene of the plasticity-related zif268 transcription factor. The results show that increased amounts of zif268 within neurones decrease gephyrin mRNA and protein levels.

The gephyrin antibody used throughout is directed against the C-terminal E-domain, an area crucial for many of gephyrin's binding partners, and has been frequently cited in the literature as being highly specific for use with western blotting (Feng *et al.* 1998; Kneussel & Betz 2000) and immunofluorescence (Giesemann *et al.* 2003).

In the first instance, gephyrin was localised within the PC-12 cell line. A brief period of nerve growth factor stimulation differentiated the cells partially. PC-12 cells become a neuronal-like cell type once treated with NGF and can stop dividing, extend processes from the cell body and become electrically excitable. The cells were probed with anti-gephyrin and subsequently displayed distinct puncta when compared to cells probed only with the secondary antibody as control. This provided evidence that gephyrin protein is expressed in PC-12 cells. The punctate labelling is consistent with previous reports in neurones (Craig *et al.* 1996), and in PC-12 cells may relate to the non-receptor clustering functions of gephyrin.

We then verified findings from the original microarray data presented by James *et al.* (2005). Confirmatory analysis involved the transient transfection of PC-12 cells with either a full length or a truncated version of zif268. The truncated form of the zif268 transcription factor is inactive due to an N-terminal deletion (ΔN3-372), inhibiting endogenous full-length zif268. Harvesting mRNA after 48 hours and utilising RT-PCR displayed a decrease in gephyrin expression in the presence of full-length zif268 when compared to truncated zif268. This was mirrored in the findings when investigating gephyrin protein levels by western blot after zif268 transient transfection, revealing a small, but significant, decrease in gephyrin expression. In this particular experiment, a one-tailed one-sample t-test was used as a decrease in gephyrin protein was anticipated from the RNA findings.

Ponceau S was used in all western blotting experiments (PC-12 and primary cultured cortical neurones) to check the uniformity of protein transfer, the normalisation of protein concentration starting material and loading of lysate onto the polyacrylamide gel. If all the sample lanes stained equally, especially within the sizing area expected for the protein, then the experiment was continued. If an uneven distribution of stained proteins was witnessed, the samples were either re-assayed for normalisation of protein concentration or re-loaded onto the gel depending on the nature of variation. Hence, it is very unlikely that the differences in protein levels detected could result from uneven loading or transfer of protein samples. Blotting with an antibody against a “housekeeping" protein, such as actin or GAPDH, would also have helped to confirm protein loading was consistent for each lane.

It seems somewhat surprising that a transcription factor would suppress gene expression rather than activate transcription, especially when considering the pivotal role of zif268 in learning and memory. However, as demonstrated in James *et al.* (2005), it is becoming increasingly evident that zif268 target genes are generally down regulated (Fukada & Tonks 2001; Bahouth *et al.* 2002; Davis *et al.* 2003; Zhang & Liu 2003). The findings presented in this chapter therefore reinforce the suppressive nature of this particular transcription factor as previously published.

Transient transfection of zif268 into neuronal cells was attempted for immunocytochemistry however, this was technically very challenging. There is an increased tendency for neurones to migrate towards each other and 'clump' together the longer the cells are *in vitro*. Combined with the low transfection efficiency, which necessitates the use of assay methods with cellular resolution, such as immunocytochemistry, this can make it very difficult to find measurable cells, especially when the cell to be measured is dictated arbitrarily by transfection success within viable cells.

The RT-PCR results were derived from information gleaned over three data points as this allows for a high degree of confidence in the results obtained. GAPDH is treated as a steady state control that is not affected by treatment (Spanakis 1993; Spanakis & Brouty-Boye 1994), however, when dealing with PCR over time there is a need to adjust for the effect of independent biological variables, as reference genes have been found to alter with treatment type (Bond *et al.* 2002). ANCOVA

allows for an improvement in the sensitivity of analysis and enables the variation common to both test and reference gene to be explained and removed from the analysis (Bond *et al.* 2002).

After 6 hours of NMDA stimulation, gephyrin mRNA levels in cortical neurones (7-10 DIV) are significantly decreased compared to controls. By 24 hours, mRNA levels have returned to basal levels. By western blot detection, gephyrin protein levels are not significantly different from controls at 3 or 6 hours of NMDA stimulation but are significantly downregulated at 24 hours in cultured cortical neurones (7-10 DIV). These results are consistent, whereby an increase in zif268 expression would decrease gephyrin mRNA levels, which would eventually lead to a decrease in gephyrin protein. In contrast are the results found by immunocytochemistry. In this experiment, gephyrin protein levels are found to be downregulated at 3 hours in cultured cortical neurones (21 DIV) stimulated with NMDA, but not significantly after 6 or 24 hours, when compared to controls. There are several reasons for this seeming discrepancy. Firstly, and most obviously, the techniques used are very different. Whilst measurements obtained from immunocytochemistry can be localised appropriately, in this case within dendrites, western blotting and RT-PCR harvests all proteins within all cells giving a more global idea of the effects of experimentation. Secondly, the length of time the cultures spent *in vitro* was dramatically different for each experiment. Cultured cortical neurones treated immunocytochemically were approximately 14 days more mature than the cultured cells processed for western blotting and RT-PCR. Although it was reasoned that whole cell measures of gephyrin protein didn't require localisation at the synapse, this could have a marked effect on the results. At 21 DIV approximately 90% of gephyrin clusters are synaptic and 85% of these are co-localised with $GABA_A$Rs at synaptic sites. However, at 7-10 days, the number of gephyrin clusters associated with $GABA_A$Rs is decreased dramatically to approximately 25% (Danglot *et al.* 2003). In addition, there is a clear tendency for the dendritic gephyrin immunoreactivity to be suppressed by NMDA treatment at both 6 and 24 hours as well as 3 hours, implying that there may be a sustained suppression of gephyrin expression. It is also possible that the early fall in gephyrin levels are mediated by some non-transcriptional mechanism, such as increased degradation.

The NMDA treatment experiments within this thesis used a concentration of 100 µM in 20mM KCl. As excessive or prolonged activation of NMDARs leads to

increased intracellular calcium concentrations, excitotoxicity and neuronal cell death, an XTT assay (Roehm *et al.* 1991) was performed (Professor B.J. Morris, personal communication). This colorimetric assay, based on the reduction of a tetrazolium salt (XTT), showed no change in the number of viable striatal or cortical neurones in primary culture after 24 and 48 hours treatment with 100 µM in 20mM KCl. Further tests of this nature, for longer periods of time, would ensure that the zif268 results reported here were true results of a plasticity-related pathway and not the beginnings of an excitotoxic pathway.

RT-PCR of adult cerebral tissue from zif268 knockout mice shows no difference detected in gephyrin expression when compared to wildtype controls; a result reflected in the western blotting results. This is most likely due to the fact that zif268 is a member of the large Egr family, generating the potentiality of compensation. Egr-2, egr-3 and egr-4 for instance encode proteins that can bind to the zif268 binding motif and there is considerable overlap in their binding sites and functional roles (Crosby *et al.* 1992; Vesque & Charnay 1992; Swirnoff & Milbrandt 1995). In fact, it is known that egr-4 can compensate for zif268 in the zif268 knockout mouse (Tourtellotte *et al*. 2000) and egr-3 has been found to co-localise with zif268, suggesting the possibility of further compensation (Yamagata *et al.* 1994). Egr 2 and egr3 are also regulated by the induction of LTP (Yamagata *et al.* 1994; Williams *et al.* 1995). Indeed, gephyrin is an essential cellular component, as homozygous disruption of the murine gephyrin gene is lethal at birth, suggesting that gephyrin is dispensable for embryonic development but absolutely essential for postnatal survival (Feng *et al.* 1998). Therefore the knockout mice would need to be developmentally effective at compensating for zif268 loss. Hence the lack of any detectable change in gephyrin expression in the zif268 knockout mice does not preclude an important role for zif268 as the transcriptional regulator of the gephyrin gene.

A model of CNS plasticity was used to increases zif268 and enkephalin within the striatum by way of haloperidol administration *in vivo* (Morris et al. 1988; Nguyen et al. 1992; Simpson & Morris 1994; Keefe and Gerfen 1995; Cochran et al. 2002). Haloperidol-induced responses within zif268 knockout mice were measured indirectly by way of enkephalin mRNA levels, which showed a significant increase when compared with animals treated with vehicle. The induction of enkephalin was smaller than expected. This may reflect the genetic background of the mice, as this has been shown to have a profound effect in the response of striatal

neurones to haloperidol treatment (Patel *et al.* 1998). In addition, it may be that the desired effect of increased glutamate at synapses did not occur due to haloperidol antagonistic actions on NR2B-containing NMDARs (Gallagher *et al.* 1998). There were no effects of genotype within the results confirming that enkephalin levels are not altered by the presence or absence of zif268. This is consistent with previous studies in the hippocampus (Johnston & Morris 1994). It was hypothesised that, even in the absence of any change in the basal level of gephyrin expression in the zif268 knockout mice, there might be an impairment in any response to haloperidol treatment. Unfortunately, measuring gephyrin levels by *in situ* hybridisation could not be completed within the time constraints imposed.

The mouse gephyrin promoter is described by Ramming *et al.* (1997) and was used to identify the rat gephyrin promoter region with the use of bioinformatics. Once the likely promoter region had been identified it was cloned for transfecting into PC-12 cells with either full length or truncated zif268. Within this promoter region, there were 3 potential zif268 sites, 3 potential Sp1 sites and a general zinc finger transcription factor known to enhance promoter activity (Dynan *et al.* 1986), amongst other transcription factor binding sites (www.genomatix.de). The promoter reporter assay, a CAT ELISA, is used quantitatively to measure CAT expression in eukaryotic cells transfected with a plasmid bearing a CAT encoding reporter gene.

A β-gal ELISA was performed in order to monitor transfection efficiencies, but it was found that β-gal is significantly affected by the presence of forskolin. This can be explained either by the fact that forskolin is decreasing the rate of transfection or that forskolin is causing the enzyme to decrease its activity. Since there are reports suggesting that forskolin may increase β-galactosidase activity (Löser *et al.* 1998), the latter explanation is likely, and any differences in cell types may contribute to the reversal of effect. This effect negates the use of this protein as a means to normalise for any variation in transfection efficiencies and so data were analysed without further normalisation.

The results from the CAT ELISA were several fold. Firstly, we looked at the effect that transfecting zif268 into the cell had on CAT activity. Full-length zif268 significantly decreased CAT expression, which is puzzling as pBLCAT3 is a promoter-less vector and therefore should not have been affected. Although zif268 was suppressing the CAT empty vector, transfecting gephyrin with zif268

led to a further significant decrease in CAT activity, suggesting regulation of the gephyrin promoter by full-length zif268. This effect was also significantly reduced when compared to truncated (control) zif268.

The surprising result that pGHPN displays less CAT activity than pBLCAT3 led to further data mining (using MatInspector) of the targeted promoter region. A diagrammatic overview (figure 4.22) displays a few of the pertinent transcription factor binding sites. Of particular interest is the potential Neural Restrictive Silencer Element (NRSE) site, which is found in promoters which binds NRSF (Neural Restrictive Silencer Factor)/REST (Repressor Element-1 silencing factor), a known endogenous transcriptional repressor of several genes encoding neurotransmitter receptors and ion channels in neurones (Chong *et al.* 1995; Schoenherr & Anderson 1995; Schoenherr *et al.* 1996; Shimojo & Hersh 2006). This NRSE is conserved in human, rat and mouse upstream regions at equivalent positions, relative to the gephyrin transcriptional start site. In PC-12 cells, NRSF transcriptionally represses the Na+ channel type II (Tapia-Ramirez *et al*. 1997). It has been proposed that NRSF is localised to the nucleus PKA dependently as, in environments which lack PKA, NRSF remains in the cytosol, repressing overall NRSF activity and allowing increased target gene expression (Shimojo & Hersh 2006). Therefore, there may be an influence of cAMP levels in NRSF function, which might predict less suppression of promoter activity by NRSF in the presence of forskolin. There are some suggestions that this may be the case in these results (figure 4.21).

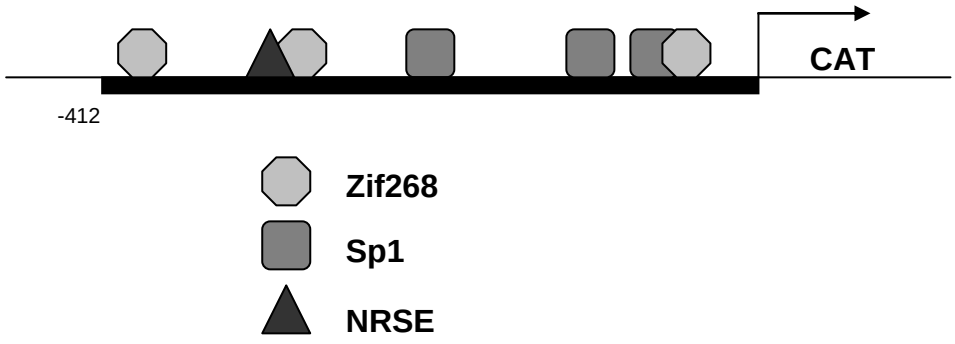

Figure 4.22 Diagram of the targeted gephyrin promoter cloned into the pBLCAT3 promoter-less vector plasmid. Positions of some of the known binding sites are annotated. Zif268 recognition sequences are located at positions -408 to -392, -294 to -278 and -22 to -6 relative to the end of the cloned gephyrin sequence and putative CAT transcription start site (at 0). Sp1 (Stimulating protein 1) recognition sequences are located at positions -193 to -179, -42 to -28 and -24 to -10 relative to the end of the cloned gephyrin sequence. The NRSE (Neural Restrictive Silencer Element) recognition site is at position -316 to -296.

It can be proposed that the introduction of the gephyrin 'promoter' region upstream of the CAT coding sequence suppresses expression via this NRSE. Ramming *et al.* (1997) observed increased expression of their reporter gene downstream of the mouse gephyrin promoter, but they used a longer 'promoter' fragment that may contain other elements that interact with the NRSE. The promoter-reporter results also confirm our earlier findings that full-length zif268 decreases gephyrin expression when compared to truncated zif268.

Zif268 expression decreased the activity of the cloned gephyrin promoter, relative to both empty vector and the truncated zif268 expression vector. This is consistent with a direct action of zif268 on one or more of the potential zif268 binding sites shown in figure 4.22, to suppress transcriptional activity. The effect was more marked in the absence of forskolin than in the presence of forskolin. However, the original microarray detection of gephyrin transcripts being modulated by zif268 and the confirmatory studies monitoring gephyrin mRNA and protein levels in PC-12 cells after zif268 transfection, were performed in the presence of forskolin. A likely explanation for this apparent discrepancy is that complete endogenous gephyrin promoter is not fully represented by the ~1 kb fragment studies here. It is well known that functionally important promoter elements are frequently located more than 1 kb upstream of the transcription start site, or downstream, in coding or intronic regions. Such elements in the endogenous gene may modify the response to zif268.

The 'promoter' region cloned in our study also contained an overlapping recognition site for Sp1 and zif268. Competition or interaction of Sp1 and zif268 binding is considered important for gene regulation and occurs in many promoters (Huang et al. 1997; Srivastava et al. 1998; Fukada and Tonks 2001; Davis et al. 2003). The ability of zif268 to modulate gephyrin expression could therefore involve competitive binding with Sp1.

Overall, we have presented strong evidence that gephyrin is a direct downstream target of zif268 and is generally suppressed during periods of neuronal plasticity (Chhatwal *et al.* 2005). Gephyrin's interactions with the cytoskeleton and $GABA_A$Rs, introduced in the general introduction, will be discussed with relevance to zif268-induced downregulation in the general discussion.

Chapter 5

Ubiquilin as a downstream target of zif268

5.1 Introduction

5.1.1 Ubiquilin and related homologues

In humans there are currently four known ubiquilin genes: ubiquilin 1 (Mah *et al.* 2000), ubiquilin 2 (originally called Chap1) (Kaye *et al.* 2000), ubiquilin 3 (Conklin *et al.* 2000) and ubiquilin 4 (A1Up) (Davidson *et al.* 2000). Ubiquilin and its forms are also known as Plic-1 and Plic-2 (Proteins that Link IAP (integrin-associated protein) with the cytoskeleton) in mouse (Wu *et al.* 1999), DA41 in rat (Ozaki *et al.* 1997a), XDRP1 in frog (Funakoshi *et al.* 1999) and Dsk2 in yeast (Biggins *et al.* 1996). In addition, alternative names in humans are hPlic-1 and hPlic-2, (Kleijnen *et al.* 2000) and human DA41 (Hanaoka *et al.* 2000).

Ubiquilin 1 was discovered in humans by Mah *et al.* (2000) as a novel 66kDa interactor with presenilin proteins, which are linked to early onset Alzheimer's Disease (AD), a property that will be discussed later in this chapter. It has 2 transcript variants, one with exon 8 (transcript 1) and one without (transcript 2) and was found to have a 60% homology with XDRP1 (*Xenopus* Dsk2-related protein 1) discovered in Xenopus *laevis* (Funakoshi *et al.* 1999). XDRP1 is a nuclear phosphoprotein and binds to cyclin A1 and A2, proteins that seem to be importantly involved in mitosis, as their degradation is necessary to enter the next cell cycle and is highly regulated. This interaction requires the N-terminal UBL domain of XDRP1 and inhibits cyclin A degradation, allowing overall involvement of XDRP1 with the spindle function in mitosis, and therefore cell cycle regulation. Dsk2, human Chap1 and DA41 have also been implicated as regulators of the cell cycle (Biggins *et al.* 1996; Kaye *et al.* 2000; Ozaki *et al.* 1997b).

Plic-1 and Plic-2 were discovered in 1999 by Wu *et al.* and share over 80% sequence identity. Plic-1 displays 84% homology to ubiquilin 1 and Plic-2 shows 60% homology. It has since been found that ubiquilin 1 is more closely related to Plic-1, and ubiquilin 2 more close to Plic-2. They were found by yeast dihybrid screening using two isoforms of IAP with distinctly different cytoplasmic tails. Integrins associate with microfilaments, and IAP is thought to mediate the interaction of both Plic-1 and -2 with integrin $\alpha v\beta 3$. In addition, Plic proteins were found to interact with IAP and vimentin, anchoring the intermediate filaments to the plasma membrane. Moreover, the transfection of either Plic-1 or -2 into a stable cell line containing an IAP isoform increased the area of the cell when compared

to control. Therefore, the affiliation of the Plic proteins and IAP could lead to alterations in the cytoskeleton.

Kliejnen *et al.* (2000) also utilised yeast dihybrid screening, to find cDNAs encoding human Plic-2 and Plic-1. As mentioned in the Chapter 1, this was the first paper to propose that the Plic proteins had an association with the ubiquitination machinery and the proteasome.

Ubiquilin staining pattern is variable in different cell types (Mah *et al.* 2000). However, analysis of tissue distribution in mouse Plic-1, rat DA41 and human DA41 show that it is ubiquitously expressed (Ozaki *et al.* 1997a; Wu *et al.* 1999; Hanaoka *et al*. 2000). Northern blot analysis of human tissues found that ubiquilin is highly expressed in the brain and pancreas. In addition, in adult human neurones, ubiquilin localises to the nucleus, cytoplasm and to long axonal processes (Mah *et al.* 2000).

5.1.2 The Role of Ubiquilin in Neurodegenerative Disease

5.1.2.1 General Aggresomal Diseases

Massey *et al.* (2004) located ubiquilin proteins within the inner core of aggresomes, structures involved with the sequestration of misfolded proteins in cells. This could suggest a role for ubiquilin within general aggresomal disease states. Small protein aggregates singularly form throughout the cytoplasm and are quickly dynein-dependently transported on microtubules to form a large aggresome (Johnston *et al.* 1998; Garcia-Mata *et al.* 1999). In an attempt to dispose of the aggresome, chaperones, the ubiquitination machinery and the proteasome arrive, closely followed by autophagosomes and lysosomes (Mortimore *et al.* 1996). The many known aggresome-related diseases provide circumstantial evidence that aggresomes are involved in cellular degeneration in disease states. Possible mechanisms for cell death include the sequestration of chaperones and proteasomes, a disruption of cellular trafficking (Johnston *et al.* 2000), and the ability of aggresomes to attract other proteins on a ‘like for like’ basis, whereby aggresomal proteins attract structurally similar proteins (Huang *et al.* 1998).

5.1.2.2 Alzheimer's Disease

The majority of recent publications regarding ubiquilin have argued over the relevance and role it may play in Alzheimer's disease (AD). AD is a neurodegenerative disorder responsible for the majority of dementia cases found in the elderly. It is characterised by amyloid plaques and neurofibrillary tangles formed in various brain areas. The majority of cases are found in individuals over the age of 65, however, the less common early-onset AD can affect approximately 5% of the overall number of AD patients (Farrer *et al.* 1997).

So far three genetic mutations have been related to early onset familial (FAD) AD: β-amyloid precursor protein (APP), presenilin-1 (PSEN1) and presenilin-2 (PSEN2) (Hardy 1997; Price *et al.* 1998), and only one genetic mutation has been related to late-onset AD in the ε4 allele of apolipoprotein E (APOE) (Kamboh 2004). However, there are genetic variations found in AD, so many more genes probably need to be identified (Daw *et al.* 2000), in addition, it is not fully understood how mutations in these known genes can cause AD. Ubiquilin was found as a novel interactor of both PSEN1 and PSEN2 (Mah *et al.* 2000). An *in vitro* binding assay provided evidence that only the UBA containing COOH-terminal of ubiquilin was able to bind the presenilins. Co-expression of ubiquilin with PSEN2 resulted in a marked increase of PSEN2 protein accumulation, compared with overexpression of PSEN2 alone, in the presence and absence of proteasome inhibitors. In addition, they discovered by immunohistochemistry that neurones containing neurofibrillary tangles (from AD patients) had more intense ubiquilin staining than control neurones.

The catalytic core of the γ-secretase complex is formed from presenilin proteins and is responsible for cleaving APP, leading to a build up of fragments in the extracellular space (Edbauer *et al.* 2003; Kimberly *et al.* 2003; De Strooper 2003). In order for the catalytic core to form, the presenilins must undergo endoproteolysis by 'presenilinase' to create C-terminal and N-terminal fragments (Thinakaran *et al.* 1996; Kim *et al.* 1997; Thinakaran *et al.* 1997; Ratovitski *et al.* 1997), which interact with each other and are responsible for the γ-secretase activity (Esler *et al.* 2000; Li *et al.* 2000). Ubiquilin is thought to promote the accumulation of presenilin full-length proteins, and to regulate its endoproteolysis by blocking access to the 'presenilinase', an unknown activity. Ubiquilin also modulated the levels of other key members of the γ-secretase complex such as

pen2 and nicastrin (Massey *et al.* 2005). Further evidence linking ubiquilin with the presenilin proteins includes the co-localisation of ubiquilin and PSEN1 in primary cultured neurones. In addition, evidence suggests an interaction between the two proteins at the cell surface. However, this interaction was not significantly different in AD patients compared to controls (Thomas *et al.* 2006).

The first clinical study linking ubiquilin with AD was by Bertram *et al.* (2005) utilising two family-based samples. They used neural tissue from 25 late-onset AD patients and 17 controls and studied a single nucleotide C/T polymorphism located within the ubiquilin gene (UBQ-8i) that they state was consistently mutated in AD brains. They also found that the level of ubiquilin transcript 2 was increased in AD brains. However, genotyping the transcript 2 sample for the UBQ-8i risk allele did not reveal significant linkage to AD, possibly due to their small sample size. This article created a wave of responses, most of which disagreed with the findings (Bensemain *et al.* 2006; Brouwers *et al.* 2006; Slifer *et al.* 2006; Smemo *et al.* 2006).

5.1.2.3 Huntingdon's Disease

The fatal, hereditary, neurodegenerative Huntingdon's Disease (HD) is caused by the expansion of a CAG repeat found in exon 1 of the gene encoding huntingtin protein. This gene product is then translated with an expanded polyglutamine (polyQ) stretch, which is thought to cause intracellular nuclear aggregates to form (Scherzinger *et al.* 1997; Michalik & Van Broeckhoven 2003). Numerous proteins interact with the aggregates, which are ubiquilin rich, but it is unclear whether these aggregates are protective or toxic. Doi *et al.* (2004) identified ubiquilin 1, as well as ubiquilin 2, as novel proteins that interact with aggregates, in addition to their interaction with ubiquitin. PolyQ aggregates have been reported to contain several UBA domain-containing proteins, as well as ubiquitin interacting motif (UIM) domain-containing proteins (Donaldson *et al.* 2003; Wang *et al.* 2000; Davidson *et al.* 2000). PolyQ aggregates are thought to sequester ubiquitin-interacting proteins through these domains, disrupting normal neuronal function.

Recently, Wang *et al.* (2006) co-transfected ubiquilin into neuronal cells with a GFP-tagged protein containing 74 polyQ repeats (GFP-Htt(Q74-3)) and found that overexpression of ubiquilin promotes increased cell survival. They also showed that cells stably expressing GFP-Htt(Q74-3) were more sensitive to oxidative

stress induced by exposure to H_2O_2 or serum deprivation than a lower polyQ repeat protein, GFP-Htt(Q28-2). The GFP-Htt(Q74-3) cell death was reduced by approximately 80% and 50% respectively when ubiquilin was transiently transfected into the cells. They also investigated the effects of reducing ubiquilin by siRNA in the GFP-Htt(Q74-3) stably expressing HeLa cells. They observed a corresponding halt in cell proliferation, an increase in cell death and the accumulation of expanded GFP-immunoreactive aggregates when knocking down ubiquilin.

5.1.3 Additional Functions of Ubiquilin

Prolonged exposure to nicotine can upregulate the surface expression of nicotinic acetylcholine receptors (nAChRs) in neurones (Wonnacott 1990; Darsow *et al.* 2005). Ubiquilin was found to bind to the mouse α3 subunit of nAChRs by yeast dihybrid screening (Ficklin *et al.* 2005). By co-transfecting ubiquilin and the α3 nAChR subunit into COS-7 cells they found that ubiquilin redistributed the subunit to the 20S proteasome subunit. They also found that ubiquilin decreased the surface expression of receptors in a stably expressed α3 and β2 subunit HEK293 cell line. In addition, ubiquilin was able to reduce the number of surface nAChRs upregulated by nicotine in cultured mouse superior cervical ganglion cells. Taken together, this may mean that ubiquilin can limit nAChR subunits for assembly and trafficking.

Protein-disulfide isomerase (PDI) forms and rearranges disulfide bonds within the rough endoplasmic reticulum (RER) in order to aid the folding of proteins (Lyles & Gilbert 1991). An increase in the amount of unfolded proteins within the ER can lead to a stress response (Sidrauski *et al.* 1998), which in mild cases, can be dealt with by stress proteins like PDI. PDI has been shown to up-regulate in response to hypoxia *in vitro* and brain ischemia *in vivo* in glial cells (Tanaka *et al.* 2000). Ubiquilin has been identified as a PDI-interacting protein and therefore a possible protective factor against hypoxia. Ubiquilin binds *in vitro* and *in vivo* to PDI's C-terminus and, when over-expressed, could be found localised to the ER. Ubiquilin mRNA and proteins levels were increased in response to hypoxia in astrocytes and co-expression of ubiquilin and PDI had a protective effect against hypoxia in human neuroblastoma cells (Ko *et al.* 2002).

Ubiquilin also interacts with Eps15 (epidermal growth factor (EGF) receptor pathway substrate 15) a protein that interacts with AP2, the linker protein involved in clathrin coated pit formation (Benmerah *et al.* 1995; Morgan *et al.* 2003). The UIM (ubiquitin-interacting motif) domains of Eps15, Eps15R (Eps15-related) and another endocytic protein, Hrs, interact with ubiquilin through the UBL domain although this interaction was not related to endocytic compartments (Regan-Klapisz *et al.* 2005).

Overall, there is considerable evidence that ubiquilin is involved in the cell cycle, the cytoskeleton, proteasome activity and ligand gated ion channel receptors and signalling molecules and is implicated in certain neurodegenerative diseases. This chapter introduces ubiquilin as a downstream target of zif268, implicating this relatively new protein in synaptic plasticity.

5.2 Aims & Objectives

- Identify and verify the presence of ubiquilin within the PC-12 cell line.

- Validate the original microarray experiment by transfecting PC-12 cells with full length or truncated zif268 and investigating ubiquilin expression at RNA and protein levels.

- Extend the findings found within the cell-line by utilising primary cortical neurones stimulated with either NMDA or vehicle over 24 hours and investigating ubiquilin expression at the RNA and protein levels.

- Look at ubiquilin RNA and protein levels harvested from zif268 knockout and wildtype mice to investigate the effects of genetic manipulation.

5.3 Results

5.3.1 PC-12 cells stain positively for ubiquilin

To assess ubiquilin expression within the PC-12 cell line, immunocytochemistry was performed on partially differentiated and undifferentiated cells using a rabbit anti-ubiquilin antibody. As illustrated in Figure 5.1A & 5.1B, using only a secondary antibody as a control shows very little or no staining on cells treated or untreated with nerve growth factor. In contrast, undifferentiated cells stained with anti-ubiquilin show diffuse staining and distinct puncta (figure 5.1C). PC-12 cells treated with nerve growth factor for 2 hours before fixing with formaldehyde show the appearance of dendrite-like processes. In addition, they show ubiquilin immunoreactivity throughout the cells, including punctuate staining along processes, and display stronger staining than the undifferentiated cells (figure 5.1D).

5.3.2 Ubiquilin is downregulated in PC-12 cells after transient transfection with zif268

Transient transfection of 1 μg/mL full-length zif268 into PC-12 cells treated with 50 ng/mL nerve growth factor showed a statistically significant reduction in ubiquilin RNA when compared to cells transfected with 1 μg/mL of a truncated control zif268 ($p<0.05$, one sample t-test, $n=5$; see figure 5.2). RT-PCR was performed using GAPDH primers and exon-intron spanning primers for ubiquilin. A single cycle within the logarithmic linear phase was taken for each transcript and the log GAPDH normalised pixel intensity value subtracted from the log ubiquilin normalised pixel intensity value. This revealed a 13% reduction in ubiquilin RNA in PC-12 cells transiently transfected with full length zif268 compared to control.

Utilising western blotting, it was found that protein levels of ubiquilin were not significantly downregulated within the same experimental paradigm, with full length transiently transfected zif268 PC-12 cells displaying a non-significant 8% reduction in normalised pixel intensity when compared to control ($n=6$; see figure 5.3 A & B).

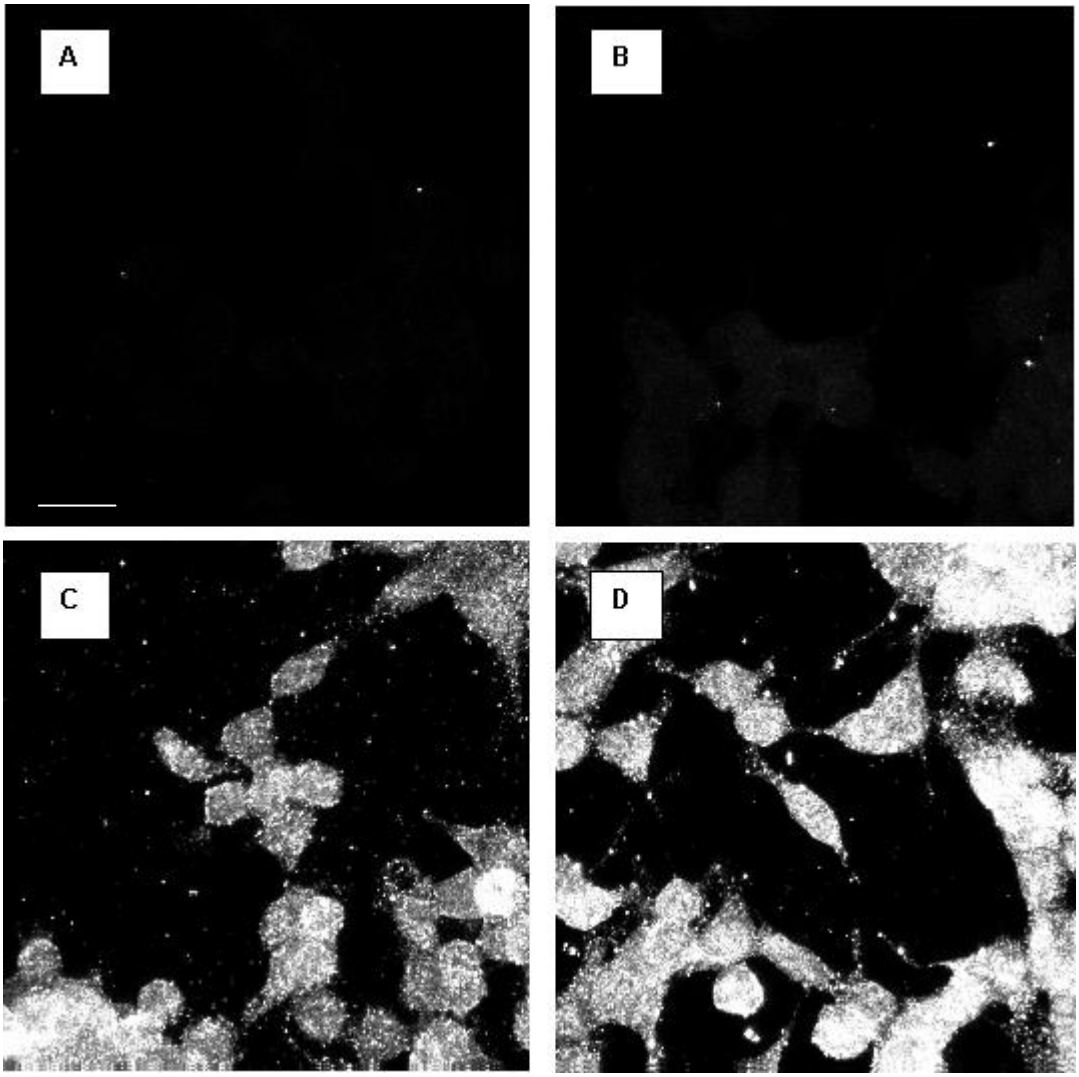

Figure 5.1: Confocal images of ubiquilin staining in PC-12 cells. *A*, undifferentiated cells stained only with 1:100 anti-rabbit Alexa 594. *B*, PC-12 cells pre-incubated for 2 hours with 50ng/mL NGF-7S and stained only with 1:100 anti-rabbit Alexa 594. *C*, undifferentiated PC-12 cells stained with 1:100 anti-ubiquilin and 1:100 anti-rabbit Alexa 594. *D*, PC-12 cells pre-incubated for 2 hours with 50ng/ml NGF-7S and stained with 1:100 anti-ubiquilin and 1:100 anti-rabbit Alexa 594. Scale bar 15μm.

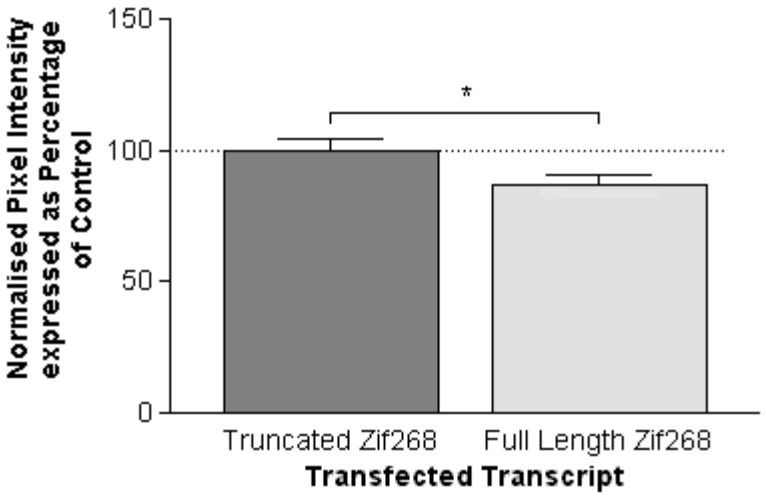

Figure 5.2: The effect of zif268 on ubiquilin mRNA in PC-12 cells. Graph comparing ubiquilin RNA levels as assessed by signal intensities at a single RT-PCR cycle from differentiated PC-12 cells transiently transfected with either full length or truncated zif268. Results are presented as ubiquilin normalised pixel intensity after normalisation to corresponding GAPDH values. All data expressed as mean percentage of control ± SEM. *p<0.05 one sample t-test, n=5.

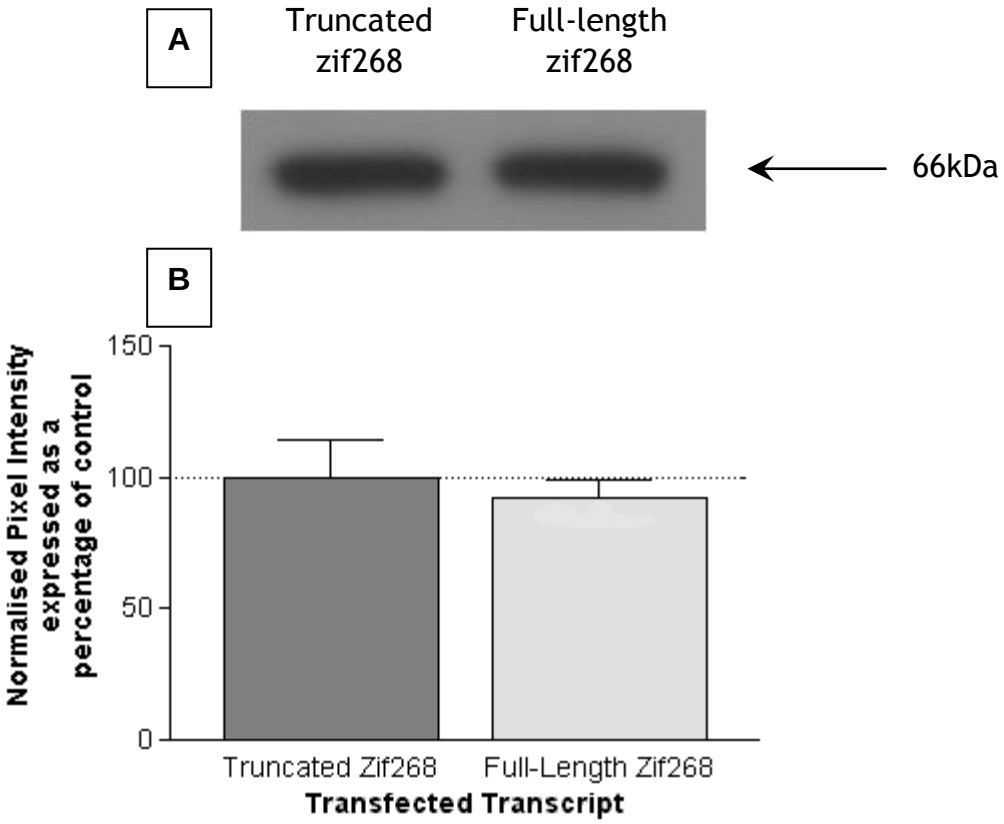

Figure 5.3: The effect of zif268 on ubiquilin protein levels in PC-12 cells *A,* Representative image of western blot comparing ubiquilin protein levels from PC-12 cells transfected with either full length or truncated zif268. *B,* Graph comparing protein levels of differentiated PC-12 cells transiently transfected with either full length or truncated zif268, as determined by western blotting. Results are presented as ubiquilin normalised pixel intensity. All data expressed as a mean percentage of control ± SEM, n=6.

5.3.3 Ubiquilin is time-dependently downregulated in cultured cortical neurones after NMDA treatment

NMDA stimulation (100µM NMDA in 20mM KCl) of cultured primary cortical neurones for 6 hours displayed a statistically significant downregulation of approximately 23% in ubiquilin RNA levels when compared to vehicle as determined by RT-PCR ($p<0.01$, ANCOVA, n=4; see figure 5.4). Statistically, we employed the ANCOVA in order to adjust for variances, with GAPDH as the covariate. Looking at protein levels, ubiquilin is significantly downregulated when stimulated with NMDA for 3 hours (29.8 $\pm$ 5.8% of control) and 6 hours (30.9 $\pm$ 7.3% of control) as determined by immunocytochemistry ($p<0.05$ and $p<0.01$ respectively, two-way ANOVA with Tukeys *post-hoc* test; see figure 5.6). Figure 5.7 contains representative confocal images of primary cultured neurones treated for 3 hours with NMDA or control.

In contrast, when comparing RNA and protein levels after 24-hour stimulation with NMDA, ubiquilin is not significantly different from primary cortical neurones treated with vehicle for 24 hours (see figures 5.5 and 5.6). Western blotting of protein levels after 3 hours, 6 hours or 24 hours NMDA stimulation showed no significant differences when compared with controls (see figure 5.8A & B).

5.3.4 Ubiquilin RNA is downregulated in zif268 knockout mice

A comparison of RNA extracted from zif268 knockout mice and their associated wildtype counterparts by RT-PCR show that ubiquilin is significantly downregulated (ANCOVA $p<0.01$; see figure 5.9). At the protein level however, western blotting shows no significant difference between zif268 knockout mice and the wildtypes (figures 5.10 A & B).

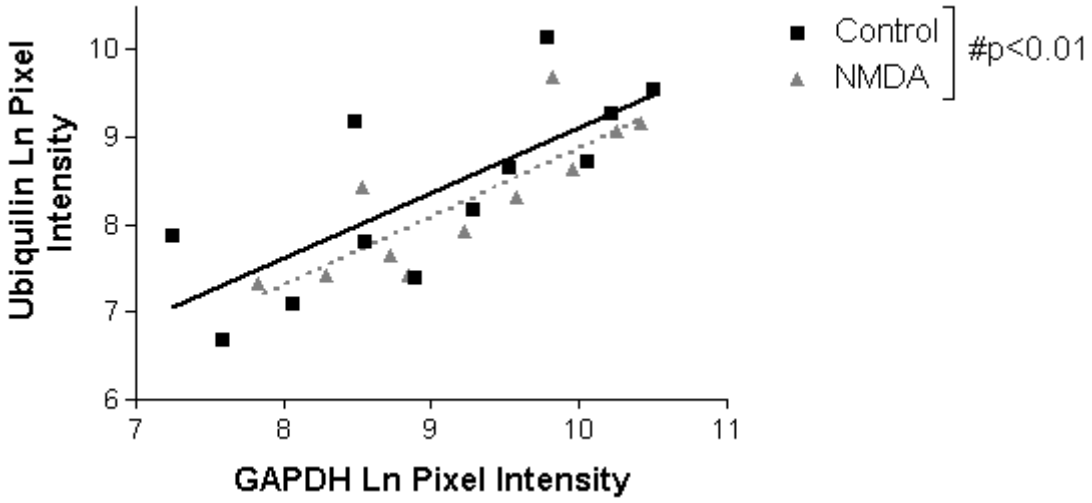

Figure 5.4: The effect of 6 hours NMDA stimulation on ubiquilin mRNA in cultured neurones. Graph illustrating ubiquilin log pixel intensity as a function of GAPDH log pixel intensity, as determined by RT-PCR of cultured primary cortical neurones stimulated for 6 hours with either 100µM NMDA in 20mM KCl or Vehicle. Effect of NMDA treatment #p<0.01, F(1,15)=8.45, ANCOVA n=4.

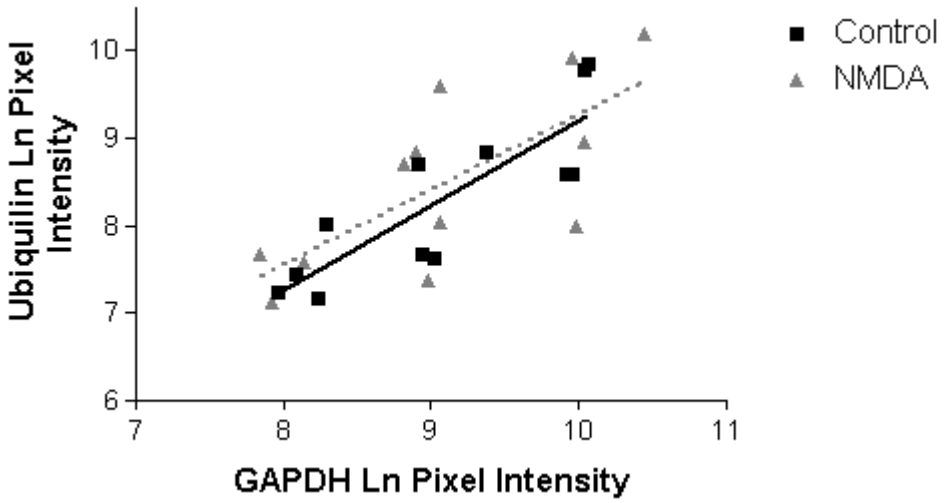

Figure 5.5: The effect of 24 hours NMDA stimulation on ubiquilin mRNA in cultured neurones. Graph illustrating ubiquilin log pixel intensity as a function of GAPDH log pixel intensity as determined by RT-PCR of cultured primary cortical neurones stimulated for 24 hours with either 100µM NMDA in 20mM KCl or Vehicle. n=4.

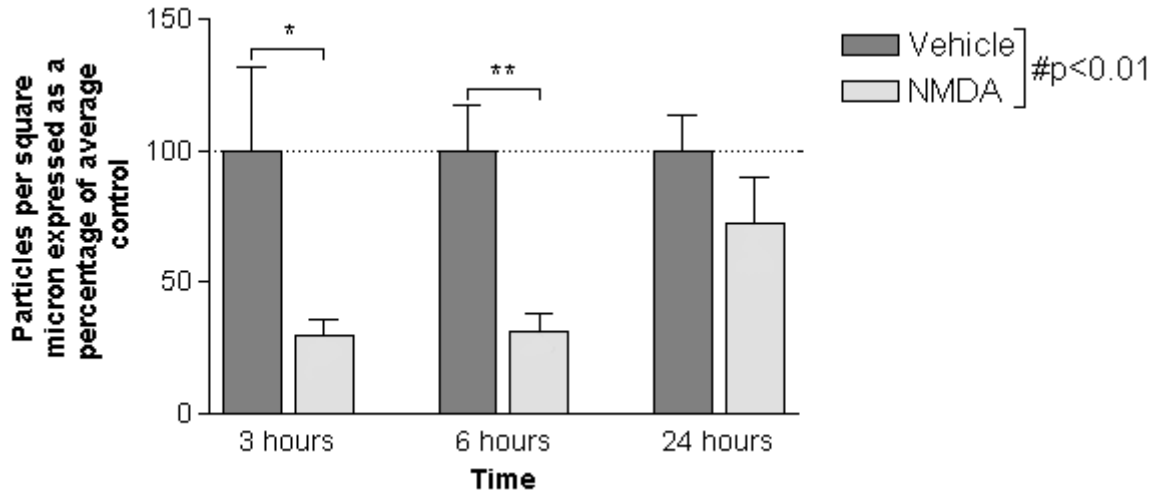

Figure 5.6: The effect of NMDA stimulation on ubiquilin protein levels in cultured neurones. Graph illustrating the effect of treatment of cultured cortical neurones (21DIV) for either 3 hours, 6 hours or 24 hours with either 100µM NMDA in 20mM KCl or vehicle on ubiquilin immunoreactivity, as detected by immunocytochemistry. Results are presented as the number of particles measured per square micron and expressed as a mean percentage of the signal in control (vehicle treated) cells ± SEM. Effect of treatment, #p<0.01, F(1,27) = 22.44, two-way ANOVA. Effect of time **p<0.01, *p<0.05, Tukeys *post hoc* test, n=5

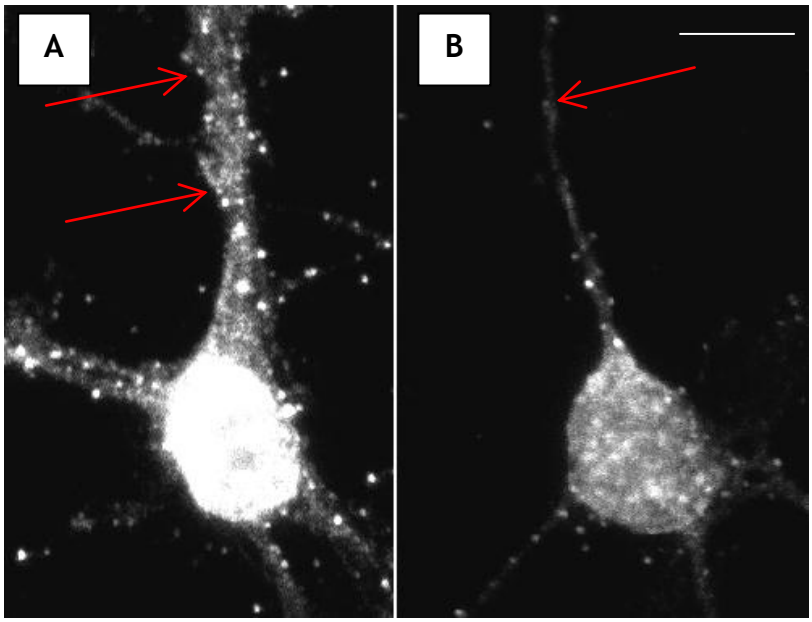

Figure 5.7: Images of ubiquilin within cultured neurones after 3 hours NMDA stimulation. A representative image comparing primary cultured cortical neurones (21 DIV) treated for 3 hours with vehicle (A) or with 100 µM NMDA in 20 mM KCl (B), probed with anti-ubiquilin and visualised with a confocal microscope as per the immunocytochemistry protocol. Arrows depict the measured puncta within cells A and B. Scale bar 15 µm.

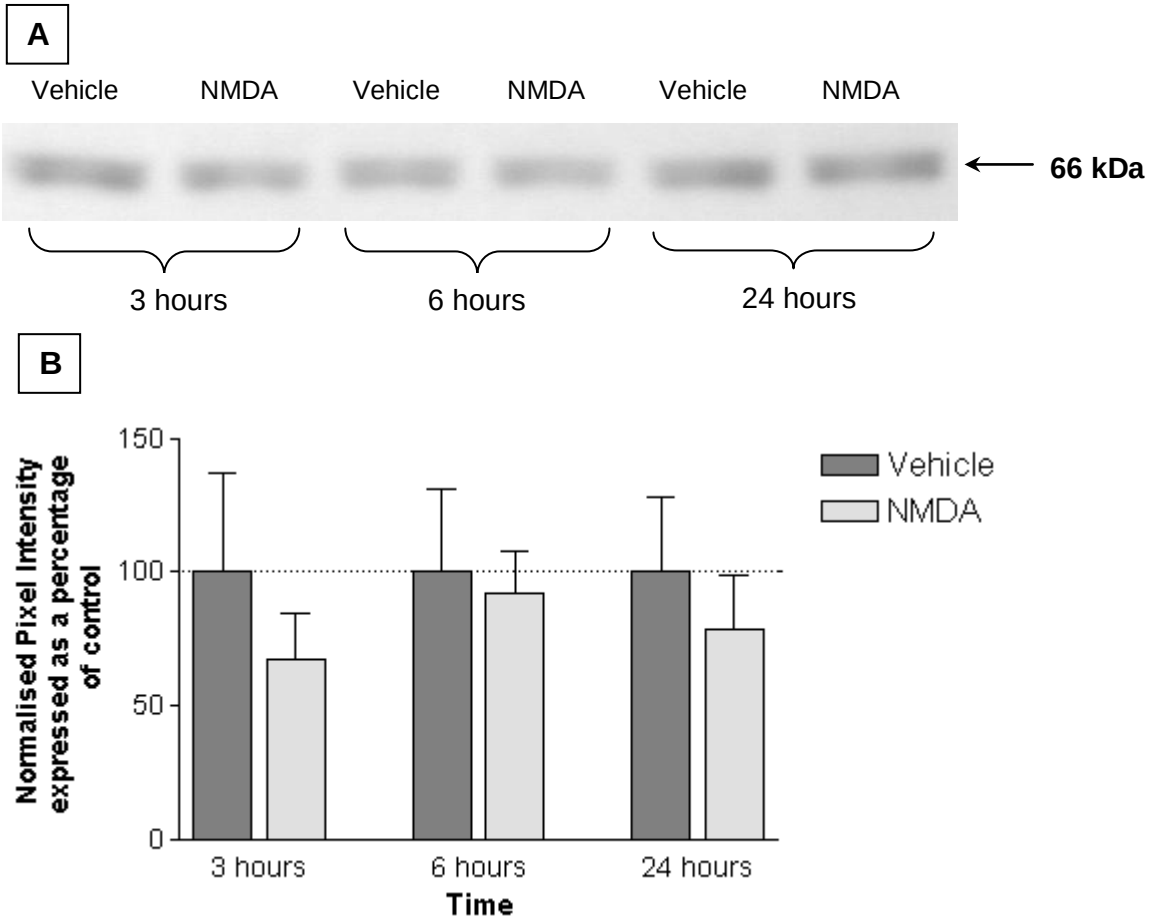

Figure 5.8: The effect of NMDA stimulation on ubiquilin protein levels in cultured neurones by western blot *A:* Representative western blot of ubiquilin immunoreactivity in cultured cortical neurones stimulated for either 3 hours, 6 hours or 24 hours with either 100µM NMDA in 20mM KCl or vehicle and probed with anti-ubiquilin. *B:* Graph comparing ubiquilin immunoreactive signal intensities from western blots of cultured cortical neurones (7-10 DIV) stimulated for either 3 hours, 6 hours or 24 hours with either 100µM NMDA in 20mM KCl or vehicle. Results are presented as normalised pixel intensity and expressed as a mean percentage of control (vehicle treatment) ± SEM. ANOVA revealed no significant effect of NMDA treatment and no significant interaction with time. Effect of NMDA $F(1,18) = 2.07$, $p>0.05$, interaction of time and treatment $F(2,18) = 0.55$, $p>0.05$, $n=4$.

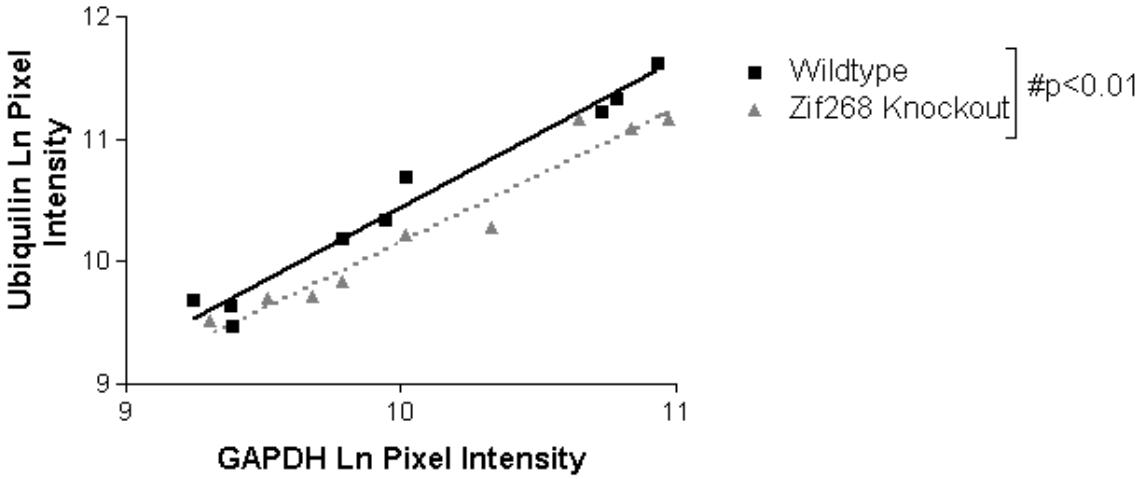

Figure 5.9: The effect of a zif268 targeted deletion on ubiquilin mRNA in the adult cortex. Graph illustrating ubiquilin log pixel intensity as a function of GAPDH log pixel intensity, as determined by RT-PCR of adult cerebral cortex tissue from either wildtype or zif268 knockout mice. #p<0.01 F(1,11) = 11.90, ANCOVA, n=3.

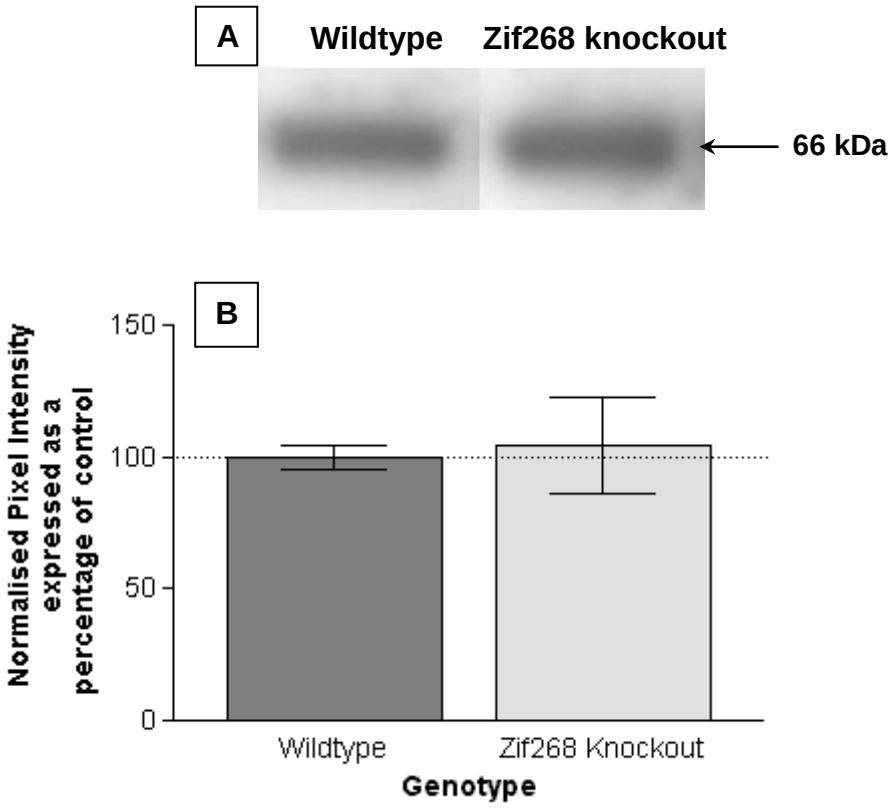

Figure 5.10: The effect of a zif268 targeted deletion on ubiquilin protein levels in the adult cortex. *A:* Representative western blot comparing ubiquilin immunoreactivity signal in cortical tissue from wildtype and zif268 knockout mice. *B:* Graph comparing ubiquilin immunoreactivity signal intensities from western blots of adult cerebral cortex tissue extracted from either wildtype or knockout zif268 mice. Results are presented as normalised pixel intensity and expressed as a mean percentage of total control (wildtype tissue) ± SEM. Wildtype, n=7, knockout zif268, n=5.

5.4 Discussion

This is the first study to identify ubiquilin as a downstream target gene of the inducible transcription factor zif268. Ubiquilin RNA and protein levels are downregulated by increased amounts of zif268 and ubiquilin mRNA levels are decreased in cortical tissue from zif268 knockout mice, implying that ubiquilin is a transcriptional target of this plasticity related gene.

Initial experiments used a pheochromocytoma derived cell line in order to establish the validity of the original microarray experiment (James *et al.* 2005). In the first instance, PC-12 cells were partially differentiated with nerve growth factor. Applying an anti-ubiquilin antibody revealed punctate staining throughout the cytoplasm and processes, confirming the presence of ubiquilin protein. The ubiquilin antibody used has not been widely cited, however, it is directed towards amino acid residues 2-18 of ubiquilin and displayed a high level of specificity in western blot experiments.

The upregulation of zif268 by transient transfection in the presence of forskolin produced a significant decrease in ubiquilin RNA when compared with a truncated control form of zif268. This validated the significant result achieved previously by James *et al.* (2005). At the protein level however, no significant result was achieved. Western blotting has changed very little since its development in 1979 (Towbin *et al.* 1979). Among this technique's limitations is the problem of restricted quantitative capability and PCR is generally a more sensitive method of detection (Liu *et al.* 2004).

We next looked at the effect increasing zif268 had on cultured dissociated primary cortical neurones. Zif268 protein levels peak at 2 hours after stimulation (Richardson *et al*. 1992) whereby it enters the nucleus to regulate downstream targets. Therefore, cells were harvested at 2 time points in order to delineate any time dependent effects of zif268 stimulation. At 6 hours, ubiquilin RNA levels were significantly decreased in cells stimulated with NMDA when compared to vehicle-stimulated cells. This result is echoed in the protein levels, which are also significantly decreased when looking at the immunocytochemistry results. An additional time point of 3 hours stimulation was examined with the protein levels allowing a further insight into ubiquilin actions after zif268 induction. At 3 hours, ubiquilin protein levels are significantly decreased when compared to controls.

However, at 24 hours both RNA and protein levels have returned towards a basal level, inferring that zif268's actions could be time-dependent. This is consistent with the ubiquilin gene being regulated by transient induction of zif268 following NMDA receptor stimulation.

Changes in ubiquilin protein levels were apparent using immunocytochemical techniques. The paraformaldehyde fixation stage of immunofluorescence procedures can produce artefacts in immunocytochemistry. In addition, unfortunately, optimal antibody concentrations were determined by visualisation with an inverted light microscope, before the availability of image capture with the confocal microscope. The specific laser used in the confocal microscope has a wavelength of 568nm, which means that the fluorescent Alexa 594 secondary antibody is only reaching 50% excitation. This required an increase in laser power which uniformly increased background and could have created less than optimal conditions for ubiquilin immunoreactivity detection. However, we attempted to circumvent any possible problems with generic staining by using the Image J program. This allows a certain threshold to be set in order to minimise any background noise, which can be individually altered for each image, and all the results were performed blind. Hence, the data obtained can be viewed with considerable confidence. Earlier data from our laboratory (McDermot & Morris, unpublished) showed no evidence of apoptosis or necrosis at extended times after this NMDA treatment protocol. It is also encouraging to note that the return of ubiquilin RNA and protein to basal levels after 24 hours suggests that any changes at earlier time points were due to a genuine downregulation in ubiquilin and not to cell death.

Western blotting to detect protein levels of ubiquilin after zif268 induction by NMDA stimulation produced no significant results at 3 hours, 6 hours or 24 hours. However, contradictory results in protein levels detected by western blot compared to immunocytochemistry have been obtained by others (Salvador-Silva *et al.* 2001; Lindahl & Keifer 2004) and may reflect the fundamental difference between the techniques: western blotting detects whole cell proteins whilst immunocytochemistry has a more directed approach.

When comparing RNA levels of zif268 knockout mice compared to wildtypes a significant reduction in ubiquilin was detected. This result was surprising, as an absence of zif268 would suggest an increase in ubiquilin RNA. There are many

inherent problems with knockout mice however, especially those that deal with immediate early genes (Prof. Hugh Piggins, Manchester University; personal communication). There is an element of redundancy in many control systems allowing for developmental compensation. In particular, there is strong evidence that another member of the Egr family, Egr4 can compensate for the absence of zif268 in these knockout mice (Tourtellotte *et al.* 2000). Propitiously, it does demonstrate that ubiquilin is ultimately a target of zif268, as ubiquilin's expression is significantly affected by zif268's absence. The western blot did not detect any changes in ubiquilin protein levels in zif268 knockout mice compared to wildtypes, possibly due to limitations inherent in the technique. As a complimentary experiment to the RNA work and to extend protein detection, we had hoped to culture zif268 knockout and wildtype cortical tissues for 21 days, genotype the cultures by removing additional tissue at dissection, and perform immunocytochemistry with the ubiquilin antibody. Unfortunately, colony breeding was intermittent, delivering minimal litter sizes and creating time constraint problems. Ubiquilin labelling in zif268 knockout and wildtype mice treated with haloperidol to produce an *in vivo* model of synaptic plasticity sadly did not produce results. More time would be needed to optimise the oligonucleotide labelling. Overall, however, these results provide strong support for the hypothesis that ubiquilin expression is regulated by zif268.

The overall hypothesis of the effect zif268 has on ubiquilin concerns the effects this may produce in $GABA_A$Rs at the synapse, which will be discussed later. The number of cellular functions in which ubiquilin has been implicated leads to further consequences of ubiquilin downregulation that could affect a myriad of different systems. Ubiquilin is localised to neuropathological inclusions in AD, PD (Mah *et al.* 2000) and HD (Doi *et al.* 2004) and has been shown to modulate the accumulation of presenilin proteins (Mah *et al.* 2000). This suggests that increased ubiquilin levels are involved in or associated with neuronal disease. Zif268 expression is decreased in AD transgenic mouse models modelling amyloid deposition (APP+PS1) (Dickey *et al.* 2003; Dickey *et al*. 2004), although zif268 actions still remain controversial in neurodegenerative diseases (Rensink *et al.* 2002).

In addition, ubiquilin is upregulated in response to hypoxia (Ko et al. 2002), whereas zif268 mRNA expression is inhibited (Hung *et al*. 2000). Zif268 has many different roles, as it is induced by DNA damaging agents (Quinones *et al.* 2003),

and may have a role in the cellular reaction to hyperoxia (Jones and Agani 2003) and apoptosis (Pignatelli *et al.* 2003). Chaperones assist the folding of newly synthesised proteins and refolding of proteins damaged by stress and cellular injuries. Incorrectly folded proteins are delivered to the ubiquitin-proteasome system, and ubiquilin is known to act post transcriptionally like a molecular chaperone (Funakoshi *et al.* 1999; Davidson *et al.* 2000; Kaye *et al*. 2000). A decrease in ubiquilin therefore may increase the number of misfolded and unrepaired proteins within the cell, increasing the number of proteins delivered to the proteasome.

At the level of the cytoskeleton, mouse Plic-1 and Plic-2 have an involvement in linking integrins via integrin-associated proteins to the intermediate filaments (Wu *et al.* 1999). Ubiquilin, therefore, could connect the plasma membrane and the cytoskeleton and may be involved in regulating adhesion and migration, an important property for synaptic plasticity.

In summary, the diversity of studies leave it unclear exactly what the consequences of altered ubiquilin expression will be. Clearly, a lot more experimentation is required to find out the many and varied roles of this protein. Nevertheless, the data provides strong evidence that expression of the ubiquilin gene is regulated during plasticity by zif268.

Chapter 6

Potential downstream effects of the modulation of gephyrin & ubiquilin expression by zif268

6.1 Introduction

Gephyrin and ubiquilin have been functionally linked to both the $GABA_AR$ and mTOR (mammalian target of rapamycin). In order to gain a greater understanding of the possible downstream consequences in response to altered zif268 expression, the effects potentially resulting from changes in gephyrin and ubiquilin levels were the subjects of a preliminary investigation.

6.1.1 The $GABA_AR$ at the synapse

$GABA_ARs$ are ligand-gated chloride channels that exist in numerous distinct subunit combinations, but the $\alpha1\beta2\gamma2$ combination is the most predominantly expressed receptor multimers, followed by $\alpha2\beta3\gamma2$ and $\alpha3\beta3\gamma2$ (Fritschy *et al.* 2003). $GABA_ARs$ containing α and β subunits can reach the cell surface (Connolly *et al.* 1996b) however, there is a necessity for the γ subunit for synaptic localisation (Essrich *et al.* 1998). Gephyrin has been linked with the α1-3, β3 and γ2 subunits of the $GABA_ARs$ at postsynaptic sites (Kirsch *et al.* 1995; Essrich *et al.* 1998; Sassoe-Pognetto *et al.* 2000; Danglot *et al.* 2003), and ubiquilin binds to the α1-3, α6 and β1-3 subunits of the $GABA_AR$ (Bedford *et al.* 2001). Reduced gephyrin expression is predicted to decrease the number of $GABA_ARs$ clustered at synaptic sites, while decreased ubiquilin expression is predicted to reduce $GABA_AR$ number via enhanced proteasomal degradation.

6.1.2 Downstream effectors of mTOR

mTOR, also known as FRAP (FKBP-rapamycin-associated protein), RAFT1 (rapamycin and FKBP target) and RAPT1 (rapamycin target) (Brown *et al.* 1994; Chiu *et al.* 1994; Sabatini *et al.* 1994; Sabers *et al.* 1995) is a highly conserved serine-threonine kinase regulated by growth factors, and is involved in the regulation of translation activity. The dendritic translation of a subset of mRNAs involved in the protein-synthesis dependent induction of LTP is regulated by mTOR (Raught *et al.* 2001; Tang *et al.* 2002; Cammalleri *et al.* 2003). mTOR is a target of the immunosuppressant drug, and is inhibited by, rapamycin (Kunz *et al.* 1993; Helliwell *et al.* 1994). Rapamycin inhibits high frequency stimulation-induced protein synthesis, long term facilitation in *Aplysia* and late-phase LTP in the hippocampus (Casadio *et al.* 1999; Tang *et al.* 2002; Cammalleri *et al.* 2003;

Karpova et al. 2006). Figure 6.1 depicts a summary of the many ways that mTOR can be activated within cells.

Downstream targets of mTOR mainly comprise those proteins involved in ribosome recruitment to mRNA. 4E-BP1 (eIF4E-binding protein) is a repressor of mRNA translation until it becomes phosphorylated, an enzymatic action carried out by mTOR. eIF4E, a eukaryotic initiation factor that binds to the 5'cap of mRNA allowing the 40S ribosomal subunit to bind (Gingras *et al.* 1999), is inhibited when bound by 4E-BP1 (Schmelzle & Hall 2000). Phosphorylation of 4E-BP1, initially at Thr37 and Thr46 (Gingras *et al.* 1999), by mTOR releases it from eIF4E, allowing the initiation factor to bind with eIF4G, form a complex in association with eIF4A and permit translation (Haghighat *et al.* 1995; Marcotrigiano *et al.* 1999; Gingras *et al.* 1999).

mTOR also phosphorylates and activates p70 ribosomal S6 kinase (S6K), which leads to translational activation and ultimately, cell growth (Montagne *et al.* 1999; Radimerski *et al.* 2002). p70 S6K phosphorylates the 40S ribosomal protein S6 and allows the increased translation of mRNAs coding for components of the translational machinery, specifically the 5'TOP (terminal oligopyrimidine tract) mRNAs, including all the ribosomal proteins and elongation factors (Schwab *et al.* 1999; Gingras *et al.* 2001).

Rapamycin blocks phosphorylation of mTOR and, therefore, 4E-BP1 and p70 S6K inactivation and activation respectively. It has been demonstrated that both 4E-BP1 and p70 S6K are inhibited/activated by rapamycin *in vivo* and phosphorylated by mTOR in *vitro* (Brunn *et al.* 1997; Burnett *et al.* 1998). P70S6K or 4E-BP1 phosphorylation can be used as an *in vivo* readout of mTOR activity.

Utilising yeast di-hybrid systems, it has been found that mTOR interacts with both ubiquilin and gephyrin (Sabatini et al. 1999; Wu et al. 2002). We reasoned that in PC-12 cells, containing no $GABA_A$Rs, gephyrin and ubiquilin may modulate cellular signalling through mTOR. To this end we monitored levels of phospho-4E-BP1 and phospho-p70 S6K as an indication of mTOR activity.

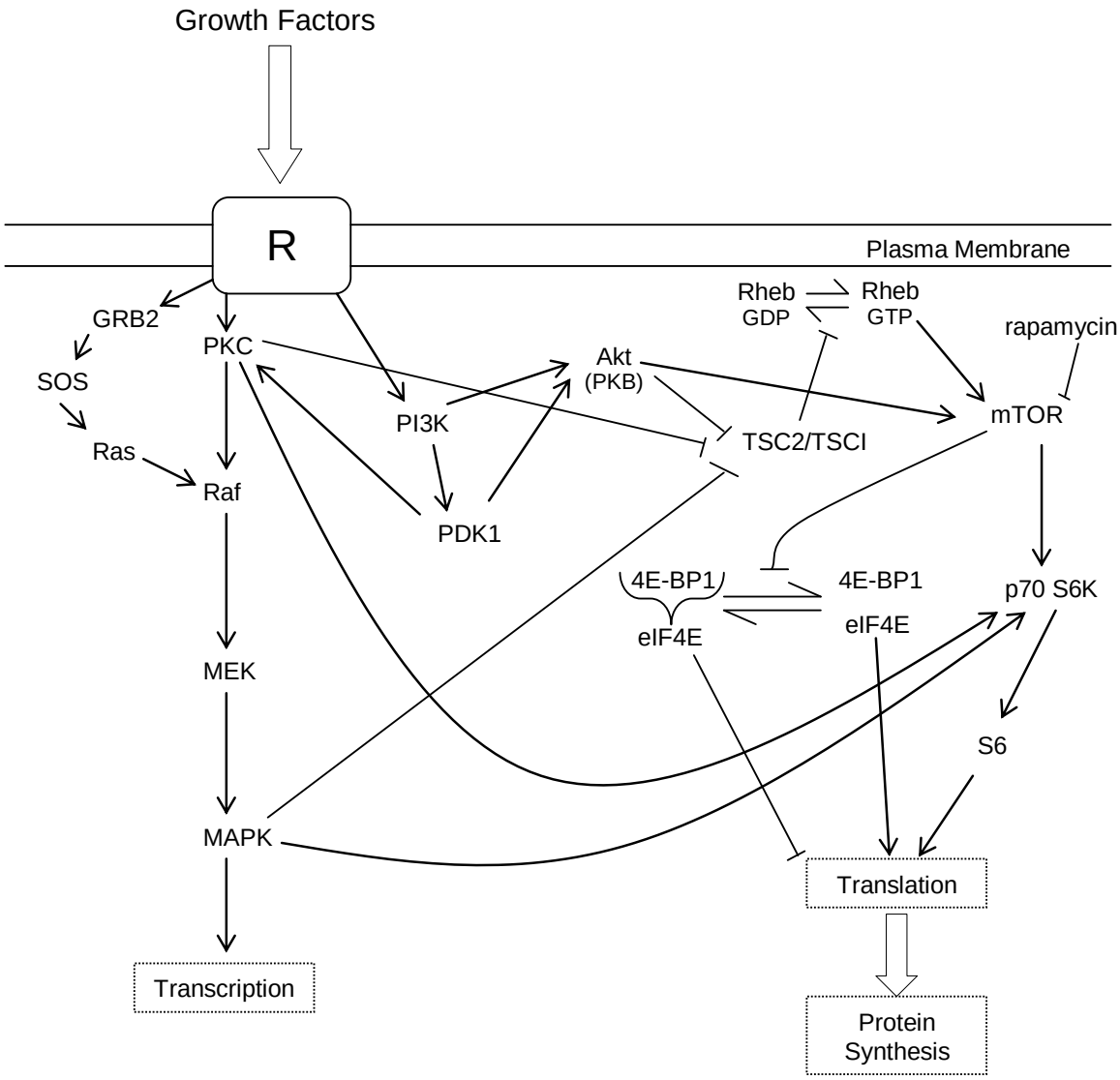

Figure 6.1: A simplified diagram of the activation and downstream effects of mTOR on protein synthesis. Growth factors activate receptors (R depicts the growth factor receptor) leading to the activation of many protein kinases and signalling pathways, ultimately culminating in the activation of mTOR. eIF4E, an initiation factor, is inhibited when bound by its repressor 4E-BP1. The phosphorylation of 4E-BP1 by mTOR releases eIF4E and activates translation. mTOR also phosphorylates the S6 kinase, activating translation. Diagram produced from information reviewed in Hay and Sonenberg (2004) and Asnaghi *et al.* (2004).

6.2 Aims & Objectives

- Investigate the effect of NMDA stimulation on the number of $GABA_A$ receptor β2/3 and γ2 subunits localised to the plasma membrane of primary cultured cortical neurones.

- Study the effects of altered zif268 expression on mTOR effectors, p70 S6 kinase and 4E-BP1.

6.3 Results

6.3.1 $GABA_AR$ β 2/3 numbers are not altered in response to NMDA stimulation

Primary cortical neurones were aged *in vitro* for 3 weeks as most $GABA_ARs$ are expressed postnatally (Laurie *et al.* 1992) and inhibitory synapse maturation takes approximately 21 days in cultured hippocampal neurones (Craig *et al*. 1996; Levi *et al*. 2002).

No effect of NMDA stimulation was found on the density of punctate $GABA_AR$ β chain immunoreactivity when compared to vehicle treated cultured primary cortical neurones by immunocytochemistry ($p>0.05$, 2-way ANOVA, n=6; see figure 6.2 and 6.3). Specifically, there was no overall effect of treatment or time and no interaction between treatment and time. However, there was a tendency for NMDA treatment to reduce the density of the labelled puncta at later time points. For normalisation and resultant statistical analysis, the log value of pixel intensities was used. For graphs, all values are presented as percentages of vehicle treated cells.

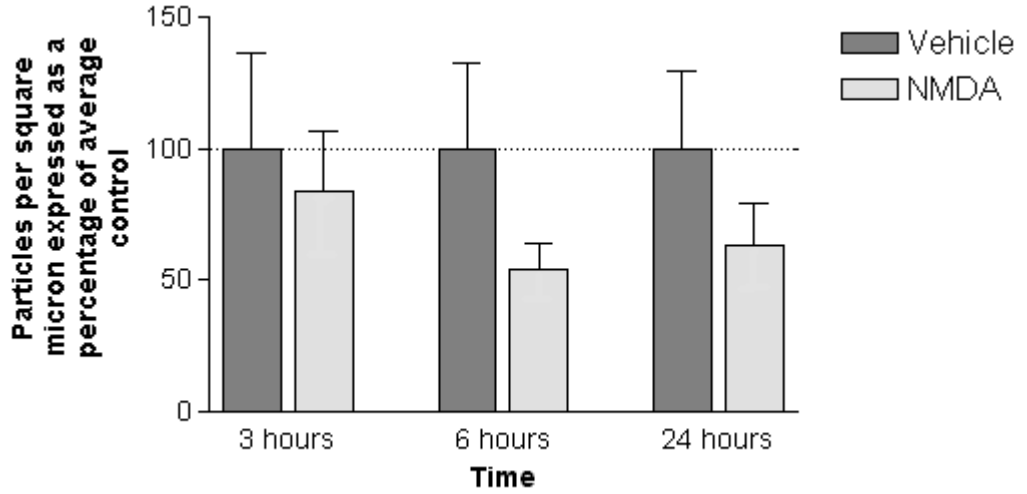

Figure 6.2: The effect of NMDA stimulation on the density of puncta immunoreactive for the $GABA_AR$ β chain in cultured cortical neurones. Graph illustrating the effect of treatment of 3, 6 or 24 hour stimulation of 100μM NMDA in 20mM KCl or vehicle on $GABA_A$ β2/3 subunits immunoreactivity of 21 DIV primary cultured cortical neurones as detected by immunocytochemistry. Results are presented as the number of puncta measured per square micron and expressed as a mean percentage of the signal in control (vehicle-treated) cells ± SEM, The effect of treatment, $p>0.05$, $F(1,29)=1.20$, 2-way ANOVA, n=6.

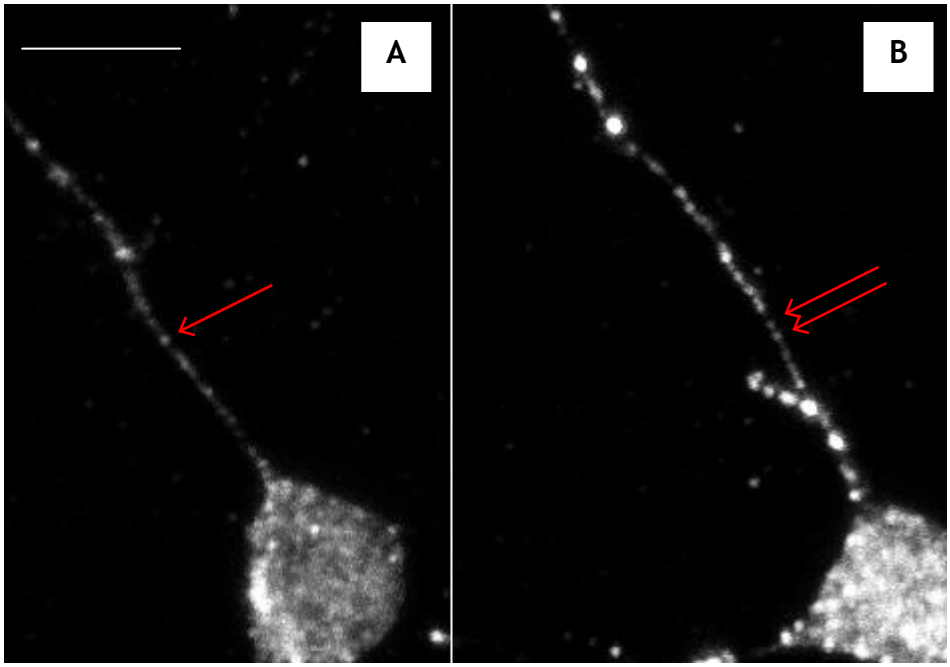

Figure 6.3: Images of $GABA_A$ β chains within cultured neurones after 6 hours NMDA stimulation. A representative image comparing primary cultured cortical neurones (21 DIV) treated for 6 hours with 100 μM NMDA in 20 mM KCl (A) or vehicle (B), probed with anti- $GABA_A$ β2/3 subunit antibody and visualised with a confocal microscope as per the immunocytochemistry protocol. Arrows depict examples of the measured puncta within cells A and B. Scale bar 15 μm.

6.3.2 $GABA_A$ γ2 subunits are downregulated in response to NMDA stimulation

Using immunocytochemistry, an overall effect of NMDA treatment was found on the density of punctate $GABA_A$ γ2 subunit immunoreactivity within cultured primary cortical neurones when compared to control (vehicle treated) cells ($p<0.01$ effect of treatment, $F(1,11) = 9.16$, 2-way ANOVA, factors: time and treatment, n=3; see figure 6.4). There was no overall effect of time ($p = 0.311$, $F(2,11) = 1.30$) and no interaction between treatment and time ($p = 0.257$, $F(2,11) = 1.54$). The log value of pixel intensities was used for normalisation and resultant statistical analysis. For graphical presentation all values are presented as percentages of control (vehicle treatment). Figure 6.5 contains representative confocal images of primary cortical neurones treated with either vehicle or NMDA for 3 hours.

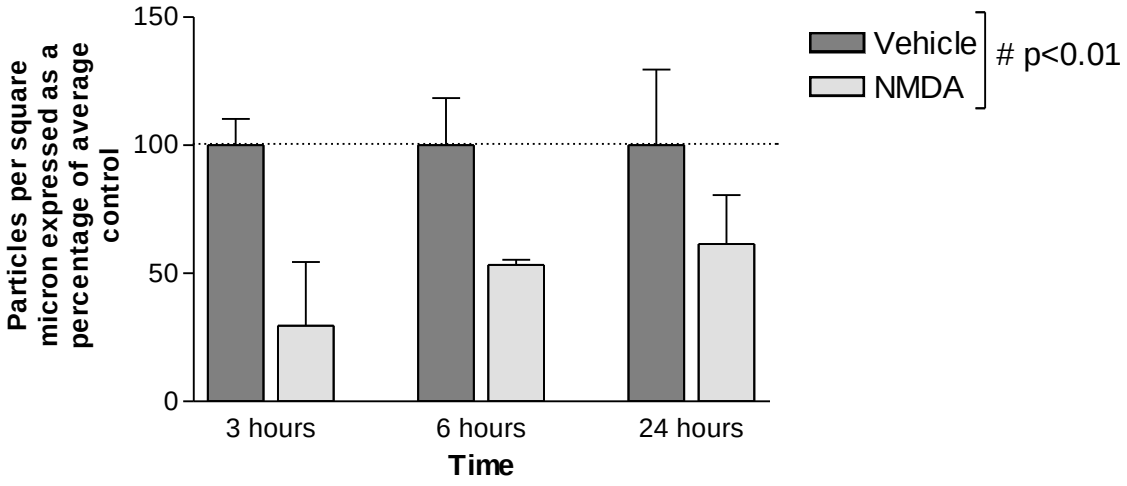

Figure 6.4: The effect of NMDA stimulation on the density of puncta immunoreactive for $GABA_A$ γ2 subunit in cultured cortical neurones. Graph illustrating the effect of treatment of 3, 6 or 24 hour stimulation of 100μM NMDA in 20mM KCl or vehicle on the $GABA_A$ γ2 subunit immunoreactivity of 21 DIV primary cultured cortical neurones as detected by immunocytochemistry. Results are presented as the number of puncta measured per square micron and expressed as a mean percentage of the signal in control (vehicle-treated) cells ± SEM, The effect of treatment #p<0.01, F(1,11)=9.16, 2-way ANOVA n=3.

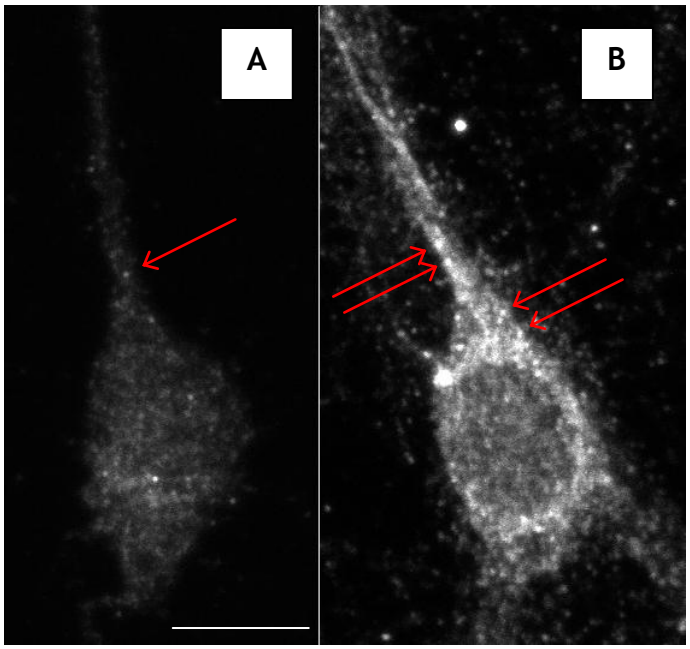

Figure 6.5: Images of $GABA_A$ γ2 subunits within cultured neurones after 3 hours NMDA stimulation. A representative image comparing primary cultured cortical neurones (21 DIV) treated for 6 hours with 100 μM in 20 mM KCl (A) or vehicle (B), probed with anti- $GABA_A$ γ2 and visualised with a confocal microscope as per the immunocytochemistry protocol. Arrows depict examples of the measured puncta within cells A and B. Scale bar 15 μm.

6.3.3 Phosphorylation of mTOR targets is not altered in response to zif268 overexpression in PC-12 cells

4E-BP1 and p70S6K phospho-protein levels within PC-12 cells transiently transfected with 1 μg/mL full-length zif268 pre-treated with 50 ng/mL nerve growth factor show no effect compared to control (truncated) transfected cells as determined by western blotting ($p>0.05$, one sample t-test, n=3; see figures 6.6 A & B and 6.7 A & B).

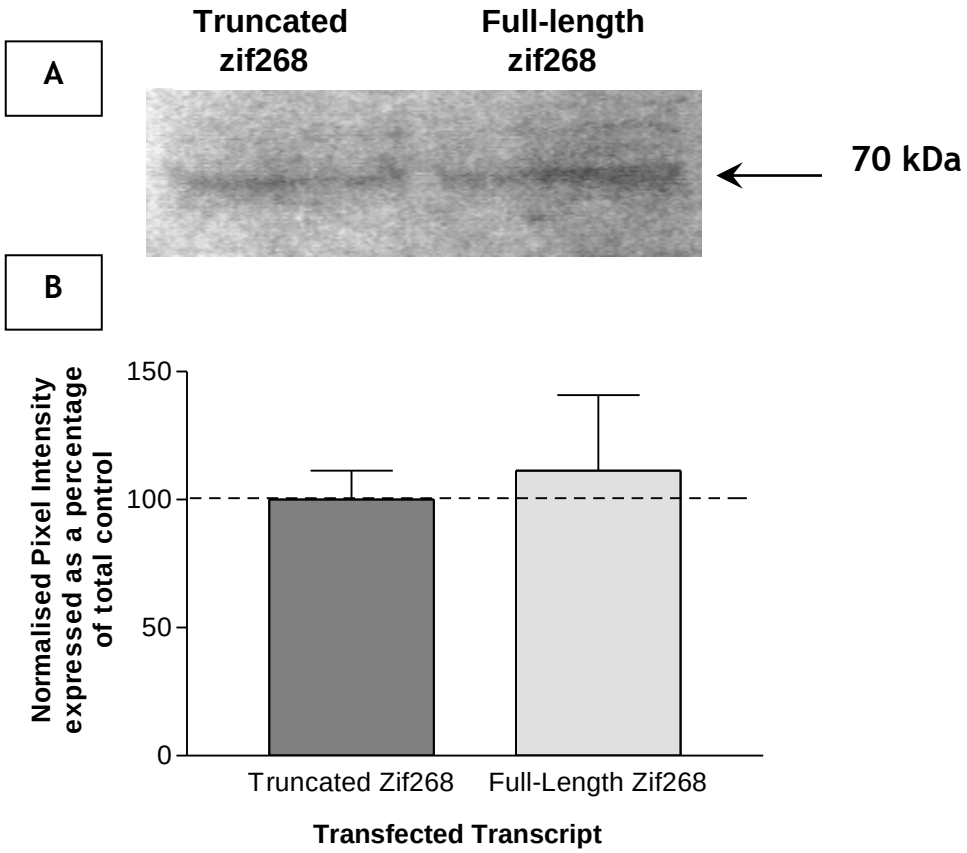

Figure 6.6: The effect of zif268 on phospho-p70S6K protein levels in PC-12 cells. *A,* Representative western blot comparing phospho-p70S6K immunoreactivity in PC-12 cells transiently transfected with either truncated or full-length zif268. *B,* Graph comparing phospho-p70S6K protein levels from PC-12 cells transiently transfected with either truncated or full-length zif268 as determined by western blotting. Results are presented as phospho-p70S6K normalised pixel intensity. All data is expressed as a mean percentage of control ± SEM, n=3.

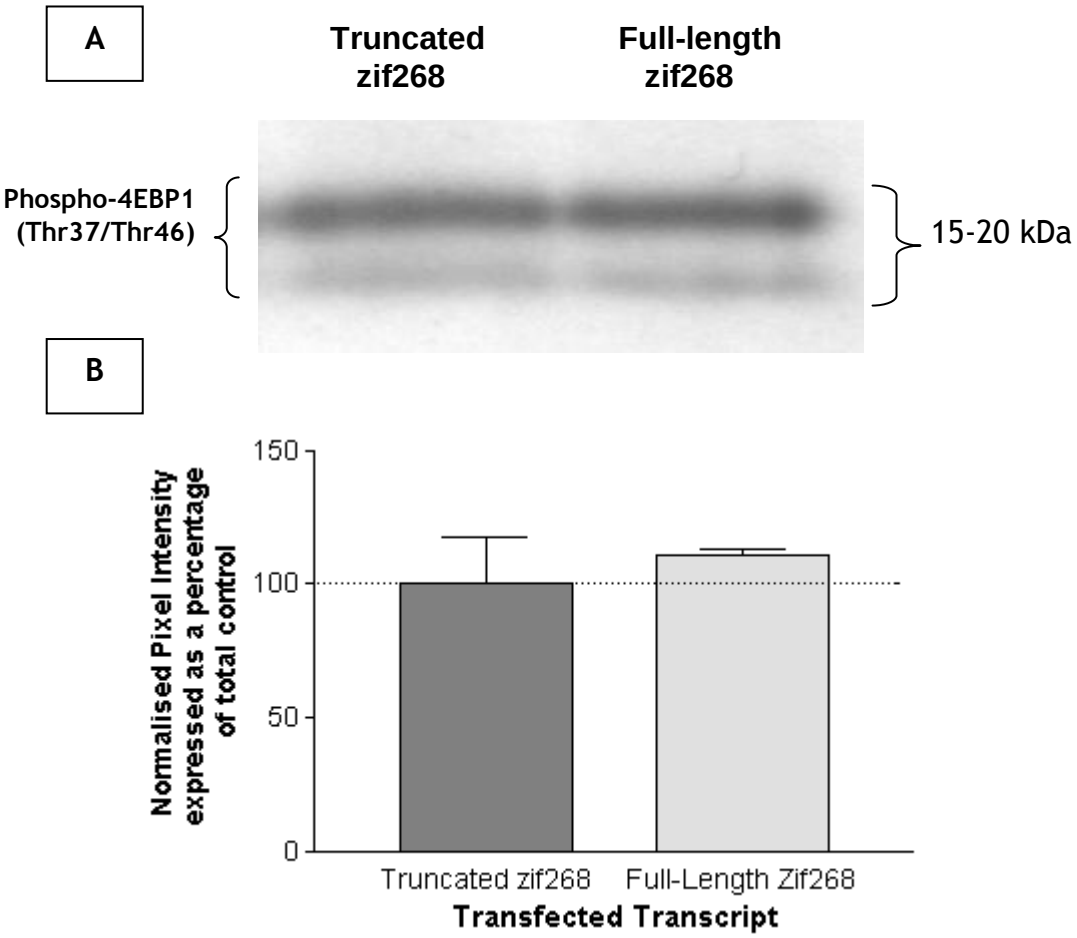

Figure 6.7: The effect of zif268 on phospho-4E-BP1 protein levels in PC-12 cells. *A,* Representative western blot comparing phospho-4E-BP1 (Thr37/Thr46) immunoreactivity in PC-12 cells transiently transfected with either truncated or full-length zif268. *B,* Graph comparing phospho-4EB-BP1 protein levels from PC-12 cells transiently transfected with either truncated or full-length zif268 as determined by western blotting. Results are presented as phospho-4E-BP1 normalised pixel intensity. All data is expressed as a mean percentage of control ± SEM, n=3.

6.4 Discussion

6.4.1 $GABA_AR$ density in response to NMDAR stimulation

This chapter attempted to investigate the joint downstream effects of gephyrin and ubiquilin downregulated by an increase in zif268 levels. Gephyrin is thought to mediate clustering and/or synaptic anchoring (Craig *et al.* 1996; Kneussel *et al.* 1999a) and ubiquilin is involved in membrane trafficking of $GABA_AR$s (Bedford *et al.* 2001). Hence it can be postulated that decreased expression of gephyrin and ubiquilin following zif268 induction might affect synaptic $GABA_AR$ levels.

The application of NMDA for up to 24 hours produced no significant effect on the density of receptors containing the β chain. However, receptors containing the γ subunit displayed an overall effect of NMDA treatment when compared to vehicle treated cells.

The co-transfection of $GABA_AR$ $\beta3$ subunits and gephyrin into HEK293 cells causes the intracellular co-localisation of both elements (Kirsch *et al.* 1995), and co-expressing ubiquilin with receptors containing the $\beta3$ subunit creates co-localised clusters below the plasma membrane (Bedford *et al.* 2001). The $\beta2$ subunit is necessary for $GABA_A$ receptor cell surface expression (Connolly *et al*. 1996b), and therefore the extracellular antibody against the $\beta2/3$ subunits recognizes most $GABA_A$ receptor subtypes in cortical neurones and was used by Bedford *et al.* (2001) and Danglot *et al.* (2003) among many others.

The γ subunit, along with gephyrin, is critical for synaptic targeting (Essrich *et al.* 1998), and so $\gamma2$ subunits were visualised to look specifically at gephyrin clustering of $GABA_AR$ at synapses. The antibody was utilised by O'Sullivan *et al.* (2005) and was directed at extracellular sequences of the subunit and so only visualised those receptors at the cell surface. Without the use of double labelling, we were not able to differentiate between synaptic and extrasynaptic $GABA_AR$ clusters, however, at 21 DIV, 82.2% of gamma subunits are synaptically located (Danglot *et al.* 2003).

A thorough investigation into the percentage of ubiquilin associated with $GABA_AR$ within or just below the synaptic membrane has not been published, however, 90% of gephyrin clusters at 21DIV are synaptic and, although these were not always associated with the $\beta3$ subunit, only 1.8% of γ subunits are localised at the

synapse without gephyrin (Danglot *et al.* 2003). The fact that β 2/3 clusters were not significantly affected by NMDA, but γ subunits were, may be due to the fact that 33.4% of β2/3 clusters are extrasynaptic at 21 DIV whilst only 11.6% of clusters containing both gephyrin and γ are extrasynaptic. As gephyrin and ubiquilin are associated predominantly with the synapse, the higher percentage of extrasynaptic β 2/3 subunits may have negatively affected the measured puncta. Alternatively, as γ subunit containing $GABA_A$Rs decreased, there could have been compensatory effects from other $GABA_A$Rs containing β (e.g. β1), but not γ subunits, that served to maintain receptor numbers at the cell surface, and remained undetected in this particular experiment. However, it is interesting to note that the $GABA_A$R γ subunit graph is strikingly similar to the gephyrin graph for NMDAR stimulation over 24 hours (Figures 6.4 and 4.8 respectively). The results are therefore consistent with induction of zif268 following NMDAR activation leading to reductions in synaptic $GABA_A$Rs via reduced gephyrin expression.

Both gephyrin and ubiquilin are significantly downregulated after NMDA treatment in cultured cortical neurones (chapters 4 & 5). As noted above, NMDA treatment will have many actions on neurones apart from zif268 induction and likely suppression of gephyrin and ubiquilin levels. Therefore the reduced density of $GABA_A$R-immunoreactive clusters observed (with the γ subunit-specific antibody) cannot be unequivocally linked to the actions of zif268 via gephyrin and ubiquilin. Nevertheless, the hypothesis of reduced synaptic $GABA_A$R density after NMDAR stimulation was generated on the basis of detection of gephyrin and ubiquilin as zif268 target genes, and the results are certainly consistent with, mediation by this pathway.

It is possible that $GABA_A$Rs within the cytoplasm after NMDA treatment will be in diffuse 'microclusters' throughout the cell and not ordered into synaptic clusters by gephyrin (Kneussel *et al.* 1999a). It is known that the inhibition of gephyrin leads to dramatic decreases in $GABA_A$R clusters (Essrich *et al*. 1998; Feng *et al*. 1998; Kneussel *et al.* 1999a). Image J was used to detect immunoreactivity and allowed the enforcement of a threshold for relative optical density and mean puncta size, which was found empirically for each z-stacked image. This makes it unlikely that micro-clusters would have been measured as they would be below the minimum size. Although the assumption is that internalised receptors have not been measured, there is the possibility that they have in fact been counted and may

skew the results. This would mean that the results presented are a global count of $GABA_A$Rs, though they would still be in favour of receptor downregulation after NMDA induced zif268 activation. In addition, immunocytochemistry can produce artefacts from the paraformaldehyde fixation of immunofluorescence procedures, and it is known that extracellular antibodies can have difficulty gaining access to synapses. However, all the results presented were investigated blind, and the result for $GABA_AR$ γ subunits show a significant ($p<0.01$) effect of NMDA treatment, suggesting that there is a genuine reduction in clustered $GABA_A$Rs after NMDA treatment.

A number of further experiments were planned to test whether zif268 can be unequivocally linked to the regulation of $GABA_AR$ density. In particular, γ subunit immunoreactive cluster density was to be assessed after transfection of cortical neurones with active or inactive zif268 and in cortical neurones cultured from wildtype or zif268 knockout mice. However, following various technical problems, there was insufficient time for these studies.

6.4.2 mTOR in response to changes in zif268 expression levels

4E-BP1 and p70 S6K are downstream effectors of mTOR, promote cell growth (Schmelzle & Hall 2000), and are implicated in diseases such as cancer and diabetes (Vogt 2001). Both are found at postsynaptic sites (Tang *et al.* 2002) and can be activated by the ERK pathway activating mTOR (Kelleher *et al.* 2004). In addition, both are phosphorylated during hippocampal LTP. Therefore, mTOR could be part of pathway that regulates protein synthesis during LTP.

Phosphorylation of 4E-BP1 by mTOR dissociates it from eIF-4E, relieving the translational block; the concurrent phosphorylation of p70 S6K also increases protein synthesis. Transient transfection of full-length zif268 in PC-12 cells had no effect on either phospho-4E-BP1 or phospho-p70 S6K when compared to truncated (control) zif268. Transient transfection of zif268 in PC-12 cells significantly reduces mRNA levels of gephyrin and ubiquilin; in addition, 4E-BP1 and p70 S6K have both been detected and activated in PC-12 cells in previous studies (Kleijn & Proud 2000).

In rat embryos mTOR and gephyrin are expressed widely, with large amounts located to the CNS. In rat brain they are localised to synaptic vesicles and

presynaptic membranes. Sequence similarity between mTOR and the glycine receptor means that gephyrin can bind mTOR in this region. Mutations in the mTOR binding region cannot bind gephyrin and subsequently do not activate 4E-BP1 or p70 S6K, suggesting that gephyrin may be necessary for mTOR function in HEK293 cells. In addition, gephyrin may control the localisation of mTOR in HeLa cells to cellular membranes (Sabatini *et al.* 1999). We found no evidence to link decreased gephyrin levels with the mTOR effectors, 4E-BP1 or p70 S6K, in PC-12 cells.

Ubiquilin was found to bind to mTOR through a yeast 2-hybrid experiment, however, there seemed to be no evidence of cellular co-localisation, although both proteins were found to co-sediment in some fractions of membrane proteins. mTOR did not phosphorylate ubiquilin *in vitro*, ubiquilin does not effect mTORs phosphorylation of 4E-BP1 or p70S6K and therefore the functional activity remains unclear (Wu *et al.* 2002). Our results also showed no effect of ubiquilin on mTOR, via 4E-BP1 or p70 S6K, in PC-12 cells.

Rapamycin has been shown to inhibit zif268 expression in rat myoblast cells (Sarker & Lee 2004), and so mTOR can increase zif268 expression by activating p70 S6K. This suggests that zif268 is in fact a target of mTOR and may explain why we witnessed no effect of altering zif286 levels. mTOR may activate its downstream effector, p70 S6K, and activate zif268 which would then decrease the levels of gephyrin and ubiquilin within the cells. Bypassing mTOR activation by artificially increasing zif268 levels through transient transfection would then explain why no changes in mTOR were detected.

Chapter 7

Novel gene urma is a downstream target of zif268

7.1 Introduction

Bioinformatics is a vital discipline that provides the computational management of all kinds of biological information. It has revolutionised our understanding of basic biological processes, and is a valuable tool capable of turning data into knowledge. Database technologies and software tools enable the collection, display, storage and retrieval of large volumes of detailed and complex gene and protein sequence data which, when combined with molecular function, results in a considerable amount of information. Bioinformatics can include DNA and protein sequences, genotype, expression microarray, protein structure and many other kinds of genetic and genomic data, which can be compared, interpreted and analysed through the use of a computer. With genomics technologies generating experimental data ranging from gene sequences, to gene expression levels, to protein-protein interactions, it is possible to delineate preparatory functional genomics before physical experimentation.

Known genes found on existing biological databases are derived from a range of expressed genes. Undiscovered genes are expressed at very low levels, and only occur at certain developmental stages or are cell type specific. The identification of these genes can include the approach of Expressed Sequence Tag (EST) analysis, whereby partial cDNA clones are sequenced from mRNA, ensuring the partial capture of expressed genes. EST sequences can be found on the NCBI website (http://www.ncbi.nlm.nih.gov/) and generally represent 200–800 bp of sequence information extending towards the gene origin, usually from the mRNA 3' end.

Within microarrays, thousands of expressed gene cDNA tags are arrayed on a glass slide and incubated with labelled first-strand cDNA produced from cellular mRNA. The subsequent hybridisation of the endogenous sequence to the complementary array-based sequence allows relative quantitation of expression levels within a given paradigm. This technology allows widespread changes in expression patterns to be probed in a single experiment.

In 2005, James *et al.* published data from a microarray experiment performed on PC-12 cells and verified in primary hippocampal neurones. Increased zif268 protein levels were induced in a cell line by transfecting a plasmid construct containing the zif268 gene, whilst primary cultured neurones received NMDA in

the presence of KCl. Known genes from the Affymetrix GeneChip® A were monitored, categorised, investigated and reported as downstream targets of zif268. In addition to the published data, there were also GeneChips® B & C which, in contrast to the defined genes on GeneChip® A, mainly contained ESTs. Those tags affected by experimentation were subsequently identified as parts of known, or unknown, genes by bioinformatics (please see appendix).

This chapter looks at two of these ESTs in greater detail as downstream targets of zif268 and presents one of them, AI169020, as a potential novel gene, named urma (from the Gaelic for ‘brand new’).

7.2 Aims & Objectives

- Investigate all of the ESTs significantly altered in the microarray experiment performed by James *et al.* (2005).

- Select interesting ESTs for further investigation as potential novel genes.

- Determine the exact locus and sequence of any prospective novel gene candidates.

- Complete bench work performed on PC-12 cells and primary cortical neurons to validate any predictions.

7.3 Results

7.3.1 Microarray results present 144 ESTs as downstream targets of zif268

Significant Analysis of Microarrays (SAM) software (Tusher *et al.* 2001) was utilised to calculate the expression levels of mRNA extracted from full-length zif268 transfected PC-12 cells compared to a transfections with a control (truncated) form of zif268 (as published by James *et al.* (2005)). SAM allows the false positive rate to be set by the user, permitting the selection of the number of candidate genes with respect to the likelihood of false positives. On Genechips B & C, 72 ESTs were selected on each chip with a false discovery rate of 7.02 and 1.26 respectively. This means that, of the 144 ESTs affected by treatment, approximately 8 of them are likely to be false positives.

Each of the ESTs was investigated in turn and the results are detailed in the appendix. After the retrieval of EST sequence data from NCBI (www.ncbi.nim.nih.gov/), tags were compared to the *Rattus norvegicus* genome as detailed on Ensembl in January 2004 (www.ensembl.org) by BLAST analysis. Criteria were set allowing the identity of ESTs to be revealed as part of a known and annotated gene or as an unknown transcript as detailed in Chapter 2. From this list, AI169020 and AI176839 were highlighted as potentially interesting. AI176839 is found on *Rattus norvegicus* chromosome 3q42, which shows high synteny with *Homo sapiens* chromosome 20q13, whilst AI169020 is located on *Rattus norvegicus* chromosome 4q13, which shows high synteny with *Homo sapiens* chromosome 7q21.2. Furthermore, ESTs AA998964 and AI112362 were also highlighted, due to minimal information regarding their origin and their close proximity to one another (4q13, between 27.98MB and 28.16MB), suggesting that they may be part of one transcript. AA998964 and AI112362 are currently under a separate investigation and will not be dealt with in this thesis.

7.3.2 AI176839 is down regulated in PC-12 cells after transient transfection of full-length zif268

In the first instance, results from the microarray were verified in PC-12 cells by repeating the transient transfection performed by James *et al.* (2005). mRNA was harvested and primers designed against the EST were used to produce an amplicon of approximately 209 bps. The sequence of AI176839 is detailed in

figure 7.1 along with the primer locations. RNA expression is significantly downregulated in PC-12 cells transiently transfected with 1 μg/mL full-length zif268 when compared to cells transiently transfected with 1 μg/mL of a control truncated zif268 (one sample t-test, $p<0.001$, $n=5$; see figure 7.2). A single cycle within the logarithmic linear phase was taken and GAPDH values were used to normalise the data. This gave a 50% reduction in AI176839 RNA in PC-12 cells transiently transfected with full-length zif268 compared to control.

AI176839

AAAAACATCACCAAGTCAGATTTTTATTTCTACAGACAGAAGGCCAAAAGTTTCTATTTC
AGTAGCAGTGTACACCAAACCACTCCTCCCCAGCCAAAGCTGACTCTTCTTTGCATCCTG
CATGCCTTTGAACCATGCCCAGCCTTGTGGGGGTGGCAGCAGGACTAGACTGCTATTCTG
TGTTCCAAGGGGTACCTGAAAG**CAAGAATAGACCAACACTGGCATCC**GTGGGTTCCTCAG
GCCAACGCGCTCCCCTCTGAGTTCACCATTCATTCAAAGCCTGGTCTTGGCCGTCAGCAA
ACCTTGAGACTTAAGGTGCTCGGCGATTTCTCATCTCCCTGGAGGACCTTCTCTCCCTCC
GACCTCCATTCTGTACTGCTTGATCAGTCCAGCCATCTGCAAATGAATATCACAGGGAAG
AGACCTATCGTAACCACGAGAACACCTCACGGAGACTCACCTCGTGCCGACTGGTGCC

Figure 7.1: cDNA sequence data for EST AI176839. This data was detailed in and retrieved from the NCBI website (http://www.ncbi.nlm.nih.gov/). Sequence data in bold represents the forward primer location and underlined sequences represent reverse primer targets.

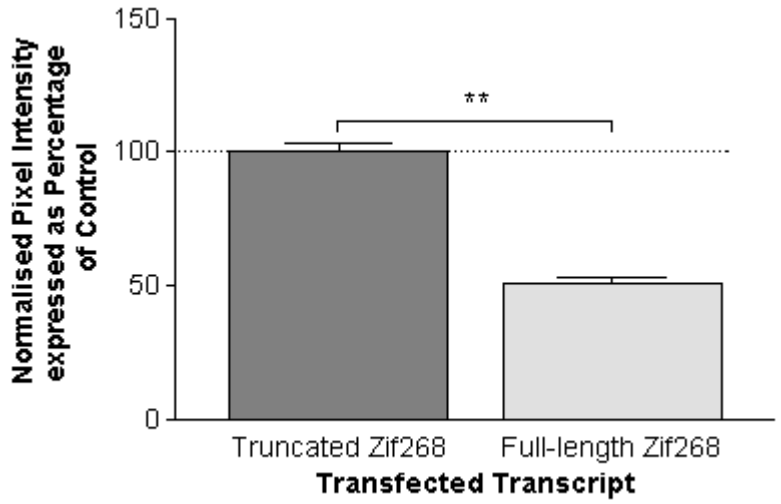

Figure 7.2: The effect of zif268 transfection on AI176839 RNA in PC-12 cells. Graph comparing EST AI176839 RNA from PC-12 cells transiently transfected with either truncated or full-length zif268, as assessed by signal intensities at a single RT-PCR cycle. Results are presented as AI176839 normalised pixel intensity after normalisation to the corresponding GAPDH value. All data is expressed as a mean percentage of control ± SEM, **$p<0.001$, one sample t-test, $n=5$.

7.3.3 AI176839 is downregulated in primary cortical neurones after NMDA stimulation to induce zif268

NMDA stimulation (100µM NMDA in 20mM KCl) of cultured primary cortical neurones for 6 hours displayed a statistically significant downregulation of approximately 10% in EST AI176839 RNA levels when compared to vehicle as determined by RT-PCR (ANCOVA, $p<0.05$, $F(1,16)=6.48$, $n=4$; see figure 7.3). A window of 5 PCR cycles within the logarithmic phase of the PCR reaction was established empirically for both AI176839 and the co-variate, GAPDH.

In contrast, evaluating RNA levels after 24-hour stimulation of primary cortical neurones with NMDA, EST AI176839 RNA is not significantly different from primary cortical neurones treated with vehicle for 24 hours ($p=0.606$, $F(1, 16) = 0.28$, $n=3$, see figure 7.4).

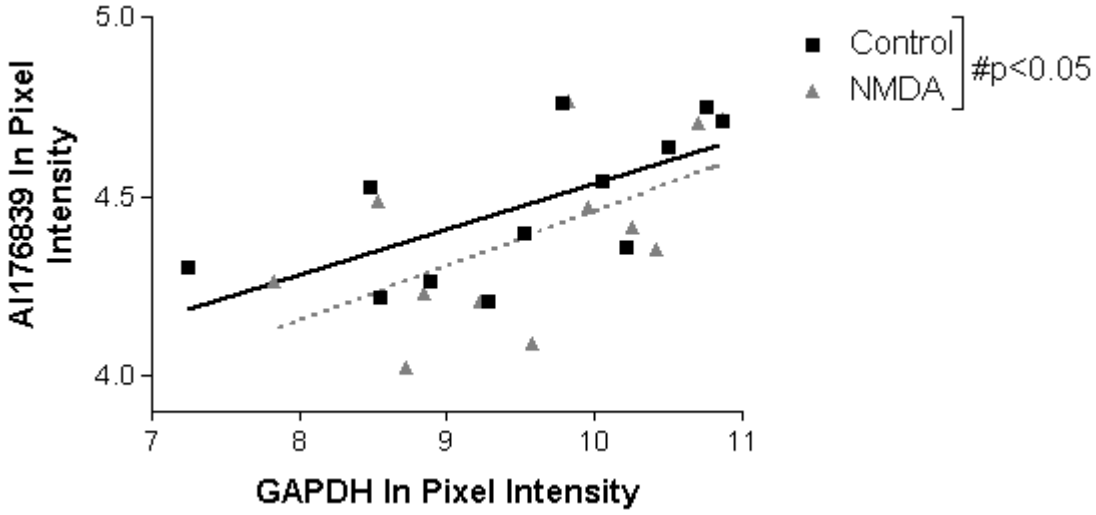

Figure 7.3: The effect of 6 hour NMDA stimulation on AI176839 RNA levels in primary cortical neurones. Graph illustrating AI176839 ln pixel intensity as a function of GAPDH ln pixel intensity, as determined by RT-PCR of cultured primary cortical neurones stimulated for 6 hours with either 100µM NMDA in 20mM KCl or Vehicle. ANCOVA, #p<0.05, $F(1, 16) = 6.48$, $n=4$.

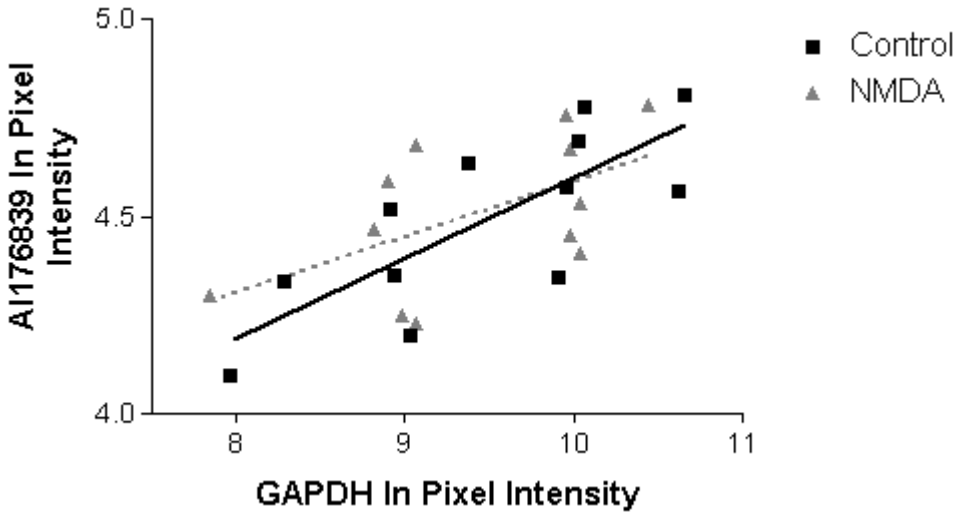

Figure 7.4: The effect of 24 hour NMDA stimulation on AI176839 RNA levels in primary cortical neurones. Graph illustrating AI176839 ln pixel intensity as a function of GAPDH ln pixel intensity as determined by RT-PCR of cultured primary cortical neurones stimulated for 24 hours with either 100µM NMDA in 20mM KCl or Vehicle. ANCOVA, $p>0.05$, $F(1, 16) = 0.28$, $n=3$.

7.3.4 AI169020 may be part of novel predicted transcript ENSRNOT00000012253

AI169020 is found on chromosome 4 between genomic locations 27305926 and 27306502 bases. In 2005, further investigation of AI169020 with Ensembl version 34 suggested that it might be part of the novel predicted transcript ENSRNOT00000012253, which was a transcript of gene ENSRNOG00000009163. This was due to the fact that many ESTs were found in the area of the genome between and including EST AI169020 and transcript ENSRNOT00000012253, with very little known annotated data (see figure 7.5). In addition, a genscan prediction (Burge & Karlin 1997) was present within the same genomic contig. Data mining Ensembl for all the orthologue predictions of ENSRNOT00000012253 led to the *Mus musculus* gene prediction NM_026583 (ensembl gene identifier ENSMUSG00000058503) on chromosome 5A1, which led to *Homo sapiens* gene XP_376148.1 (Ensembl known gene prediction ENSG00000183055, transcript ENST00000332869) on chromosome 5q12.1, which in turn was linked to protein reference sequence NP_690002.1. This referred to a hypothetical protein LOC257415 isoform 1 [Homo sapiens] from gene "MGC40405".

In order to find the reference and original data from which this information was derived, NCBI was consulted and 'Homo sapiens hypothetical protein MGC40405 (MGC40405), mRNA' (744 bp) found. However, this had the gene identifier NM_152789 and the nucleotide sequence for translation to predicted protein LOC257415 (XP_376148.1, Ensembl gene identifier ENSG00000183055; transcript ENST00000332869) is not the same nucleotide sequence as NM_152789. In addition, the nucleotide sequence was placed on *Homo sapiens* chromosome 7 (7q21.1) by NCBI and not 5 (5q12.1) as per Ensembl. However, on UniProt (www.ebi.uniprot.org) hypothetical protein MGC40405 (their entry name and accession number Q8N0W8) was placed on chromosome 7q21.3.

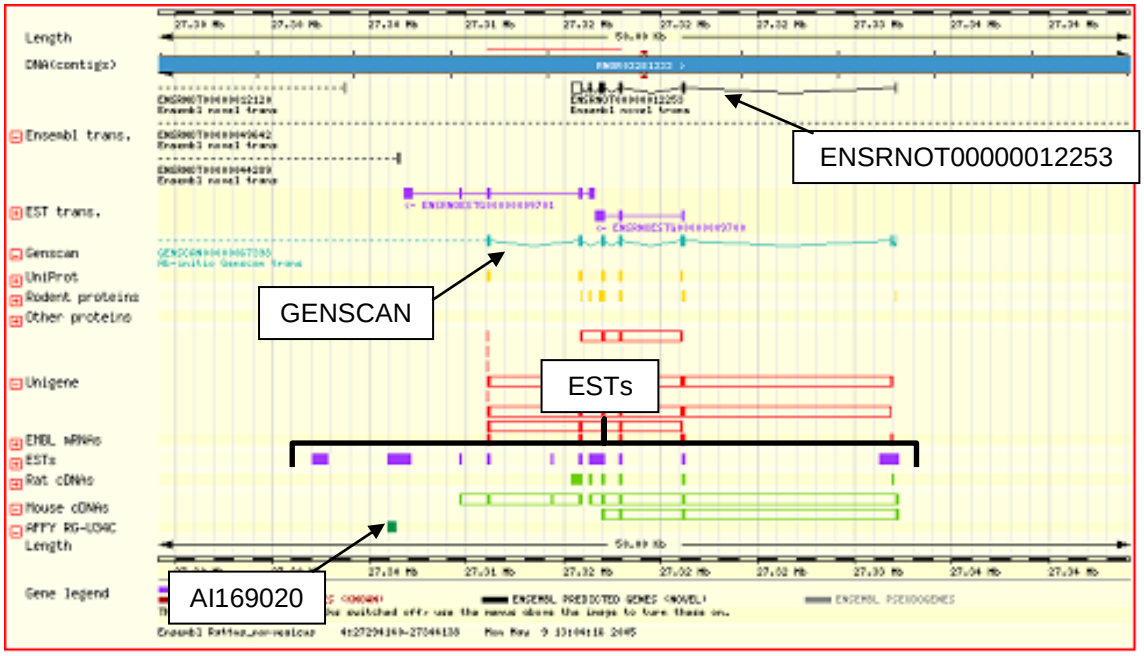

Figure 7.5: BLAST analysis of AI169020 on Ensembl. A screengrab of the genomic area surrounding EST AI169020. Of note are the highlighted ESTs and GENSCAN gene. In addition, the predicted transcript ENSRNOT00000012253 is also of interest.

Further investigation uncovered a protein LOC257415 isoform 2, which displayed a marked similarity to the predicted protein of transcript ENSRNOT00000012253 and to protein MGC40405 (see figure 7.6).

The information for hypothetical protein MGC40405 was derived from human brain tissue mRNA and submitted to EMBL/GenBank/DDBJ databases and published by Strausberg *et al.* (2002) and Scherer *et al.* (2003). The nucleic acid records are supported by experimental data however the protein sequence is predicted. Performing a BLAST search with MGC40405 nucleotide sequence against the rat

genome places it in the same vicinity as AI169020 and ENSRNOT00000012253, highlighting this genomic area of interest (see figure 7.7). In addition, BLAST searching the MGC40405 nucleotide sequence against the human genome places it on chromosome 7q21.2.

ENSRNOT00000012253
ATGAACCCAATAGCAATGGCGAGATCAAGGGGTCCAATCCAGTCTTCAGGGCCAACAATA
CAGGATTATCTGAATCGACCAAGGCCTACCTGGGAAGAAGTAAAAGAGCAACTAGAAAAG
GAAAAGAAAGGCTCCAAGGCTTTGGCTGAATTTGAAGAAAAAATGAATGAGAACTGGAAG
AAAGAACTGGAAAAACACAGAGAGAAATTGTTAAGTGGAAGTGAGAGCTCATCCAAAAAA
AGACAGAGAAAGAAAAAAGAAAAGAAGAAATCTGGTAGGTATTCATCTTCTTCTTCATCA
AGCTCTGATTCTTCCAGCAGTTCTTCTGATTCTGAAGATGAGGATAAGAAACAAGGAAAA
CAGAGAAAGAAAAAGAAGAACCGTTCACATAAATCTTCTGAAAGCTCCATGTCAGAAACT
GAATCAGACAGTAAGGATAGTTTAAAAAAGAAAAAGAAGTCAAAAGATGGAACTGAGAAA
GAAAAGGATATTAAAGGACTCAGCAAAAAGAGAAAGATGTATTCTGAAGATAAACCTTTA
TCATCTGAGTCCTTGTCAGAATCAGAGTATATTGAGGAGGTGCAAGCAAAAAAGAAGAAA
AGCAGTGAAGAACGAGAAAAAGCAACAGAAAAAACAAAAAAGAAAAAGAAGCATAAGAAA
CACAGTAAGAAGAAGAAAAAGAAGGCTGCTAGTTCAAGTCCTGACTCACCGTAA

Predicted protein of transcript ENSRNOT00000012253
MNPIAMARSRGPIQSSGPTIQDYLNRPRPTWEEVKEQLEKKKKGSKALAEFEEKMNENWK
KELEKHREKLLSGNESSSKKRQKKKKEKKKSGRYSSSSSSSSDSSSSSSDSEEEDKKQTK
RRKKKKSHCHKSPETSVSDSDSDSKDGSKKKKKSKDITEREKDTKGLSKKRKMYEDKPLS
SESLSESDCGEVQAKKKKSGEERERTT

LOC257415 isoform 1
MGKRDNRVAYMNPIAMARSRGPIQSSGPTIQDYLNRPRPTWEEVKEQLEKKKKGSKALAE
FEEKMNENWKKELEKHREKLLSGSESSSKKRQRKKKEKKKSGRYSSSSSSSSDSSSSSSD
SEDEDKKQGKRRKKKKKNRSHKSSESSMSETESDSKDSLKKKKKSKDGTEKEKDIKGLSKK
RKMYSEDKPLSSESLSESEYIEEVRAKKKKSSEEREKATEKTKKKKKKHKKHSKKKKKKAA
SSSPDSP

LOC257415 isoform 2
MNPIAMARSRGPIQSSGPTIQDYLNRPRPTWEEVKEQLEKKKKGSKALAEFEEKMNENWK
KELEKHREKLLSGSESSSKKRQRKKKEKKKSGRYSSSSSSSSDSSSSSSDSEDEDKKQGK
RRKKKKNRSHKSSESSMSETESDSKDSLKKKKKSKDGTEKEKDIKGLSKKRKMYSEDKPL
SSESLSESEYIEEVRAKKKKSSEEREKATEKTKKKKKHKKHSKKKKKKAASSSPDSP

MGC40405
ATGAACCCAATAGCAATGGCGAGATCAAGGGGTCCAATCCAGTCTTCAGGGCCAACAATA
CAGGATTATCTGAATCGACCAAGGCCTACCTGGGAAGAAGTAAAAGAGCAACTAGAAAAG
AAAAAGAAAGGCTCCAAGGCTTTGGCTGAATTTGAAGAAAAAATGAATGAGAACTGGAAG
AAAGAACTGGAAAAACACAGGGAGAAATTGTTAAGTGGAAGTGAGAGCTCATCCAAAAAA
AGACAGAGAAAGAAAAAAGAAAAGAAGAAATCTGGTAGGTATTCATCTTCTTCTTCATCA
AGCTCTGATTCTTCCAGCAGTTCTTCTGATTCTGAAGATGAGGATAAGAAACAAGGAAAA
CGGAGAAAGAAAAAGAAGAACCGTTCACATAAATCTTCTGAAAGCTCCATGTCAGAAACT
GAATCAGACAGTAAGGATAGTTTAAAAAAGAAAAAGAAGTCAAAAGATGGAACTGAGAAA
GAAAAGGATATTAAAGGACTCAGCAAAAAGAGAAAGATGTATTCTGAAGATAAACCTTTA
TCATCTGAGTCCTTGTCAGAATCAGAGTATATTGAGGAGGTGCGAGCAAAAAAGAAGAAA
AGCAGTGAAGAACGAGAAAAAGCAACAGAAAAAACAAAAAAGAAAAAGAAGCATAAGAAA
CACAGTAAGAAGAAGAAAAAGAAGGCTGCTAGTTCAAGTCCTGACTCACCATAA

MGC40405 Predicted protein
MNPIAMARSRGPIQSSGPTIQDYLNRPRPTWEEVKEQLEKKKKGSKALAEFEEKMNENWK
KELEKHREKLLSGSESSSKKRQRKKKEKKKSGRYSSSSSSSSDSSSSSSDSEDEDKKQGK
RRKKKKNRSHKSSESSMSETESDSKDSLKKKKKSKDGTEKEKDIKGLSKKRKMYSEDKPL
SSESLSESEYIEEVRAKKKKSSEEREKATEKTKKKKKHKKHSKKKKKKAASSSPDSP

Figure 7.6: Sequence data for transcript ENSRNOT00000012253, LOC257415 and MGC40405. A list of information presented for transcript ENSRNOT00000012253 and its predicted protein along with the information it was derived from, LOC257415 isoform 1 (as found on www.ensemble.org). In addition, the sequence data for protein LOC257415 isoform 2 and the nucleotide and predicted protein sequence of MGC40405 (as found on www.ncbi.nim.nih.gov/).

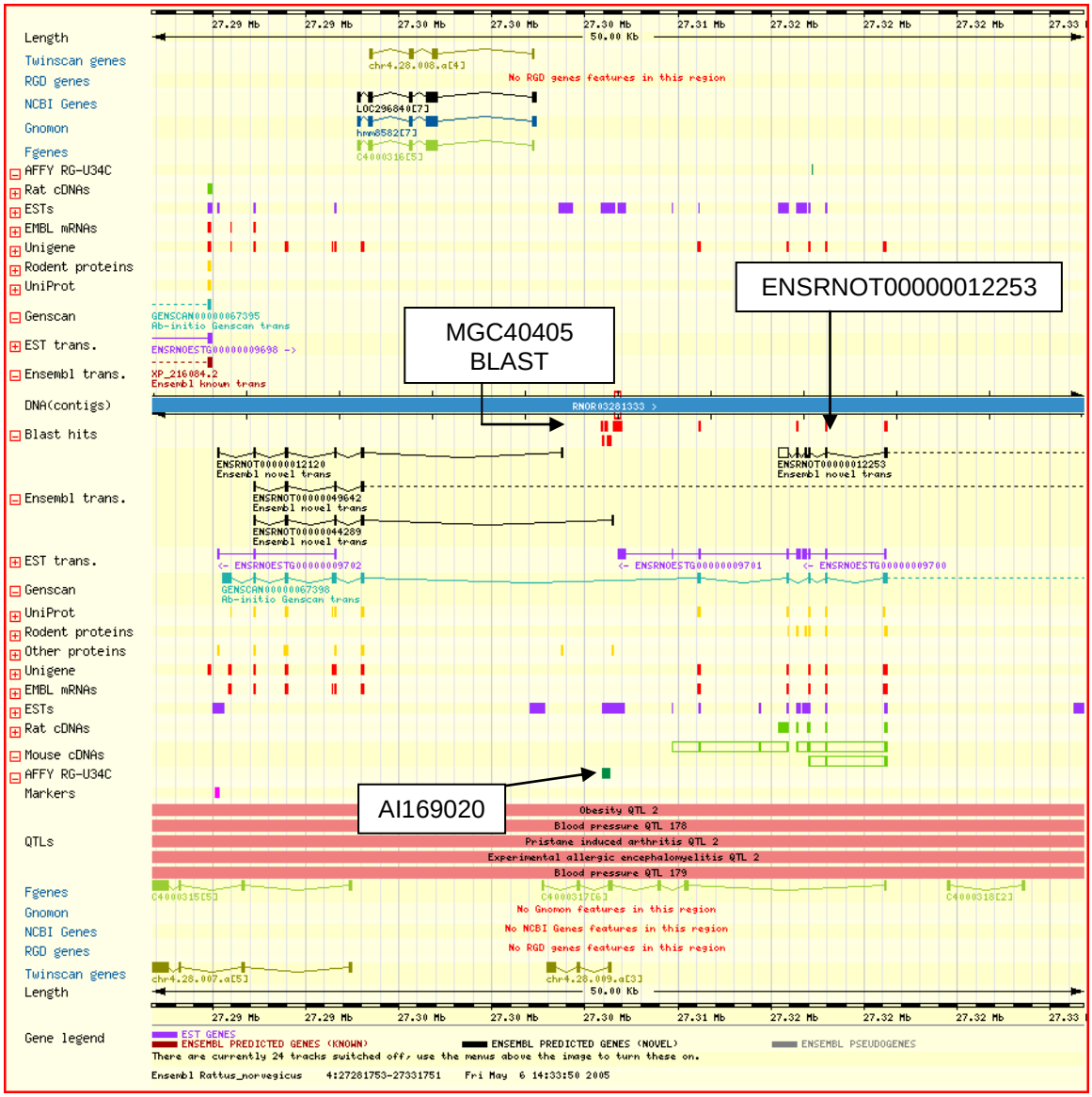

Figure 7.7: A BLAST search of the MGC40405 nucleotide sequence. A screen grab from an Ensembl BLAST search of MGC40405 places the sequence in the same genomic area (4q13) as the EST AI169020 and the transcript of interest, ENSRNOT00000012253.

The accumulation of contradictory evidence suggested that, in contrast to the information presented by Ensembl, the protein sequence was actually that of LOC257415 variant 2, not variant 1 and the MGC40405 protein was localised to chromosome 7. Overall, there is the implication that this is indeed an area of interest with little verified data, warranting further investigation.

7.3.5 AI169020 is not significantly downregulated in PC-12 cells after transient transfection with zif268

The microarray transient transfections were repeated in PC-12 cells by replicating the experiments performed by James *et al.* (2005). The sequence of AI169020 is detailed in figure 7.8 along with the primer locations. RNA expression was not significantly affected in PC-12 cells transiently transfected with 1 μg/mL full-length

zif268 when compared to cells transiently transfected with 1 μg/mL of a control truncated zif268 (n=5; see figure 7.9) although there was a tendency for decreased expression in the zif268-transfected cells.

7.3.6 AI169020 and ENSRNOT00000012253 primers produce an amplicon from PC-12 cells RNA

Using RNA extracted from PC-12 cells, several reactions were simultaneously monitored via PCR for 45 cycles. EST AI169020 forward and reverse primers produced a predicted amplicon of 148 bps and ENSRNOT00000012253 forward and reverse primers (Tr12253 Fwd and Rev) produced a predicted amplicon of 371 bps, with the addition of minor products, when electrophoresed on a 1.5% agarose gel.

AI169020
AAAACAAGTGTTTACTAAAATTCTGGCAATAGCTTTATGTAACAAGATACAGCATACCAG
GCCTGCCACTCAACTTGTTTGTGGTAAGTCTCAGCTTCAATATGAAGCCGTTAAAAACAA
AAACCAAAAGTCCTGCTTTTTACATGCTAAATATCTTGAAAGTGTGCCATTAAACATAGT
TATGAACTTAAGACAGCAAGAGTTAGTTAAAAGCTAAACACTGCAGCCTAAACAAAGTTT
ATACAAAACATGAAGTGTCTATCACTGGCTACGTAAAAATCTCCTGACTGGTTAAAACTT
GTGTAACACATGCGCTTTACAACTGTCAGCTGTCAAGCTCAGAAAGTACCAGTGTCTACT
AAACCATCCCTTTCCAAAGCCAAAGTGTAGT**CAAAATGAATTCAAATGACGCAACA**CAAC
GTAACCCTAAAAACATTCAGTTATTATTGATGTGGAGGTAATTCCAGAGCTTTGGGGGCT
TTCTCATGCTGCAAAGGGCCGGGTACCTCTGGTTCATTCCAAGCAGCTTACGACAAAGTC
TAAGGATGTCATTAACCTCAGTCAGGGCAGGACTGAC

Figure 7.8: cDNA sequence data for EST AI169020. This data was detailed and retrieved from the NCBI website (http://www.ncbi.nlm.nih.gov/). Sequence data in bold represents the forward primer location and underlined sequences represent reverse primer targets.

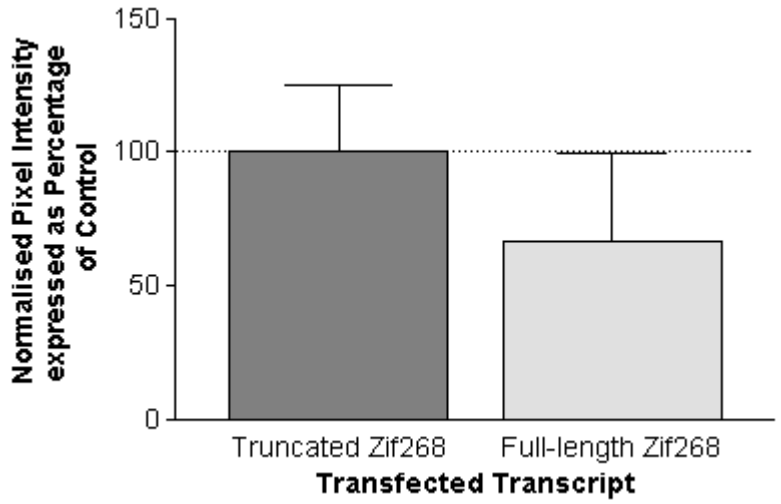

Figure 7.9: The effect of zif268 transfection on AI169020 RNA in PC-12 cells. Graph comparing EST AI169020 RNA from PC-12 cells transiently transfected with either truncated or full-length zif268, as assessed by signal intensities at a single RT-PCR cycle. Results are presented as AI169020 normalised pixel intensity after normalisation to the corresponding GAPDH value. All data is expressed as a mean percentage of control ± SEM, n=5.

In addition, the forward primer of AI169020 and Tr12253 Fwd (the sequences are presented on opposite strands) produced an amplicon of approximately 1,200 base pairs with a minor product at approximately 570 bps. As negative controls, the Tr12253 Fwd and Rev primers and the AI169020 Fwd and Tr12253 Fwd were also investigated with no cDNA present. The Tr12253 Fwd and Rev primers produced no bands (see figure 7.10), however, the AI169020 Fwd and Tr12253 Fwd produced a minor band of a few tens of bases, which is likely to be primer-dimers.

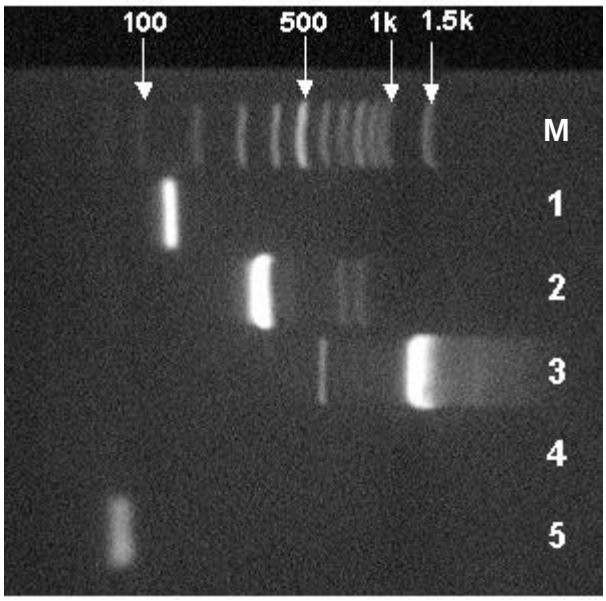

Figure 7.10: Agarose gel image of the novel product PCR fragment. PCR amplified products electrophoresed on a 1.5% agarose gel after 45 cycles. *M*, 100 bp DNA marker (Promega, Southampton, UK), *1*, EST AI169020 forward & reverse primers, *2*, Tr12253 forward & reverse primers, *3*, EST AI169020 forward & Tr12253 forward primers, *4*, ENSRNOT12253 forward & reverse primers, no cDNA, *5*, EST AI169020 forward & Tr12253 forward primers, no cDNA.

7.3.7 AI169020 and ENSRNOT00000012253 primers produce a novel transcript from adult rat cerebral cortex mRNA

cDNA was generated from rat cerebral cortex tissue using Oligo(dT), which hybridises to 3' poly(A) tails, ensuring that only expressed mRNAs were used as template. The cDNA was then amplified with AI169020 and Tr12253 Fwd primers for 45 cycles in order to generate enough product to sequence. Previous attempts at PCR had unfortunately necessitated such a high number of cycles in order to achieve the cDNA concentration required. Primers were designed utilising a predicted sequence of the novel gene ascertained from EST and predicted gene information. Firstly, all the ESTs present between AI169020 and transcript

ENSRNOT00000012253 were collated in order from 5' to 3' (using the AI169020 sense strand to orientate). This comprised ESTs BF542993, CF977261, CB765971, BF288214 and BF522287, none of which were present on the Affymetrix GeneChips and therefore were not present in the microarray experiment (James *et al.* 2005). Sequential BLAST analyses were performed to find overlapping regions of sequence, allowing all 6 ESTs (including AI169020) and ENSRNOT00000012253 to form a coherent single theoretical cDNA strand. This created 1414 bps of theoretically expressed sequence, which was used as the basis of the novel transcript (see figure 7.11 A & B). Primers were designed using this information and sequenced from AI169020 as the lead primer (as this was the originally affected transcript from the microarray experiment). The actual sequence returned contained a number of bases denoted 'N', which were manually identified by scrutinising the chromatogram and verifying with the details found on NCBI (see figure 7.12 A & B). However, the sequencing company only provided a single read and, combined with any PCR-introduced errors, it is possible that the DNA sequence may contain some inaccuracies. The sequence returned comprised 1477 bases and showed approximately 90% homology to the predicted sequence (figure 7.12 C), suggesting the discovery of a novel gene which I propose to call urma.

7.3.8 Urma may code for a novel transcription factor of unknown function

With the addition of the AI169020 EST and Transcript ENSRNOT00000012253 sequences outwith the primers, the total length of urma identified is 1879 bases. As AI169020 is a 3' EST, the correct orientation is on the complementary strand to that sequenced.

By running the entire nucleotide sequence through two different websites ExPASy and ATGpr (Nishikawa et al. 2000) (http://ca.expasy.org/tools/dna.html and http://www.hri.co.jp/atgpr/ respectively; see figure 7.13) the results returned were exactly the same and therefore, the predicted protein sequence of urma is:

MNPIAMARSRGPIQSSGPTIQDYLNRPRPTWEEVKEQLEKKKKGSKALAEFEEKMNENWKKELEKH
REKLLSGNESSSKKRQKKKKEKKKSGRYSSSSSSSSDSSSSSSDSEEEDKKQTKRRKKKKSHCHKS
PETSVSDSDSDSKDGSKKKKKSKDITEREKDTKGLSKKRKMYEDKPLSSESLSESDCGEVQAKKKK
SGEERERTTDKAKKRRKHKKHSKKKKKKAASSSSDSP

A

1. AI169020

AAAACAAGTG TTTACTAAAA TTCTGGCAAT AGCTTTATGT AACAAGATAC AGCATACCAG
GCCTGCCACT CAACTTGTTT GTGGTAAGTC TCAGCTTCAA ATGAAGCCGT AAAAACAAAA
ACCAAAAGTC TGCTTTTTAA TGCTAAATAT TTGAAAGTGT CCATTAAACA AGTTATGAAC
TTAAGACAGA AGAGTTAGTA AAAGCTAAAC CTGCAGCCTA ACAAAGTTTA ACAAAACATG
AAGTGTCTAC ACTGGCTACT AAAAATCTCC GACTGGTTAA ACTTGTGTAA ACATGCGCTT
TACAACTGTA GCTGTCAAGT CAGAAAGTAC AGTGTCTACT AACCATCCCT TCCAAAGCCA
AGTGTAGT**CA AAATGAATTA AATGACGCAA A**CAACGTAAC CTAAAAACAT CAGTTATTAT
TGATGTGGAG TAATTCCAGG CTTTGGGGGC TTCTCATGCT CAAAGGGCCG GTACCTCTGG
TTCATTCCAA GCAGCTTACG ACAAAGTCTA AGGATGTCAT TAACCTCAGT CAGGGCAGGA
CTGAC

2. BF542993

CACGAGGTTT GACTACACTT TGGCTTTGGA GAGGGATGGT TTAGTACACA CTGGTACTTT
CTGAGCTTGA CAGCTGACAG TTGTAAAGCG CATGTGTTAC ACAAGTTTTA ACCAGTCAGG
AGATTTCTAC GTAGCCAGTG ATAGACACTT CATGTTTTGT ATAAACTTTG TTTAGGCTGC
AGTGTTTAGC TTTTAACTAA CTCTTGCTGT CTTAAGTTCA TAACTATGTT TAATGGCACA
CTTTCAAGAT ATTTAGCATG TAAAAAGCAG GACTTTTGGT TTTTGTTTTT AACGGCTTCA
TATTGAAGCT GAGACTTACC ACAAACAAGT TGAGTGGCAG GCCTGGTATG CTGTATCTTG
TTACATAAAG CTATTGCCA

3. CF977261

GGGGAACTGA ATCTGGATCC ATCTTTTAAG ATGTAACCAG AAATAACGAG TAAAGATTTT
CAAAGTAGGG ATTTCATTAA TATTTCAAAA TCCTTACTCT GTAGATAAGT ATATTTTAAT
TTTTCCCCAC GTATGCTTTG ATTTACTTGG GGAAGGAGCT TTTAAAGAGG GGGTGGTTTG
CTATCTCTTT AGCTACCAGA ACAGCGTGCC TTTGATCTCA CACATCCTAC TTTTGTGGAC
ACAGTAGCCA TGCTTCCTGG GAGGACAGAG CTGGGCACGG TCAGTCCTGC CCTGACTGAG
GTTAATGACA TCCTTAGACT TTGTCGTATG CTGCTTGGAA TGAACCAGAG GTACCCGGCC
CTTTGCAGCA TGAGAAAGCC CCCAAAGCTC TGGAATTACC TCCACATCAA TAATAACTGA
ATGTTTTTAG GGTTACGTTG TGTTGCGTCA TTTGAATTCA TTTTGACTAC ACTTTGGCTT
TGGAGAGGGA TGGTTTAGTA AACACTGGTA CTTTCTGAGC TTGACAGCTG ACAGTTGTAA
AGCGCATGTG TTACACAAGT TTTAACCAGT CAG

4. CB765971

CGTAGCATCC AGAAGACCAG GGTCCTTACA GAGTGCAATG TCAAAGGAGC TCTCAACTGT
GAAGATTATG ACTTACTTAG TAACGTGCAT GAATCCCCTT GTTTTTAGAC TTGTCCTGGA
CTAGTCAGTA GTCACTTGGA TTCCGCTGTG TGAAGGGCCA TGAATGTTGC CTGCTGCTTG
AACACCTTTT CCTCTTCCAG TGCTTGGTGA CTCTGGGAGA TAGTACTTTG CAGTCATACT
AGTGGTTAAG ATATTTGGAA TAAAGCTAAT ATTTTTTACT AGAAGTACTT AAGAATAAAT
CAACAGGAAC TGAATCTGGA TCCATCTTTT AAGATGTAAC CAGAAATAAC GAGATGACTC
TAGTAAAGAT TTTCAAAGTA TGGATTTCAT TAATATTTCA AAATCCTTAC TCTGTAGA

5. BF288214

CAGTTCCTGT TAATTTATTC TTAAGTACTT CTAGTAAAAA ATATTAGCTT TATTCCAAAT
ATCTTAACCA CTAGTATGAC TGCAAAGTAC TATCTCCCAG AGTCACCAAG CACTGGAAGA
GGAAAAGGTG TTCAAGCAGC AGGCAACATT CATGGCCCTT CACACAGCGG AATCCAAGTG
ACTACTGACT AGTCCAGGAC AAGTCTAAAA ACAAGGGGAT TCATGCACGT TACTAAGTAA
GTCATAATCT TCACAGTTGA GAGCTCCTTT GACATTGCAC TCTGTAAGGA CCCTGGTCTT
CTGGATGCTA CGGCGAGTCT GAGCTTGAAC TGGCAGCCTT CTTTTTCTTC TTCTTGCTGG
GTTTCTTATG CTTCCTTCTC TTTTTAGCTT TGTCTGTTGT TCTCTCTCGC TCTTCACCGC
TTTTCTTCTT TTTCGCTTGC ACCTCTCCAC AGTCTGACTC TGACAATGAC TCANC

6. BF522287

CACGAGGGCT TTGTTGAGCT TTTGTGGGAG GGAAATGGCT TTGATATTTT AGTTTCTAAA
TCCTGTGAAT ATGGCATCTG TTTCTTAGAC ACTAGATTGA TTTCACTAAG TGCTTGAGAG
ACTTAGTAAA AGAAACCAAT TCCTGCATCT CACAAGCTTT AATTGTTTTG TGCTTGGTCA
AGTATTCATC TTCTTCTTCA TCGAGCTCTG ATTCTTCCAG CAGTTCTTCA GATTCTGAGG
AGGAGGATAA AAAGCAAACA AAAAGAAGGA AGAAAAAGAA GAGCCATTGC CATAAGTCTC
CGGAGACCTC CGTGTCGGAT TCAGACTCAG ACAGCAAGGA CACTAAAGGA CTCAGCAAAA
AGAGAAAGAT GTATGAGGAT AAACCTTTGT CATCTGAGTC ATTGTCAGAG TCAGACTGTG
GAGAGGTGCA AGCGAAAAAG AAGAAAAGCG GTGAAGAGCG AGAGAGAACA AC

7. ENSRNOT00000012253

ATGGGGAAGC GAGACAATCG CGTGGCCTAC ATGAATCCAA TAGCAATGGC TCGGTCAAGG

GGTCCAATCC AGTCTTCAGG ACCAACAATC CAGGATTATC TGAATCGACC AAGGCCTACC
TGGGAGGAAG TGAAGGAGCA GCTGGAAAAG AAAAAGAAGG GCTCCAAGGC TTTGGCTGAG
TTTGAAGAGA AAATGAATGA GAATTGGAAG AAAGAACTAG AAAAACATAG AGAAAAACTA
TTAAGTGGAA ATGAGAGCTC ATCCAAAAAG CGACAGAAAA AGAAAAAAGA AAAGAAGAAA
TCTGGTAGGT ATTCATCTTC TTCTTCATCG AGCTCTGATT CTTCCAGCAG TTCTT**CAGAT**
TCTGAGGAGG AGGATAAAAA GCAAACAAAA AGAAGGAAGA AAAAGAAGAG CCATTGCCAT
AAGTCTCCGG AGACCTCCGT GTCGGATTCA GACTCAGACA GCAAGGTGAG ACTCAGCCCT
GGACTGCTGA GAGCAAAAAC AGCCATTTTC CTGTCTGCTT TTCCTGTCTA GCGCTTCAGT
TAGAAAGCAC ATTTGATTTC ATTTTTGGAT TTTTGAGACA GAGTTTTTCT CTGTATAGAC
CTAGATCAGG CTGGCCTCAA AGTCACTGAG ATCCAACCTG CCTTCCTGTG CAGCCTGAGT
GCTGGCACTA AAGGGGTGCA CTAGCACCAC CACTCCCAGC CACATTTGAC TTTTGTACTT
TGAGGTTCTG CACCAGTCGA CAGGTGTATT TAATATTGTA CATGTAGCAT CTTTTTATCC
TTTATTCTTC ATATGCATGT TTGTATGATT CCATGATAGT GTTTCCTTTG TTTGTAAAAT
AATATTTGCA ATTCTAGGTT

B

caaaatgaattcaaatgacgcaacacaacgtaaccctaaaaacattcagttattatt
gatgtggaggtaattccagagctttgggggctttctcatgctgcaaagggccgggta
cctctggttcattccaagcagcttacgacaaagtctaaggatgtcattaacctcagt
cagggcaggactgaccgtgcccagctctgtcctcccaggaagcatggctactgtgtc
cacaaaagtaggatgtgtgagatcaaaggcacgctgttctggtagctaaagagatag
caaaccacccctctttaaaagctccttccccaagtaaatcaaagcatacgtgggga
aaaattaaaatatacttatctacagagtaaggattttgaaatattaatgaaatccct
actttgaaaatctttactcgttatttctggttacatcttaaaagatgqatccaqatt
caqttccccagttcctgttaatttattcttaagtacttctagtaaaaaatattagc
tttattccaaatatcttaaccactagtatgactgcaaagtactatctcccagagtca
ccaagcactggaagaggaaaaggtgttcaagcagcaggcaacattcatggcccttca
cacagcggaatccaagtgactactgactagtccaggacaagtctaaaaacaaggggga
ttcatgcacgttactaagtaagtcataatcttcacagttgagagctcctttgacatt
gcactctgtaaggaccctggtcttctggatgctacggcgagtctgagcttgaactgg
cagccttctttttcttcttcttgctgggtttcttatgcttccttctctttttagctt
tgtctgttgttctctctcgctcttcaccgcttttcttctttttcgcttgcacctctc
cacagtctgactctgacaatgactcagatgacaaaggtttatcctcatacatctttc
tctttttgctgagtcctttagtgtccttgctgtctgagtctgaatccgacacggagg
tctccggagacttatggcaatggcatcctcctcctcagaatctgaagaactgctgga
agaatcagagctcgatgaagaagaagatgaatacctaccagatttcttcttttcttt
tttctttttctgtcgctttttggatgagctctcatttccacttaatagttttctct
atgtttttctagttctttcttccaattctcattcattttctcttcaaactcagccaa
agccttggagcccttctttttctttccagctgctccttcacttcctcccaggtagg
ccttggtcgattcagataatcctggattgttggtcctgaagactggattggacccct
tqaccqaqccattqctattqqatt**catgtaggccacgcgattgtct**

Figure 7.11: Sequence data for the predicted transcript of urma. *A,* The sequences of ESTs AI169020, BF542993, CF977261, CB765971, BF288214, BF522287 and transcript ENSRNOT00000012253 in genomic order. B, The collated sequence of the predicted urma transcript after sequential BLAST analyses of the ESTs presented in *A*. Primer locations of AI169020 forward and Tr12253 forward are in bold. Additional primers for sequencing are underlined.

This protein sequence is 86% homologous to the protein sequence detailed for ENSRNOT00000012253 on Ensembl and 86% homologous to that of MGC40405 as detailed by NCBI (with areas of similarity differing slightly). Upstream EST sequences to that of urma (CF977260 and BF393377) were collated and added to the 5'end and the extended sequence run through both protein prediction websites again. This did not alter the translation start site of the protein, suggesting that the true translational start site has indeed been located.

As a control, the *Rattus norvegicus* gephyrin genome sequence (as detailed on NCBI, accession number NM_022865) was entered into the ATGpr website. A protein sequence with 99% homology to the experimentally derived protein sequence detailed on NCBI, accession number NP_074056, and with the correct translational start site, was retrieved.

A

NNNNNNNNNNNNNANNANNTTNNGTTATTATTGATGTGGAGGTAATTCCAGAGCTTTGGGGGCTTTCTC
ATGCTGCAAAGGGCCGGGTACCTCTGGTTCATTCCAAGCAGCATACGACAAAGTCTAAGGATGTCATTA
ACCTCAGTCAGGGCAGGACTGACCGTGCCCAGCTCTGTCCTCCCAGGAAGCATGGCTACTGTGTCCACA
AAAGTAGGATGTGTGAGATCAAAGGCACGCTGTTCTGGTAGCTAAAGAGATAGCAAACCACCCCCTCTT
TAAAAGCTCCTTCCCCAAGTAAATCAAAGCATACGTGGGGAANAATTAAAATATACTTATCTACAGAGT
AAGGATTTTGAAATATTAATGAAATCCCTACTTTGAAAATCTTTACTAGAGTCATCTCGTTATTTCTGG
TTACATCTTAAAAGATGGATCCAGATTCAGTTCCTGTTGATTTATTCTTAAGTACTTCTAGTAAAAAAT
ATTAGCTTTATTCCAAATATCTTAACCACTAGTATGACTGCAAAGTACTATCTCCCAGAGTCACCAAGC
ACTGGAAGAGGAAAAGGTGTTCAAGCAGCAGGCAACATTCATGGCCCTTCACACAGCGGAATCCAAGTG
ACTACTGACTAGTCCAGGACAAGTCTAAAAACAAGGGGATTCATGCACGTTACTAAGTAAGTCATAATC
TTCACAGTTGAGAGCTCCTTTGACATTGCACTCTGTAAGGACCCTGGTCTTCTGGATGCTACGGCGAGT
CTGAGCTTGAACTGGCAGCCTTCTTTTTCTTCTTCTTGCTGTGTTTCTTATGCTTCCTTCTCTTTTTAG
CTTTGTCTGTTGTTCTCTCTCGCTCTTCACCGCTTTTCTTCTTTTTCGCTTGCACCTCTCCACAGTCTG
ACTCTGACAATGACTCAGATGACAAAGGTTTATCCTCATACATCTTTCTCTTTTTGCTGAGTCCTTTAG
TGTCCTTTTCTCTTTCNNTTATATCCTTTGACTTCTTTTTCTTTTTTGAACCATCCTTGCTGTCTGAGT
CTGAATCCGACACGGAGGTCTCCGGANACTTATGGNANTGGCTCTTCTTTTTCTTCCTTCTTTTTGTTT
GCTTTTTATCCTCCTCCTCAGAATCTGAAGAACTGCTGGAAGAATCAGAGCTCGATGAAGAAGAAGATG
AATACCTACCAGATTTCTTCTTTTCTTTTTTCTTTTTCTGTCGCTTTTTGGATGAGCTCTCATTTCCAC
TTAATAGTTTTTCTCTATGTTTTTCTAGTTCTTTCTTCCAATTCTCATTCATTTTCTCTTCAAACTCAG
CCAAAGCCTTGGAGCCCTTCTTTTTCTTTTCCAGCTGCTCCTTCACTTCCTCCCAGGTAGGCCTTGGTC
GATTCAGATAATCCTGGATTGTTGGTCCTGAAGACTGGATTGGACCCCTTGACCGAGCCATTGCTATTG
GATTCATGTAGGCCACGCGATTGTCTAA

B

CAACGTAACCCTAAAAACATTCAGTTATTATTGATGTGGAGGTAATTCCAGAGCTTTGGGGGCTTTCTC
ATGCTGCAAAGGGCCGGGTACCTCTGGTTCATTCCAAGCAGCATACGACAAAGTCTAAGGATGTCATTA
ACCTCAGTCAGGGCAGGACTGACCGTGCCCAGCTCTGTCCTCCCAGGAAGCATGGCTACTGTGTCCACA
AAAGTAGGATGTGTGAGATCAAAGGCACGCTGTTCTGGTAGCTAAAGAGATAGCAAACCACCCCCTCTT
TAAAAGCTCCTTCCCCAAGTAAATCAAAGCATACGTGGGGAAAAATTAAAATATACTTATCTACAGAGT
AAGGATTTTGAAATATTAATGAAATCCCTACTTTGAAAATCTTTACTAGAGTCATCTCGTTATTTCTGG
TTACATCTTAAAAGATGGATCCAGATTCAGTTCCTGTTGATTTATTCTTAAGTACTTCTAGTAAAAAAT
ATTAGCTTTATTCCAAATATCTTAACCACTAGTATGACTGCAAAGTACTATCTCCCAGAGTCACCAAGC
ACTGGAAGAGGAAAAGGTGTTCAAGCAGCAGGCAACATTCATGGCCCTTCACACAGCGGAATCCAAGTG
ACTACTGACTAGTCCAGGACAAGTCTAAAAACAAGGGGATTCATGCACGTTACTAAGTAAGTCATAATC
TTCACAGTTGAGAGCTCCTTTGACATTGCACTCTGTAAGGACCCTGGTCTTCTGGATGCTACGGCGAGT
CTGAGCTTGAACTGGCAGCCTTCTTTTTCTTCTTCTTGCTGTGTTTCTTATGCTTCCTTCTCTTTTTAG
CTTTGTCTGTTGTTCTCTCTCGCTCTTCACCGCTTTTCTTCTTTTTCGCTTGCACCTCTCCACAGTCTG
ACTCTGACAATGACTCAGATGACAAAGGTTTATCCTCATACATCTTTCTCTTTTTGCTGAGTCCTTTAG
TGTCCTTTTCTCTTTCAGTTATATCCTTTGACTTCTTTTTCTTTTTTGAACCATCCTTGCTGTCTGAGT
CTGAATCCGACACGGAGGTCTCCGGAGACTTATGGCAATGGCTCTTCTTTTTCTTCCTTCTTTTTGTTT
GCTTTTTATCCTCCTCCTCAGAATCTGAAGAACTGCTGGAAGAATCAGAGCTCGATGAAGAAGAAGATG
AATACCTACCAGATTTCTTCTTTTCTTTTTTCTTTTTCTGTCGCTTTTTGGATGAGCTCTCATTTCCAC
TTAATAGTTTTTCTCTATGTTTTTCTAGTTCTTTCTTCCAATTCTCATTCATTTTCTCTTCAAACTCAG
CCAAAGCCTTGGAGCCCTTCTTTTTCTTTTCCAGCTGCTCCTTCACTTCCTCCCAGGTAGGCCTTGGTC
GATTCAGATAATCCTGGATTGTTGGTCCTGAAGACTGGATTGGACCCCTTGACCGAGCCATTGCTATTG
GATTCATGTAGGCCACGCGATTGTCTAA

C

```
1 _____________________________NNNNNNNNNNNNNANNANNTTNN
1 CAAAATGAATTCAAATGACGCAACACAACGTAACCCTAAAAACATTCA

GTTATTATTGATGTGGAGGTAATTCCAGAGCTTTGGGGGCTTTCTCATGCTGCAAAGGGCCGGGTACCT
GTTATTATTGATGTGGAGGTAATTCCAGAGCTTTGGGGGCTTTCTCATGCTGCAAAGGGCCGGGTACCT

CTGGTTCATTCCAAGCAGCATACGACAAAGTCTAAGGATGTCATTAACCTCAGTCAGGGCAGGACTGAC
CTGGTTCATTCCAAGCAGCTTACGACAAAGTCTAAGGATGTCATTAACCTCAGTCAGGGCAGGACTGAC

CGTGCCCAGCTCTGTCCTCCCAGGAAGCATGGCTACTGTGTCCACAAAAGTAGGATGTGTGAGATCAAA
CGTGCCCAGCTCTGTCCTCCCAGGAAGCATGGCTACTGTGTCCACAAAAGTAGGATGTGTGAGATCAAA

GGCACGCTGTTCTGGTAGCTAAAGAGATAGCAAACCACCCCCTCTTTAAAAGCTCCTTCCCCAAGTAAA
GGCACGCTGTTCTGGTAGCTAAAGAGATAGCAAACCACCCCCTCTTTAAAAGCTCCTTCCCCAAGTAAA

TCAAAGCATACGTGGGGAANAATTAAAATATACTTATCTACAGAGTAAGGATTTTGAAATATTAATGAA
TCAAAGCATACGTGGGGAAAAATTAAAATATACTTATCTACAGAGTAAGGATTTTGAAATATTAATGAA

ATCCCTACTTTGAAAATCTTTACTAGAGTCATCTCGTTATTTCTGGTTACATCTTAAAAGATGGATCCA
ATCCCTACTTTGAAAATCTTTA__________CTCGTTATTTCTGGTTACATCTTAAAAGATGGATCCA

GATTCAGT_________TCCTGTTGATTTATTCTTAAGTACTTCTAGTAAAAAATATTAGCTTTATTCC
GATTCAGTTCCCCCAGTTCCTGTTAATTTATTCTTAAGTACTTCTAGTAAAAAATATTAGCTTTATTCC

AAATATCTTAACCACTAGTATGACTGCAAAGTACTATCTCCCAGAGTCACCAAGCACTGGAAGAGGAAA
AAATATCTTAACCACTAGTATGACTGCAAAGTACTATCTCCCAGAGTCACCAAGCACTGGAAGAGGAAA

AGGTGTTCAAGCAGCAGGCAACATTCATGGCCCTTCACACAGCGGAATCCAAGTGACTACTGACTAGTC
AGGTGTTCAAGCAGCAGGCAACATTCATGGCCCTTCACACAGCGGAATCCAAGTGACTACTGACTAGTC

CAGGACAAGTCTAAAAACAAGGGGATTCATGCACGTTACTAAGTAAGTCATAATCTTCACAGTTGAGAG
CAGGACAAGTCTAAAAACAAGGGGATTCATGCACGTTACTAAGTAAGTCATAATCTTCACAGTTGAGAG

CTCCTTTGACATTGCACTCTGTAAGGACCCTGGTCTTCTGGATGCTACGGCGAGTCTGAGCTTGAACTG
CTCCTTTGACATTGCACTCTGTAAGGACCCTGGTCTTCTGGATGCTACGGCGAGTCTGAGCTTGAACTG

GCAGCCTTCTTTTTCTTCTTCTTGCTGTGTTTCTTATGCTTCCTTCTCTTTTTAGCTTTGTCTGTTGTT
GCAGCCTTCTTTTTCTTCTTCTTGCTGGGTTTCTTATGCTTCCTTCTCTTTTTAGCTTTGTCTGTTGTT

CTCTCTCGCTCTTCACCGCTTTTCTTCTTTTTCGCTTGCACCTCTCCACAGTCTGACTCTGACAATGAC
CTCTCTCGCTCTTCACCGCTTTTCTTCTTTTTCGCTTGCACCTCTCCACAGTCTGACTCTGACAATGAC

TCAGATGACAAAGGTTTATCCTCATACATCTTTCTCTTTTTGCTGAGTCCTTTAGTGTCCTTTTCTCTT
TCAGATGACAAAGGTTTATCCTCATACATCTTTCTCTTTTTGCTGAGTCCTTTAGTGTCCTT_______

TCNNTTATATCCTTTGACTTCTTTTTCTTTTTTGAACCATCCTTGCTGTCTGAGTCTGAATCCGACACG
_____________________________________________GCTGTCTGAGTCTGAATCCGACACG

GAGGTCTCCGGANACTTATGGNANTGGCTCTTCTTTTTCTTCCTTCTTTTTGTTTGCTTTTTATCCTCC
GAGGTCTCCGGAGACTTATGGCAATGGC_____________________________________ATCCTCC

TCCTCAGAATCTGAAGAACTGCTGGAAGAATCAGAGCTCGATGAAGAAGAAGATGAATACCTACCAGAT
TCCTCAGAATCTGAAGAACTGCTGGAAGAATCAGAGCTCGATGAAGAAGAAGATGAATACCTACCAGAT

TTCTTCTTTTCTTTTTTCTTTTTCTGTCGCTTTTTGGATGAGCTCTCATTTCCACTTAATAGTTTTTCT
TTCTTCTTTTCTTTTTTCTTTTTCTGTCGCTTTTTGGATGAGCTCTCATTTCCACTTAATAGTTTTTCT

CTATGTTTTTCTAGTTCTTTCTTCCAATTCTCATTCATTTTCTCTTCAAACTCAGCCAAAGCCTTGGAG
CTATGTTTTTCTAGTTCTTTCTTCCAATTCTCATTCATTTTCTCTTCAAACTCAGCCAAAGCCTTGGAG

CCCTTCTTTTTCTTTTCCAGCTGCTCCTTCACTTCCTCCCAGGTAGGCCTTGGTCGATTCAGATAATCC
CCCTTCTTTTTCTTTTCCAGCTGCTCCTTCACTTCCTCCCAGGTAGGCCTTGGTCGATTCAGATAATCC

TGGATTGTTGGTCCTGAAGACTGGATTGGACCCCTTGACCGAGCCATTGCTATTGGATTCATGTAGGCC
TGGATTGTTGGTCCTGAAGACTGGATTGGACCCCTTGACCGAGCCATTGCTATTGGATTCATGTAGGCC

ACGCGATTGTCTAA
ACGCGATTGTCT
```

Figure 7.12: Sequencing data from urma transcript. *A*, The collated sequence returned from Geneservice (Cambridge, UK). *B*, Sequence information of urma once the N's have been replaced with bases derived from the chromatograms and NCBI. *C*, Alignment of the predicted sequence (from figure 7.11B) (in red text) and the actual sequence (from A) (in black text).

A

http://ca.expasy.org/tools/dna.html

5'3' Frame 1

```
L D N R V A Y Met N P I A Met A R S R G P I Q S S G P T I Q D Y L N R P R
P T W E E V K E Q L E K K K K G S K A L A E F E E K Met N E N W K K E L E
K H R E K L L S G N E S S S K K R Q K K K E K K K S G R Y S S S S S S S D S S S S S D S E E E D K K Q T K R R K K K K S H C H K S
P E T S V S D S D S D S K D G S K K K K K S K D I X E R E K D T K G L S K K R K M Y E D K P L S S E S L S E S D C G E V Q A K K K K
S G E E R E R T T D K A K K R R K H K K H S K K K K K K A A S S S S D S P
```

B

http://www.hri.co.jp/atgpr/

```
No.of ATG from 5'end:                          1

Frame:                                         1

Identity to Kozak rule A/GXXATGG:              tXXATGa

Start(bp):                                     22

Finish (bp):                                   726

ORF Length(aa):                                235

Stop codon found?:                             Yes

Sequence:

MNPIAMARSRGPIQSSGPTIQDYLNRPRPTWEEVKEQLEKKKKGSKALAEFEEKMNENWKKELEKH
REKLLSGNESSSKKRQKKKKEKKKSGRYSSSSSSSSDSSSSSSDSEEEDKKQTKRRKKKKSHCHKS
PETSVSDSDSDSKDGSKKKKKSKDIXEREKDTKGLSKKRKMYEDKPLSSESLSESDCGEVQAKKKK
SGEERERTTDKAKKRRKHKKHSKKKKKKAASSSSDSP
```

Figure 7.13: Predicted protein sequence of urma. *A,* The predicted protein sequence of urma as returned from ExPASy. *B,* The predicted protein sequence of urma as returned from ATGpr.

The urma protein sequence is not predicted to span the cell membrane nor be secreted, as per the Centre for Biological Sequence Analysis (http://www.cbs.dtu.dk/services/TMHMM/). Presumably, this implies that urma does not contain a hydrophobic membrane-spanning domain. Furthermore, when investigated using the PredictProtein website (http://www.predictprotein.org), urma is predicted to contain 7 cAMP- and cGMP-dependent protein kinase phosphorylation sites and 7 PKC phosphorylation sites. In addition, it may be localised to the nucleus and bind to DNA, as various nuclear localisation signals

and DNA binding domains were identified throughout the protein sequence. These data suggest that urma may be a transcription factor.

Although the translation start site is predicted, the transcription initiation site has still to be elucidated. However, by examining 11,000 base pairs of the rat genome upstream of the translation start site, we reasoned that any exons, introns and the promoter region would be included. Using Signal Scan (http://thr.cit.nih.gov/molbio/signal/) to investigate, we found evidence of 3 TATA boxes, 2 CAAT boxes, 1 CREB site and 1 zif268 binding site with an overlapping Sp-1 recognition sequence, all within 2000 base pairs of each other (see figure 7.14).

7.3.9 Urma is significantly downregulated in primary cortical neurons after zif268 induction by NMDA stimulation

The predicted protein results were used to design primers within the coding region of urma. These were used to monitor effects within that part of the transcript that may have direct, or indirect, actions on other cellular components. Evaluating RNA levels after 6-hour stimulation of primary cortical neurones with NMDA, urma mRNA levels are not significantly different from those in primary cortical neurones treated with vehicle for 6 hours ($p=0.09$, $F(1, 11) = 3.46$, $n=3$, see figure 7.15). In contrast, NMDA stimulation (100µM NMDA in 20mM KCl) of cultured primary cortical neurones for 24 hours induced a statistically significant downregulation in mRNA levels when compared to vehicle as determined by RT-PCR (ANCOVA, $p<0.05$, $F(1,11) = 4.93$, $n=3$; see figure 7.16). A window of 3 PCR cycles within the logarithmic phase of the PCR reaction was established empirically for both urma and the co-variate, GAPDH.

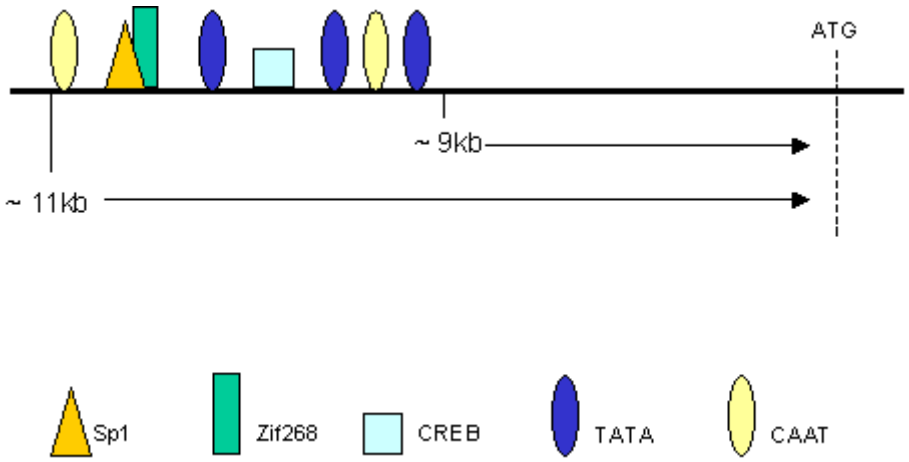

Figure 7.14: A diagram of the DNA recognition sequences upstream of the urma translation start site. Positions of some of the possible binding sites for CREB, Zif268 and Sp1, as well as TATA and CAAT box locations are presented. Note that distances in kb are to the translation start site as the transcription start site is not known.

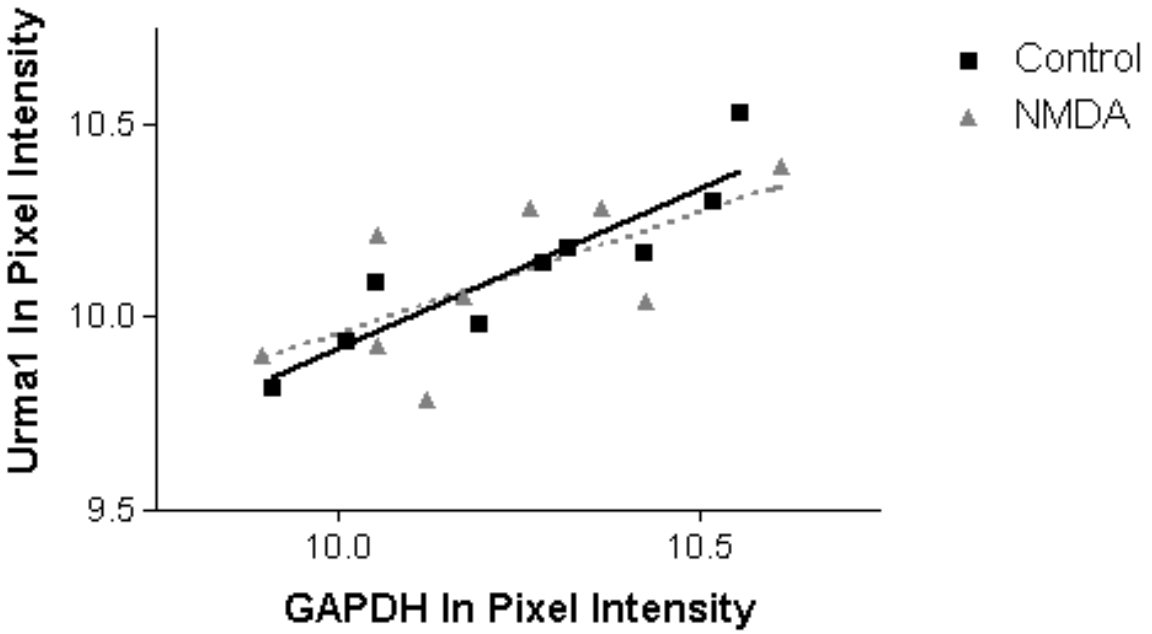

Figure 7.15: The effect of 6 hour NMDA stimulation on urma mRNA levels in primary cortical neurones. Graph illustrating urma coding amplimer ln pixel intensity as a function of GAPDH ln pixel intensity, as determined by RT-PCR of cultured primary cortical neurones stimulated for 6 hours with either 100µM NMDA in 20mM KCl or vehicle (control). ANCOVA, $p>0.05$, $F(1, 11) = 3.46$, $n=3$.

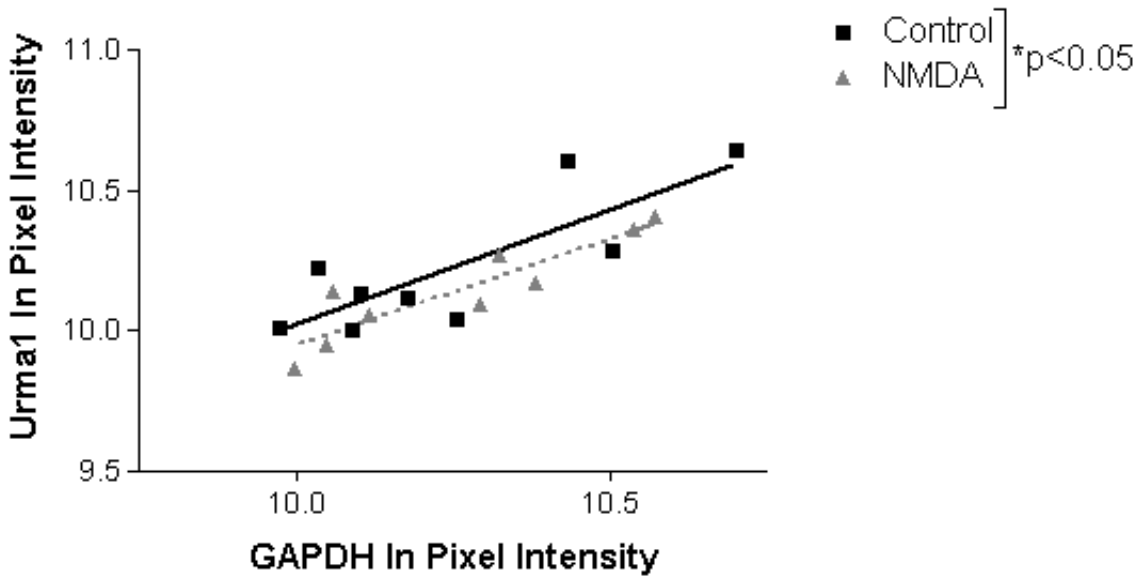

Figure 7.16: The effect of 24 hour NMDA stimulation on urma mRNA levels in primary cortical neurones. Graph illustrating urma coding amplimer ln pixel intensity as a function of GAPDH ln pixel intensity, as determined by RT-PCR of cultured primary cortical neurones stimulated for 24 hours with either 100µM NMDA in 20mM KCl or vehicle (control). ANCOVA, *p<0.05, F(1, 11) = 4.93, n=3.

7.3.10 Urma is significantly down regulated in zif268 knockout mice

Urma mRNA is significantly downregulated by 7% in cerebral cortex tissue from zif268 knockout mice compared to their counterpart wildtype mice as determined by RT-PCR (p<0.01 F(1,13) = 9.61, ANCOVA, n=9; see figure 7.17).

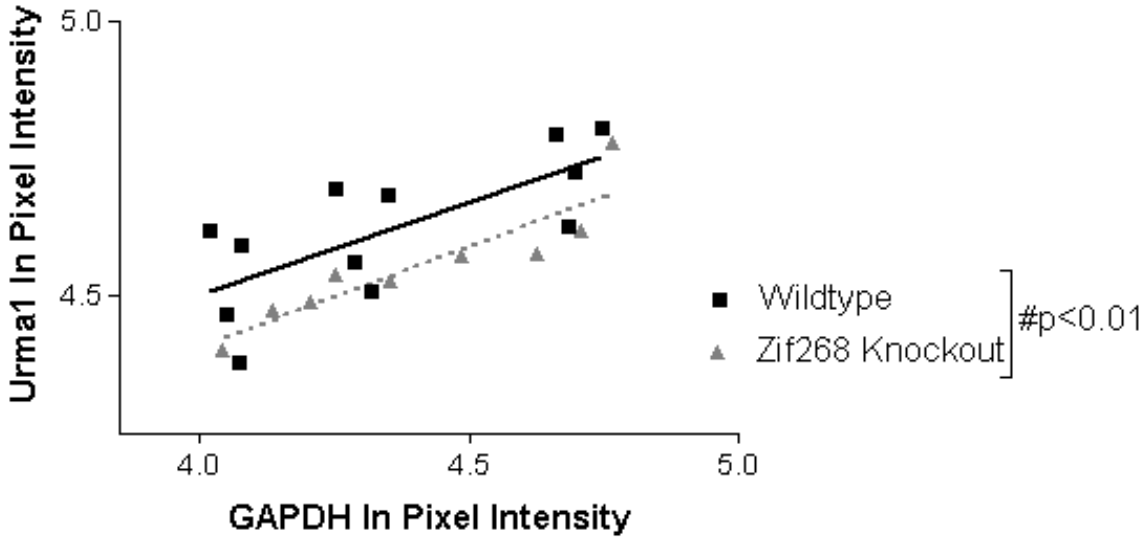

Figure 7.17: The effect of genotype on urma RNA levels. Graph illustrating urma log pixel intensity as a function of GAPDH log pixel intensity, as determined by RT-PCR of adult cerebral cortex tissue from either wildtype or zif268 knockout mice. ANCOVA, #p<0.01 F(1,13) = 9.61, n=9.

7.3.11 Updated Bioinformatics for Urma

On the 25th November 2004, both Ensembl and NCBI were contacted to clarify the mismatched information regarding the whereabouts of protein MGC40405. Both organisations replied that they would investigate and update their databases. In Ensembl version 42 (December 2006), AI169020 is lined up with Ensembl known protein coding NP_001019970.1 (Ensembl Gene ENSRNOG00000009163, transcript ENSRNOT00000012253), which still has no functional description, but has an orthologue prediction straight to an MGC40405 fragment (although this is still placed on chromosome 5) (see figure 7.18). The NP_001019970.1 information is described as 'hypothetical protein LOC362320 [Rattus norvegicus]', which now has no variants and presents data that was originally associated with isoform 1. The updated predicted protein sequence of ENSRNOT00000012253 matches this, although our results suggest that the transcript had a greater similarity to their, now missing, isoform 2. The information is from the Sanger Institute and was updated in December 2005. This Ensembl entry NP_001019970.1 corresponds to the Rat Genome database RGD1306302 (Rattus norvegicus similar to RIKEN cDNA 5830415L20).

In contrast, the entry on NCBI regarding MGC40405 now has 2 variants: MGC40405 isoform 1, described as 'hypothetical protein LOC257415 isoform 1' and MGC40405 isoform 2, described as 'hypothetical protein LOC257415 isoform 2'. This information was updated in November 2006. Our predicted protein results for urma are similar to MGC40405 isoform 2 protein results.

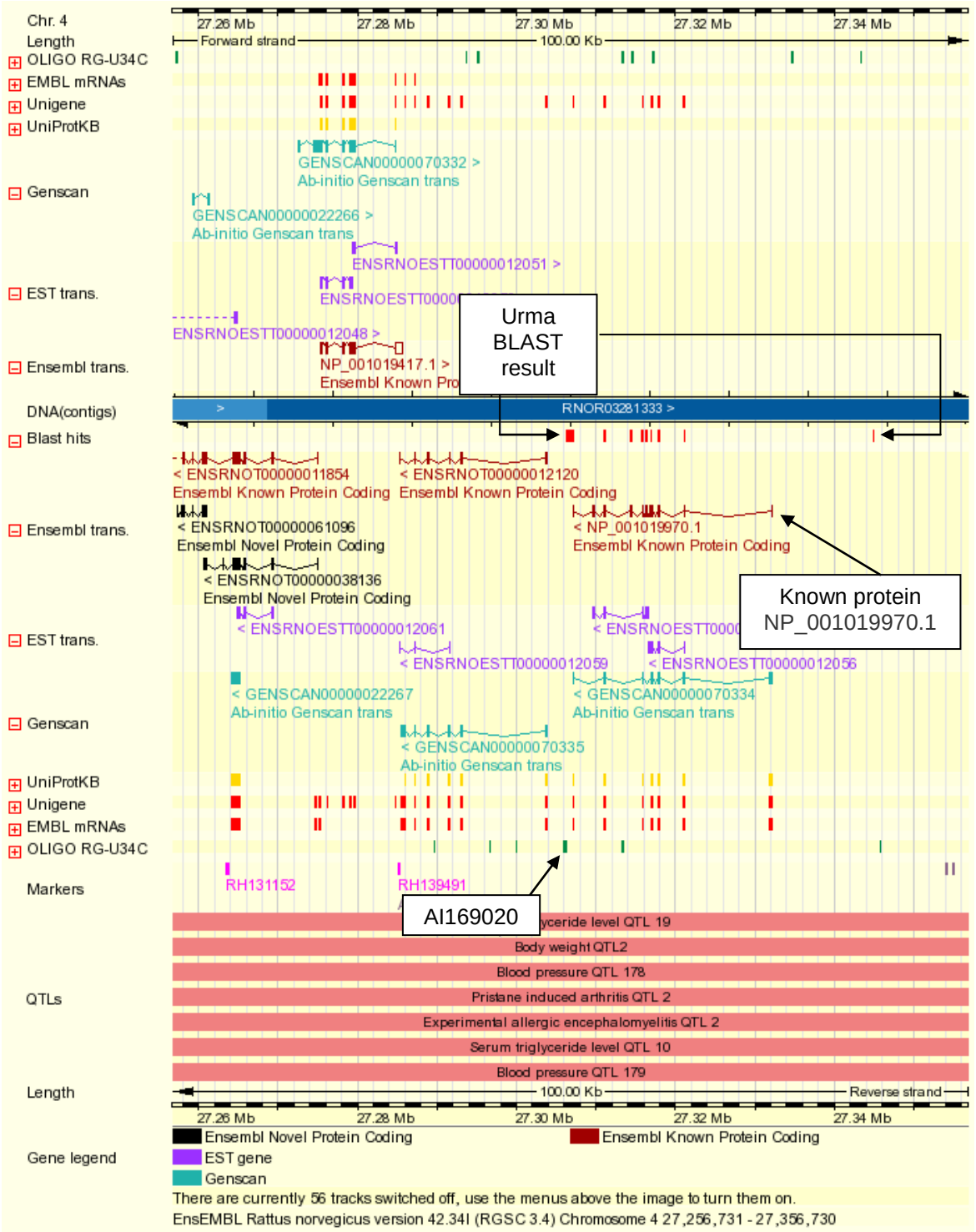

Figure 7.18 Updated BLAST search of urma, using only the sequenced nucleotide information returned from Geneservice. Highlighted are the BLAST results for urma, Ensembl Known Protein Coding NP_001019970.1 and EST AI169020.

7.4 Discussion

This chapter is a first introduction to the novel gene urma and describes it as a downstream target of zif268 and predicted transcription factor. Increasing levels of zif268 in PC-12 cells shows a tendency to suppress urma mRNA levels, NMDA stimulation in cortical neurones decreases urma mRNA levels, and the absence of zif268 altogether significantly decreases urma levels in the cerebral cortex in zif268 knockout mice.

Microarrays can produce enormous amounts of information, which can be effectively interpreted with the use of SAM analysis. The use of this statistical package provides an accurate estimate of the percentage of genes identified by chance, and hence is superior to the performance of multiple uncorrected statistical tests. Of the 144 ESTs affected, only 4 were nominated for further investigation. The remaining 140 ESTs, mainly of known origin, warrant further investigation to determine their potential role in plasticity via the transcription factor zif268. Gene identification is one of the major tasks of bioinformatics and the comparison of ESTs to each other and to genome sequences is useful for gene discovery. ESTs are characteristically redundant and naturally error prone due to the fact that they are single-read sequences, however, they are generated from oligo(dT)-primed cDNA libraries and can therefore identify authentic mRNAs, even when there are long 3'UTRs.

More than half of the genes within the genome of an organism can be located through their homology to other known proteins. In order to determine the remaining genes, genefinder programs can be utilised. GENSCAN, in the most basic of explanations, is a probabilistic HMM-based[2] program that searches for consensus sequences on both strands of DNA, allowing for occurrences of multiple genes. In general it scans for features recognised by transcriptional, splicing and translational machinery which process all of the protein coding genes; therefore it locates such characteristics as exons, introns, splice sites and promoters. It was chosen as a benchmark model for locating areas of interest as, in 1997, it could identify 75-80% of exons completely (Burge & Karlin 1997) and is

[2] Hidden Markov Model - A probabilistic model used to align and analyze sequence datasets by generalization from a sequence profile

currently recommended by others (Nadershahi *et al.* 2004). GENSCAN can predict about 65% of translation initiation sites and 76% of termination codons exactly, whilst correctly identifying 90% of internal splice sites (Burge & Karlin 1997).

EST AI176839 is significantly downregulated by an increase in zif268 levels as determined by RT-PCR within a cell line and verified in primary neurones. The effect within cultured primary neurones may be time dependent as RNA levels of the EST were significantly downregulated at 6 hours, an effect that had diminished by 24 hours. These results indicate that an area of interest has been identified. There is now an 'Ensembl known protein coding' (transcript ENSRNOT00000055127, NP_001041325.1, gene ENSRNOG00000008194, similar to known gene NFX1-type zinc finger-containing protein 1 (ZNFX1)) in this area however, AI176839 does not line up with any of the exons and is situated at the 5' end, suggesting that it may not be part of the annotated gene. Additional exploration of the genomic region is warranted to determine the full-length sequence of this mRNA, investigate the presence of a novel gene, and locate the transcription and translation start sites, the open reading frame and overall function.

The generation of a product from oligo(dT) primed cDNA by pooling the primers designed for EST AI169020 and transcript ENSRNOT00000012253 shows that an actual transcript can be recovered from this area of the genome. In addition to this, knitting together other expressed transcripts in the form of ESTs produced the information for the overall sequenced product returned from Geneservice. This suggested that the predicted transcript ENSRNOT00000012253 was in fact a real transcript with an extended, only just discovered, 3' UTR. Once the coding sequence of urma had been predicted by two separate programs, and delivered very similar results to those published for transcript ENSRNOT00000012253 and MGC40405 on Ensembl and NCBI respectively, primers were designed to monitor effects within this region only. This assumes that any effects noted are true responses of a novel gene modulated by the transcription factor zif268. An increase in zif268 by NMDA stimulation in cultured primary cortical neurones caused RNA levels of urma to decrease after 24 hours, an effect that seems slow acting as there was no difference in RNA levels between NMDA stimulated cells and controls after only 6 hours. This may imply that zif268 has an indirect effect on urma, whereby an unknown transcription factor gene could mediate the

activation of urma. However, the presence of a zif268 binding site in the proposed 'promoter' area may argue a direct interaction.

The likely translation start site was identified using the software ATGpr, which is the most sensitive and accurate of the various approaches available (Nadershahi *et al.* 2004). The optimal context for initiation of translation is GCCRCCaugG whereby R denotes a purine (adenine or guanine). Within this sequence, the purine (-3) and the G (+4) (the only effective base in this position) are most important for strong activation of the start codon (Kozak 1986; Kozak 1997). When both of these are intact, the AUG is in its strongest context and can function more than 10 times more efficiently than any gene with the start codon in a weak context (Kozak 1987). Urma has a kozak sequence of GCCTACatgA, where underlined letters indicate the important bases, and in both cases it can be seen that the environment is less than optimal. When the context is less than favourable and translation is not strongly stimulated, some protein synthesis may occur but most will start at the next downstream AUG codon. This means that some ribosomes may bypass the weak context AUG codon in favour of a stronger context further downstream, in a manner termed leaky scanning (Kozak 2005). This can enable the generation of long and short forms of the protein, if they are in the same frame, or completely different proteins if they are in different frames. However, less than 10% of all eukaryotic mRNAs do not use the first ATG for the start codon (Kozak 1989). Additional possible effects may be an alteration in mRNA stability or splicing (Kozak 2003). Indeed, it is reported that 35-59% of human genes display evidence of at least one splice variant (Modrek & Lee 2002). Further experimentation is required to determine whether the suboptimal context of the kozak rule within urma has any effect on protein length, number, sequence and/or function.

Analysing gene promoters bioinformatically to identify transcription factor consensus sequences has aided the detection of functional transcription factor binding sites (Tullai *et al.* 2004; Chowdhary *et al.* 2005; Kamalakaran *et al.* 2005; Xie *et al.* 2005). The difficulty in this instance is that we have not definitively identified a transcriptional start site and it is very difficult to obtain data on the average length of 5'UTRs in the *Rattus norvegicus* genome. However, a statistical analysis in 1999 (Deutsch & Long 1999) of 74 genes with descriptive 5'UTRs, taken from 10 eukaryotic model organisms, records a range of 96 to 8214 nucleotides for intron length in this area. Eukaryotic genes tend to have very long

genes with very short exons (e.g. *Arabidopsis* has exons of 3 bps) and long introns (e.g. the human dystrophin gene has introns of >100 kbs) (Mathe *et al*. 2002). In fact, first introns in the human genome were found to be longer than median length introns more often than expected at random (Kalari *et al.* 2006). In addition, it has been shown that transcripts with an optimal start codon context tend to have shorter 5' UTRs, whereas an increased length of 5' UTR correlates with a 'weak' start codon context (Rogozin *et al.* 2001). Overall, this therefore led to the analysis of a large genomic area.

The urma promoter may contain a TATA box, CAAT box, CREB site and a zif268 binding site with an overlapping Sp-1 recognition sequence. An interesting feature of these consensus sequences is that they are all located within 2000 base pairs of each other. The TATA box to cap site is 30 to 36 bps from the first T of the TATA box matrix to the cap site (start of transcription), and the CAAT is generally found upstream at –60 to –100. However, the TATA box only seems to be present in about 70% of human promoters, and the CAAT box found in about 50% of vertebrate promoters (Fickett & Hatzigeorgiou 1997). The presence of a zif268 binding site located close to recognition sites that may signal the immediacy of the transcriptional start site is very encouraging. In many known zif268 targets the consensus sequence(s) are in proximal promoter regions (James *et al.* 2006). The presence of a zif268 binding site does not prove an interaction with urma but does increase the likelihood that it is a direct target. Interestingly, the zif268 binding site is overlapped by an Sp-1 binding site. It has been reported that the competitive binding between Sp-1 and zif268 at overlapping sites leads to a suppression in transcription mediated by zif268 as it blocks the binding of Sp-1 to its recognition sequence (Ackerman *et al.* 1991; Bahouth *et al.* 2002). Furthermore, additional studies suggest that displaced Sp1 binds to and activates the endogenous zif268 gene, thereby leading to "facilitated inhibition" of Sp1 function by the resulting increased zif268 (Liu *et al.* 1996).

The bioinformatically-derived localisation of urma to the nucleus, with the prediction that it will bind to DNA, suggests that urma may be transcription factor. The presence of many PKA/PKC/PKG phosphorylation sites within the protein sequence are also typical of a transcription factor responding to extracellular signals, to rapidly induce or suppress gene expression. This allows several layers of control with overlapping functions to tightly regulate the activity of transcription factors and therefore, their downstream targets.

Within zif268 knockout mice, urma levels are significantly downregulated. As with the ubiquilin results, this is surprising as the expected result would be an upregulation in the absence of zif268, however, it does identify urma as a genuine downstream target. It was planned to determine the distribution of urma mRNA throughout the whole mouse brain, as well as comparing mRNA levels in the striatum of zif268 knockout and wildtype mice after haloperidol administration, by *in situ* hybridisation. However, there was not enough time to optimise these experiments.

Evidence that urma could be involved in synaptic plasticity comes from a paper published recently describing a girl of 10.5 years of age with mental retardation. This has been located to an interstitial deletion of chromosome 7q21.1-q22 and is the third case of its kind (Young *et al.* 1984; Chitayat *et al*. 1988; Manguoglu *et al.* 2005). In addition a case of a 7q21.2 to q22.1 duplication resulted in moderate mental retardation (Lukusa & Fryns 1998), and a proximal interstitial deletion of 7q (q11.23q22) produced severe mental retardation (McElveen *et al*. 1995). In all of the above cases, many other symptoms were also reported, most frequently of which is ectrodactyly (split hand/split foot malformation), which appears to be localised between 7q21.2 and 7q22.1. While clearly there are many genes located in this region that could be responsible for the mental retardation, the above evidence linking urma to neuronal plasticity makes urma an interesting candidate.

Biological websites are updated continuously but the annotation of all the information presented by researchers is not keeping pace with the volume of raw sequence data. In addition, the multitude of databases, each with their specific accession numbers, can be very confusing. However, as each part of genome is investigated and interpreted, the situation should become more manageable. Experimental approaches remain necessary in order to confirm the exact locations, transcriptional activity and splicing patterns of novel genes and the existence of virtual proteins, their biological functions and condition of expression within an organism. Although the complete gene structure and physical evidence of the protein have not been elucidated yet, urma may be a rarely expressed transcription factor that can target genes involved in plasticity.

Chapter 8

General Discussion

8.1 Discussion

8.1.1 Significance of Investigation

This thesis introduces gephyrin, ubiquilin and a novel gene, urma, as downstream targets of the plasticity-related immediate early gene, zif268. It also proposes that zif268, activated during neuronal plasticity, transcriptionally downregulates gene expression of gephyrin and ubiquilin, which impacts on the number of $GABA_A$Rs localised to the synapse. This effect may also indirectly influence proteasome activity and the cytoskeleton at inhibitory synapses.

8.1.2 Plasticity

It is assumed that memories are represented in the brain as spatio-temporal patterns of cellular activity within a neural network, with adaptations occurring at a cellular level to store experiences. LTP is the pairing of input stimulation and postsynaptic depolarisation, with a resulting long-term increase in the strength and efficiency of the synaptic connection. Stable LTP has been produced in the medial and lateral perforant pathways for up to a year (Abraham *et al.* 2002). It is therefore studied as a possible cellular correlate of learning and memory.

Several protein kinases, including Src, ERK, CaMKII, PKC, cGMP-dependent kinase (PKG) and PKA are downstream effectors of synaptic signalling, as selectively inhibiting their actions can prevent hippocampal LTP induction. Interactions between kinase pathways suggests that ERK may be a point of convergence integrating CaMK, PKA and PKC signals (Impey *et al.* 1998). These kinases are thought to play a role in the early phases of LTP, leading to the changes necessary for the slower, more sustained phases requiring increased gene transcription and new protein synthesis which occur after approximately 3 hours of LTP maintenance (Krug *et al.* 1984; Otani *et al.* 1989; Fazeli *et al.* 1993).

Many articles cite the effects that plasticity have on excitatory synapses. Seventeen to twenty percent of the neurones in the brain are GABAergic, each of which receives approximately 6000 connections (Somogyi *et al.* 1998). Seventeen percent of these cells innervate other GABAergic cells (Freund & Buzsaki 1996). This body of work looks at inhibitory synapses found on cells that are involved in excitatory synaptic transmission; those cells that may be glutamatergic, but

contain synapses that are activated by GABA, leading to a suppression of their activity.

8.1.3 The transcription factor, zif268

Zif268 is one of the few proteins consistently implicated in many different forms of plasticity. Within 1 hour of LTP induction, zif268 mRNA is increased (Cole *et al.* 1989; Wisden *et al*. 1990; Richardson *et al*. 1992). It is also induced during periods of learning, whilst the threshold and duration of hippocampal LTP correlates with the degree of zif268 induction (Richardson *et al*. 1992; Worley *et al.* 1993). Sustained changes in neuronal activity with a concurrent induction of zif268 has been recorded in the hippocampus, visual or temporal cortex and spinal cord, in diverse species from primates to songbirds (Cole *et al*. 1989; Wisden *et al.* 1990; Jarvis *et al.* 1998; Kaczmarek *et al.* 1999; Mello *et al.* 2004; Morris, 2004).

Zif268 knockout mice show an intact short-term memory but display deficits in late phase LTP, whilst long term memory is significantly impaired (Jones *et al.* 2001), confirming the importance of zif268 induction for long term plasticity. With training however, these mice can overcome deficits in memory as illustrated by a number of memory tasks (Jones *et al.* 2001). This may suggest that other mechanisms can compensate for the lack of zif268 in certain behavioural conditions. For instance, egr-2 mRNA is upregulated and returns to basal levels within a timeframe similar to that of zif268. However, the corresponding egr-2 protein increase outlasts that of zif268 by approximately 16 hours (Williams *et al.* 1995). In addition, certain binding sites on the promoter region of zif268 are equally present on egr-2 and egr-4, as well as other IEGs such as c-fos and arg3.1 (Davis *et al.* 2003), and egr-2 and egr-3 are induced during periods of synaptic activity in the CNS (Yamagata *et al.* 1994; Beckmann *et al.* 1997). This may go some way to explain our results for gephyrin, ubiquilin and urma in the knockout mouse. A preferable paradigm would have included a targeted deletion that could be induced in the adult mouse and knock down the zif268 gene in a controlled manner.

Within this thesis both primary cortical neurones and PC-12 cells were utilised. Zif268 has been identified within the PC-12 cell line, and although it is activated by the addition of 50ng/mL NGF (Milbrandt 1987), this returns to basal level within 120 minutes (Day *et al.* 1990), the minimum amount of time that was allowed to

elapse after NGF treatment of PC-12 cells before transient transfection of the full-length or truncated zif268 constructs. In addition, NMDA stimulation with a depolarising agent induced zif268 in primary cultured cortical cells in a physiologically relevant manner. However, zif268 is also activated during cellular stress & pathology (Jones & Agani 2003; Pignatelli *et al.* 2003; Quinones *et al.* 2003) which could feasibly occur through *in vitro* cell culture work. We performed the majority of experiments on aged cultures, when presumably, any stress-related IEG activation has returned to basal levels. If time had allowed, gephyrin, ubiquilin and urma would have been monitored with an *in vivo* LTP model; haloperidol administration to zif268 knockout mice in order to block striatal D2 receptors. This induces glutamate release from corticostriatal neurones, and produces LTP at corticostriatal synapses, whilst increasing protein levels of zif268 (Nguyen *et al.* 1992; Simpson & Morris 1994; Keefe & Gerfen 1995; Calabresi *et al.* 1997; Cepeda *et al.* 2001).

8.1.4 Urma as a neuronal target of zif268

A full characterisation of urma is still required to elucidate many aspects of this potential neuronal plasticity gene. However, this thesis has presented a transcribed sequence that is downregulated in response to an increase in zif268 as determined by microarray and NMDA stimulation of primary cortical neurones. In addition, urma mRNA levels are downregulated in zif268 knockout mice. This information was collected after the design of unique primers using an EST and closely located predicted transcript. The sequence provided from this product after only amplifying the transcriptome was used to locate a putative translation start site. This information drove the design of further primers to examine the translated region of the gene after experimental manipulation. The likelihood of a novel gene within this area of the genome is increased by the annotations now found on regularly used bioinformatic websites. Although the descriptions on these websites are currently blank, the presence of a known gene symbol adds to the probability that urma is a newly discovered transcript. The submission of urma to genomic databases will officially flag this locus as a zif268-modulated gene. Urma may be a transcription factor involved in learning and memory, as it has putative sites for nuclear localisation, DNA binding, contains multiple phosphorylation sites and is regulated by zif268 in primary cultured neurones.

8.1.5 Gephyrin as a neuronal target of zif268

The downstream target genes of zif268 in neurones were recently discovered and published by James *et al.* (2005). In their microarray experiment, gephyrin mRNA was suggested to be downregulated by 26% in response to an increase in zif268 expression. A downregulation of gephyrin in response to elevated zif268 expression was confirmed within this thesis.

8.1.5.1 Gephyrin and the cytoskeleton

Gephyrin has a tendency to assemble into highly structured complexes both *in vitro* and in transfected cells (Schmitt *et al.* 1987; Kirsch & Betz 1995; Meyer *et al.* 1995), which can occur without the aid of additional proteins (Choquet & Triller 2003) to form a submembraneous scaffold. It is highly enriched at the cytoplasmic face of inhibitory postsynaptic membrane differentiations and is proposed to recruit membrane receptors and subsynaptic structural and signalling proteins to inhibitory synapses. In only one study however, gephyrin clusters have been found opposite glutamate synapses in cultured hippocampal neurones (Brunig *et al.* 2002).

Gephyrin, a major structural component of inhibitory postsynaptic membranes, localises and anchors inhibitory receptors at the synapse, minimising receptor diffusion. Although individual $GABA_A$ receptors at the synapse are continually recycled and exchanged between the cell surface and intracellular compartments the number of receptors at the plasma membrane is generally a stable arrangement. The exception is during periods of intense activity, like that encountered during long-term potentiation and synaptic plasticity. It is thought that synaptic activity could control the cytoskeleton to influence the number of receptors at synapses. Cytoskeleton disruption has been shown to induce rapid variations in GlyR numbers at synapses, decreasing receptor dwell times and causing a rapid diffusion of receptors in the extrasynaptic membrane (Kirsch & Betz 1995; van Zundert *et al.* 2002; van Zundert *et al.* 2004; Charrier *et al.* 2006).

Cytoskeletal anchoring of inhibitory receptors may be mediated by an interaction of gephyrin with tubulin (Kirsch *et al.* 1991) as evidence shows that alkaloids, which disrupt the microtubular network, cause a loss of gephyrin from synaptic sites in cultured spinal cells (Kirsch & Betz 1995; van Zundert *et al*. 2004). In addition, gephyrin interacts with the 'barbed' end of filamentous F-actin, a crucial

protein at the early stages of synaptogenesis (Zhang & Benson 2001). Gephyrin may be laid down at $GABA_AR$ containing membrane domains by an interaction with actin, as microfilaments are essential for gephyrin scaffold formation during postsynaptic membrane development. However this interaction could be transient, as disruption of the actin cytoskeleton and microtubule network in differentiated cells has no effect on the number of postsynaptic $GABA_AR$ and gephyrin clusters (Allison *et al.* 2000). This may suggest that the receptor and scaffold complex, once formed, remains clustered independently without the aid of conventional cytoskeletal proteins.

Mena/VASP acts as an adaptor between actin and gephyrin (Bausen *et al.* 2006) and, along with profilin, is considered an essential and ubiquitous component of the cortical microfilament web, linking gephyrin and GlyRs to the microfilament system (Mammoto *et al.* 1998; Giesemann *et al.* 2003). Profilin, which stimulates actin polymerisation *(*Mammoto *et al.* 1998*)*, is a gephyrin ligand that may contribute to the activity dependent processes underlying synaptic plasticity, as both profilin I and II are redistributed to dendritic spines after synaptic activity, which, in the case of profilin II, occurs after calcium influx (Ackermann & Matus 2003; Neuhoff *et al.* 2005).

Gephyrin mRNA and protein levels were downregulated by increased zif268 levels in PC-12 cells, and following NMDA treatment of primary cortical neurones, as determined by reverse transcription PCR, western blotting, immunocytochemistry and ELISA. A zif268-mediated downregulation of gephyrin therefore could decrease cytoskeletal elements at the cell membrane either directly, or indirectly, decreasing the number of receptors at the synapse. The sub-synaptic scaffolds in general govern the mobility of many membrane-associated or transmembrane proteins. As synaptic gephyrin appears to restrict the mobility of inhibitory receptors diffusing in the plane of the plasma membrane, the loss of gephyrin would decrease the protein availability for interaction with the cortical microfilament web, resulting in a reduced size and low packing density of gephyrin scaffolds, alleviating restrictions on the lateral mobility of neuronal receptors. This would directly influence the number of postsynaptic receptors localised to the synapse, and therefore the size of the synaptic response and ultimately the synaptic efficacy (Lim *et al.* 1999; Meier *et al.* 2001). Gephyrin, via a plasticity-induced upregulation of zif268, may therefore act as a molecular switch that

converts alterations in synaptic activity into morphological changes of synaptic structure.

In addition to the static gephyrin lattices located to the postsynaptic cell membrane, there are a number of small mobile gephyrin particles located throughout the cytoplasm. These represent approximately 2% of the total clusters (Lorenzo *et al.* 2004; Maas *et al.* 2006), and seem to combine and dissociate with the bigger clusters. This mechanism could increase, and reduce, the size of pre-existing gephyrin scaffolds. This infers that 98% of gephyrin locates at plasma membrane regions (Lorenzo *et al.* 2004), and confirms our immunocytochemical results as depicting gephyrin immunoreactivity at the membrane. However, if the 2% of mobile gephyrin has been included in the immunocytochemistry result, it would illustrate a reduction of global gephyrin, therefore depleting the available pool of gephyrin protein that seems to be reserved for maintaining large gephyrin clusters, or represents the gephyrin molecules transportation from their site of production in the cytoplasm. Global gephyrin levels were detected by western blotting and showed a significant downregulatory effect of NMDA treatment on protein levels within primary cultured cortical neurones.

8.1.5.2 Gephyrin and the $GABA_A$ Receptor

During plastic processes, the lateral diffusion of neurotransmitter receptors in and out of synapses rapidly alters receptor numbers and is a key component of receptor renewal and concentration as shown by electrophysiology (Tovar & Westbrook 2002; Adesnik *et al.* 2005; Thomas *et al.* 2005) and imaging techniques (Dahan *et al.* 2003; Tardin *et al.* 2003; Groc *et al.* 2004). This serves to swiftly restore synaptic function during periods of intense activity, whereby lateral diffusion reduces once the receptor reaches the postsynaptic specialisation (Jacob *et al.* 2005).

Gephyrin colocalises with both GlyRs and $GABA_A$Rs in spinal cord, retina and various brain regions (Triller *et al.* 1985; Sassoe-Pognetto *et al.* 1995; Todd *et al.* 1996; Sassoe-Pognetto *et al.* 2000). $GABA_A$ and glycine receptors together with gephyrin can also accumulate at the same postsynaptic sites (Dumoulin *et al*. 2001) indicating that gephyrin can provide a common anchoring scaffold for both types of inhibitory neurotransmitter receptors, although glycine receptors are relatively rare in the forebrain (Luscher & Keller 2004). Gephyrin restricts the

mobility of diffusing hetero-oligomeric GlyRs (Meier *et al.* 2001), and regulates their packing density at the postsynaptic membrane (Kirsch & Betz 1995). In addition, gephyrin has a strong association with the γ2 subunit of $GABA_AR$, restricts lateral mobility and regulates clustering and cluster stability of $GABA_AR$ at postsynaptic sites (Essrich *et al.* 1998, Kneussel *et al.* 1999; Jacob *et al.* 2005).

Gephyrin knockout mice display a total loss of postsynaptic $GABA_AR$ α2 and γ2 immunoreactivities (Kneussel *et al.* 1999), and the targeted deletion of the γ2 subunit of $GABA_ARs$ prevents postsynaptic clustering (Essrich *et al.* 1998). In addition, gephyrin KO mice have a marked increase in the number of intracellular aggregates of $GABA_ARs$ (Kneussel *et al.* 1999). Therefore, clusters of $GABA_ARs$ at the synapse may be formed by the intracellular loop of the γ2 subunit interacting with gephyrin, as part of a postsynaptic scaffold, which then increases their half-life at the synapse and prevents internalisation (Kneussel *et al.* 1999). LTP driven gephyrin protein downregulation would therefore decrease the number of $GABA_ARs$ at the postsynaptic membrane. Indeed, decreasing gephyrin expression by RNAi does not modify the total cell surface expression levels of $GABA_ARs$, but significantly reduces the number of synaptic receptor clusters (Jacob *et al.* 2005). Our results displayed a significant reduction in γ2 containing, but not β containing, $GABA_ARs$ in cortical neurones after NMDA treatment. Although the neurones were not simultaneously stained with anti-gephyrin and anti-$GABA_AR$, the experimental procedures in all treatment groups were identical and therefore a relationship can be drawn between the decrease in gephyrin immunoreactivity and corresponding decrease in γ2 subunit containing $GABA_ARs$. It has been suggested that gephyrin and $GABA_ARs$ are not stably organised with the cytoskeleton and instead rely on the γ2 subunit for long term maintenance at the synapse and recycling at post synaptic sites (Schweizer *et al*. 2003). Our results specifically monitored and reported a significant decrease in the γ2 subunit of $GABA_ARs$. Although a significant fraction of $GABA_ARs$ at postsynaptic sites are not accessible to antibodies in intact cells (van Rijnsoever *et al.* 2005), and $GABA_ARs$ can gephyrin-independently cluster at non-synaptic sites (Christie *et al*. 2002; Scotti & Reuter 2001), the cultured cells were permeabilised with triton X-100 (Sigma-Aldrich, Dorset, UK) and therefore may have allowed the labelling of the majority of the 82% of γ2 subunits that are localised to the synapse (Danglot *et al.* 2003).

A prerequisite for fast and efficient synaptic transmission is a high concentration of neurotransmitter-gated ion channels located directly opposite presynaptic nerve terminals. Inhibitory synaptic currents are significantly affected by the number of synaptic $GABA_A$Rs at the plasma membrane (Otis *et al.* 1994; Nusser *et al.* 1997; Nusser *et al.* 1998), so a reduction of $GABA_A$Rs at the synapse by a zif268-induced downregulation of gephyrin would decrease the likelihood of receptor activation and therefore inhibitory currents entering the cell. $GABA_A$Rs are located to and exert their effects preferentially in the neuronal dendrites (Miles *et al.* 1996; Allison *et al.* 2000; Megias *et al.* 2001), whilst gephyrin immunoreactivity is localised mainly to the dendrites after 3 weeks in culture (Craig *et al.* 1996). As mechanisms that regulate the density and localisation of $GABA_A$Rs on the surface of cortical neurones influence neuronal excitability and inhibitory GABAergic networks are known to adapt to changes in the strength of their excitatory inputs (Nusser *et al.* 1998; Ives *et al.* 2002; Leroy *et al.* 2004; Suzuki *et al.* 2005), it is therefore likely that this adaptation could include a downregulation of inhibitory receptors at synapses.

It is possible that the downstream effects of LTP directly interact with the $GABA_A$Rs at the synapse as they are phosphorylated by PKA, PKC, PKG, CaMKII and Src, an interaction that is thought to cause enhancement or inhibition of inhibitory currents (Moss & Smart 2001; Smart 1997; McDonald *et al.* 1998). After PKC activation, receptors containing the γ2 subunit are reduced at the plasma membrane (Connolly *et al.* 1999b) as this prevents internalised receptors from returning to the surface, although conflicting evidence has been reported (Chapell *et al*. 1998; Cinar & Barnes 2001). Although this may be the case, this thesis presents evidence that zif268 activation directly downregulates gephyrin levels in neurones in the first instance and that this downregulation is remarkably mirrored in the downregulation of $GABA_A$Rs, a receptor that gephyrin has been linked with on many occasions.

Circumstantial evidence has previously linked gephyrin and zif268 within a learning and memory paradigm. It was reported that kainic acid-induced plasticity and fear conditioning by light shock treatment and odour-shock associative learning, induces an upregulation of zif268 mRNA after 0 to 60 minutes and extensive downregulation of gephyrin after 30 – 120 minutes, implying that gephyrin may be involved in the long-term storage of fear memory (Resslar *et al.* 2002). These alterations were detected by *in situ* hybridisation and paired within

the basolateral amygdala, the piriform cortex, perirhinal cortex and habenula. Strikingly, in the areas displaying no changes in zif268 mRNA levels, the investigators also found that gephyrin levels were unaffected (Ressler *et al*. 2002).

8.1.6 Ubiquilin as a neuronal target of zif268

The decrease of gephyrin, which causes a decrease of $GABA_A$Rs localised to the synapse could increase the number of intracellular receptor microclusters throughout the cell, as reported in gephyrin knockout mice (Feng *et al*. 1998). These microclusters would either be recycled or require clearance from the cell. Ubiquilin, found to be downregulated in the microarray experiment (James *et al.* 2005) and in this thesis, has been linked to the $GABA_A$R and the proteasome. Ubiquilin therefore may play a role in receptor degradation.

8.1.6.1 Ubiquilin and $GABA_A$Rs

$GABA_A$Rs are constantly removed from the cell surface by endocytosis and cycled between synaptic sites and intracellular endocytic structures, in a 'holding and recycling' pattern (Tehrani & Barnes 1993; Kittler *et al.* 2000). This allows the quick recovery and reinsertion of receptors into the plasma membrane during periods of intense synaptic activity. Ubiquilin is associated with the plasma membrane (N'Diaye & Brown 2003) and is found in clathrin-coated vesicles as well as on intracellular membranes, so is well placed to stabilise recycled and de novo synthesised receptors (Bedford *et al.* 2001). It can modulate the membrane insertion of $GABA_A$R, by binding its UBA domain to $GABA_A$R α and β subunits, which has a profound effect on the efficacy of synaptic transmission by inhibiting $GABA_A$R polyubiquitylation, reducing receptor targeting to the proteasome and promoting their recruitment to the cell surface. Importantly, blocking the interaction of ubiquilin with $GABA_A$R reduces the number of receptors at the cell surface (Bedford *et al.* 2001).

Ubiquilin possesses an N-terminal ubiquitin like domain, which interacts with subunits of the 19S complex, and a C-terminal UBA domain that interacts with K48-linked polyubiquitin chains (Funakoshi *et al.* 2002; Ko *et al.* 2002; Raasi & Pickart 2003), interfering with the degradation of ubiquitin-dependent proteasome substrates *in-vivo*, increasing their half-life (Kleijnen *et al.* 2000). Ubiquilin interacts with the ubiquitin ligase E6-AP and proteasomes in large complexes (Kleijnen *et al.* 2000), and polyubiquitylated proteins are recognised by a complex

containing the E4 enzymes cdc48/p97 and ubiquitin-fusion degradation 2 enzyme (Ufd2). Ufd2 extends the ubiquitin chain by a few ubiquitin residues and recruits Dsk2, an ubiquilin homologue, which may bind to the ubiquitin-protein conjugate and interact with the proteasome via Rpn1/S2 (Funakoshi *et al.* 2002; Kim *et al*. 2004; Richly *et al*. 2005). This could suggest that ubiquilin delivers the substrate to the proteasome. However, evidence that increasing ubiquilin levels increases $GABA_AR$ immunoreactivity (Bedford *et al.* 2001) suggests that the interaction with the proteasome blocks the degradation of ubiquilin-bound polyubiquitylated proteins, at least in the case of $GABA_AR$ at the synapse.

This thesis reports a reduction in ubiquilin mRNA and protein levels in PC-12 cells and primary neurones as determined by RT-PCR and immunocytochemistry after treatment upregulating zif268 levels. In addition, ubiquilin mRNA is downregulated in zif268 mice compared to wildtypes. As we did not look at proteasome activity directly, this leads to a purely theoretical relationship between LTP, zif268, ubiquilin, $GABA_AR$ and the proteasome. Thus, a zif268 mediated decrease in ubiquilin could increase the degradation of the $GABA_AR$, as ubiquilin would no longer be able to 'protect' the $GABA_AR$ from the proteasome. This in turn would decrease the size of the intracellular pool of inhibitory receptors in GABA receptive synapses available for membrane insertion. It has been shown that PKC activation prevents the recycling of receptors back to the cell surface after endocytosis (Connolly *et al.* 1999b; Kittler & Moss 2001), though this does not seem to be due to a direct phosphorylation of the receptor. It is feasible therefore that this effect could be induced via zif268 and a resultant decrease in the availability of ubiquilin protein.

Ubiquilin interacts with the α and β subunits of $GABA_AR$, subunits that are found throughout the cell and not specifically localised to synapses. In fact, α and β subunits are preferentially extrasynaptic (Fritschy *et al.* 1998; Sassoe-Pognetto *et al.* 2000) suggesting that ubiquilin may play a role in the regulation of global $GABA_AR$, rather than synapse specific receptors. Although Bedford *et al.* (2001) localised ubiquilin to subsynaptic spaces and internal structures, there is the capacity for ubiquilin to exert its effects on extrasynaptic $GABA_AR$ and therefore influence tonic inhibition. Extrasynaptic receptors are not in a cluster formation and therefore the threshold setting for measuring the immunocytochemistry results may have overlooked those receptors that did not meet the minimum size requirements. This would explain why our results do not show a significant

reduction in β subunit containing $GABA_A$Rs throughout the cell, although there was a trend for a reduction of these subunits after NMDA treatment. A reduction of $GABA_A$Rs involved in tonic inhibition would lower the threshold needed for action potentials, allowing the cell to act more responsively to afferent excitatory input.

8.1.6.2 Plasticity and the proteasome

James *et al.* (2005) were the first to discover that many downstream targets of zif268 are either subunits of the proteasome or proteins that function with the proteasome within the CNS. This is additional evidence that LTP and neuronal plasticity are dependent on protein degradation, as well as protein formation, and that regulation of the proteasome could be essential for normal CNS function. Zif268 is involved in the suppression of these genes, leading to a corresponding decrease in proteasome activity, whereas the absence of zif268 by gene knockout is associated with elevated cerebral cortex proteasome activity. These alterations may be subtle but prolonged, as CNS plasticity has been associated with long-term modifications of proteasome gene expression.

The levels of proteins involved in synaptic communication are regulated by the proteasome (Boehmer *et al.* 2003; Colledge *et al*. 2003; Ehlers 2003; Pak & Sheng 2003; Boehmer *et al.* 2004), and the altered expression of a number of proteasome genes has been observed in a variety of plasticity models (El-Khodor *et al.* 2001; Becker *et al.* 2003; Blalock *et al.* 2003; Cirelli *et al.* 2004). In addition, NMDAR activation leads to proteasome sequestration to synaptic spines (Bingol & Schuman 2004) however, APV does not block HFS-induced protein degradation (Karpova *et al*. 2006). HFS-induced phosphorylation of the transcription factor CREB (Leutgeb *et al.* 2005) depends on a functional proteasome system (Ehlers 2003), and therefore the activity of postsynaptic glutamate receptors may regulate the expression of proteasome subunits via zif268 and possibly other inducible transcription factors.

In light of these findings, the activation of zif268, which decreases ubiquilin levels and therefore potentially increases proteasome activity, seems contradictory. It is possible that a zif268 mediated decrease in ubiquilin and in proteasome subunits may not increase $GABA_A$R degradation, but the $GABA_A$Rs are spatially restricted from returning to the membrane or that the downregulation of gephyrin means internalised $GABA_A$Rs cannot be re-localised and anchored to the synapse.

However, our immunocytochemistry results display a decrease in $GABA_AR$ immunoreactivity in response to NMDA treatment. An explanation therefore could be that $GABA_AR$ subunits interact with the AP2 complex (Marsh & McMahon 1999; Kittler *et al.* 2000), which in turn interacts with Eps-15 (Benmerah *et al*. 1995; Morgan *et al*. 2003). Eps-15 also interacts with polyubiquitinated receptors, possibly to sort them into endocytic compartments (Polo *et al.* 2002; Riezman 2002; Bache *et al.* 2003; de Melker *et al.* 2004). Ubiquilin binds to $GABA_AR$ (Bedford *et al.* 2001) and can interact with Eps-15 (Regan-Klapisz *et al.* 2005). During periods of proteasome downregulation, ubiquilin forms cytoplasmic aggresomes that are highly enriched in polyubiquitinated proteins. The $GABA_AR$, through its interaction with Eps-15, ubiquilin, and its possible ubiquitination as a signal for endocytosis, could be recruited to cytoplasmic aggregates after a zif268-induced downregulation of the proteasome. Antibodies would encounter difficulties in trying to penetrate the aggresome and could therefore give the impression of reduced proteins levels of $GABA_AR$ and could explain our western blotting results for ubiquilin.

A simpler explanation could be that the proteasome is indeed upregulated at inhibitory synapses in response to LTP, an effect that would not be identified using the techniques of James *et al.* (2005), which looked at global proteasome activity. Excitatory synapses along the dendrites of cultured hippocampal neurones outnumber inhibitory synapses by 4:1 (Liu *et al.* 2004). An overriding downregulation at excitatory synapses would therefore overshadow any specific effect at inhibitory synapses when monitored at the cellular level.

The role of the proteasome within LTP therefore remains controversial and is probably due to the precise balance of proteins required throughout the cell to provide alterations in neural network properties.

8.1.7 Inhibitory transmission and Long Term Potentiation

Normal brain function relies on tightly controlled synaptic inhibition to influence neuronal excitability. GABA ensures that neurones avoid overexcitation, preventing the development of pathological states of network activity; experimental animal models of temporal lobe epilepsy often involve impaired dendritic inhibition (Cossart *et al.* 2001). Clinically, $GABA_ARs$ deal with disorders of excitability and

are the site of action for benzodiazepines, barbiturates and neurosteroids to combat such conditions as stress, anxiety, epilepsy and pain (McKernan & Whiting 1996; Moss & Smart 2001).

Regulating the number of receptors at the postsynaptic membrane allows alterations in the efficacy of inhibitory synaptic transmission. A decrease in inhibition may be required for the potentiated activation of excitatory synapses allowing the encoding of new information. To this end, it has been reported that interneurones display a reduced level of activity during novel spatial experiences as determined by electrophysiology (Wilson & McNaughton 1993; Fyhn *et al.* 2002). Enhancing network activity in hippocampal slices leads to increased internalisation of $GABA_A$Rs (Blair *et al.* 2004). Decreasing $GABA_A$R at the synapse would increase the probability of neuronal firing as the cell would be more receptive to repeated action potentials due to a decrease in the voltage threshold for firing. This may play some part in the strengthening of synapses that occurs during LTP implying that changes in excitability could be secondary to, or facilitated by, changes in inhibitory synaptic transmission.

Synaptic scaling, a form of homeostatic plasticity, has been described for both AMPAR and NMDAR (Watt *et al.* 2000). This phenomenon affects all the synapses of a cell, proceeds over long periods of time and scales synapses proportionally to their synaptic strength (Turrigiano *et al.* 1998). As all neurones in the CNS appear to be responsive to GABA (Peran *et al.* 2001), this could imply that changes in synaptic efficacy at excitatory synapses would result in a cellular decrease in $GABA_A$Rs.

The site of action for benzodiazepines, a treatment for anxiety and stress, is the γ subunit of the $GABA_A$R, suggesting that $GABA_A$ receptor–mediated inhibitory currents are most likely involved in fear and associated behaviours. The frontotemporal amygdala has been implicated in fear memory acquisition (Fanselow & Gale 2003), and contains a powerful GABA inhibitory circuit within the basolateral amygdala complex (Takagi & Yamamoto 1981; Washburn & Moises 1992a, b). The formation of new fear memories displays a requirement for reduced GABA inhibitory neurotransmission (Rodriguez et al. 2005). Zif268 has also been implicated in fear conditioning and behavioural learning (Malkani & Rosen 2000; Hall *et al*. 2000).

There is evidence to suggest that synaptic $GABA_A$Rs may be downregulated during forms of plasticity involving zif268 induction. Hippocampal LTP is associated with the suppression of GABAergic synaptic events (Lu *et al.* 2000). Similarly BDNF treatment or epileptogenesis cause a downregulation of synaptic $GABA_A$Rs (Brunig *et al.* 2001; Blair *et al*. 2004). Activity dependent modulation of GABAergic transmission may therefore contribute to long-lasting plasticity. The potential suppression by zif268 by gephyrin and/or ubiquilin expression provides a molecular substrate for this phenomenon.

8.1.8 Summary

In summary, neuronal plasticity can stimulate the activation of the inducible transcription factor zif268. Zif268 in turn suppresses the transcription of the neuronal proteins gephyrin, ubiquilin and also the novel gene urma. This downregulation is accompanied by a downregulation of synaptically located $GABA_A$Rs. Postsynaptic receptor accumulation is likely to depend on several highly regulated processes, such as receptor synthesis, intracellular trafficking, membrane insertion, lateral diffusion, internalisation and degradation. Each neurone in the mammalian brain receives, on average, 10^3-10^4 synaptic inputs from other nerve cells. In cultured hippocampal neurones, neural output is determined by the dynamic balance of active excitatory and inhibitory synapses (Liu 2004). The neurone therefore must act as a whole entity, with the nucleus directing overall protein movement; subsequently, orchestrated local protein synthesis would be briefly outsourced to the dendrites during periods of intense activity. Thus, zif268 may play a role in inhibitory synapse receptor clustering during synaptic plasticity.

8.2 Future Studies

- Double stained immunocytochemistry of gephyrin with $GABA_A$Rs or with synapse specific proteins VIAAT, synapsin or the GABA synthesising enzyme GAD-65 would confirm a relationship between the gephyrin and $GABA_A$Rs after zif268 activation.

- The elucidation of endocytosis at the membrane driven by direct LTP induced phosphorylation of $GABA_A$R or lack of gephyrin could prove interesting in ascertaining zif268 actions at inhibitory synapses. Therefore, co-immunofluorescence with endogenous, constitutively recycling, transferrin receptors in permeabilised cells could be informative.

- In order to determine the full sequence of urma, rapid amplification of cDNA ends (RACE) or a primer extension reaction could be performed.

- A yeast 2 hybrid assay would determine the binding partners of urma and enable further characterisation of the function of the urma protein.

- To characterise urma further, the gene could be cloned into a FLAG-tagged vector (or equivalent), transfected into neurones, or a cell line and immunocytochemistry performed to determine the subcellular localisation, as well as any physical effects. In addition, western blotting could also be performed to find the molecular mass of the protein and *in situ* hybridisation would determine the neuro-anatomical expression pattern.

- Transient transfection of zif268 into cultured neurones would elucidate the specific effect of this transcription factor on gephyrin, ubiquilin and a tagged urma by immunocytochemistry.

- Culturing cortical tissue from zif268 knockout mice could verify the effect of zif268 on gephyrin, ubiquilin and urma protein levels as determined by immunocytochemistry.

- CAT reporter assays could be performed for ubiquilin and urma to investigate promoter regulation by zif268. In addition, an interaction with, and direct binding of, zif268 with the promoters of the genes encoding gephyrin, ubiquilin and urma could be determined by EMSA.

- A behavioural paradigm of synaptic plasticity, in which gephyrin, ubiquilin and urma mRNA levels are monitored after zif268 induction in the striatum, could be examined by *in situ* hybridisation.

- Hippocampal tissue, where LTP has been induced 3 hours previously, could be scrutinized relative to control tissue for alterations in mRNA levels of gephyrin, ubiquilin and urma.

Appendix

The details of the results for GeneChips® B & C in the microarray experiment (James *et al.* 2005), whereby PC-12 cells were transiently transfected with either a full-length zif268 or a truncated control, as described in Chapter 7, are tabulated on the following pages.

In each table, the individual ESTs are listed with the fold change reported by the microarray experiment (Fold Change) and length of the EST (Length (bp)). In addition, the results from the BLAST analysis (www.ensembl.org) are detailed. The percentage of similarity to that area of the genome (BLAST Similarity (%)), how many base pairs are involved in this percentage (Length Similarity) and the precise location of the genomic area are all presented (Chromosome Location). Then follows a database reference for any known gene within the vicinity of the BLAST hit (Database Reference), the description that accompanies this reference (Description) and whether a known gene is annotated within the area (Known Gene?).

Table Key:

mm *Mus musculus*

hs *Homo sapiens*

rn *Rattus norvegicus*

B	EST Name	Fold Change	Length (bp)	BLAST similarity (%)	Length similarity (bp)	Chromosome Location (Rat)	Database Reference	Description	Known Gene?
1	AA851237	5.697356	494	97.65	383	4q42			rn: predicted (EST) (genscan exon)
2	AA850583	6.775527	391	99.74	391	12q16	hs: Q15646 mm: NM_145209	hs&mm: 2' 5' oligoadenylate synthetase like protein (P59OASL) (Thyroid R interacting protein 14) (TRIP14)	rn: predicted (ensembl, genscan, NCBI) hs: OASL or TRIP14 mm: OASL1 or OASL2
3	AA899109	4.858614	430	100	413	10q32.3	hs: Q98HCL8	NCBI: similar to chromosome 17 open reading frame 27	rn: predicted (ensembl) (genscan, NCBI exons) hs: Q98HCL8 mm: predicted
4	AA849827	3.290448	446	96.71	243	9q22	rn: NM_032612 hs: P42224 mm: P42225	rn: Signal transducer and activator of transcription 1	rn: NM_032612 hs: STAT1 mm: Stat1 *** 4kbp away from BLAST
5	AA998964	4.615527	511	99.8	496	4q13	hs: NM_0152703 mm: AA175286	no description	rn: predicted (ensembl, genscan) hs: NM_0152703 (BRH) mm: AA175286 (RHS)
6	AI014130	6.250391	431	100	431	6q16	hs: Q96AL8 mm: NM_020557	mm: Thymidylate Kinase family LPS inducible member; thymidylate kinase homologue	rn: predicted (ensembl, EST, genscan, NCBI) hs: Q96AL8 mm: Tyki
7	AI030615	4.981072	278	81.25	160	11q12	rn: P18589 hs: P20591 mm: NM_13606	rn: interferon-induced GTP-binding protein MX2	rn: MX2_RAT hs: MX1 (BRH) mm: MX2
8	AA945915	2.41762	671	100	434	11q22	hs: NM_138287	hs: Rhysin 2	rn: predicted (ensembl, EST, genscan) hs: NM_138287 mm: predicted

B	EST Name	Fold Change	Length (bp)	BLAST similarity (%)	Length similarity (bp)	Chromosome Location (Rat)	Database Reference	Description	Known Gene?
9	AA943147	5.983724	437	99.31	437	4q24	hs: NM_017912 mm: NM_028075	mm: HECT domain and RLD3	rn: predicted (ensembl, EST, genscan, NCBI) hs: NM_017912 (RHS) mm: Herc3 (RHS)
10	AA965186	6.084946	525	100	340	1q37	hs: Q92985 mm: P704434 *opposite direction:* rn: NM_139093 hs: Q9P1Y6	hs&mm: Interferon regulatory protein 7 rn: CTD-binding SR-like protein rA9	rn: predicted (ensembl, genscan, NCBI) hs: IRF7 mm: Irf7 rn: NM_139093 hs: Q9P1Y6 mm: predicted
11	AA999171	2.617801	403	99.74	386	9q22	hs: P42224 mm: P42225	rn: Signal transducer and activator of transcription 1	rn: NM_032612 hs: STAT1 mm: Stat1 *** 4kbp away from BLAST
12	AA924764	2.489172	520	98.82	169	8q24			***closest prediction 6kbp away from BLAST ***no other EST's in vicinity
13	AA997288	2.962963	417	99.74	388	4q22	hs: NM_02275 mm: NM_172893	NCBI: similar to 9930021O16 protein	rn: predicted (ensembl, EST, genscan, NCBI) hs: NM_02275 mm: NM_172893
14	AA955246	6.131208	249	94.83	232	10q21	rn: NM_172019 mm: NM_008330	rn: Interferon gamma inducible protein 1	rn: NM_172019 mm: Ifi47
15	AA997077	2.701461	367	100	350	8q32	mm: NM_011637	mm: three prime repair exonuclease 1; trophoblast expressed 1; three prime exonuclease 1	rn: predicted (ensembl, EST, genscan, NCBI) mm: Trex1

B	EST Name	Fold Change	Length (bp)	BLAST similarity (%)	Length similarity (bp)	Chromosome Location (Rat)	Database Reference	Description	Known Gene?
16	AI012235	1.991437	636	98.58	636	14p22	hs: O14625 mm:Q9JHH5	hs&mm: Small inducible cytokine b11 precursor (cxcl11) (interferon-inducible t-cell alpha chemoattractant) (i-tac) (interferon-gamma-inducible protein-9) (ip-9) (h174) (beta-r1).	rn: predicted (ensembl, EST, NCBI) (genscan exon) hs: CXCL11 mm: Cxcl11
17	AA946088	1.675014	493	97.57	493	1q55	rn: NM_022260 hs: P55210 mm: P97864	rn: Caspase-7	rn: NM_022260 hs: CASP7 mm: Casp7
18	AA946160	1.572179	430	93.49	430	20p12	hs: Q12899 mm: Q9WUH5	hs&mm: Zinc finger protein 173 (tripartite motif-containing protein 26) (acid finger protein) (AFP)	rn: predicted (ensembl, genscan, NCBI) hs: TRIM26 or ZNF173 mm: Trim26 or RNF9 or HERF1
19	AI008397	1.774528	485	75.49	102	18q12.2			rn: predicted (genscan exon)
20	AA998576	2.128611	457	99.78	457	4q22			removed from further distribution at the submitters request
21	AA851040	1.602795	494	92.42	396	20p12			*** closest exon 5kbp away from BLAST *** EST clusters
22	AA945683	2.032149	411	95.39	412	1q54	hs: NM_031212 mm: NM_145156	hs&mm: Putative mitochondrial solute carrier; hypothetical protein NPD016; putative mitochondrial solute carrier	rn: predicted (ensembl, EST, genscan, NCBI) hs: NM_031212 mm: Mrs3/4-pending
23	AI045789	3.264773	388	100	376	7q34	hs: NM_032789 mm: Q8R133	NCBI: similar to Plec1 protein	rn: predicted (ensembl, EST, genscan, NCBI) hs: NM_032789 mm: Q8R133

B	EST Name	Fold Change	Length (bp)	BLAST similarity (%)	Length similarity (bp)	Chromosome Location (Rat)	Database Reference	Description	Known Gene?
24	AI029217	2.097755	389	97.3	370	12q16	hs: Q9Y6K5 mm: P11928	hs&mm: 2'-5'-oligoadenylate synthetase 3 (ec 2.7.7.-) ((2-5')oligo(a) synthetase 3) (2-5a synthetase 3) (p100 OAS) (p100oas)	rn: OAS1_RAT hs: OAS3 (BRH) mm: Oas1g (BRH)
25	AI009156	1.931285	493	98.51	403	3q42	hs: Q9Y508 mm: Q9ET26	hs&mm: zinc finger protein 313	rn: predicted (ensembl, EST, genscan, NCBI) hs: ZNF313 mm: Zfp313
26	AA955213	1.867483	496	99.79	471	18q12.1	mm: Q8R5D8	NCBI: similar to interferon-inducible GTPase	rn: predicted (ensembl, EST, genscan, NCBI) mm: Q8R5D8 (BRH)
27	AI045075	2.888838	395	92.1	367	1q31	hs: NM_002201 mm: NM_020583	hs&mm: interferon stimulated gene (20kDa)	rn: predicted (ensembl, EST, genscan, NCBI) hs: ISG20 mm: Isg20
28	AI070325	2.959543	280	98.09	262	7q34	hs: O95236 mm: Q8VDU3	hs: apoliprotein L3 (apolipoprotein L-III) (APOL-III) (TNF-inducible protein CG12-1) (CG12_1)	rn: predicted (ensembl, EST, genscan) hs: APOL3 (RHS) mm: Q8VDU3
29	AI070313	2.453626	543	87.5	384	9q35	hs: Q9HB58	hs: nuclear body protein (speckled 110 kDa) (transcriptional co-activator SP110) (interferon induced protein 41/75)	rn: predicted (ensembl, EST, NCBI) hs: SP110 mm: predicted
30	AI012552	1.743102	565	98.22	561	1q32	hs: NM_033034 mm: P15533	hs&mm: tripartite motif protein trim5 isoform alpha; tripartite motif protein trim5; tripartite motif protein 5 (down regulatory protein of interleukin 2 receptor)	rn: predicted (ensembl, genscan, NCBI) hs: TRIM5 mm: TRIM30

B	EST Name	Fold Change	Length (bp)	BLAST similarity (%)	Length similarity (bp)	Chromosome Location (Rat)	Database Reference	Description	Known Gene?
31	AA848811	1.542258	367	92.16	255	3q35	hs: P01884 mm: P01887	hs&mm: Beta-2-microglobulin precursor	rn: B2MG_RAT hs: BM2 mm: Bm2
32	AA945204	1.845121	587	85.56	374	6q32	rn: NM_130743 hs: Q96BMO hs: Q9H2X8	rn: Interferon, alpha-inducible protein 27-like	rn: NM_130743 hs: FAM14A or TLH29 (RHS) hs: FAM14B (RHS) mm: D12Ertd647e
33	AI044879	1.970482	410	99.72	355	9q33	hs: NM_005444 mm: NM_021383	hs&mm: RCD1 required for cell differentiaton 1 homolog; protein involved in sexual development	rn: predicted (ensembl, EST, genscan, NCBI) hs: RQCD1 mm: Rqcd1 (or FL10)
34	AI044792	1.807697	429	76.46	429	11q21	rn: NM_019195 hs: Q08722 mm: NM_010581	rn: integrin-associated protein	rn: NM_019195 hs: CD47 mm: Cd47
35	AA955249	1.488516	298	100	281	5q22	hs: Q14142	hs: Tripartite motif protein TRIM14	rn: predicted (ensembl, genscan, NCBI) hs: TRIM14 mm: 5830400N10Rik *** ensembl 4kbp away from BLAST
36	AI011981	1.443584	476	99.58 99.52	239 208	15p13 17p14	rn: Q63798 hs: Q9UL46 mm: P97372 rn: NM_017257	lines up with exon of Proteosome activator complex subunit 2	rn: PSE2_RAT hs: PSME2 mm: PSE2_MOUSE RGD: Psme2
37	AI059254	1.860603	436	89.86	148	3q42	hs: Q9Y508 mm: Q9ET26	hs&mm: Zinc finger protein 313	rn: predicted (ensembl, EST, genscan, NCBI) hs: ZNF313 mm: Zfp313

B	EST Name	Fold Change	Length (bp)	BLAST similarity (%)	Length similarity (bp)	Chromosome Location (Rat)	Database Reference	Description	Known Gene?
38	AA997015	1.732952	476	99.13	460	1q43			rn: predicted (EST, genscan)
39	AA849015	1.491958	623	99.7	334	10q11	rn: Q9QX78 hs: O15524 mm: O35716	hs&mm: suppressor of cytokine signalling(Jak binding protein) (STAT induced STAT inhibitor 1) (tec-interacting protein 3)	rn: SOC1_RAT hs: SOCS1 or SSI1 or TIP3 mm: Socs1
40	AA944197	1.272005	537	98.08	260	10q24	rn: NM_023092 hs: O00159 mm: Q9WT17	rn: unconventional myosin MYR2 1 heavy chain	rn: NM_023092 hs: MYO1C mm: Myo1c
41	AA850552	1.242266	496	100	496	4q24			genscan prediction (approx. 3kbp upstream)
42	AA963884	1.517473	504	99.66	296	3q42			genscan prediction (& EST in opposite direction)
43	AI010116	1.394991	528	98.3	528	8q12	hs: Q9NVC6 mm: NM_144933	hs&mm: co-factor required for SP1 transcriptional activation subunit 6 (transcriptional co-activator CRSP77) (vitamin D3 receptor-interacting protein complex 80kDa component DRIP80) (thyroid hormone receptor-assoc.protein complex 80kDa component TRAP80)	rn: predicted (ensembl, EST, genscan, NCBI) hs: CRSP6 or DRIP80 or TRAP80 or ARC77 mm: Crsp6
44	AA851265	1.736533	230	76.21	227	20p12	rn: P15978 hs: P30460	rn: Class 1 histocompatibility antigen non-RT1.A Alpha-1 chain precursor	rn: HA11_RAT hs: HLA-B or HLAB
45	AI043759	1.964945	429	93.45	412	8q13	hs: NM_018381 mm: NM_175687 *opposite direction:* hs: NM_031917 mm: NM_145154	no description hs&mm: angiopoietin-related protein 5	rn: predicted (ensembl) hs: NM_018381 mm: NM_175687 rn: predicted (ensembl, EST, genscan, NCBI) hs: ANGPTL6 mm: 6330404E11Rik

B	EST Name	Fold Change	Length (bp)	BLAST similarity (%)	Length similarity (bp)	Chromosome Location (Rat)	Database Reference	Description	Known Gene?
46	AA850907	1.372024	560	95.72	561	1p12		no description	rn: predicted (ensembl, genscan exon)
47	AI060296	1.213283	345	92.75	207	3q21	hs: NM_172070	hs: similar to F10G7.10.P (KIAA2024)	rn: predicted (ensembl, EST, genscan, NCBI exons) hs: NM_172070 mm: predicted
48	AI012340	1.930762	512	97.57	288	20p12	rn: P28077 hs: P28065 mm: P28076	rn: proteasome subunit beta type 9 precursor (proteasome chain 7) (macropain chain 7) (multicatalytic endopeptidase complex chain 7) (ring 12 protein) (low mol. mass protein 2)	rn: PSB9_RAT hs: PSMB9 mm: Psmb9
49	AI044795	2.022081	359	99.65	286	3q43	rn: Q9QXY4 hs: Q9NZT2 mm: Q99PG2	rn: opioid growth factor receptor (OGFR) (zeta type opioid receptor)	rn: OGFR_RAT hs: OGFR mm: Ogfr
50	AA851169	1.450284	403	80.49	287	15p13	rn: Q63798 hs: Q9UL46 mm: P97372	Proteosome activator complex subunit 2 (proteasome activator 28-beta subunit) (PA28BETA) (PA28B) (activator of multicatalytic protease subunit 2) (11S regulator complex beta subunit) (reg-beta)	rn: PSE2_RAT hs: PSME2 mm: PSE2_MOUSE
51	AI058400	1.292373	351	99.05	316	2q45	hs: O14772	hs: Fucose-1-phosphate guanalyl tansferase (GDP-L-Fucosepyrophosphor-ylase) (GDP-L-Fucosediphosphorylase)	rn: predicted (ensembl, EST, genscan, NCBI) hs: FPGT or GFPP
52	AA850608	1.464707	556	100	277	6q16			no predictions within 2kbp *** Ensembl & genscan approx 3kbp away

B	EST Name	Fold Change	Length (bp)	BLAST similarity (%)	Length similarity (bp)	Chromosome Location (Rat)	Database Reference	Description	Known Gene?
53	AA851017	1.244911	423	99.21	253	2q14		NCBI:similar to Molybdenum cofactor synthesis protein 2 large subunit (Molybdopterin synthase large subunit) (MPT synthase large subunit) (MOCS2B) (MOCO1-B	rn: predicted (EST, genscan, NCBI)
54	AA900198	1.350785	400	100	383	1q21			rn: predicted (EST & genscan)
55	AI059449	1.450641	515	92.4	500	1q34	hs: NM_002645 mm: O11083	hs&mm: phosphoinositide-3-kinase, class 2, alpha polypeptide; C2-containing phosphatidylinositol kinase	rn: predicted (ensembl, EST, genscan, NCBI) hs: PIK3C2A mm: Pik3c2a
56	AI070270	1.392079	400	99.74	381	7q34	hs: Q14106 mm: Q9JM55	hs: TOB2 protein (transducer of ERBB-2 2)	rn: predicted (ensembl, EST, genscan, NCBI) hs: TOB2 or TOB4 or KIAA1663 mm: Tob2
57	AA848487	1.516116	539	96.1	539	17q12.1		NCBI : similar to proteasome activator complex unit 1 Proteasome activator 28-alpha subunit) (PA28alpha) (PA28a) (Activator of multicatalytic protease subunit 1) (11S regulator complex alpha subunit) (REG-alpha)	rn: predicted (ensembl, genscan, NCBI)
58	AA850501	1.569242	620	92.59	486	5q22	rn: NM_138871 hs: NM_014290 mm: AI447170	rn: Tudor repeat associator with pctaire 2	rn: NM_138871 hs: NM_014290 mm: AI447170
59	AA956379	1.311905	456	99.76	421	15p14	hs: NM_153331	NCBI: similar to hypothetical protein MGC27385	rn: predicted (ensembl, NCBI, genscan) hs: NM_153331 mm: predicted

B	EST Name	Fold Change	Length (bp)	BLAST similarity (%)	Length similarity (bp)	Chromosome Location (Rat)	Database Reference	Description	Known Gene?
60	AA849560	1.633453	442	99.1	442	3p12	rn: NM_153303 hs: O14657 mm: Q9ER41 *opposite direction* hs: O14656 mm: Q9ER39	rn: dystonia 1, torsin (autosomal dominant; torsin A) hs&mm: Torsin B precursor (torsin family 1 member B) hs&mm: Torsin A precursor (torsin family 1 member A) dystonia 1 protein	rn: NM_153303 hs: TOR1B or DQ1 or FKSG18 mm: Tor1b rn: predicted (ensembl, EST, genscan, NCBI) hs: DYT1 or TOR1A or DQ2 mm: Dyt1
61	AA998506	2.112735	419	98.01	402	18q12.1	mm: Q8R5D8	NCBI: similar to interferon-inducible GTPase	rn: predicted (ensembl, EST, genscan, NCBI) mm: Q8R5D8 (BRH also several RHS)
62	AA850909	1.415247	641	96.72	641	1q21	hs: Q92692 mm: P32507	hs&mm: poliovirus receptor related protein 2 precursor (herpes virus entry mediator B) (HVEB) (nectin 2) (CD112 antigen)	rn: predicted (ensembl, EST, genscan, NCBI) hs: PVRL2 (BRH) or PRR2 or HVEB mm: Pvrl2
63	AA942995	1.338276	461	99.69	320	5q36	hs: NM_018715	hs: RCC1-like (TD-60) NCBI: similar to CG9135-PA	rn: predicted (ensembl, EST, genscan, NCBI) hs: NM_018715 mm: predicted
64	AA800994	1.455138	489	99.8	489	2q41	hs: NM_021190 mm: NM_019550	hs&mm: polypyrimidine tract binding protein 2; neural polypyrimidine tract binding protein; ptb-like protein	rn: predicted (ensembl, EST, NCBI) hs: PTBP2 mm: NM_019550
65	AA943011	1.277416	595	99.13	461	8q22	hs: Q9H270 mm: Q91W86	hs&mm: vacuolar protein sorting 11 (HVSP11) (APP3476)	rn: predicted (ensembl, EST, genscan, NCBI) hs: VPS11 mm: Vps11

B	EST Name	Fold Change	Length (bp)	BLAST similarity (%)	Length similarity (bp)	Chromosome Location (Rat)	Database Reference	Description	Known Gene?
66	AI059844	1.856010	424	99.43	351	12q16	rn: Q99MM4 hs: NM_006700 mm: NM_172275	rn: Traf-interacting zinc finger protein fln29 (fragment) hs&mm: FLN29 gene product	rn: Q99MM4 hs: NM_006700 mm: NM_172275
67	AA849028	1.410556	657	97.87	957	6q24	hs: P25788 mm: O70435	hs&mm: proteasome subunit alpha type 3 (proteasome component C8) (macropain subunit C8) (multicatalytic endopeptidase complex subunit C8)	rn: predicted (ensembl, EST, genscan, NCBI) hs: PSMA3 or PSC8 mm: Psma3 ***large EST Cluster
68	AA955175	1.260318	512	97.58	495	10q26	hs: P52429 mm: Q9R1C6	hs&mm: diacylglycerol kinase, epsilon (diglyceride kinase) (DGK-epsilon) (DAG kinase epsilon)	rn: predicted (ensembl, genscan) hs: DGKE or DAGK5 mm: Dgke *** 4kbp away from BLAST
69	AI044222	1.397194	479	99.34	151	14p22	rn: NM_145672 hs: Q07325 mm: P18340	rn: small inducible cytokine B9 hs&mm: small inducible cytokine B9 precursor (gamma interferon induced monokine) (MIG)	rn: NM_145672 hs: CXCL9 or SCYB9 or MIG mm: Cxc19
70	AA900506	1.270857	527	99.17	361	3q36	hs: NM_022662 mm: P53995	hs: anaphase-promoting complex 1 (meiotic checkpoint regulator) (ANAPC1) mm: protein TSG24 (meiotic regulator)	rn: predicted (ensembl, EST, genscan, NCBI) hs: NM_022662 mm: Mcpr
71	AI070047	1.448225	479	99.57	462	5q36	hs: Q9Y692 mm: Q9JL60	hs&mm: glucocorticoid modulatory element binding protein 1 (GMEB-1) (parvovirus initiation factor P96) (DNA binding protein P96PIF)	rn: predicted (ensembl, genscan) hs: GMEB1 mm: Gmeb1
72	AI030755	1.503307	523	99.8	492	17p14		NCBI: similar to 1110064L07Rik protein	rn: predicted (ensembl, EST, genscan, NCBI) mm: predicted

Table i: Table containing all the information gleaned from www.ensembl.org pertaining to the ESTs significantly affected by zif268 on GeneChip® B of the microarray experiment performed by James *et al.* (2005). Please see Chapter 7.

C	EST Name	Fold Change	Length (bp)	BLAST similarity (%)	Length similarity (bp)	Chromosome Location (Rat)	Database Reference	Description	Known Gene?
1	AI112362	5.812263	440	99.52	417	4q13			rn: predicted (genscan)
2	AI111492	8.059316	414	92.95	397	6q16	hs: Q96AL8 mm: NM_020557	mm: Thymidylate kinase family LPS-inducible member; thymidylate kinase homologue	rn: predicted (ensembl, EST, genscan, NCBI) hs: Q96AL8 mm: Tyki
3	AI180075	3.419621	423	98.58	423	7q11		NCBI: similar to signal transducer & activator of transcription 2	rn: predicted (EST, genscan, NCBI)
4	AI073001	4.377708	463	99.22	383	10q24	hs: NM_153230	NCBI: similar to hypothetical protein MGC35179	rn: predicted (ensembl, NCBI exon) hs: NM_153230 mm: predicted
5	AA819679	2.725092	554	99.44	537	11q22	hs: NM_031458	B aggressive lymphoma gene (BAL)	rn: predicted (ensembl, genscan exon, NCBI) hs: NM_031458 mm: BC003281
6	AI169624	4.349338	602	84.72	458	12q16	rn: Q05961 hs: Q9Y6K5 mm: P11928	rn: 2'-5' oligoadenylate synthetase 1	rn: OAS1_RAT hs: OAS3 mm: Oas1g
7	AI176721	2.242152	599	100	599	1q32	hs: Q8NH66 mm: NM_147079	hs: seven transmembrane helix receptor mm: olfactory receptor Mor31-4	rn: predicted (ensembl, genscan) hs: Q8NH66 mm: NM_147079
8	AI137038	2.667022	495	98.76	483	13q21	hs: NM_022371 mm: NM_023141	hs&mm: torsin family 3, member A; ATP-dependent interferon response protein 1; ATP-dependent interferon Responsive, NCBI: similar to ADIR1	rn: predicted (ensembl, genscan, NCBI) hs: TOR_3A mm: Tor3a EST cluster close with no predictions
9	AA799298	1.964366	593	99.42	515	1q52	hs: P09913 mm: Q64112	hs&mm: interferon induced protein with tetratricopeptide repeats 2 (glucocorticoid-attenuated response gene 39 protein GARG-39)	rn: predicted (ensembl, genscan, NCBI) hs: IFIT2 mm: Ifit2

C	EST Name	Fold Change	Length (bp)	BLAST similarity (%)	Length similarity (bp)	Chromosome Location (Rat)	Database Reference	Description	Known Gene?
10	AI236003	2.399980	529	87.95	332	14q22	hs: NM_033109 mm: NM_027869	hs&mm: 3'-5' RNA exonuclease; polynucleotide phosphorylase-like (polyribonucleotide nucleotidyltransferase 1)	rn: predicted (ensembl, EST, NCBI) hs: PNPT1 mm: 1200003F12Rik
11	AA858505	2.177984	558	98.7	539	7q34	hs: O95236	hs: apoliprotein L3 (APOL-III) (TNF-inducible protein CG12-1)	rn: predicted (ensembl, EST, genscan, NCBI) hs: APOL3 mm: 9130022K13Rik
12	AI102236	2.117253	518	98.84	518	3q42	hs: Q9Y3Z3 mm: Q60710	hs&mm: sam domain & HD domain-containing protein 1 (dendritic cell-derived IFNG-induced protein DCIP) (monocyte protein 5 MOP_5) (interferon-gamma inducible protein MGII)	rn: predicted (ensembl) hs: SAMHD1 or MOP5 mm: Samhd1
								in opposite direction	
								NCBI: similar to dJ132F21.2 - contains a novel protein similar to the L82E from drosophila	rn: predicted (EST, genscan, NCBI)
13	AA819034	2.945161	458	100	209	6q32	hs: Q9H2X8 mm: NM_145449	hs: protein fam14a precursor (TLH29 protein) (pif127-like protein)	rn: predicted (ensembl, EST, genscan, NCBI) hs: FAM14A (BRH) or TLH29 mm: NM_145449
14	AI169676	1.785363	583	100	572	7q13	hs: Q9NV91	NCBI: similar to CGi3957-PA	rn: predicted (EST, genscan, NCBI) hs: Q9NV91 mm: predicted

C	EST Name	Fold Change	Length (bp)	BLAST similarity (%)	Length similarity (bp)	Chromosome Location (Rat)	Database Reference	Description	Known Gene?
15	AI178800	1.937421	568	100	559	3q24	hs: O14933 mm: NM_19949	hs&mm: ubiquitin-conjugating enzyme E2- 18kDa UBCH8 (ubiquitin-protein ligase) (ubiquitin carrier protein) (retinoic acid induced gene B protein) (RIG-B) riken cDNA 2810489121 *opposite direction* NCBI: similar to RIKEN cDNA 1110030K22	rn: predicted (ensembl, EST, genscan, NCBI) hs: UBE2L6 or UBCH8 mm: Ubce8 rn: predicted (ensembl, EST, genscan, NCBI) hs: predicted mm: 1110030K22Rik
16	AI105268	2.842362	514	100	367	9q22	rn: NM_032612 hs: P42224 mm: P42225	rn: signal transducer and activator of transcription 1	rn: NM_032612 hs: STAT1 mm: Stat1 *** 4kbp away from BLAST
17	AI071868	1.642953	271	100	254	1q32	hs: P19474 mm: Q62191	hs&mm: 52kDa RO protein (SJOGREN syndrome type A antigen) (RO(SS-A)) (52kDa ribonucleoprotein autoantigen ro/ss-A) (SS-A) (tripartite motif protein 2)	rn: predicted (ensembl, genscan, NCBI) hs: SSA1 (BRH) mm: Trim 21
18	AI177755	1.818049	590	99.83	590	6q16	rn: NM_177928 hs: P43490 mm: NM_021524	rn: pre-B-cell colony-enhancing factor	rn: NM_177928 hs: PBEF_Human mm: NM_021524
19	AA818937	3.017592	394	99.47	377	20p12	rn: P15978 hs: P30460	rn: Class 1 histocompatibility antigen, B-8 B*0801 alpha chain precursor	rn: HAII_RAT hs: HLA-B
20	AA818055	1.651773	594	100	457	15q12	rn: NM_053520 hs: P32519 mm: Q60775	rn: E74-like factor 1 (ETS domain transcription factor)	rn: NM_053520 hs: ELF1 mm: Elf1

C	EST Name	Fold Change	Length (bp)	BLAST similarity (%)	Length similarity (bp)	Chromosome Location (Rat)	Database Reference	Description	Known Gene?
21	AI178386	1.867204	443	96.06	254	9q21	hs: NM_138798	NCBI: similar to hypothetical protein BC018453	rn: predicted (ensembl, EST, NCBI) hs: NM_138798 mm: 1500032H18Rik
22	AI229172	2.188327	319	97.48	318	8q13	hs: NM_018381 mm: NM_175687 hs: NM_031917 mm: NM_145154	no description hs&mm: angiopoietin-related protein 5	rn: predicted (ensembl) hs: NM_018381 mm: NM_175687 rn: predicted (ensembl, EST, genscan, NCBI) hs: ANGPTL6 rn:6330404E11Rik
23	AI171280	1.831267	628	71.92	146	4q34	hs: NM_014497 mm: NM_008717	hs&mm: NP220 nuclear protein; CTCL tumour antigen SE33-1	rn: predicted (EST) (ensembl, NCBI exons) hs: NM_014497 mm: Np220 *** >2kbp away
24	AI231086	1.518925	541	99.6	252	2q43	rn: Q9QXN1 hs: Q9UJU2 mm: P27782	rn: lymphoid enhancer binding factor 1	rn: LEF1_RAT hs: LEF1 mm: Lef1
25	AI171480	1.517404	519	100	519	1q32			rn: predicted (genscan)
26	AI102643	1.612565	496	92.14	496	15p13	hs: Q00978 mm: Q61179	hs&mm: transcriptional regulator ISGF3 gamma subunit (IFN-alpha responsive transcription factor subunit) (interferon stimulated gene factor 3 gamma) (ISGF3 P48 subunit) (ISGF-3 gamma)	rn: predicted (ensembl, EST, genscan, NCBI) hs: ISGF3G mm: Isgf3g
27	AA818887	1.712270	522	99.79	477	20p12	rn: NM_012646 hs: P30460 mm: P14432	rn: RTI class 1B gene, H2-TL-like, GRC region	rn: NM_012646 hs: HLA-B mm: H2-T10
28	AI071755	1.261304	263	100	146	9q31			rn: predicted (genscan)

C	EST Name	Fold Change	Length (bp)	BLAST similarity (%)	Length similarity (bp)	Chromosome Location (Rat)	Database Reference	Description	Known Gene?
29	AI227666	1.651391	573	96.86	573	11q21	rn: NM_019195 hs: Q08722 mm: NM_010581	rn: integrin-associated protein	rn: NM_019195 hs: CD47 mm: Cd47
30	AI234967	1.793207	416	100	376	20p12	hs: Q9C019 mm: Q8R096	hs&mm: tripartite motif protein 15 (zinc finger protein B7)	rn: predicted (ensembl, EST, genscan, NCBI) hs: Trim15 or ZNFB7 mm: Q8R096 (BRH)
31	AI103500	1.616213	519	87.35	304	20p1	rn: P15978 hs: P30460	rn: Class 1 histocompatibility antigen, non- rH.A alpha-1 chain precursor	rn: HAII_RAT hs: HLA-B
32	AI177396	1.819174	507	9137	241	8q32		NCBI: similar to ubiquitin-activating enzyme E1-like; ubiquitin-activating enzyme-2; ubiquitin-activating enzyme E1 like	rn: predicted (EST) (genscan, NCBI exons)
33	AA818849	2.103757	417	86.8	250	10q32.1	hs: NM_024119	NCBI: similar to hypothetical protein FLJ11354	rn: (ensembl, genscan, NCBI) hs: NM_024119 mm: DIILgp2e
34	AA819788	1.878639	517	99.8	503	11q23		NCBI: similar to 5830458k16Rik protein	rn: predicted (EST, genscan, NCBI)
35	AI177481	2.16080728	457	97.92	289	20p12	rn: P28077 hs: P28065 mm: P28076	rn: proteasome subunit beta type 9 precursor (proteasome chain 7) (macropain chain 7) (multicatalytic endopeptidase complex chain 7) (ring 12 protein) (low mol. mass protein 2)	rn: PSB9_RAT hs: PSMB9 mm: Psmb9
36	AI170410	1.436327	638	99.84	638	11p12	hs: NM_173824	NCBI: similar to 4930453N24Rik	rn: predicted (ensembl, EST, genscan, NCBI) hs: NM_173824 mm: predicted
37	AI176839	1.853808	478	97.63	211	3q42			rn: predicted (EST, genscan)

C	EST Name	Fold Change	Length (bp)	BLAST similarity (%)	Length similarity (bp)	Chromosome Location (Rat)	Database Reference	Description	Known Gene?
38	AI228291	1.841349	461	98.26	287	1q22	hs: NM_031448	NCBI: similar to cDNA 160001410	rn: predicted (ensembl, genscan, NCBI) hs: NM_031448 mm: 1600014C10Rik
39	AA819629	1.460664	529	98.82	510	2.fragment	hs: NM_006820	hs: histocompatibility 28	rn: predicted (ensembl, EST) (genscan exon) hs: Clorf29
40	AI179939	1.917067	398	100	268	20p12	rn: NM_033098 hs: O15533 mm: Q9R233 hs: O15211 mm: Q61193	rn: Tapasin hs&mm: RAL guanine nucleotide dissociation stimulator-like 2 (RALGDS-like factor (ras-associated protein rab21)	rn: NM_033098 hs: TAPBP or TAPA or NGS17 mm: TPSN_MOUSE rn: predicted (ensembl, EST, NCBI) hs: RAB2L or RGL2 mm: RGL2_Mouse
41	AI235748	1.819836	537	98.19	497	9q12		NCBI: similar to cDNA 0610009D16	rn: predicted (ensembl, genscan, EST, NCBI) hs: MAD2LIBP mm: 0610009D16Rik
42	AI113020	1.588865	503	97.94	486	20p12	hs: NM_015050	NCBI: similar to Riken cDNA 1300018105 no description	rn:predicted(ensembl,EST,genscan)(NCBI exon) hs: NM_015050 mm: 1300018105Rik rn: predicted (EST, genscan)
43	AI071800	1.292724	259	99.08	109	14q21	rn: NM_031352 hs: NM_014063 mm: NM_013810	rn: Drebrin-like	rn: NM_031352 (Ensembl exon) hs: NM_014063 mm: Dbn1
44	AA818912	1.701085	615	95.32	598	1q41	hs: NM_022466	hs: zinc finger protein, subfamily 1A,5; zinc finger transcription factor pegasus	rn: predicted (ensembl, genscan, NCBI) hs: NM_022466 mm: predicted

C	EST Name	Fold Change	Length (bp)	BLAST similarity (%)	Length similarity (bp)	Chromosome Location (Rat)	Database Reference	Description	Known Gene?
45	AI178869	1.717091	408	99.65	289	3p12	rn: NM_153303 hs: O14657 mm: Q9ER41	rn: dystonia 1, torsin (autosomal dominant; torsin A) hs&mm: Torsin B precursor (torsin family 1 member B)	rn: NM_153303 hs: TOR1B or DQ1 or FKSG18 mm: Tor1b
46	AI177734	1.334543	550	99.64	551	11q11		NCBI: similar to hypothetical protein KIAA0136	rn: predicted (NCBI) (genscan exon)
47	AI145609	1.800893	528	98.79	495	18q11	hs: P23508	hs: Colorectal mutant cancer protein (MCC protein	rn: predicted (ensembl, genscan, EST, NCBI) hs: MCC mm: predicted *** 4kbp away from Blast ***Large EST Cluster
48	AA817937	1.683501	360	100	343	16p14	rn: Q811A2 hs: Q10589 mm: Q8R2Q8	rn: DAMP-1 protein	rn: Q811A2 hs: BST2 mm: Q8R2Q8
49	AI104907	1.432870	587	99.63	534	14q22	rn: NM_023986 mm: Q8K0K0	mm: similar to TEMO (fragment) NCBI: TEMO (WITHDRAWN)	rn: NM_023986 hs: PSME4 mm: AA409398 (BRH)
50	AA684879	1.729296	326	93.19	235	20p12	rn: Q8V1B2 hs: Q9UER7 mm: O35613	rn: death domain-associated protein 6 (DAXX)	rn: DAXX_RAT hs: DAXX or BING2 mm: DAXX_MOUSE
51	AA858877	1.501456	487	100	459	2q43	rn: Q9QXN1 hs: Q9UJU2 mm: P27782	rn: lymphoid enhancer binding factor 1	rn: LEF1_RAT hs: LEF1 mm: Lef1
52	AA818264	1.760532	494	100	402	12q12	hs: NM_006989	hs: Ca++-promoted Ras inactivator; GTPase activating protein-like; Ca++-promoted ras inactivator (Rasp21 protein activator 4 (RASA4))	rn: predicted (ensembl, genscan, EST, NCBI) hs: NM_006989 mm: predicted

C	EST Name	Fold Change	Length (bp)	BLAST similarity (%)	Length similarity (bp)	Chromosome Location (Rat)	Database Reference	Description	Known Gene?
53	AI176976	1.369938	510	98.2	501	3q24	hs: NM_15308 mm: NM_018828	hs&mm: formin binding protein 4 (or 30)	rn: predicted (ensembl, genscan, EST, NCBI) hs: FNBP4 mm: Fnbp4
54	AI231494	1.518741	588	98.13	588	15p14	rn: P22288 hs: P30793 mm: Q05915	rn: GTP cyclohydrolase 1 precursor (GTP- CH-1)	rn: GCH1_RAT hs: GCH1 or GCH or DYT5 mm: Gch
55	AI178629	1.641470	438	98.97	290	20p12	rn: P28064 hs: P28062 mm: P28063	rn: proteasome subunit beta type 8 precursor (proteasome component C13) (multicatalytical endopeptidase complex subunit C13) (fragment)	rn: PSB8_RAT hs: PSMB8 or LMP7 or RING10 or Y2 mm: Psmb8
56	AI176183	1.350876	453	97.57	453	Xq34	hs: P06280 mm: P51569	hs&mm: alpha galactosidase A precursor (melibiase) (alpha-D-galactoside galactohyd- rolase) (alpha-D-galactosidase A)	rn: predicted (ensembl, genscan, NCBI) hs: GLA mm: Gla
57	AI176479	1.341039	416	100	261	1q41	rn: P26376 hs: Q01628 mm:NM_0285378	rn: interferon-inducible protein	rn: INIB_RAT hs: IFITM3 mm: Fgls - pending (BRH)
58	AI072951	1.363177	516	94.44	216	10q26	hs: NM_144975	NCBI: similar to hypothetical protein FLJ34922	rn: predicted (ensembl, EST, NCBI) hs: NM_144975 mm: predicted (RHS only)
59	AI071534	1.292306	464	97.54	447	11p12	hs: NM_173824	NCBI: similar to 4930453N24Rik protein	rn: predicted (ensembl, EST, genscan, NCBI) hs: NM_173824 mm: predicted (BRH)

C	EST Name	Fold Change	Length (bp)	BLAST similarity (%)	Length similarity (bp)	Chromosome Location (Rat)	Database Reference	Description	Known Gene?
60	AI179403	1.560792	541	99.81	532	20q13	hs: NM_022091	hs: DJ467N11.1 protein NCBI: similar to RNA helicase family	rn: predicted (ensembl, EST, genscan, NCBI) hs: NM_006828 mm: Q8K292
61	AI232313	1.628982	575	97.91	575	4q11	hs: Q9Y5A7 mm: P54729	hs&mm: BS4 protein (NY-REN-18 antigen) (NEDD8 ultimate buster-1)	rn: predicted (ensembl, EST, genscan, NCBI) hs: BS4_Human or NUB1 or NYREN 18 mm: Nyren 18 - pending
62	AI112633	1.272086	446	96.74	429	12p12		NCBI: similar to proteasome subunit alpha type 6 (proteasome iota chain)(macropain iota chain) (multicatalytic endopeptidase complex iota chain)(27kDa prosomal protein) (PROS-27) (p27k)	rn: predicted (genscan) (ensembl pseudogene)
63	AI176007	1.695461	653	99	400	4q44			rn: predicted (EST)
64	AI137689	1.272232	457	98.44	384	14q22	rn: NM_173147 hs: NM_016516 mm: NM_139061	rn: VPS54-like hs&mm: Tumour antigen SLP-8P	rn: NM_173147 hs: VPS54 mm: Vps54
66	AI071570	1.220613	429	100	118	20p12	hs: P00751 mm: P04186	hs&mm: complement factor B precursor (C3/C5 convertase) (properdin factor B) (glycine-rich beta glycoprotein)(GBG)(PBF2)	rn: predicted (ensembl, EST, genscan, NCBI) hs: BF mm: CFAB_Mouse
67	AI171503	1.436843	479	74.31	432	2q11	rn: Q9JJ22 hs: Q9NZ08 mm: Q9EQH2	rn: adipocyte-derived leucine aminopeptidase precursor (A-lap) (ARTS-1) (aminopeptidase pils) (puromycin-insensitive leucyl-specific aminopeptidase) (pils-AP)	rn: ART1-RAT hs: ART1-HUMAN mm: Arts-1 pending

C	EST Name	Fold Change	Length (bp)	BLAST similarity (%)	Length similarity (bp)	Chromosome Location (Rat)	Database Reference	Description	Known Gene?
68	AI227647	1.227656	339	80.07	301	19p12	rn: O55145 hs: P78423 mm: O35188	rn: fractalkaline precursor (CX3CLI) (neurotactin) (CX3C membrane-anchored chemokine) (small inducible cytokine D1)	rn: SYD1-RAT hs: CX3CLI or SCYDI or FKN or NTT or A-152E5.2 mm: AB030188
69	AI169020	1.420293	577	99.31	577	4q13	 hs: NM_152789	no description no description	rn: predicted (ensembl) mm: 1700109H08Rik rn: predicted (ensembl) hs: NM_152789 (BRH) mm: 5830415L20Rik (RHS only)
70	AI227994	1.487453	569	94.76	572	11q21	rn: NM_019195 hs: Q08722 mm: NM_010581	rn: integrin-associated protein	rn: NM_019195 hs: CD47 mm: Cd47
71	AI071265	1.489646	443	99.29	424	15p13	hs: Q00978 mm: Q61179	hs&mm: transcriptional regulator ISGF3 gamma subunit (IFN-alpha responsive transcription factor subunit) (interferon stimulated gene factor 3 gamma) (ISGF3 P48 subunit) (ISGF-3 gamma)	rn: predicted (ensembl, EST, genscan, NCBI) hs: ISGF3G mm: Isgf3g
72	AI178746	1.400854	542	97.42	542	8q32		NCBI: similar to TGF-beta induced apoptosis protein 3	rn: predicted (EST, genscan, NCBI)

Table ii: Table containing all the information gleaned from www.ensembl.org pertaining to the ESTs significantly affected by zif268 on GeneChip® C of the microarray experiment performed by James *et al.* (2005). Please see Chapter 7.

List of References

Abel, T., Nguyen, P. V., Barad, M., Deuel, T. A., Kandel, E. R. and Bourtchouladze, R. (1997) Genetic demonstration of a role for PKA in the late phase of LTP and in hippocampus-based long-term memory. *Cell* **88,** 615-626.

Abeliovich, A., Chen, C., Goda, Y., Silva, A. J., Stevens, C. F. and Tonegawa, S. (1993a) Modified hippocampal long-term potentiation in PKC gamma-mutant mice. *Cell* **75,** 1253-1262.

Abeliovich, A., Paylor, R., Chen, C., Kim, J. J., Wehner, J. M. and Tonegawa, S. (1993b) PKC gamma mutant mice exhibit mild deficits in spatial and contextual learning. *Cel,* **75,** 1263-1271.

Abraham W. C., Mason S. E., Demmer J., Williams J. M., Richardson C. L., Tate W. P., Lawlor P. A. and Dragunow M. (1993) Correlations between immediate early gene induction and the persistence of long-term potentiation. *Neuroscience* **56,** 717-727.

Abraham W. C., Christie B. R., Logan B., Lawlor P. and Dragunow M. (1994) Immediate early gene expression associated with the persistence of heterosynaptic long-term depression in the hippocampus. *Proc Natl Acad Sci U S A* **91,** 10049-10053.

Abraham W. C., Logan B., Greenwood J. M. and Dragunow M. (2002) Induction and experience-dependent consolidation of stable long-term potentiation lasting months in the hippocampus. *J Neurosci* **22,** 9626-9634.

Ackerman S. L., Minden A. G., Williams G. T., Bobonis C. and Yeung C. Y. (1991) Functional significance of an overlapping consensus binding motif for Sp1 and Zif268 in the murine adenosine deaminase gene promoter. *Proc Natl Acad Sci U S A* **88,** 7523-7527.

Ackermann, M. and Matus, A. (2003) Activity-induced targeting of profilin and stabilization of dendritic spine morphology. *Nat Neurosci,* **6,** 1194-1200.

Adesnik, H., Nicoll, R. A. and England, P. M. (2005) Photoinactivation of native AMPA receptors reveals their real-time trafficking. *Neuron,* **48,** 977-985.

Akopian G., Musleh W., Smith R. and Walsh J. P. (2000) Functional state of corticostriatal synapses determines their expression of short- and long-term plasticity. *Synapse* **38,** 271-280.

Alberts, A. S., Montminy, M., Shenolikar, S. and Feramisco, J. R. (1994) Expression of a peptide inhibitor of protein phosphatase 1 increases phosphorylation and activity of CREB in NIH 3T3 fibroblasts. *Mol Cell Biol,* **14,** 4398-4407.

Alexandropoulos, K., Qureshi, S. A., Bruder, J. T., Rapp, U. and Foster, D. A. (1992a) The induction of Egr-1 expression by v-Fps is via a protein kinase C-independent intracellular signal that is sequentially dependent upon HaRas and Raf-1. *Cell Growth Differ,* **3,** 731-737.

Alexandropoulos, K., Qureshi, S. A., Rim, M., Sukhatme, V. P. and Foster, D. A. (1992b) v-Fps-responsiveness in the Egr-1 promoter is mediated by serum response elements. *Nucleic Acids Res,* **20,** 2355-2359.

Allison D. W., Chervin A. S., Gelfand V. I. and Craig A. M. (2000) Postsynaptic scaffolds of excitatory and inhibitory synapses in hippocampal neurons: maintenance of core components independent of actin filaments and microtubules. *J Neurosci* **20,** 4545-4554.

Altschuler R. A., Betz H., Parakkal M. H., Reeks K. A. and Wenthold R. J. (1986) Identification of glycinergic synapses in the cochlear nucleus through immunocytochemical localization of the postsynaptic receptor. *Brain Res* **369,** 316-320.

Amaral D.G., Witter M.P. (1989) The three-dimensional organization of the hippocampal formation: a review of anatomical data. *Neuroscience* **31**(3):571-91

Anwyl, R. (2006) Induction and expression mechanisms of postsynaptic NMDA receptor-independent homosynaptic long-term depression. *Prog. Neurobiol*. **78**, 17–37

Arthur, J. S., Fong, A. L., Dwyer, J. M., Davare, M., Reese, E., Obrietan, K. and Impey, S. (2004) Mitogen- and stress-activated protein kinase 1 mediates cAMP response element-binding protein phosphorylation and activation by neurotrophins. *J Neurosci,* **24,** 4324-4332.

Artola, A., Brocher, S. and Singer, W. (1990) Different voltage-dependent thresholds for inducing long-term depression and long-term potentiation in slices of rat visual cortex. *Nature* **347**,69-72

Artola, A. and Singer, W. (1993) Long-term depression of excitatory synaptic transmission and its relationship to long-term potentiation. *Trends Neurosci.* **16**, 480–487

Asnaghi L., Bruno P., Priulla M. and Nicolin A. (2004) mTOR: a protein kinase switching between life and death. *Pharmacol Res* **50,** 545-549.

Athos J., Impey S., Pineda V. V., Chen X. and Storm D. R. (2002) Hippocampal CRE-mediated gene expression is required for contextual memory formation. *Nat Neurosci* **5,** 1119-1120.

Bache, K. G., Raiborg, C., Mehlum, A. and Stenmark, H. (2003) STAM and Hrs are subunits of a multivalent ubiquitin-binding complex on early endosomes. *J Biol Chem,* **278,** 12513-12521.

Baer K., Essrich C., Benson J. A., Benke D., Bluethmann H., Fritschy J. M. and Luscher B. (1999) Postsynaptic clustering of gamma-aminobutyric acid type A receptors by the gamma3 subunit in vivo. *Proc Natl Acad Sci U S A* **96,** 12860-12865.

Bagni C., Mannucci L., Dotti C. G. and Amaldi F. (2000) Chemical stimulation of synaptosomes modulates alpha -Ca2+/calmodulin-dependent protein kinase II mRNA association to polysomes. *J Neurosci* **20,** RC76.

Bahouth, S. W., Beauchamp, M. J. and Vu, K. N. (2002) Reciprocal regulation of beta(1)-adrenergic receptor gene transcription by Sp1 and early growth response gene 1: induction of EGR-1 inhibits the expression of the beta(1)-adrenergic receptor gene. *Mol Pharmacol,* **61,** 379-390.

Baimbridge K. G. and Miller J. J. (1981) Calcium uptake and retention during long-term potentiation of neuronal activity in the rat hippocampal slice preparation. *Brain Res* **221,** 299-305.

Bamford, N. S., Zhang, H., Schmitz, Y. et al. (2004) Heterosynaptic dopamine neurotransmission selects sets of corticostriatal terminals. *Neuron,* **42,** 653-663.

Barnes C. A., Jung M. W., McNaughton B. L., Korol D. L., Andreasson K. and Worley P. F. (1994) LTP saturation and spatial learning disruption: effects of task variables and saturation levels. *J Neurosci* **14,** 5793-5806.

Barnes E. M., Jr. (2000) Intracellular trafficking of GABA(A) receptors. *Life Sci* **66,** 1063-1070.

Barria, A., Derkach, V. and Soderling, T. (1997a) Identification of the Ca2+/calmodulin-dependent protein kinase II regulatory phosphorylation site in the alpha-amino-3-hydroxyl-5-methyl-4-isoxazole-propionate-type glutamate receptor. *J Biol Chem,* **272,** 32727-32730.

Barria, A., Muller, D., Derkach, V., Griffith, L. C. and Soderling, T. R. (1997b) Regulatory phosphorylation of AMPA-type glutamate receptors by CaM-KII during long-term potentiation. *Science,* **276,** 2042-2045.

Barrionuevo G., Schottler F., Lynch G. (1980) The effects of repetitive low frequency stimulation on control and "potentiated" synaptic responses in the hippocampus. *Life Sci*. **15**;27(24):2385-91

Basarsky T. A., Parpura V. and Haydon P. G. (1994) Hippocampal synaptogenesis in cell culture: developmental time course of synapse formation, calcium influx, and synaptic protein distribution. *J Neurosci* **14,** 6402-6411.

Bausen M., Fuhrmann J. C., Betz H. and O'Sullivan G A. (2006) The state of the actin cytoskeleton determines its association with gephyrin: role of ena/VASP family members. *Mol Cell Neurosci* **31,** 376-386.

Bayer K. U., De Koninck P., Leonard A. S., Hell J. W. and Schulman H. (2001) Interaction with the NMDA receptor locks CaMKII in an active conformation. *Nature* **411,** 801-805.

Bear J. E., Svitkina T. M., Krause M., Schafer D. A., Loureiro J. J., Strasser G. A., Maly I. V., Chaga O. Y., Cooper J. A., Borisy G. G. and Gertler F. B. (2002) Antagonism between Ena/VASP proteins and actin filament capping regulates fibroblast motility. *Cell* **109,** 509-521.

Bear M. F. (1996) A synaptic basis for memory storage in the cerebral cortex. *Proc Natl Acad Sci U S A* **93,** 13453-13459.

Bear M. F. and Abraham W. C. (1996) Long-term depression in hippocampus. *Annu Rev Neurosci* **19,** 437-462.

Bechade C., Colin I., Kirsch J., Betz H. and Triller A. (1996) Expression of glycine receptor alpha subunits and gephyrin in cultured spinal neurons. *Eur J Neurosci* **8,** 429-435.

Becker A. J., Chen J., Zien A., Sochivko D., Normann S., Schramm J., Elger C. E., Wiestler O. D. and Blumcke I. (2003) Correlated stage- and subfield-associated hippocampal gene expression patterns in experimental and human temporal lobe epilepsy. *Eur J Neurosci* **18,** 2792-2802.

Beckmann A. M., Davidson M. S., Goodenough S. and Wilce P. A. (1997) Differential expression of Egr-1-like DNA-binding activities in the naive rat brain and after excitatory stimulation. *J Neurochem* **69,** 2227-2237.

Bedet C., Bruusgaard J. C., Vergo S., Groth-Pedersen L., Eimer S., Triller A. and Vannier C. (2006) Regulation of gephyrin assembly and glycine receptor synaptic stability. *J Biol Chem* **281,** 30046-30056.

Bedford F. K., Kittler J. T., Muller E., Thomas P., Uren J. M., Merlo D., Wisden W., Triller A., Smart T. G. and Moss S. J. (2001) GABA(A) receptor cell surface number and subunit stability are regulated by the ubiquitin-like protein Plic-1. *Nat Neurosci* **4,** 908-916.

Benmerah, A., Gagnon, J., Begue, B., Megarbane, B., Dautry-Varsat, A. and Cerf-Bensussan, N. (1995) The tyrosine kinase substrate eps15 is constitutively associated with the plasma membrane adaptor AP-2. *J Cell Biol,* **131,** 1831-1838.

Bensemain F., Chapuis J., Tian J., Shi J., Thaker U., Lendon C., Iwatsubo T., Amouyel P., Mann D. and Lambert J. C. (2006) Association study of the Ubiquilin gene with Alzheimer's disease. *Neurobiol Dis* **22,** 691-693.

Bertram, L., Hiltunen, M., Parkinson, M. et al. (2005) Family-based association between Alzheimer's disease and variants in UBQLN1. *N Engl J Med,* **352,** 884-894.

Betz H. (1998) Gephyrin, a major player in GABAergic postsynaptic membrane assembly? *Nat Neurosci* **1,** 541-543.

Biggins, S., Ivanovska, I. and Rose, M. D. (1996) Yeast ubiquitin-like genes are involved in duplication of the microtubule organizing center. *J Cell Biol,* **133,** 1331-1346.

Bingol B. and Schuman E. M. (2004) A proteasome-sensitive connection between PSD-95 and GluR1 endocytosis. *Neuropharmacology* **47,** 755-763.

Bingol B. and Schuman E. M. (2006) Activity-dependent dynamics and sequestration of proteasomes in dendritic spines. *Nature* **441,** 1144-1148.

Bito H., Deisseroth K. and Tsien R. W. (1996) CREB phosphorylation and dephosphorylation: a Ca(2+)- and stimulus duration-dependent switch for hippocampal gene expression. *Cell* **87,** 1203-1214.

Blalock, E. M., Chen, K. C., Sharrow, K., Herman, J. P., Porter, N. M., Foster, T. C. and Landfield, P. W. (2003) Gene microarrays in hippocampal aging: statistical profiling identifies novel processes correlated with cognitive impairment. *J Neurosci,* **23,** 3807-3819.

Blendy J. A., Schmid W., Kiessling M., Schutz G. and Gass P. (1995) Effects of kainic acid induced seizures on immediate early gene expression in mice with a targeted mutation of the CREB gene. *Brain Res* **681,** 8-14.

Bliss T. V. and Lomo T. (1973) Long-lasting potentiation of synaptic transmission in the dentate area of the anaesthetized rabbit following stimulation of the perforant path. *J Physiol* **232,** 331-356.

Bliss T. V. and Collingridge G. L. (1993) A synaptic model of memory: long-term potentiation in the hippocampus. *Nature* **361,** 31-39.

Blitzer, R. D., Connor, J. H., Brown, G. P., Wong, T., Shenolikar, S., Iyengar, R. and Landau, E. M. (1998) Gating of CaMKII by cAMP-regulated protein phosphatase activity during LTP. *Science,* **280,** 1940-1942.

Blitzer R. D., Wong T., Nouranifar R., Iyengar R. and Landau E. M. (1995) Postsynaptic cAMP pathway gates early LTP in hippocampal CA1 region. *Neuron* **15,** 1403-1414.

Boehmer, C., Embark, H. M., Bauer, A. et al. (2004) Stimulation of renal Na+ dicarboxylate cotransporter 1 by Na+/H+ exchanger regulating factor 2, serum and glucocorticoid inducible kinase isoforms, and protein kinase B. *Biochem Biophys Res Commun,* **313,** 998-1003.

Boehmer, C., Henke, G., Schniepp, R., Palmada, M., Rothstein, J. D., Broer, S. and Lang, F. (2003) Regulation of the glutamate transporter EAAT1 by the ubiquitin ligase Nedd4-2 and the serum and glucocorticoid-inducible kinase isoforms SGK1/3 and protein kinase B. *J Neurochem,* **86,** 1181-1188.

Bolshakov V. Y. and Siegelbaum S. A. (1994) Postsynaptic induction and presynaptic expression of hippocampal long-term depression. *Science* **264,** 1148-1152.

Bond B. C., Virley D. J., Cairns N. J., Hunter A. J., Moore G. B., Moss S. J., Mudge A. W., Walsh F. S., Jazin E. and Preece P. (2002) The quantification of gene expression in an animal model of brain ischaemia using TaqMan real-time RT-PCR. *Brain Res Mol Brain Res* **106,** 101-116.

Bonnert T. P., McKernan R. M., Farrar S., le Bourdelles B., Heavens R. P., Smith D. W., Hewson L., Rigby M. R., Sirinathsinghji D. J., Brown N., Wafford K. A. and Whiting P. J. (1999) theta, a novel gamma-aminobutyric acid type A receptor subunit. *Proc Natl Acad Sci U S A* **96,** 9891-9896.

Boulton, T. G., Nye, S. H., Robbins, D. J. et al. (1991) ERKs: a family of protein-serine/threonine kinases that are activated and tyrosine phosphorylated in response to insulin and NGF. *Cell,* **65,** 663-675.

Bourtchuladze R., Frenguelli B., Blendy J., Cioffi D., Schutz G. and Silva A. J. (1994) Deficient long-term memory in mice with a targeted mutation of the cAMP-responsive element-binding protein. *Cell* **79,** 59-68.

Bradford M. M. (1976) A rapid and sensitive method for the quantitation of microgram quantities of protein utilizing the principle of protein-dye binding. *Anal Biochem* **72,** 248-254.

Bradshaw K. D., Emptage N. J. and Bliss T. V. (2003) A role for dendritic protein synthesis in hippocampal late LTP. *Eur J Neurosci* **18,** 3150-3152.

Brambilla R., Gnesutta N., Minichiello L., White G., Roylance A. J., Herron C. E., Ramsey M., Wolfer D. P., Cestari V., Rossi-Arnaud C., Grant S. G., Chapman P. F., Lipp H. P., Sturani E. and Klein R. (1997) A role for the Ras signalling pathway in synaptic transmission and long-term memory. *Nature* **390,** 281-286.

Braun B. C., Glickman M., Kraft R., Dahlmann B., Kloetzel P. M., Finley D. and Schmidt M. (1999) The base of the proteasome regulatory particle exhibits chaperone-like activity. *Nat Cell Biol* **1,** 221-226.

Brennan P. A., Hancock D. and Keverne E. B. (1992) The expression of the immediate-early genes c-fos, egr-1 and c-jun in the accessory olfactory bulb during the formation of an olfactory memory in mice. *Neuroscience* **49,** 277-284.

Brennan P. A., Schellinck H. M. and Keverne E. B. (1999) Patterns of expression of the immediate-early gene egr-1 in the accessory olfactory bulb of female mice exposed to pheromonal constituents of male urine. *Neuroscience* **90,** 1463-1470.

Brickley S. G., Cull-Candy S. G. and Farrant M. (1999) Single-channel properties of synaptic and extrasynaptic GABAA receptors suggest differential targeting of receptor subtypes. *J Neurosci* **19,** 2960-2973.

Broutman G. and Baudry M. (2001) Involvement of the secretory pathway for AMPA receptors in NMDA-induced potentiation in hippocampus. *J Neurosci* **21,** 27-34.

Brouwers N., Sleegers K., Engelborghs S., Bogaerts V., van Duijn C. M., De Deyn P. P., Van Broeckhoven C. and Dermaut B. (2006) The UBQLN1 polymorphism, UBQ-8i, at 9q22 is not associated with Alzheimer's disease with onset before 70 years. *Neurosci Lett* **392,** 72-74.

Brown, E. J., Albers, M. W., Shin, T. B., Ichikawa, K., Keith, C. T., Lane, W. S. and Schreiber, S. L. (1994) A mammalian protein targeted by G1-arresting rapamycin-receptor complex. *Nature,* **369,** 756-758.

Brunig I., Penschuck S., Berninger B., Benson J. and Fritschy J. M. (2001) BDNF reduces miniature inhibitory postsynaptic currents by rapid downregulation of GABA(A) receptor surface expression. *Eur J Neurosci* **13,** 1320-1328.

Brunig I., Suter A., Knuesel I., Luscher B. and Fritschy J. M. (2002) GABAergic terminals are required for postsynaptic clustering of dystrophin but not of GABA(A) receptors and gephyrin. *J Neurosci* **22,** 4805-4813.

Bruning, J. C., Gillette, J. A., Zhao, Y. et al. (2000) Ribosomal subunit kinase-2 is required for growth factor-stimulated transcription of the c-Fos gene. *Proc Natl Acad Sci U S A,* **97,** 2462-2467.

Burge C. and Karlin S. (1997) Prediction of complete gene structures in human genomic DNA. *J Mol Biol* **268,** 78-94.

Brunn, G. J., Hudson, C. C., Sekulic, A., Williams, J. M., Hosoi, H., Houghton, P. J., Lawrence, J. C., Jr. and Abraham, R. T. (1997) Phosphorylation of the translational repressor PHAS-I by the mammalian target of rapamycin. *Science,* **277,** 99-101.

Burbea M., Dreier L., Dittman J. S., Grunwald M. E. and Kaplan J. M. (2002) Ubiquitin and AP180 regulate the abundance of GLR-1 glutamate receptors at postsynaptic elements in C. elegans. *Neuron* **35,** 107-120.

Burnett P. E., Barrow R. K., Cohen N. A., Snyder S. H. and Sabatini D. M. (1998) RAFT1 phosphorylation of the translational regulators p70 S6 kinase and 4E-BP1. *Proc Natl Acad Sci U S A* **95,** 1432-1437.

Burt D. R. (2003) Reducing GABA receptors. *Life Sci* **73,** 1741-1758.

Burt D. R. and Kamatchi G. L. (1991) GABAA receptor subtypes: from pharmacology to molecular biology. *Faseb J* **5,** 2916-2923.

Butler M. H., Hayashi A., Ohkoshi N., Villmann C., Becker C. M., Feng G., De Camilli P. and Solimena M. (2000) Autoimmunity to gephyrin in Stiff-Man syndrome. *Neuron* **26,** 307-312.

Calabresi P., Saiardi A., Pisani A., Baik J. H., Centonze D., Mercuri N. B., Bernardi G. and Borrelli E. (1997) Abnormal synaptic plasticity in the striatum of mice lacking dopamine D2 receptors. *J Neurosci* **17,** 4536-4544.

Cammalleri M., Lutjens R., Berton F., King A. R., Simpson C., Francesconi W. and Sanna P. P. (2003) Time-restricted role for dendritic activation of the mTOR-p70S6K pathway in the induction of late-phase long-term potentiation in the CA1. *Proc Natl Acad Sci U S A* **100,** 14368-14373.

Casadio, A., Martin, K. C., Giustetto, M., Zhu, H., Chen, M., Bartsch, D., Bailey, C. H. and Kandel, E. R. (1999) A transient, neuron-wide form of CREB-mediated long-term facilitation can be stabilized at specific synapses by local protein synthesis. *Cell,* **99,** 221-237.

Cascio, P., Call, M., Petre, B. M., Walz, T. and Goldberg, A. L. (2002) Properties of the hybrid form of the 26S proteasome containing both 19S and PA28 complexes. *Embo J,* **21,** 2636-2645.

Castro-Alamancos M. A., Donoghue J. P. and Connors B. W. (1995) Different forms of synaptic plasticity in somatosensory and motor areas of the neocortex. *J Neurosci* **15,** 5324-5333.

Centonze D., Usiello A., Costa C., Picconi B., Erbs E., Bernardi G., Borrelli E. and Calabresi P. (2004) Chronic haloperidol promotes corticostriatal long-term potentiation by targeting dopamine D2L receptors. *J Neurosci* **24,** 8214-8222.

Cepeda C., Buchwald N. A. and Levine M. S. (1993) Neuromodulatory actions of dopamine in the neostriatum are dependent upon the excitatory amino acid receptor subtypes activated. *Proc Natl Acad Sci U S A* **90,** 9576-9580.

Cepeda C., Hurst R. S., Altemus K. L., Flores-Hernandez J., Calvert C. R., Jokel E. S., Grandy D. K., Low M. J., Rubinstein M., Ariano M. A. and Levine M. S. (2001) Facilitated glutamatergic transmission in the striatum of D2 dopamine receptor-deficient mice. *J Neurophysiol* **85,** 659-670.

Chain D. G., Schwartz J. H. and Hegde A. N. (1999) Ubiquitin-mediated proteolysis in learning and memory. *Mol Neurobiol* **20,** 125-142.

Chandler L. J., Sutton G., Dorairaj N. R. and Norwood D. (2001) N-methyl D-aspartate receptor-mediated bidirectional control of extracellular signal-regulated kinase activity in cortical neuronal cultures. *J Biol Chem* **276,** 2627-2636.

Chang Y., Wang R., Barot S. and Weiss D. S. (1996) Stoichiometry of a recombinant GABAA receptor. *J Neurosci* **16,** 5415-5424.

Chapell R., Bueno O. F., Alvarez-Hernandez X., Robinson L. C. and Leidenheimer N. J. (1998) Activation of protein kinase C induces gamma-aminobutyric acid type A receptor internalization in Xenopus oocytes. *J Biol Chem* **273,** 32595-32601.

Chapman N. R. and Perkins N. D. (2000) Inhibition of the RelA(p65) NF-kappaB subunit by Egr-1. *J Biol Chem* **275,** 4719-4725.

Charpier S. and Deniau J. M. (1997) In vivo activity-dependent plasticity at cortico-striatal connections: evidence for physiological long-term potentiation. *Proc Natl Acad Sci U S A* **94,** 7036-7040.

Charrier C., Ehrensperger M. V., Dahan M., Levi S. and Triller A. (2006) Cytoskeleton regulation of glycine receptor number at synapses and diffusion in the plasma membrane. *J Neurosci* **26,** 8502-8511.

Chen W. R., Lee S., Kato K., Spencer D. D., Shepherd G. M. and Williamson A. (1996) Long-term modifications of synaptic efficacy in the human inferior and middle temporal cortex. *Proc Natl Acad Sci U S A* **93,** 8011-8015.

Cherubini E. and Conti F. (2001) Generating diversity at GABAergic synapses. *Trends Neurosci* **24,** 155-162.

Chetkovich D. M., Gray R., Johnston D. and Sweatt J. D. (1991) N-methyl-D-aspartate receptor activation increases cAMP levels and voltage-gated Ca2+ channel activity in area CA1 of hippocampus. *Proc Natl Acad Sci U S A* **88,** 6467-6471.

Chetkovich, D. M. and Sweatt, J. D. (1993) nMDA receptor activation increases cyclic AMP in area CA1 of the hippocampus via calcium/calmodulin stimulation of adenylyl cyclase. *J Neurochem,* **61,** 1933-1942.

Chhatwal J. P., Myers K. M., Ressler K. J. and Davis M. (2005) Regulation of gephyrin and GABAA receptor binding within the amygdala after fear acquisition and extinction. *J Neurosci* **25,** 502-506.

Chitayat D., McGillivray B. C., Wood S., Kalousek D. K., Langlois S. and Applegarth D. A. (1988) Interstitial 7q deletion [46,XX,del(7)(pter----q21.1::q22----qter)] and the location of genes for beta-glucuronidase and cystic fibrosis. *Am J Med Genet* **31,** 655-661.

Chiu, M. I., Katz, H. and Berlin, V. (1994) RAPT1, a mammalian homolog of yeast Tor, interacts with the FKBP12/rapamycin complex. *Proc Natl Acad Sci U S A,* **91,** 12574-12578.

Chong, J. A., Tapia-Ramirez, J., Kim, S. et al. (1995) REST: a mammalian silencer protein that restricts sodium channel gene expression to neurons. *Cell,* **80,** 949-957.

Choquet D. and Triller A. (2003) The role of receptor diffusion in the organization of the postsynaptic membrane. *Nat Rev Neurosci* **4,** 251-265.

Chowdhary R., Ali R. A., Albig W., Doenecke D. and Bajic V. B. (2005) Promoter modeling: the case study of mammalian histone promoters. *Bioinformatics* **21,** 2623-2628.

Christie S. B., Miralles C. P. and De Blas A. L. (2002) GABAergic innervation organizes synaptic and extrasynaptic GABAA receptor clustering in cultured hippocampal neurons. *J Neurosci* **22,** 684-697.

Christy, B. and Nathans, D. (1989) DNA binding site of the growth factor-inducible protein Zif268. *Proc Natl Acad Sci U S A,* **86,** 8737-8741.

Christy B. A., Lau L. F. and Nathans D. (1988) A gene activated in mouse 3T3 cells by serum growth factors encodes a protein with "zinc finger" sequences. *Proc Natl Acad Sci U S A* **85,** 7857-7861.

Ciechanover A. and Schwartz A. L. (1998) The ubiquitin-proteasome pathway: the complexity and myriad functions of proteins death. *Proc Natl Acad Sci U S A* **95,** 2727-2730.

Cinar H. and Barnes E. M., Jr. (2001) Clathrin-independent endocytosis of GABA(A) receptors in HEK 293 cells. *Biochemistry* **40,** 14030-14036.

Cochran S. M., McKerchar C. E., Morris B. J. and Pratt J. A. (2002) Induction of differential patterns of local cerebral glucose metabolism and immediate-early genes by acute clozapine and haloperidol. *Neuropharmacology* **43,** 394-407.

Cole A. J., Saffen D. W., Baraban J. M. and Worley P. F. (1989) Rapid increase of an immediate early gene messenger RNA in hippocampal neurons by synaptic NMDA receptor activation. *Nature* **340,** 474-476.

Colin I., Rostaing P. and Triller A. (1996) Gephyrin accumulates at specific plasmalemma loci during neuronal maturation in vitro. *J Comp Neurol* **374,** 467-479.

Colin I., Rostaing P., Augustin A. and Triller A. (1998) Localization of components of glycinergic synapses during rat spinal cord development. *J Comp Neurol* **398,** 359-372.

Colledge, M., Snyder, E. M., Crozier, R. A., Soderling, J. A., Jin, Y., Langeberg, L. K., Lu, H., Bear, M. F. and Scott, J. D. (2003) Ubiquitination regulates PSD-95 degradation and AMPA receptor surface expression. *Neuron,* **40,** 595-607.

Collingridge G. L., Kehl S. J. and McLennan H. (1983) The antagonism of amino acid-induced excitations of rat hippocampal CA1 neurones in vitro. *J Physiol* **334,** 19-31.

Collingridge G. L., Herron C. E. and Lester R. A. (1988) Frequency-dependent N-methyl-D-aspartate receptor-mediated synaptic transmission in rat hippocampus. *J Physiol* **399,** 301-312.

Condorelli, D. F., Dell'Albani, P., Amico, C., Lukasiuk, K., Kaczmarek, L. and Giuffrida-Stella, A. M. (1994) Glutamate receptor-driven activation of transcription factors in primary neuronal cultures. *Neurochem Res,* **19,** 489-499.

Conklin, D., Holderman, S., Whitmore, T. E., Maurer, M. and Feldhaus, A. L. (2000) Molecular cloning, chromosome mapping and characterization of UBQLN3 a testis-specific gene that contains an ubiquitin-like domain. *Gene,* **249,** 91-98.

Connolly C. N., Wooltorton J. R., Smart T. G. and Moss S. J. (1996a) Subcellular localization of gamma-aminobutyric acid type A receptors is determined by receptor beta subunits. *Proc Natl Acad Sci U S A* **93,** 9899-9904.

Connolly C. N., Krishek B. J., McDonald B. J., Smart T. G. and Moss S. J. (1996b) Assembly and cell surface expression of heteromeric and homomeric gamma-aminobutyric acid type A receptors. *J Biol Chem* **271,** 89-96.

Connolly C. N., Uren J. M., Thomas P., Gorrie G. H., Gibson A., Smart T. G. and Moss S. J. (1999a) Subcellular localization and endocytosis of homomeric gamma2 subunit splice variants of gamma-aminobutyric acid type A receptors. *Mol Cell Neurosci* **13,** 259-271.

Connolly C. N., Kittler J. T., Thomas P., Uren J. M., Brandon N. J., Smart T. G. and Moss S. J. (1999b) Cell surface stability of gamma-aminobutyric acid type A receptors. Dependence on protein kinase C activity and subunit composition. *J Biol Chem* **274,** 36565-36572.

Conti F., Minelli A., DeBiasi S. and Melone M. (1997) Neuronal and glial localization of NMDA receptors in the cerebral cortex. *Mol Neurobiol* **14,** 1-18.

Coogan, A. N., O'Leary, D. M. and O'Connor, J. J. (1999) P42/44 MAP kinase inhibitor PD98059 attenuates multiple forms of synaptic plasticity in rat dentate gyrus in vitro. *J Neurophysiol,* **81,** 103-110.

Cossart, R., Dinocourt, C., Hirsch, J. C., Merchan-Perez, A., De Felipe, J., Ben-Ari, Y., Esclapez, M. and Bernard, C. (2001) Dendritic but not somatic GABAergic inhibition is decreased in experimental epilepsy. *Nat Neurosci,* **4,** 52-62.

Craig A. M., Banker G., Chang W., McGrath M. E. and Serpinskaya A. S. (1996) Clustering of gephyrin at GABAergic but not glutamatergic synapses in cultured rat hippocampal neurons. *J Neurosci* **16,** 3166-3177.

Crosby S. D., Puetz J. J., Simburger K. S., Fahrner T. J. and Milbrandt J. (1991) The early response gene NGFI-C encodes a zinc finger transcriptional activator and is a member of the GCGGGGGCG (GSG) element-binding protein family. *Mol Cell Biol* **11,** 3835-3841.

Crosby S. D., Veile R. A., Donis-Keller H., Baraban J. M., Bhat R. V., Simburger K. S. and Milbrandt J. (1992) Neural-specific expression, genomic structure, and chromosomal localization of the gene encoding the zinc-finger transcription factor NGFI-C. *Proc Natl Acad Sci U S A* **89,** 4739-4743.

D'Andrea A. and Pellman D. (1998) Deubiquitinating enzymes: a new class of biological regulators. *Crit Rev Biochem Mol Biol* **33,** 337-352.

Dahan M., Levi S., Luccardini C., Rostaing P., Riveau B. and Triller A. (2003) Diffusion dynamics of glycine receptors revealed by single-quantum dot tracking. *Science* **302,** 442-445.

Dalby B., Cates S., Harris A., Ohki E. C., Tilkins M. L., Price P. J. and Ciccarone V. C. (2004) Advanced transfection with Lipofectamine 2000 reagent: primary neurons, siRNA , and high throughput applications. *Methods* **33**, 95-103

Dale N., Schacher S. and Kandel E. R. (1988) Long-term facilitation in Aplysia involves increase in transmitter release. *Science* **239,** 282-285.

Danglot, L., Triller, A. and Bessis, A. (2003) Association of gephyrin with synaptic and extrasynaptic GABAA receptors varies during development in cultured hippocampal neurons. *Mol Cell Neurosci,* **23,** 264-278.

Darsow T., Booker T. K., Pina-Crespo J. C. and Heinemann S. F. (2005) Exocytic trafficking is required for nicotine-induced up-regulation of alpha 4 beta 2 nicotinic acetylcholine receptors. *J Biol Chem* **280,** 18311-18320.

Dash P. K., Karl K. A., Colicos M. A., Prywes R. and Kandel E. R. (1991) cAMP response element-binding protein is activated by Ca2+/calmodulin- as well as cAMP-dependent protein kinase. *Proc Natl Acad Sci U S A* **88,** 5061-5065.

Davidson, J. D., Riley, B., Burright, E. N., Duvick, L. A., Zoghbi, H. Y. and Orr, H. T. (2000) Identification and characterization of an ataxin-1-interacting protein: A1Up, a ubiquitin-like nuclear protein. *Hum Mol Genet,* **9,** 2305-2312.

Davis H. P. and Squire L. R. (1984) Protein synthesis and memory: a review. *Psychol Bull* **96,** 518-559.

Davis S., Bozon B. and Laroche S. (2003) How necessary is the activation of the immediate early gene zif268 in synaptic plasticity and learning? *Behav Brain Res* **142,** 17-30.

Davis, S., Vanhoutte, P., Pages, C., Caboche, J. and Laroche, S. (2000) The MAPK/ERK cascade targets both Elk-1 and cAMP response element-binding protein to control long-term potentiation-dependent gene expression in the dentate gyrus in vivo. *J Neurosci,* **20,** 4563-4572.

Davis, W., Jr., Chen, Z. J., Ile, K. E. and Tew, K. D. (2003) Reciprocal regulation of expression of the human adenosine 5'-triphosphate binding cassette, sub-family A, transporter 2 (ABCA2) promoter by the early growth response-1 (EGR-1) and Sp-family transcription factors. *Nucleic Acids Res,* **31,** 1097-1107.

Davy A., Bello P., Thierry-Mieg N., Vaglio P., Hitti J., Doucette-Stamm L., Thierry-Mieg D., Reboul J., Boulton S., Walhout A. J. M., Coux O. and Vidal M. (2001) A protein-protein interaction map of the Caenorhabditis elegans 26S proteasome. *Embo Reports* **2,** 821-828.

Daw E. W., Payami H., Nemens E. J., Nochlin D., Bird T. D., Schellenberg G. D. and Wijsman E. M. (2000) The number of trait loci in late-onset Alzheimer disease. *Am J Hum Genet* **66,** 196-204.

Day M. L., Fahrner T. J., Aykent S. and Milbrandt J. (1990) The zinc finger protein NGFI-A exists in both nuclear and cytoplasmic forms in nerve growth factor-stimulated PC12 cells. *J Biol Chem* **265,** 15253-15260.

de Melker, A. A., van der Horst, G. and Borst, J. (2004) c-Cbl directs EGF receptors into an endocytic pathway that involves the ubiquitin-interacting motif of Eps15. *J Cell Sci,* **117,** 5001-5012.

De Strooper B. (2003) Aph-1, Pen-2, and Nicastrin with Presenilin generate an active gamma-Secretase complex. *Neuron* **38,** 9-12.

Deadwyler S. A., Dunwiddie T. and Lynch G. (1987) A critical level of protein synthesis is required for long-term potentiation. *Synapse* **1,** 90-95.

Deak, M., Clifton, A. D., Lucocq, L. M. and Alessi, D. R. (1998) Mitogen- and stress-activated protein kinase-1 (MSK1) is directly activated by MAPK and SAPK2/p38, and may mediate activation of CREB. *Embo J,* **17,** 4426-4441.

Decker, E. L., Nehmann, N., Kampen, E., Eibel, H., Zipfel, P. F. and Skerka, C. (2003) Early growth response proteins (EGR) and nuclear factors of activated T cells (NFAT) form heterodimers and regulate proinflammatory cytokine gene expression. *Nucleic Acids Res,* **31,** 911-921.

Derkach V., Barria A. and Soderling T. R. (1999) Ca2+/calmodulin-kinase II enhances channel conductance of alpha-amino-3-hydroxy-5-methyl-4-isoxazolepropionate type glutamate receptors. *Proc Natl Acad Sci U S A* **96,** 3269-3274.

Deutsch M. and Long M. (1999) Intron-exon structures of eukaryotic model organisms. *Nucleic Acids Res* **27,** 3219-3228.

Deveraux Q., van Nocker S., Mahaffey D., Vierstra R. and Rechsteiner M. (1995) Inhibition of Ubiquitin-mediated Proteolysis by the Arabidopsis 26 S Protease Subunit S5a. *J. Biol. Chem.* **270,** 29660-29663.

Di Cristo, G., Berardi, N., Cancedda, L., Pizzorusso, T., Putignano, E., Ratto, G. M. and Maffei, L. (2001) Requirement of ERK activation for visual cortical plasticity. *Science,* **292,** 2337-2340.

Dickey C. A., Loring J. F., Montgomery J., Gordon M. N., Eastman P. S. and Morgan D. (2003) Selectively reduced expression of synaptic plasticity-related genes in amyloid precursor protein + presenilin-1 transgenic mice. *J Neurosci* **23,** 5219-5226.

Dickey C. A., Gordon M. N., Mason J. E., Wilson N. J., Diamond D. M., Guzowski J. F. and Morgan D. (2004) Amyloid suppresses induction of genes critical for memory consolidation in APP + PS1 transgenic mice. *J Neurochem* **88,** 434-442.

Ding Q. and Keller J. N. (2001) Proteasomes and proteasome inhibition in the central nervous system. *Free Radic Biol Med* **31,** 574-584.

Doble A. (1995) Excitatory amino acid receptors and neurodegeneration. *Therapie* **50,** 319-337.

Doi H., Mitsui K., Kurosawa M., Machida Y., Kuroiwa Y. and Nukina N. (2004) Identification of ubiquitin-interacting proteins in purified polyglutamine aggregates. *FEBS Lett* **571,** 171-176.

Dolphin A. C., Errington M. L. and Bliss T. V. (1982) Long-term potentiation of the perforant path in vivo is associated with increased glutamate release. *Nature* **297,** 496-498.

Donaldson, K. M., Li, W., Ching, K. A., Batalov, S., Tsai, C. C. and Joazeiro, C. A. (2003) Ubiquitin-mediated sequestration of normal cellular proteins into polyglutamine aggregates. *Proc Natl Acad Sci U S A,* **100,** 8892-8897.

Drapeau C., Pellerin L., Wolfe L. S. and Avoli M. (1990) Long-term changes of synaptic transmission induced by arachidonic acid in the CA1 subfield of the rat hippocampus. *Neurosci Lett* **115,** 286-292.

Dudek, S. M. and Bear, M. F. (1992) Homosynaptic long-term depression in area CA1 of hippocampus and effects of N-methyl-D-aspartate receptor blockade. *Proc. Natl Acad. Sci.USA* **89**, 4363--4367

Duffy C., Teyler T. J. and Shashoua V. E. (1981) Long-term potentiation in the hippocampal slice: evidence for stimulated secretion of newly synthesized proteins. *Science* **212,** 1148-1151.

Dumoulin, A., Triller, A. and Dieudonne, S. (2001) IPSC kinetics at identified GABAergic and mixed GABAergic and glycinergic synapses onto cerebellar Golgi cells. *J Neurosci,* **21,** 6045-6057.

Dunwiddie T. V. and Lynch G. (1979) The relationship between extracellular calcium concentrations and the induction of hippocampal long-term potentiation. *Brain Res* **169,** 103-110.

Dynan W. S., Sazer S., Tjian R. and Schimke R. T. (1986) Transcription factor Sp1 recognizes a DNA sequence in the mouse dihydrofolate reductase promoter. *Nature* **319,** 246-248.

Edbauer, D., Winkler, E., Regula, J. T., Pesold, B., Steiner, H. and Haass, C. (2003) Reconstitution of gamma-secretase activity. *Nat Cell Biol,* **5,** 486-488.

Edeline J. M., Pham P. and Weinberger N. M. (1993) Rapid development of learning-induced receptive field plasticity in the auditory cortex. *Behav Neurosci* **107,** 539-551.

Ehlers M. D. (2003) Activity level controls postsynaptic composition and signaling via the ubiquitin-proteasome system. *Nat Neurosci* **6,** 231-242.

Ehrengruber, M. U., Muhlebach, S. G., Sohrman, S., Leutenegger, C. M., Lester, H. A. and Davidson, N. (2000) Modulation of early growth response (EGR) transcription factor-dependent gene expression by using recombinant adenovirus. *Gene,* **258,** 63-69.

Ekerot C.F. and Kano M. (1985) Long-term depression of parallel fibre synapses following stimulation of climbing fibres. *Brain Res* **342**(2):357-60

El-Khodor, B. F., Kholodilov, N. G., Yarygina, O. and Burke, R. E. (2001) The expression of mRNAs for the proteasome complex is developmentally regulated in the rat mesencephalon. *Brain Res Dev Brain Res,* **129,** 47-56.

English J. D. and Sweatt J. D. (1996) Activation of p42 mitogen-activated protein kinase in hippocampal long term potentiation. *J Biol Chem* **271,** 24329-24332.

Esler, W. P., Kimberly, W. T., Ostaszewski, B. L. et al. (2000) Transition-state analogue inhibitors of gamma-secretase bind directly to presenilin-1. *Nat Cell Biol,* **2,** 428-434.

Essrich C., Lorez M., Benson J. A., Fritschy J. M. and Luscher B. (1998) Postsynaptic clustering of major GABAA receptor subtypes requires the gamma 2 subunit and gephyrin. *Nat Neurosci* **1,** 563-571.

Fanselow M. S. and Gale G. D. (2003) The amygdala, fear, and memory. *Ann N Y Acad Sci* **985,** 125-134.

Farrar S. J., Whiting P. J., Bonnert T. P. and McKernan R. M. (1999) Stoichiometry of a ligand-gated ion channel determined by fluorescence energy transfer. *J Biol Chem* **274,** 10100-10104.

Farrer L. A., Cupples L. A., Haines J. L., Hyman B., Kukull W. A., Mayeux R., Myers R. H., Pericak-Vance M. A., Risch N. and van Duijn C. M. (1997) Effects of age, sex, and ethnicity on the association between apolipoprotein E genotype and Alzheimer disease. A meta-analysis. APOE and Alzheimer Disease Meta Analysis Consortium. *Jama* **278,** 1349-1356.

Fazeli M. S., Corbet J., Dunn M. J., Dolphin A. C. and Bliss T. V. (1993) Changes in protein synthesis accompanying long-term potentiation in the dentate gyrus in vivo. *J Neurosci* **13,** 1346-1353.

Feng G., Tintrup H., Kirsch J., Nichol M. C., Kuhse J., Betz H. and Sanes J. R. (1998) Dual requirement for gephyrin in glycine receptor clustering and molybdoenzyme activity. *Science* **282,** 1321-1324.

Ferrell K., Wilkinson C. R., Dubiel W. and Gordon C. (2000) Regulatory subunit interactions of the 26S proteasome, a complex problem. *Trends Biochem Sci* **25,** 83-88.

Fickett J. W. and Hatzigeorgiou A. G. (1997) Eukaryotic promoter recognition. *Genome Res* **7,** 861-878.

Ficklin M. B., Zhao S. and Feng G. (2005) Ubiquilin-1 regulates nicotine-induced up-regulation of neuronal nicotinic acetylcholine receptors. *J Biol Chem* **280,** 34088-34095.

Fifkova E. and Van Harreveld A. (1977) Long-lasting morphological changes in dendritic spines of dentate granular cells following stimulation of the entorhinal area. *J Neurocytol* **6,** 211-230.

Fiore, R. S., Bayer, V. E., Pelech, S. L., Posada, J., Cooper, J. A. and Baraban, J. M. (1993a) p42 mitogen-activated protein kinase in brain: prominent localization in neuronal cell bodies and dendrites. *Neuroscience,* **55,** 463-472.

Fiore, R. S., Murphy, T. H., Sanghera, J. S., Pelech, S. L. and Baraban, J. M. (1993b) Activation of p42 mitogen-activated protein kinase by glutamate receptor stimulation in rat primary cortical cultures. *J Neurochem,* **61,** 1626-1633.

Foley A. G., Hartz B. P., Gallagher H. C., Ronn L. C., Berezin V., Bock E. and Regan C. M. (2000) A synthetic peptide ligand of neural cell adhesion molecule (NCAM) IgI domain prevents NCAM internalization and disrupts passive avoidance learning. *J Neurochem* **74,** 2607-2613.

Fordyce D. E. and Wehner J. M. (1993) Physical activity enhances spatial learning performance with an associated alteration in hippocampal protein kinase C activity in C57BL/6 and DBA/2 mice. *Brain Res* **619,** 111-119.

Fordyce D. E., Bhat R. V., Baraban J. M. and Wehner J. M. (1994) Genetic and activity-dependent regulation of zif268 expression: association with spatial learning. *Hippocampus* **4,** 559-568.

Frankland P. W., Cestari V., Filipkowski R. K., McDonald R. J. and Silva A. J. (1998) The dorsal hippocampus is essential for context discrimination but not for contextual conditioning. *Behav Neurosci* **112,** 863-874.

French P. J., O'Connor V., Jones M. W., Davis S., Errington M. L., Voss K., Truchet B., Wotjak C., Stean T., Doyere V., Maroun M., Laroche S. and Bliss T. V. (2001) Subfield-specific immediate early gene expression associated with hippocampal long-term potentiation in vivo. *Eur J Neurosci* **13,** 968-976.

Freund T. F. and Buzsaki G. (1996) Interneurons of the hippocampus. *Hippocampus* **6,** 347-470.

Frey U., Frey S., Schollmeier F. and Krug M. (1996) Influence of actinomycin D, a RNA synthesis inhibitor, on long-term potentiation in rat hippocampal neurons in vivo and in vitro. *J Physiol* **490 (Pt 3),** 703-711.

Frey U., Huang Y. Y. and Kandel E. R. (1993) Effects of cAMP simulate a late stage of LTP in hippocampal CA1 neurons. *Science* **260,** 1661-1664.

Frey, U., Krug, M., Brodemann, R., Reymann, K. and Matthies, H. (1989) Long-term potentiation induced in dendrites separated from rat's CA1 pyramidal somata does not establish a late phase. *Neurosci Lett,* **97,** 135-139.

Frey U., Krug M., Reymann K. G. and Matthies H. (1988) Anisomycin, an inhibitor of protein synthesis, blocks late phases of LTP phenomena in the hippocampal CA1 region in vitro. *Brain Res* **452,** 57-65.

Frey U. and Morris R. G. (1998) Synaptic tagging: implications for late maintenance of hippocampal long-term potentiation. *Trends Neurosci* **21,** 181-188.

Fritschy J. M. and Brunig I. (2003) Formation and plasticity of GABAergic synapses: physiological mechanisms and pathophysiological implications. *Pharmacol Ther* **98,** 299-323.

Fritschy J. M., Johnson D. K., Mohler H. and Rudolph U. (1998) Independent assembly and subcellular targeting of GABA(A)-receptor subtypes

demonstrated in mouse hippocampal and olfactory neurons in vivo. *Neurosci Lett* **249,** 99-102.

Fritschy J. M. and Mohler H. (1995) GABAA-receptor heterogeneity in the adult rat brain: differential regional and cellular distribution of seven major subunits. *J Comp Neurol* **359,** 154-194.

Fritschy J. M., Schweizer C., Brunig I. and Luscher B. (2003) Pre- and post-synaptic mechanisms regulating the clustering of type A gamma-aminobutyric acid receptors (GABAA receptors). *Biochem Soc Trans* **31,** 889-892.

Fu H., Reis N., Lee Y., Glickman M. H. and Vierstra R. D. (2001) Subunit interaction maps for the regulatory particle of the 26S proteasome and the COP9 signalosome. *Embo J* **20,** 7096-7107.

Fuhrmann, J. C., Kins, S., Rostaing, P., El Far, O., Kirsch, J., Sheng, M., Triller, A., Betz, H. and Kneussel, M. (2002) Gephyrin interacts with Dynein light chains 1 and 2, components of motor protein complexes. *J Neurosci,* **22,** 5393-5402.

Fujii, S., Mikoshiba, K., Kuroda, Y., Ahmed, T. M. and Kato, H. (2003) Cooperativity between activation of metabotropic glutamate receptors and NMDA receptors in the induction of LTP in hippocampal CA1 neurons. *Neurosci Res,* **46,** 509-521.

Fukada T. and Tonks N. K. (2001) The reciprocal role of Egr-1 and Sp family proteins in regulation of the PTP1B promoter in response to the p210 Bcr-Abl oncoprotein-tyrosine kinase. *J Biol Chem* **276,** 25512-25519.

Fukunaga K., Muller D. and Miyamoto E. (1996) CaM kinase II in long-term potentiation. *Neurochem Int* **28,** 343-358.

Funakoshi M., Geley S., Hunt T., Nishimoto T. and Kobayashi H. (1999) Identification of XDRP1; a Xenopus protein related to yeast Dsk2p binds to the N-terminus of cyclin A and inhibits its degradation. *Embo J* **18,** 5009-5018.

Funakoshi M., Sasaki T., Nishimoto T. and Kobayashi H. (2002) Budding yeast Dsk2p is a polyubiquitin-binding protein that can interact with the proteasome. *Proc Natl Acad Sci U S A* **99,** 745-750.

Fyhn M., Molden S., Hollup S., Moser M. B. and Moser E. (2002) Hippocampal neurons responding to first-time dislocation of a target object. *Neuron* **35,** 555-566.

Gallagher, M.J., Huang, H. and Lynch, D.R. (1998) Modulation of the N-Methyl-D-Aspartate Receptor by Haloperidol: NR2B-Specific Interactions. *J. Neurochem*. **70**, 2120—2128

Garcia-Mata R., Bebok Z., Sorscher E. J. and Sztul E. S. (1999) Characterization and dynamics of aggresome formation by a cytosolic GFP-chimera. *J Cell Biol* **146,** 1239-1254.

Gashler A. L., Swaminathan S. and Sukhatme V. P. (1993) A novel repression module, an extensive activation domain, and a bipartite nuclear localization signal defined in the immediate-early transcription factor Egr-1. *Mol Cell Biol* **13,** 4556-4571.

Gerfen C. R. and Young W. S., 3rd (1988) Distribution of striatonigral and striatopallidal peptidergic neurons in both patch and matrix compartments: an in situ hybridization histochemistry and fluorescent retrograde tracing study. *Brain Res* **460,** 161-167.

Gerfen C. R., McGinty J. F. and Young W. S., 3rd (1991) Dopamine differentially regulates dynorphin, substance P, and enkephalin expression in striatal neurons: in situ hybridization histochemical analysis. *J Neurosci* **11,** 1016-1031.

Gertler F. B., Niebuhr K., Reinhard M., Wehland J. and Soriano P. (1996) Mena, a relative of VASP and Drosophila Enabled, is implicated in the control of microfilament dynamics. *Cell* **87,** 227-239.

Ghansah E. and Weiss D. S. (2001) Modulation of GABA(A) receptors by benzodiazepines and barbiturates is autonomous of PKC activation. *Neuropharmacology* **40,** 327-333.

Ghosh, A., Ginty, D. D., Bading, H. and Greenberg, M. E. (1994) Calcium regulation of gene expression in neuronal cells. *J Neurobiol,* **25,** 294-303.

Giese K. P., Fedorov N. B., Filipkowski R. K. and Silva A. J. (1998) Autophosphorylation at Thr286 of the alpha calcium-calmodulin kinase II in LTP and learning. *Science* **279,** 870-873.

Giesemann T., Schwarz G., Nawrotzki R., Berhorster K., Rothkegel M., Schluter K., Schrader N., Schindelin H., Mendel R. R., Kirsch J. and Jockusch B. M. (2003) Complex formation between the postsynaptic scaffolding protein gephyrin, profilin, and Mena: a possible link to the microfilament system. *J Neurosci* **23,** 8330-8339.

Gingras A. C., Raught B. and Sonenberg N. (1999) eIF4 initiation factors: effectors of mRNA recruitment to ribosomes and regulators of translation. *Annu Rev Biochem* **68,** 913-963.

Gingras A. C., Raught B. and Sonenberg N. (2001) Regulation of translation initiation by FRAP/mTOR. *Genes Dev* **15,** 807-826.

Giustetto M., Kirsch J., Fritschy J. M., Cantino D. and Sassoe-Pognetto M. (1998) Localization of the clustering protein gephyrin at GABAergic synapses in the main olfactory bulb of the rat. *J Comp Neurol* **395,** 231-244.

Glickman M. H. and Ciechanover A. (2002) The Ubiquitin-Proteasome Proteolytic Pathway: Destruction for the Sake of Construction. *Physiol. Rev.* **82,** 373-428.

Glickman M. H. and Raveh D. (2005) Proteasome plasticity. *FEBS Lett* **579,** 3214-3223.

Glickman M. H., Rubin D. M., Coux O., Wefes I., Pfeifer G., Cjeka Z., Baumeister W., Fried V. A. and Finley D. (1998) A subcomplex of the proteasome regulatory particle required for ubiquitin-conjugate degradation and related to the COP9-signalosome and eIF3. *Cell* **94,** 615-623.

Goelet P., Castellucci V. F., Schacher S. and Kandel E. R. (1986) The long and the short of long-term memory--a molecular framework. *Nature* **322,** 419-422.

Gonzalez G. A. and Montminy M. R. (1989) Cyclic AMP stimulates somatostatin gene transcription by phosphorylation of CREB at serine 133. *Cell* **59,** 675-680.

Gosslar U., Schmid R. M. and Holzmann B. (1999) Regulation of Egr-1-dependent gene expression by the C-terminal activation domain. *Biochem Biophys Res Commun* **255,** 208-215.

Graham D., Pfeiffer F., Simler R. and Betz H. (1985) Purification and characterization of the glycine receptor of pig spinal cord. *Biochemistry* **24,** 990-994.

Greene L. A. and Tischler A. S. (1976) Establishment of a noradrenergic clonal line of rat adrenal pheochromocytoma cells which respond to nerve growth factor. *Proc Natl Acad Sci U S A* **73,** 2424-2428.

Grimm R. and Tischmeyer W. (1997) Complex patterns of immediate early gene induction in rat brain following brightness discrimination training and pseudotraining. *Behav Brain Res* **84,** 109-116.

Groc L., Heine M., Cognet L., Brickley K., Stephenson F. A., Lounis B. and Choquet D. (2004) Differential activity-dependent regulation of the lateral mobilities of AMPA and NMDA receptors. *Nat Neurosci* **7,** 695-696.

Groll M., Ditzel L., Lowe J., Stock D., Bochtler M., Bartunik H. D. and Huber R. (1997) Structure of 20S proteasome from yeast at 2.4A resolution. **386,** 463-471.

Grudzinska J., Schemm R., Haeger S., Nicke A., Schmalzing G., Betz H. and Laube B. (2005) The beta subunit determines the ligand binding properties of synaptic glycine receptors. *Neuron* **45,** 727-739.

Gupta M. P., Gupta M., Zak R. and Sukhatme V. P. (1991) Egr-1, a serum-inducible zinc finger protein, regulates transcription of the rat cardiac alpha-myosin heavy chain gene. *J Biol Chem* **266,** 12813-12816.

Guy, G. R., Cao, X., Chua, S. P. and Tan, Y. H. (1992) Okadaic acid mimics multiple changes in early protein phosphorylation and gene expression induced by tumor necrosis factor or interleukin-1. *J Biol Chem,* **267,** 1846-1852.

Guzowski, J. F. and McGaugh, J. L. (1997) Antisense oligodeoxynucleotide-mediated disruption of hippocampal cAMP response element binding protein levels impairs consolidation of memory for water maze training. *Proc Natl Acad Sci U S A,* **94,** 2693-2698.

Guzowski J. F., Setlow B., Wagner E. K. and McGaugh J. L. (2001) Experience-dependent gene expression in the rat hippocampus after spatial learning: a comparison of the immediate-early genes Arc, c-fos, and zif268. *J Neurosci* **21,** 5089-5098.

Haghighat, A., Mader, S., Pause, A. and Sonenberg, N. (1995) Repression of cap-dependent translation by 4E-binding protein 1: competition with p220 for binding to eukaryotic initiation factor-4E. *Embo J,* **14,** 5701-5709.

Hagiwara M., Alberts A., Brindle P., Meinkoth J., Feramisco J., Deng T., Karin M., Shenolikar S. and Montminy M. (1992) Transcriptional attenuation following cAMP induction requires PP-1-mediated dephosphorylation of CREB. *Cell* **70,** 105-113.

Hall J., Thomas K. L. and Everitt B. J. (2000) Rapid and selective induction of BDNF expression in the hippocampus during contextual learning. *Nat Neurosci* **3,** 533-535.

Hall, J., Thomas, K. L. and Everitt, B. J. (2001) Cellular imaging of zif268 expression in the hippocampus and amygdala during contextual and cued fear memory retrieval: selective activation of hippocampal CA1 neurons during the recall of contextual memories. *J Neurosci,* **21,** 2186-2193.

Hanaoka E., Ozaki T., Ohira M., Nakamura Y., Suzuki M., Takahashi E., Moriya H., Nakagawara A. and Sakiyama S. (2000) Molecular cloning and expression analysis of the human DA41 gene and its mapping to chromosome 9q21.2-q21.3. *J Hum Genet* **45,** 188-191.

Hanus C., Vannier C. and Triller A. (2004) Intracellular association of glycine receptor with gephyrin increases its plasma membrane accumulation rate. *J Neurosci* **24,** 1119-1128.

Harada S., Esch G. L., Holgado-Madruga M. and Wong A. J. (2001) Grb-2-associated binder-1 is involved in insulin-induced egr-1 gene expression through its phosphatidylinositol 3'-kinase binding site. *DNA Cell Biol* **20,** 223-229.

Hardingham, G. E., Arnold, F. J. and Bading, H. (2001) A calcium microdomain near NMDA receptors: on switch for ERK-dependent synapse-to-nucleus communication. *Nat Neurosci* **4,** 565-566.

Hardingham G. E. (2006) 2B synaptic or extrasynaptic determines signalling from the NMDA receptor. *J Physiol*. **572(Pt 3),**14-15

Hardy J. (1997) Amyloid, the presenilins and Alzheimer's disease. *Trends Neurosci* **20,** 154-159.

Harris E. W., Ganong A. H. and Cotman C. W. (1984) Long-term potentiation in the hippocampus involves activation of N-methyl-D-aspartate receptors. *Brain Res* **323,** 132-137.

Harris J. L., Alper P. B., Li J., Rechsteiner M. and Backes B. J. (2001) Substrate specificity of the human proteasome. *Chem Biol* **8,** 1131-1141.

Harvey K., Duguid I. C., Alldred M. J., Beatty S. E., Ward H., Keep N. H., Lingenfelter S. E., Pearce B. R., Lundgren J., Owen M. J., Smart T. G., Luscher B., Rees M. I. and Harvey R. J. (2004) The GDP-GTP exchange factor collybistin: an essential determinant of neuronal gephyrin clustering. *J Neurosci* **24,** 5816-5826.

Harvey, J. and Collingridge, G. L. (1992) Thapsigargin blocks the induction of long-term potentiation in rat hippocampal slices. *Neurosci Lett,* **139,** 197-200.

Haussinger D., Lang F. and Gerok W. (1994) Regulation of cell function by the cellular hydration state. *Am J Physiol* **267,** E343-355.

Hay N. and Sonenberg N. (2004) Upstream and downstream of mTOR. *Genes Dev* **18,** 1926-1945.

Haystead T. A., Sim A. T., Carling D., Honnor R. C., Tsukitani Y., Cohen P. and Hardie D. G. (1989) Effects of the tumour promoter okadaic acid on intracellular protein phosphorylation and metabolism. *Nature* **337,** 78-81.

Hebb D. O., (1949) The Organisation of Behaviour: A neuropsychological theory. New York: Wiley

Helliwell, S. B., Wagner, P., Kunz, J., Deuter-Reinhard, M., Henriquez, R. and Hall, M. N. (1994) TOR1 and TOR2 are structurally and functionally similar but not identical phosphatidylinositol kinase homologues in yeast. *Mol Biol Cell,* **5,** 105-118.

Herdegen T. and Leah J. D. (1998) Inducible and constitutive transcription factors in the mammalian nervous system: control of gene expression by Jun, Fos and Krox, and CREB/ATF proteins. *Brain Res Brain Res Rev* **28,** 370-490.

Hermann A., Kneussel M. and Betz H. (2001) Identification of multiple gephyrin variants in different organs of the adult rat. *Biochem Biophys Res Commun* **282,** 67-70.

Herring D., Huang R., Singh M., Robinson L. C., Dillon G. H. and Leidenheimer N. J. (2003) Constitutive GABAA receptor endocytosis is dynamin-mediated and dependent on a dileucine AP2 adaptin-binding motif within the beta 2 subunit of the receptor. *J Biol Chem* **278,** 24046-24052.

Herry C. and Garcia R. (2002) Prefrontal cortex long-term potentiation, but not long-term depression, is associated with the maintenance of extinction of learned fear in mice. *J Neurosci* **22,** 577-583.

Herry C. and Garcia R. (2003) Behavioral and paired-pulse facilitation analyses of long-lasting depression at excitatory synapses in the medial prefrontal cortex in mice. *Behav Brain Res* **146,** 89-96.

Herry C. and Mons N. (2004) Resistance to extinction is associated with impaired immediate early gene induction in medial prefrontal cortex and amygdala. *Eur J Neurosci* **20,** 781-790.

Hershko A. and Ciechanover A. (1998) The ubiquitin system. *Annual Review of Biochemistry* **67,** 425-479.

Heynen A. J. and Bear M. F. (2001) Long-term potentiation of thalamocortical transmission in the adult visual cortex in vivo. *J Neurosci* **21,** 9801-9813.

Hicke L. and Dunn R. (2003) Regulation of membrane protein transport by ubiquitin and ubiquitin-binding proteins. *Annu Rev Cell Dev Biol* **19,** 141-172.

Hicks A., Davis S., Rodger J., Helme-Guizon A., Laroche S. and Mallet J. (1997) Synapsin I and syntaxin 1B: key elements in the control of neurotransmitter

release are regulated by neuronal activation and long-term potentiation in vivo. *Neuroscience* **79,** 329-340.

Hofmann K. and Bucher P. (1996) The UBA domain: a sequence motif present in multiple enzyme classes of the ubiquitination pathway. *Trends Biochem Sci* **21,** 172-173.

Honkanen R. E. (1993) Cantharidin, another natural toxin that inhibits the activity of serine/threonine protein phosphatases types 1 and 2A. *FEBS Lett* **330,** 283-286.

Horwich A. L., Weber-Ban E. U. and Finley D. (1999) Chaperone rings in protein folding and degradation. *PNAS* **96,** 11033-11040.

Hu G. Y., Hvalby O., Walaas S. I., Albert K. A., Skjeflo P., Andersen P. and Greengard P. (1987) Protein kinase C injection into hippocampal pyramidal cells elicits features of long term potentiation. *Nature* **328,** 426-429.

Hung A. C., Huang H. M., Tsay H. J., Lin T. N., Kuo J. S. and Sun S. H. (2000) ATP-stimulated c-fos and zif268 mRNA expression is inhibited by chemical hypoxia in a rat brain-derived type 2 astrocyte cell line, RBA-2. *J Cell Biochem* **77,** 323-332.

Huang, C. C., Faber, P. W., Persichetti, F., Mittal, V., Vonsattel, J. P., MacDonald, M. E. and Gusella, J. F. (1998) Amyloid formation by mutant huntingtin: threshold, progressivity and recruitment of normal polyglutamine proteins. *Somat Cell Mol Genet,* **24,** 217-233.

Huang R. P., Fan Y., Ni Z., Mercola D. and Adamson E. D. (1997) Reciprocal modulation between Sp1 and Egr-1. *J Cell Biochem* **66,** 489-499.

Huang Y. Y., Nguyen P. V., Abel T. and Kandel E. R. (1996) Long-lasting forms of synaptic potentiation in the mammalian hippocampus. *Learn Mem* **3,** 74-85.

Hughes P. and Dragunow M. (1995) Induction of immediate-early genes and the control of neurotransmitter-regulated gene expression within the nervous system. *Pharmacol Rev* **47,** 133-178.

Huh, G. S., Boulanger, L. M., Du, H., Riquelme, P. A., Brotz, T. M. and Shatz, C. J. (2000) Functional requirement for class I MHC in CNS development and plasticity. *Science,* **290,** 2155-2159.

Huttelmaier S., Harbeck B., Steffens O., Messerschmidt T., Illenberger S. and Jockusch B. M. (1999) Characterization of the actin binding properties of the vasodilator-stimulated phosphoprotein VASP. *FEBS Lett* **451,** 68-74.

Iida, N., Namikawa, K., Kiyama, H., Ueno, H., Nakamura, S. and Hattori, S. (2001) Requirement of Ras for the activation of mitogen-activated protein kinase by calcium influx, cAMP, and neurotrophin in hippocampal neurons. *J Neurosci,* **21,** 6459-6466.

Impey, S., Obrietan, K., Wong, S. T., Poser, S., Yano, S., Wayman, G., Deloulme, J. C., Chan, G. and Storm, D. R. (1998) Cross talk between ERK and PKA is required for Ca2+ stimulation of CREB-dependent transcription and ERK nuclear translocation. *Neuron,* **21,** 869-883.

Inamura, N., Hoshino, S., Uchiumi, T., Nawa, H. and Takei, N. (2003) Cellular and subcellular distributions of translation initiation, elongation and release factors in rat hippocampus. *Brain Res Mol Brain Res,* **111,** 165-174.

Ivanov A., Pellegrino C., Rama S., Dumalska I., Salyha Y., Ben-Ari Y. and Medina I. (2006) Opposing role of synaptic and extrasynaptic NMDA receptors in regulation of the extracellular signal-regulated kinases (ERK) activity in cultured rat hippocampal neurons. *J Physiol* **572,** 789-798.

Ives J. H., Drewery D. L. and Thompson C. L. (2002) Differential cell surface expression of GABAA receptor alpha1, alpha6, beta2 and beta3 subunits in cultured mouse cerebellar granule cells influence of cAMP-activated signalling. *J Neurochem* **80,** 317-327.

Jacob T. C., Bogdanov Y. D., Magnus C., Saliba R. S., Kittler J. T., Haydon P. G. and Moss S. J. (2005) Gephyrin regulates the cell surface dynamics of synaptic GABAA receptors. *J Neurosci* **25,** 10469-10478.

James A. B., Conway A. M. and Morris B. J. (2005) Genomic profiling of the neuronal target genes of the plasticity-related transcription factor -- Zif268. *J Neurochem* **95,** 796-810.

James A. B., Conway A. M. and Morris B. J. (2006) Regulation of the neuronal proteasome by Zif268 (Egr1). *J Neurosci* **26,** 1624-1634.

James A. B., Conway A. M., Thiel G. and Morris B. J. (2004) Egr-1 modulation of synapsin I expression: permissive effect of forskolin via cAMP. *Cell Signal* **16,** 1355-1362.

Jarvis E. D., Mello C. V. and Nottebohm F. (1995) Associative learning and stimulus novelty influence the song-induced expression of an immediate early gene in the canary forebrain. *Learn Mem* **2,** 62-80.

Jarvis E. D., Scharff C., Grossman M. R., Ramos J. A. and Nottebohm F. (1998) For whom the bird sings: context-dependent gene expression. *Neuron* **21,** 775-788.

Jiang Y. H., Armstrong D., Albrecht U., Atkins C. M., Noebels J. L., Eichele G., Sweatt J. D. and Beaudet A. L. (1998) Mutation of the Angelman ubiquitin ligase in mice causes increased cytoplasmic p53 and deficits of contextual learning and long-term potentiation. *Neuron* **21,** 799-811.

Job C. and Eberwine J. (2001) Localization and translation of mRNA in dendrites and axons. *Nat Rev Neurosci* **2,** 889-898.

Johnson J. L., Wuebbens M. M., Mandell R. and Shih V. E. (1989) Molybdenum cofactor biosynthesis in humans. Identification of two complementation groups of cofactor-deficient patients and preliminary characterization of a diffusible molybdopterin precursor. *J Clin Invest* **83,** 897-903.

Johnston H. M. and Morris B. J. (1994) zif/268 does not mediate increases in proenkephalin mRNA levels after NMDA receptor stimulation. *Neuroreport* **5,** 1498-1500.

Johnston J. A., Ward C. L. and Kopito R. R. (1998) Aggresomes: a cellular response to misfolded proteins. *J Cell Biol* **143,** 1883-1898.

Johnston J. A., Dalton M. J., Gurney M. E. and Kopito R. R. (2000) Formation of high molecular weight complexes of mutant Cu, Zn-superoxide dismutase in a mouse model for familial amyotrophic lateral sclerosis. *Proc Natl Acad Sci U S A* **97,** 12571-12576.

Jones A., Korpi E. R., McKernan R. M., Pelz R., Nusser Z., Makela R., Mellor J. R., Pollard S., Bahn S., Stephenson F. A., Randall A. D., Sieghart W., Somogyi P., Smith A. J. and Wisden W. (1997) Ligand-gated ion channel subunit partnerships: GABAA receptor alpha6 subunit gene inactivation inhibits delta subunit expression. *J Neurosci* **17,** 1350-1362.

Jones, M. W., Errington, M. L., French, P. J. et al. (2001b) A requirement for the immediate early gene Zif268 in the expression of late LTP and long-term memories. *Nat Neurosci* **4,** 289-296.

Jones M. W., French P. J., Bliss T. V. and Rosenblum K. (1999) Molecular mechanisms of long-term potentiation in the insular cortex in vivo. *J Neurosci* **19,** RC36.

Jones N. and Agani F. H. (2003) Hyperoxia induces Egr-1 expression through activation of extracellular signal-regulated kinase 1/2 pathway. *J Cell Physiol* **196,** 326-333.

Joseph L. J., Le Beau M. M., Jamieson G. A., Jr., Acharya S., Shows T. B., Rowley J. D. and Sukhatme V. P. (1988) Molecular cloning, sequencing, and mapping of EGR2, a human early growth response gene encoding a

protein with "zinc-binding finger" structure. *Proc Natl Acad Sci U S A* **85,** 7164-7168.

Kaang B. K., Kandel E. R. and Grant S. G. (1993) Activation of cAMP-responsive genes by stimuli that produce long-term facilitation in Aplysia sensory neurons. *Neuron* **10,** 427-435.

Kaczmarek L., Kossut M. and Skangiel-Kramska J. (1997) Glutamate receptors in cortical plasticity: molecular and cellular biology. *Physiol Rev* **77,** 217-255.

Kaczmarek L., Zangenehpour S. and Chaudhuri A. (1999) Sensory regulation of immediate-early genes c-fos and zif268 in monkey visual cortex at birth and throughout the critical period. *Cereb Cortex* **9,** 179-187.

Kalari, K. R., Casavant, M., Bair, T. B., Keen, H. L., Comeron, J. M., Casavant, T. L. and Scheetz, T. E. (2006) First exons and introns--a survey of GC content and gene structure in the human genome. *In Silico Biol,* **6,** 237-242.

Kamalakaran, S., Radhakrishnan, S. K. and Beck, W. T. (2005) Identification of estrogen-responsive genes using a genome-wide analysis of promoter elements for transcription factor binding sites. *J Biol Chem* **280,** 21491-21497.

Kamboh M. I. (2004) Molecular genetics of late-onset Alzheimer's disease. *Annals Of Human Genetics* **68,** 381-404.

Kamdar, K. P., Shelton, M. E. and Finnerty, V. (1994) The Drosophila molybdenum cofactor gene cinnamon is homologous to three Escherichia coli cofactor proteins and to the rat protein gephyrin. *Genetics,* **137,** 791-801.

Karachot, L., Shirai, Y., Vigot, R., Yamamori, T. and Ito, M. (2001) Induction of long-term depression in cerebellar Purkinje cells requires a rapidly turned over protein. *J Neurophysiol,* **86,** 280-289.

Karpova A., Mikhaylova M., Thomas U., Knopfel T. and Behnisch T. (2006) Involvement of protein synthesis and degradation in long-term potentiation of Schaffer collateral CA1 synapses. *J Neurosci* **26,** 4949-4955.

Kasahara, J., Fukunaga, K. and Miyamoto, E. (2001) Activation of calcium/calmodulin-dependent protein kinase IV in long term potentiation in the rat hippocampal CA1 region. *J Biol Chem,* **276,** 24044-24050.

Kato K., Uruno K., Saito K. and Kato H. (1991) Both arachidonic acid and 1-oleoyl-2-acetyl glycerol in low magnesium solution induce long-term potentiation in hippocampal CA1 neurons in vitro. *Brain Res* **563,** 94-100.

Kauer J. A., Malenka R. C. and Nicoll R. A. (1988) NMDA application potentiates synaptic transmission in the hippocampus. *Nature* **334,** 250-252.

Kawaguchi Y., Wilson C. J. and Emson P. C. (1990) Projection subtypes of rat neostriatal matrix cells revealed by intracellular injection of biocytin. *J Neurosci* **10,** 3421-3438.

Kaye F. J., Modi S., Ivanovska I., Koonin E. V., Thress K., Kubo A., Kornbluth S. and Rose M. D. (2000) A family of ubiquitin-like proteins binds the ATPase domain of Hsp70-like Stch. *FEBS Lett* **467,** 348-355.

Keefe K. A. and Gerfen C. R. (1995) D1-D2 dopamine receptor synergy in striatum: effects of intrastriatal infusions of dopamine agonists and antagonists on immediate early gene expression. *Neuroscience* **66,** 903-913.

Kelleher, R. J., 3rd, Govindarajan, A., Jung, H. Y., Kang, H. and Tonegawa, S. (2004) Translational control by MAPK signaling in long-term synaptic plasticity and memory. *Cell,* **116,** 467-479.

Keller J. N., Hanni K. B. and Markesbery W. R. (2000) Possible involvement of proteasome inhibition in aging: implications for oxidative stress. *Mech Ageing Dev* **113,** 61-70.

Kim I., Mi K. and Rao H. (2004) Multiple interactions of rad23 suggest a mechanism for ubiquitylated substrate delivery important in proteolysis. *Mol Biol Cell* **15,** 3357-3365.

Kim J. J., DeCola J. P., Landeira-Fernandez J. and Fanselow M. S. (1991) N-methyl-D-aspartate receptor antagonist APV blocks acquisition but not expression of fear conditioning. *Behav Neurosci* **105,** 126-133.

Kim J. J. and Fanselow M. S. (1992) Modality-specific retrograde amnesia of fear. *Science* **256,** 675-677.

Kim T. W., Pettingell W. H., Hallmark O. G., Moir R. D., Wasco W. and Tanzi R. E. (1997) Endoproteolytic cleavage and proteasomal degradation of presenilin 2 in transfected cells. *J Biol Chem* **272,** 11006-11010.

Kimberly W. T., LaVoie M. J., Ostaszewski B. L., Ye W., Wolfe M. S. and Selkoe D. J. (2003) Gamma-secretase is a membrane protein complex comprised of presenilin, nicastrin, Aph-1, and Pen-2. *Proc Natl Acad Sci U S A* **100,** 6382-6387.

Kins S., Betz H. and Kirsch J. (2000) Collybistin, a newly identified brain-specific GEF, induces submembrane clustering of gephyrin. *Nat Neurosci* **3,** 22-29.

Kirkwood A., Dudek S. M., Gold J. T., Aizenman C. D. and Bear M. F. (1993) Common forms of synaptic plasticity in the hippocampus and neocortex in vitro. *Science* **260,** 1518-1521.

Kirsch J. (2006) Glycinergic transmission. *Cell Tissue Res* **326,** 535-540.

Kirsch J. and Betz H. (1995) The postsynaptic localization of the glycine receptor-associated protein gephyrin is regulated by the cytoskeleton. *J Neurosci* **15,** 4148-4156.

Kirsch J. and Betz H. (1998) Glycine-receptor activation is required for receptor clustering in spinal neurons. *Nature* **392,** 717-720.

Kirsch J., Kuhse J. and Betz H. (1995) Targeting of glycine receptor subunits to gephyrin-rich domains in transfected human embryonic kidney cells. *Mol Cell Neurosci* **6,** 450-461.

Kirsch J., Langosch D., Prior P., Littauer U. Z., Schmitt B. and Betz H. (1991) The 93-kDa glycine receptor-associated protein binds to tubulin. *J Biol Chem* **266,** 22242-22245.

Kirsch J., Meyer G. and Betz H. (1996) Synaptic targeting of ionotropic neurotransmitter receptors. *Mol Cell Neurosci* **8,** 93-98.

Kirsch J., Wolters I., Triller A. and Betz H. (1993) Gephyrin antisense oligonucleotides prevent glycine receptor clustering in spinal neurons. *Nature* **366,** 745-748.

Kishimoto Y., Kawahara S., Suzuki M., Mori H., Mishina M. and Kirino Y. (2001) Classical eyeblink conditioning in glutamate receptor subunit delta 2 mutant mice is impaired in the delay paradigm but not in the trace paradigm. *Eur J Neurosci* **13,** 1249-1253.

Kisselev A. F., Akopian T. N., Castillo V. and Goldberg A. L. (1999) Proteasome active sites allosterically regulate each other, suggesting a cyclical bite-chew mechanism for protein breakdown. *Mol Cell* **4,** 395-402.

Kittler, J. T., Delmas, P., Jovanovic, J. N., Brown, D. A., Smart, T. G. and Moss, S. J. (2000) Constitutive endocytosis of GABAA receptors by an association with the adaptin AP2 complex modulates inhibitory synaptic currents in hippocampal neurons. *J Neurosci,* **20,** 7972-7977.

Kittler J. T. and Moss S. J. (2001) Neurotransmitter receptor trafficking and the regulation of synaptic strength. *Traffic* **2,** 437-448.

Kittler, J. T., Rostaing, P., Schiavo, G., Fritschy, J. M., Olsen, R., Triller, A. and Moss, S. J. (2001) The subcellular distribution of GABARAP and its ability to interact with NSF suggest a role for this protein in the intracellular transport of GABA(A) receptors. *Mol Cell Neurosci,* **18,** 13-25.

Kittler J. T., Thomas P., Tretter V., Bogdanov Y. D., Haucke V., Smart T. G. and Moss S. J. (2004) Huntingtin-associated protein 1 regulates inhibitory synaptic transmission by modulating gamma-aminobutyric acid type A receptor membrane trafficking. *Proc Natl Acad Sci U S A* **101,** 12736-12741.

Kleijn M. and Proud C. G. (2000) The activation of eukaryotic initiation factor (eIF)2B by growth factors in PC12 cells requires MEK/ERK signalling. *FEBS Lett* **476,** 262-265.

Kleijnen, M. F., Shih, A. H., Zhou, P., Kumar, S., Soccio, R. E., Kedersha, N. L., Gill, G. and Howley, P. M. (2000) The hPLIC proteins may provide a link between the ubiquitination machinery and the proteasome. *Mol Cell,* **6,** 409-419.

Knapp J., Boknik P., Huke S., Gombosova I., Linck B., Luss H., Muller F. U., Muller T., Nacke P., Schmitz W., Vahlensieck U. and Neumann J. (1998) Contractility and inhibition of protein phosphatases by cantharidin. *Gen Pharmacol* **31,** 729-733.

Kneussel M. and Betz H. (2000) Receptors, gephyrin and gephyrin-associated proteins: novel insights into the assembly of inhibitory postsynaptic membrane specializations. *J Physiol* **525 Pt 1,** 1-9.

Kneussel, M., Brandstatter, J. H., Gasnier, B., Feng, G., Sanes, J. R. and Betz, H. (2001) Gephyrin-independent clustering of postsynaptic GABA(A) receptor subtypes. *Mol Cell Neurosci,* **17,** 973-982.

Kneussel, M., Brandstatter, J. H., Laube, B., Stahl, S., Muller, U. and Betz, H. (1999a) Loss of postsynaptic GABA(A) receptor clustering in gephyrin-deficient mice. *J Neurosci,* **19,** 9289-9297.

Kneussel, M., Haverkamp, S., Fuhrmann, J. C., Wang, H., Wassle, H., Olsen, R. W. and Betz, H. (2000) The gamma-aminobutyric acid type A receptor (GABAAR)-associated protein GABARAP interacts with gephyrin but is not involved in receptor anchoring at the synapse. *Proc Natl Acad Sci U S A,* **97,** 8594-8599.

Kneussel M., Hermann A., Kirsch J. and Betz H. (1999a) Hydrophobic interactions mediate binding of the glycine receptor beta-subunit to gephyrin. *J Neurochem* **72,** 1323-1326.

Ko H. S., Uehara T. and Nomura Y. (2002) Role of ubiquilin associated with protein-disulfide isomerase in the endoplasmic reticulum in stress-induced apoptotic cell death. *J Biol Chem* **277,** 35386-35392.

Koegl M., Hoppe T., Schlenker S., Ulrich H. D., Mayer T. U. and Jentsch S. (1999) A novel ubiquitination factor, E4, is involved in multiubiquitin chain assembly. *Cell* **96,** 635-644.

Kozak M. (1986) Point mutations define a sequence flanking the AUG initiator codon that modulates translation by eukaryotic ribosomes. *Cell* **44,** 283-292.

Kozak M. (1987) Effects of intercistronic length on the efficiency of reinitiation by eucaryotic ribosomes. *Mol Cell Biol* **7,** 3438-3445.

Kozak M. (1989) The scanning model for translation: an update. *J Cell Biol* **108,** 229-241.

Kozak M. (1997) Recognition of AUG and alternative initiator codons is augmented by G in position +4 but is not generally affected by the nucleotides in positions +5 and +6. *Embo J* **16,** 2482-2492.

Kozak M. (2003) Not every polymorphism close to the AUG codon can be explained by invoking context effects on initiation of translation. *Blood* **101,** 1202-1203; author reply 1203.

Kozak M. (2005) Regulation of translation via mRNA structure in prokaryotes and eukaryotes. *Gene* **361,** 13-37.

Krug M., Lossner B. and Ott T. (1984) Anisomycin blocks the late phase of long-term potentiation in the dentate gyrus of freely moving rats. *Brain Res Bull* **13,** 39-42.

Kuhnt U., Mihaly A. and Joo F. (1985) Increased binding of calcium in the hippocampal slice during long-term potentiation. *Neurosci Lett* **53,** 149-154.

Kunz, J., Henriquez, R., Schneider, U., Deuter-Reinhard, M., Movva, N. R. and Hall, M. N. (1993) Target of rapamycin in yeast, TOR2, is an essential phosphatidylinositol kinase homolog required for G1 progression. *Cell,* **73,** 585-596.

Kurino M., Fukunaga K., Ushio Y. and Miyamoto E. (1995) Activation of mitogen-activated protein kinase in cultured rat hippocampal neurons by stimulation of glutamate receptors. *J Neurochem* **65,** 1282-1289.

Lamprecht R. and Dudai Y. (1995) Differential modulation of brain immediate early genes by intraperitoneal LiCl. *Neuroreport* **7,** 289-293.

Lamprecht, R., Hazvi, S. and Dudai, Y. (1997) cAMP response element-binding protein in the amygdala is required for long- but not short-term conditioned taste aversion memory. *J Neurosci,* **17,** 8443-8450.

Langosch D., Thomas L. and Betz H. (1988) Conserved quaternary structure of ligand-gated ion channels: the postsynaptic glycine receptor is a pentamer. *Proc Natl Acad Sci U S A* **85,** 7394-7398.

Langosch D., Hoch W. and Betz H. (1992) The 93 kDa protein gephyrin and tubulin associated with the inhibitory glycine receptor are phosphorylated by an endogenous protein kinase. *FEBS Lett* **298,** 113-117.

Lau L. F. and Nathans D. (1987) Expression of a set of growth-related immediate early genes in BALB/c 3T3 cells: coordinate regulation with c-fos or c-myc. *Proc Natl Acad Sci U S A* **84,** 1182-1186.

Laurie D. J., Wisden W. and Seeburg P. H. (1992) The distribution of thirteen GABAA receptor subunit mRNAs in the rat brain. III. Embryonic and postnatal development. *J Neurosci* **12,** 4151-4172.

Le Moine C., Normand E., Guitteny A. F., Fouque B., Teoule R. and Bloch B. (1990) Dopamine receptor gene expression by enkephalin neurons in rat forebrain. *Proc Natl Acad Sci U S A* **87,** 230-234.

Lee H. and Kim J. J. (1998) Amygdalar NMDA receptors are critical for new fear learning in previously fear-conditioned rats. *J Neurosci* **18,** 8444-8454.

Lee, J. L., Everitt, B. J. and Thomas, K. L. (2004) Independent cellular processes for hippocampal memory consolidation and reconsolidation. *Science,* **304,** 839-843.

Leil T. A., Chen Z. W., Chang C. S. and Olsen R. W. (2004) GABAA receptor-associated protein traffics GABAA receptors to the plasma membrane in neurons. *J Neurosci* **24,** 11429-11438.

Lemaire, P., Revelant, O., Bravo, R. and Charnay, P. (1988) Two mouse genes encoding potential transcription factors with identical DNA-binding domains are activated by growth factors in cultured cells. *Proc Natl Acad Sci U S A,* **85,** 4691-4695.

Lemaire P., Vesque C., Schmitt J., Stunnenberg H., Frank R. and Charnay P. (1990) The serum-inducible mouse gene Krox-24 encodes a sequence-specific transcriptional activator. *Mol Cell Biol* **10,** 3456-3467.

Leonard A. S., Lim I. A., Hemsworth D. E., Horne M. C. and Hell J. W. (1999) Calcium/calmodulin-dependent protein kinase II is associated with the N-methyl-D-aspartate receptor. *Proc Natl Acad Sci U S A* **96,** 3239-3244.

Leroy C., Poisbeau P., Keller A. F. and Nehlig A. (2004) Pharmacological plasticity of GABA(A) receptors at dentate gyrus synapses in a rat model of temporal lobe epilepsy. *J Physiol* **557,** 473-487.

Leutgeb, J. K., Frey, J. U. and Behnisch, T. (2005) Single cell analysis of activity-dependent cyclic AMP-responsive element-binding protein phosphorylation during long-lasting long-term potentiation in area CA1 of mature rat hippocampal-organotypic cultures. *Neuroscience,* **131,** 601-610.

Levenson J., Weeber E., Selcher J. C., Kategaya L. S., Sweatt J. D. and Eskin A. (2002) Long-term potentiation and contextual fear conditioning increase neuronal glutamate uptake. *Nat Neurosci* **5,** 155-161.

Levey, A. I., Hersch, S. M., Rye, D. B. et al. (1993) Localization of D1 and D2 dopamine receptors in brain with subtype-specific antibodies. *Proc Natl Acad Sci U S A,* **90,** 8861-8865.

Levi S., Chesnoy-Marchais D., Sieghart W. and Triller A. (1999) Synaptic control of glycine and GABA(A) receptors and gephyrin expression in cultured motoneurons. *J Neurosci* **19,** 7434-7449.

Levi S., Logan S. M., Tovar K. R. and Craig A. M. (2004) Gephyrin is critical for glycine receptor clustering but not for the formation of functional GABAergic synapses in hippocampal neurons. *J Neurosci* **24,** 207-217.

Levi S., Grady R. M., Henry M. D., Campbell K. P., Sanes J. R. and Craig A. M. (2002) Dystroglycan is selectively associated with inhibitory GABAergic synapses but is dispensable for their differentiation. *J Neurosci* **22,** 4274-4285.

Lewis D. and Teyler T. J. (1986) Anti-S-100 serum blocks long-term potentiation in the hippocampal slice. *Brain Res* **383,** 159-164.

Li Y., Camp S., Rachinsky T. L., Bongiorno C. and Taylor P. (1993) Promoter elements and transcriptional control of the mouse acetylcholinesterase gene. *J Biol Chem* **268,** 3563-3572.

Li, Y. M., Mackintosh, C. and Casida, J. E. (1993b) Protein phosphatase 2A and its [3H]cantharidin/[3H]endothall thioanhydride binding site. Inhibitor specificity of cantharidin and ATP analogues. *Biochem Pharmacol,* **46,** 1435-1443.

Li Y. M., Xu M., Lai M. T. et al. (2000) Photoactivated gamma-secretase inhibitors directed to the active site covalently label presenilin 1. *Nature,* **405,** 689-694.

Lim R., Alvarez F. J. and Walmsley B. (1999) Quantal size is correlated with receptor cluster area at glycinergic synapses in the rat brainstem. *J Physiol* **516 (Pt 2),** 505-512.

Lim R. W., Varnum B. C. and Herschman H. R. (1987) Cloning of tetradecanoyl phorbol ester-induced 'primary response' sequences and their expression in density-arrested Swiss 3T3 cells and a TPA non-proliferative variant. *Oncogene* **1,** 263-270.

Lindahl J. S. and Keifer J. (2004) Glutamate receptor subunits are altered in forebrain and cerebellum in rats chronically exposed to the NMDA receptor antagonist phencyclidine. *Neuropsychopharmacology* **29,** 2065-2073.

Lindecke A., Korte M., Zagrebelsky M., Horejschi V., Elvers M., Widera D., Prullage M., Pfeiffer J., Kaltschmidt B. and Kaltschmidt C. (2006) Long-term depression activates transcription of immediate early transcription factor genes: involvement of serum response factor/Elk-1. *Eur J Neurosci* **24,** 555-563.

Linden D. J. and Connor J. A. (1995) Long-Term Synaptic Depression. *Ann Rev Neurosci* **18**, 319-357

Linden D. J., Wong K. L., Sheu F. S. and Routtenberg A. (1988) NMDA receptor blockade prevents the increase in protein kinase C substrate (protein F1) phosphorylation produced by long-term potentiation. *Brain Res* **458,** 142-146.

Lisman J. (1994) The CaM kinase II hypothesis for the storage of synaptic memory. *Trends Neurosci* **17,** 406-412.

Lisman J., Schulman H. and Cline H. (2002) The molecular basis of CaMKII function in synaptic and behavioural memory. *Nat Rev Neurosci* **3,** 175-190.

Liu C., Calogero A., Ragona G., Adamson E. and Mercola D. (1996) EGR-1, the reluctant suppression factor: EGR-1 is known to function in the regulation of growth, differentiation, and also has significant tumor suppressor activity and a mechanism involving the induction of TGF-beta1 is postulated to account for this suppressor activity. *Crit Rev Oncog* **7,** 101-125.

Liu G. (2004) Local structural balance and functional interaction of excitatory and inhibitory synapses in hippocampal dendrites. *Nat Neurosci* **7,** 373-379.

Liu J., Fukunaga, K., Yamamoto, H., Nishi, K. and Miyamoto, E. (1999) Differential roles of Ca(2+)/calmodulin-dependent protein kinase II and mitogen-activated protein kinase activation in hippocampal long-term potentiation. *J Neurosci,* **19,** 8292-8299.

Liu X. B., Murray K. D. and Jones E. G. (2004) Switching of NMDA receptor 2A and 2B subunits at thalamic and cortical synapses during early postnatal development. *J Neurosci* **24,** 8885-8895.

Lledo P. M., Hjelmstad G. O., Mukherji S., Soderling T. R., Malenka R. C. and Nicoll R. A. (1995) Calcium/calmodulin-dependent kinase II and long-term potentiation enhance synaptic transmission by the same mechanism. *Proc Natl Acad Sci U S A* **92,** 11175-11179.

Lorente de Nó R. (1934) Studies on the structure of the cerebral cortex. II. Continuation of the study of the ammonic system. *J Psychol Neurol (Lpz)* **46,** 113–177.

Lorenzo L. E., Barbe A. and Bras H. (2004) Mapping and quantitative analysis of gephyrin cytoplasmic trafficking pathways in motoneurons, using an optimized Transmission Electron Microscopy Color Imaging (TEMCI) procedure. *J Neurocytol,* **33,** 241-249.

Löser P., Jennings G.S., Strauss M. and Sandig V. (1998) Reactivation of the previously silenced cytomegalovirus major immediate-early promoter in the mouse liver: Involvement of NFkappaB. *J Virol* **72,**180–190.

Lovinger D. M., Colley P. A., Akers R. F., Nelson R. B. and Routtenberg A. (1986) Direct relation of long-term synaptic potentiation to phosphorylation of membrane protein F1, a substrate for membrane protein kinase C. *Brain Res* **399,** 205-211.

Lu W., Man H., Ju W., Trimble W. S., MacDonald J. F. and Wang Y. T. (2001) Activation of synaptic NMDA receptors induces membrane insertion of new AMPA receptors and LTP in cultured hippocampal neurons. *Neuron* **29,** 243-254.

Lu Y. M., Mansuy I. M., Kandel E. R. and Roder J. (2000) Calcineurin-Mediated LTD of GABAergic Inhibition Underlies the Increased Excitability of CA1 Neurons Associated with LTP. *Neuron* **26,** 197-205.

Lu Y. M., Roder J. C., Davidow J. and Salter M. W. (1998) Src activation in the induction of long-term potentiation in CA1 hippocampal neurons. *Science,* **279,** 1363-1367.

Lukusa T. and Fryns J. P. (1998) Syndrome of facial, oral, and digital anomalies due to 7q21.2-->q22.1 duplication. *Am J Med Genet* **80,** 454-458.

Luscher B. and Keller C. A. (2001) Ubiquitination, proteasomes and GABA(A) receptors. *Nat Cell Biol* **3,** E232-233.

Lyles M. M. and Gilbert H. F. (1991) Catalysis of the oxidative folding of ribonuclease A by protein disulfide isomerase: pre-steady-state kinetics and the utilization of the oxidizing equivalents of the isomerase. *Biochemistry* **30,** 619-625.

Lynch G., Halpain S. and Baudry M. (1982) Effects of high-frequency synaptic stimulation on glumate receptor binding studied with a modified in vitro hippocampal slice preparation. *Brain Res* **244,** 101-111.

Lynch G., Larson J., Kelso S., Barrionuevo G. and Schottler F. (1983) Intracellular injections of EGTA block induction of hippocampal long-term potentiation. *Nature* **305,** 719-721.

Maas C., Tagnaouti N., Loebrich S., Behrend B., Lappe-Siefke C. and Kneussel M. (2006) Neuronal cotransport of glycine receptor and the scaffold protein gephyrin. *J Cell Biol* **172,** 441-451.

MacDonald J. F. and Nowak L. M. (1990) Mechanisms of blockade of excitatory amino acid receptor channels. *Trends Pharmacol Sci* **11,** 167-172.

Madison D. V., Malenka R. C. and Nicoll R. A. (1991) Mechanisms underlying long-term potentiation of synaptic transmission. *Annu Rev Neurosci* **14,** 379-397.

Mages, H. W., Stamminger, T., Rilke, O., Bravo, R. and Kroczek, R. A. (1993) Expression of PILOT, a putative transcription factor, requires two signals and is cyclosporin A sensitive in T cells. *Int Immunol,* **5,** 63-70.

Mah, A. L., Perry, G., Smith, M. A. and Monteiro, M. J. (2000) Identification of ubiquilin, a novel presenilin interactor that increases presenilin protein accumulation. *J Cell Biol,* **151,** 847-862.

Maharjan S., Serova L. and Sabban E. L. (2005) Transcriptional regulation of tyrosine hydroxylase by estrogen: opposite effects with estrogen receptors alpha and beta and interactions with cyclic AMP. *J Neurochem* **93,** 1502-1514.

Malenka R. C., Kauer J. A., Zucker R. S. and Nicoll R. A. (1988) Postsynaptic calcium is sufficient for potentiation of hippocampal synaptic transmission. *Science* **242,** 81-84.

Malenka R. C., Kauer J. A., Perkel D. J., Mauk M. D., Kelly P. T., Nicoll R. A. and Waxham M. N. (1989) An essential role for postsynaptic calmodulin and protein kinase activity in long-term potentiation. *Nature* **340,** 554-557.

Malinow R., Schulman H. and Tsien R. W. (1989) Inhibition of postsynaptic PKC or CaMKII blocks induction but not expression of LTP. *Science* **245,** 862-866.

Malkani S. and Rosen J. B. (2000) Specific induction of early growth response gene 1 in the lateral nucleus of the amygdala following contextual fear conditioning in rats. *Neuroscience* **97,** 693-702.

Malkani S. and Rosen J. B. (2001) N-Methyl-D-aspartate receptor antagonism blocks contextual fear conditioning and differentially regulates early growth response-1 messenger RNA expression in the amygdala: implications for a functional amygdaloid circuit of fear. *Neuroscience* **102,** 853-861.

Malosio M. L., Marqueze-Pouey B., Kuhse J. and Betz H. (1991) Widespread expression of glycine receptor subunit mRNAs in the adult and developing rat brain. *Embo J* **10,** 2401-2409.

Mammen, A. L., Kameyama, K., Roche, K. W. and Huganir, R. L. (1997) Phosphorylation of the alpha-amino-3-hydroxy-5-methylisoxazole4-propionic acid receptor GluR1 subunit by calcium/calmodulin-dependent kinase II. *J Biol Chem,* **272,** 32528-32533.

Mammoto A., Sasaki T., Asakura T., Hotta I., Imamura H., Takahashi K., Matsuura Y., Shirao T. and Takai Y. (1998) Interactions of drebrin and gephyrin with profilin. *Biochem Biophys Res Commun* **243,** 86-89.

Man, H. Y., Wang, Q., Lu, W. Y. et al. (2003) Activation of PI3-kinase is required for AMPA receptor insertion during LTP of mEPSCs in cultured hippocampal neurons

Manabe T., Renner P. and Nicoll R. A. (1992) Postsynaptic contribution to long-term potentiation revealed by the analysis of miniature synaptic currents. *Nature* **355,** 50-55.

Manguoglu E., Berker-Karauzum S., Baumer A., Mihci E., Tacoy S., Luleci G. and Schinzel A. (2005) A case with de novo interstitial deletion of chromosome 7q21.1-q22. *Genet Couns* **16,** 155-159.

Marcotrigiano, J., Gingras, A. C., Sonenberg, N. and Burley, S. K. (1999) Cap-dependent translation initiation in eukaryotes is regulated by a molecular mimic of eIF4G. *Mol Cell,* **3,** 707-716.

Maren S. and Fanselow M. S. (1996) The amygdala and fear conditioning: has the nut been cracked? *Neuron* **16,** 237-240.

Markram H., Helm P. J. and Sakmann B. (1995) Dendritic calcium transients evoked by single back-propagating action potentials in rat neocortical pyramidal neurons. *J Physiol* **485 (Pt 1),** 1-20.

Marsh M. and McMahon H. T. (1999) The structural era of endocytosis. *Science* **285,** 215-220.

Martina, M., Gorfinkel, Y., Halman, S., Lowe, J. A., Periyalwar, P., Schmidt, C. J. and Bergeron, R. (2004) Glycine transporter type 1 blockade changes NMDA receptor-mediated responses and LTP in hippocampal CA1 pyramidal cells by altering extracellular glycine levels. *J Physiol,* **557,** 489-500.

Massey L. K., Mah A. L. and Monteiro M. J. (2005) Ubiquilin regulates presenilin endoproteolysis and modulates gamma-secretase components, Pen-2 and nicastrin. *Biochem J* **391,** 513-525.

Massey L. K., Mah A. L., Ford D. L., Miller J., Liang J., Doong H. and Monteiro M. J. (2004) Overexpression of ubiquilin decreases ubiquitination and degradation of presenilin proteins. *J Alzheimers Dis* **6,** 79-92.

Mathe C., Sagot M. F., Schiex T. and Rouze P. (2002) Current methods of gene prediction, their strengths and weaknesses. *Nucleic Acids Res* **30,** 4103-4117.

Matsuoka M., Kaba H., Mori Y. and Ichikawa M. (1997) Synaptic plasticity in olfactory memory formation in female mice. *Neuroreport* **8,** 2501-2504.

Matthews R. P., Guthrie C. R., Wailes L. M., Zhao X., Means A. R. and McKnight G. S. (1994) Calcium/calmodulin-dependent protein kinase types II and IV differentially regulate CREB-dependent gene expression. *Mol Cell Biol* **14,** 6107-6116.

Matthies H. and Reymann K. G. (1993) Protein kinase A inhibitors prevent the maintenance of hippocampal long-term potentiation. *Neuroreport* **4,** 712-714.

Maura G., Giardi A. and Raiteri M. (1988) Release-regulating D-2 dopamine receptors are located on striatal glutamatergic nerve terminals. *J Pharmacol Exp Ther* **247,** 680-684.

Mayer M. L. and Westbrook G. L. (1987) Permeation and block of N-methyl-D-aspartic acid receptor channels by divalent cations in mouse cultured central neurones. *J Physiol* **394,** 501-527.

McDonald B. J., Amato A., Connolly C. N., Benke D., Moss S. J. and Smart T. G. (1998) Adjacent phosphorylation sites on GABAA receptor beta subunits determine regulation by cAMP-dependent protein kinase. *Nat Neurosci* **1,** 23-28.

McElveen C., Carvajal M. V., Moscatello D., Towner J. and Lacassie Y. (1995) Ectrodactyly and proximal/intermediate interstitial deletion 7q. *Am J Med Genet* **56,** 1-5.

McKernan R. M. and Whiting P. J. (1996) Which GABAA-receptor subtypes really occur in the brain? *Trends Neurosci* **19,** 139-143.

McLennan, H. (1983) Receptors for the excitatory amino acids in the mammalian central nervous system. *Prog Neurobiol,* **20,** 251-271.

McMahon A. P., Champion J. E., McMahon J. A. and Sukhatme V. P. (1990) Developmental expression of the putative transcription factor Egr-1 suggests that Egr-1 and c-fos are coregulated in some tissues. *Development* **108,** 281-287.

Megias M., Emri Z., Freund T. F. and Gulyas A. I. (2001) Total number and distribution of inhibitory and excitatory synapses on hippocampal CA1 pyramidal cells. *Neuroscience* **102,** 527-540.

Meier J. and Grantyn R. (2004) A gephyrin-related mechanism restraining glycine receptor anchoring at GABAergic synapses. *J Neurosci* **24,** 1398-1405.

Meier J., Meunier-Durmort C., Forest C., Triller A. and Vannier C. (2000) Formation of glycine receptor clusters and their accumulation at synapses. *J Cell Sci* **113 (Pt 15),** 2783-2795.

Meier J., Vannier C., Serge A., Triller A. and Choquet D. (2001) Fast and reversible trapping of surface glycine receptors by gephyrin. *Nat Neurosci* **4,** 253-260.

Mello C. V., Vicario D. S. and Clayton D. F. (1992) Song presentation induces gene expression in the songbird forebrain. *Proc Natl Acad Sci U S A* **89,** 6818-6822.

Mello C. V., Velho T. A. and Pinaud R. (2004) Song-induced gene expression: a window on song auditory processing and perception. *Ann N Y Acad Sci* **1016,** 263-281.

Mengual E., Arizti P., Rodrigo J., Gimenez-Amaya J. M. and Castano J. G. (1996) Immunohistochemical distribution and electron microscopic subcellular localization of the proteasome in the rat CNS. *J Neurosci* **16,** 6331-6341.

Meyer G., Kirsch J., Betz H. and Langosch D. (1995) Identification of a gephyrin binding motif on the glycine receptor beta subunit. *Neuron* **15,** 563-572.

Michalik A. and Van Broeckhoven C. (2003) Pathogenesis of polyglutamine disorders: aggregation revisited. *Hum Mol Genet* **12 Spec No 2,** R173-186.

Milbrandt J. (1987) A nerve growth factor-induced gene encodes a possible transcriptional regulatory factor. *Science* **238,** 797-799.

Miles R., Toth K., Gulyas A. I., Hajos N. and Freund T. F. (1996) Differences between somatic and dendritic inhibition in the hippocampus. *Neuron* **16,** 815-823.

Miyamoto E. and Fukunaga K. (1996) A role of Ca2+/calmodulin-dependent protein kinase II in the induction of long-term potentiation in hippocampal CA1 area. *Neurosci Res* **24,** 117-122.

Miyasaka T., Miyasaka J. and Saltiel A. R. (1990) Okadaic acid stimulates the activity of microtubule associated protein kinase in PC-12 pheochromocytoma cells. *Biochem Biophys Res Commun* **168,** 1237-1243.

Mochida H., Sato K., Sasaki S., Yazawa I., Kamino K. and Momose-Sato Y. (2001) Effects of anisomycin on LTP in the hippocampal CA1: long-term analysis using optical recording. *Neuroreport* **12,** 987-991.

Modrek B. and Lee C. (2002) A genomic view of alternative splicing. *Nat Genet* **30,** 13-19.

Mody I. and Pearce R. A. (2004) Diversity of inhibitory neurotransmission through GABA(A) receptors. *Trends Neurosci* **27,** 569-575.

Mody I., De Koninck Y., Otis T. S. and Soltesz I. (1994) Bridging the cleft at GABA synapses in the brain. *Trends Neurosci* **17,** 517-525.

Mokin M. and Keifer J. (2006) Quantitative analysis of immunofluorescent punctate staining of synaptically localized proteins using confocal microscopy and stereology. *J Neurosci Methods* **157,** 218-224.

Montagne J., Stewart M. J., Stocker H., Hafen E., Kozma S. C. and Thomas G. (1999) Drosophila S6 kinase: a regulator of cell size. *Science* **285,** 2126-2129.

Morgan, J. R., Prasad, K., Jin, S., Augustine, G. J. and Lafer, E. M. (2003) Eps15 homology domain-NPF motif interactions regulate clathrin coat assembly during synaptic vesicle recycling. *J Biol Chem,* **278,** 33583-33592.

Morita K., Ebert S. N. and Wong D. L. (1995) Role of transcription factor Egr-1 in phorbol ester-induced phenylethanolamine N-methyltransferase gene expression. *J Biol Chem* **270,** 11161-11167.

Morris B. J. (2004) Neuronal plasticity. In: Molecular biology of the neuron (Davies RW, Morris BJ, eds), Ed 2 pp. 357–386. Oxford: Oxford UP

Morris B. J., Hollt V. and Herz A. (1988) Dopaminergic regulation of striatal proenkephalin mRNA and prodynorphin mRNA: contrasting effects of D1 and D2 antagonists. *Neuroscience* **25,** 525-532.

Mortimore G. E., Miotto G., Venerando R. and Kadowaki M. (1996) Autophagy. *Subcell Biochem* **27,** 93-135.

Moss S. J. and Smart T. G. (2001) Constructing inhibitory synapses. *Nat Rev Neurosci* **2,** 240-250.

Mulkeen D., Anwyl R. and Rowan M. (1988) The effects of external calcium on long-term potentiation in the rat hippocampal slice. *Brain Res* **447,** 234-238.

Mulkey, R.M. and Malenka, R.C. (1992) Mechanisms underlying induction of homosynaptic long-term depression in area CA1 of the hippocampus. *Neuron* **9**, 967–975

Murphy L. O., MacKeigan J. P. and Blenis J. (2004) A network of immediate early gene products propagates subtle differences in mitogen-activated protein kinase signal amplitude and duration. *Mol Cell Biol* **24,** 144-153.

Murphy T. H., Worley P. F. and Baraban J. M. (1991) L-type voltage-sensitive calcium channels mediate synaptic activation of immediate early genes. *Neuron* **7,** 625-635.

Nadershahi A., Fahrenkrug S. C. and Ellis L. B. (2004) Comparison of computational methods for identifying translation initiation sites in EST data. *BMC Bioinformatics* **5,** 14.

N'Diaye E. N. and Brown E. J. (2003) The ubiquitin-related protein PLIC-1 regulates heterotrimeric G protein function through association with Gbetagamma. *J Cell Biol* **163,** 1157-1165.

Neuhoff H., Sassoe-Pognetto M., Panzanelli P., Maas C., Witke W. and Kneussel M. (2005) The actin-binding protein profilin I is localized at synaptic sites in an activity-regulated manner. *Eur J Neurosci* **21,** 15-25.

Nguyen T. V., Kosofsky B. E., Birnbaum R., Cohen B. M. and Hyman S. E. (1992) Differential expression of c-fos and zif268 in rat striatum after haloperidol, clozapine, and amphetamine. *Proc Natl Acad Sci U S A* **89,** 4270-4274.

Nikolaev E., Kaminska B., Tischmeyer W., Matthies H. and Kaczmarek L. (1992) Induction of expression of genes encoding transcription factors in the rat brain elicited by behavioral training. *Brain Res Bull* **28,** 479-484.

Nishikawa T., Ota T. and Isogai T. (2000) Prediction whether a human cDNA sequence contains initiation codon by combining statistical information and similarity with protein sequences. *Bioinformatics* **16,** 960-967.

Nishizaki T., Nomura T., Matsuoka T., Enikolopov G. and Sumikawa K. (1999) Arachidonic acid induces a long-lasting facilitation of hippocampal synaptic transmission by modulating PKC activity and nicotinic ACh receptors. *Brain Res Mol Brain Res* **69,** 263-272.

Noda C., Tanahashi N., Shimbara N., Hendil K. B. and Tanaka K. (2000) Tissue distribution of constitutive proteasomes, immunoproteasomes, and PA28 in rats. *Biochem Biophys Res Commun* **277,** 348-354.

Nohno T., Kasai Y. and Saito T. (1988) Cloning and sequencing of the Escherichia coli chlEN operon involved in molybdopterin biosynthesis. *J Bacteriol* **170,** 4097-4102.

Nong, Y., Huang, Y. Q., Ju, W., Kalia, L. V., Ahmadian, G., Wang, Y. T. and Salter, M. W. (2003) Glycine binding primes NMDA receptor internalization. *Nature,* **422,** 302-307.

Nowak L., Bregestovski P., Ascher P., Herbet A. and Prochiantz A. (1984) Magnesium gates glutamate-activated channels in mouse central neurones. *Nature* **307,** 462-465.

Nusser Z., Cull-Candy S. and Farrant M. (1997) Differences in synaptic GABA(A) receptor number underlie variation in GABA mini amplitude. *Neuron* **19,** 697-709.

Nusser Z., Hajos N., Somogyi P. and Mody I. (1998) Increased number of synaptic GABA(A) receptors underlies potentiation at hippocampal inhibitory synapses. *Nature* **395,** 172-177.

Nusser Z., Naylor D. and Mody I. (2001) Synapse-specific contribution of the variation of transmitter concentration to the decay of inhibitory postsynaptic currents. *Biophys J* **80,** 1251-1261.

Obin M., Mesco E., Gong X., Haas A. L., Joseph J. and Taylor A. (1999) Neurite outgrowth in PC12 cells. Distinguishing the roles of ubiquitylation and ubiquitin-dependent proteolysis. *J Biol Chem* **274,** 11789-11795.

O'Dell T. J., Grant S. G., Karl K., Soriano P. M. and Kandel E. R. (1992) Pharmacological and genetic approaches to the analysis of tyrosine kinase function in long-term potentiation. *Cold Spring Harb Symp Quant Biol* **57,** 517-526.

O'Dell, T. J., Hawkins, R. D., Kandel, E. R. and Arancio, O. (1991) Tests of the roles of two diffusible substances in long-term potentiation: evidence for nitric oxide as a possible early retrograde messenger. *Proc Natl Acad Sci U S A,* **88,** 11285-11289.

O'Sullivan, G. A., Kneussel, M., Elazar, Z. and Betz, H. (2005) GABARAP is not essential for GABA receptor targeting to the synapse. *Eur J Neurosci,* **22,** 2644-2648.

Obin, M., Mesco, E., Gong, X., Haas, A. L., Joseph, J. and Taylor, A. (1999) Neurite outgrowth in PC12 cells. Distinguishing the roles of ubiquitylation and ubiquitin-dependent proteolysis. *J Biol Chem,* **274,** 11789-11795.

Ohno, M., Frankland, P. W., Chen, A. P., Costa, R. M. and Silva, A. J. (2001) Inducible, pharmacogenetic approaches to the study of learning and memory. *Nat Neurosci,* **4,** 1238-1243.

Okuno H. and Miyashita Y. (1996) Expression of the transcription factor Zif268 in the temporal cortex of monkeys during visual paired associate learning. *Eur J Neurosci* **8,** 2118-2128.

Oliet S. H., Malenka R. C. and Nicoll R. A. (1996) Bidirectional control of quantal size by synaptic activity in the hippocampus. *Science* **271,** 1294-1297.

Oliet S. H., Malenka R. C. and Nicoll R. A. (1997) Two distinct forms of long-term depression coexist in CA1 hippocampal pyramidal cells. *Neuron* **18,** 969-982.

Ostroff, L. E., Fiala, J. C., Allwardt, B. and Harris, K. M. (2002) Polyribosomes redistribute from dendritic shafts into spines with enlarged synapses during LTP in developing rat hippocampal slices. *Neuron,* **35,** 535-545.

Otani S., Marshall C. J., Tate W. P., Goddard G. V. and Abraham W. C. (1989) Maintenance of long-term potentiation in rat dentate gyrus requires protein synthesis but not messenger RNA synthesis immediately post-tetanization. *Neuroscience* **28,** 519-526.

Otis T. S., De Koninck Y. and Mody I. (1994) Lasting potentiation of inhibition is associated with an increased number of gamma-aminobutyric acid type A receptors activated during miniature inhibitory postsynaptic currents. *Proc Natl Acad Sci U S A* **91,** 7698-7702.

Otmakhova, N. A., Otmakhov, N., Mortenson, L. H. and Lisman, J. E. (2000) Inhibition of the cAMP pathway decreases early long-term potentiation at CA1 hippocampal synapses. *J Neurosci,* **20,** 4446-4451.

Ozaki, T., Hishiki, T., Toyama, Y., Yuasa, S., Nakagawara, A. and Sakiyama, S. (1997a) Identification of a new cellular protein that can interact specifically with DAN. *DNA Cell Biol,* **16,** 985-991.

Ozaki T., Kondo K., Nakamura Y., Ichimiya S., Nakagawara A. and Sakiyama S. (1997b) Interaction of DA41, a DAN-binding protein, with the epidermal growth factor-like protein, S(1-5). *Biochem Biophys Res Commun* **237,** 245-250.

Paarmann I., Saiyed T., Schmitt B. and Betz H. (2006) Gephyrin: does splicing affect its function? *Biochem Soc Trans* **34,** 45-47.

Pak, D. T. and Sheng, M. (2003) Targeted protein degradation and synapse remodeling by an inducible protein kinase. *Science,* **302,** 1368-1373.

Papanikolaou N. A. and Sabban E. L. (1999) Sp1/Egr1 motif: a new candidate in the regulation of rat tyrosine hydroxylase gene transcription by immobilization stress. *J Neurochem* **73,** 433-436.

Papanikolaou N. A. and Sabban E. L. (2000) Ability of Egr1 to activate tyrosine hydroxylase transcription in PC12 cells. Cross-talk with AP-1 factors. *J Biol Chem* **275,** 26683-26689.

Parker J. C. and Colclasure G. C. (1992) Macromolecular crowding and volume perception in dog red cells. *Mol Cell Biochem* **114,** 9-11.

Partridge, J. G., Tang, K. C. and Lovinger, D. M. (2000) Regional and postnatal heterogeneity of activity-dependent long-term changes in synaptic efficacy in the dorsal striatum. *J Neurophysiol,* **84,** 1422-1429.

Patel N., Hitzemann B. and Hitzemann R. (1998) Genetics, haloperidol, and the Fos response in the basal ganglia: a comparison of the C57BL/6J and DBA/2J inbred mouse strains. *Neuropsychopharmacology* **18,** 480-491.

Patrick G. N., Bingol B., Weld H. A. and Schuman E. M. (2003) Ubiquitin-mediated proteasome activity is required for agonist-induced endocytosis of GluRs. *Curr Biol* **13,** 2073-2081.

Patterson, S. L., Pittenger, C., Morozov, A., Martin, K. C., Scanlin, H., Drake, C. and Kandel, E. R. (2001) Some forms of cAMP-mediated long-lasting potentiation are associated with release of BDNF and nuclear translocation of phospho-MAP kinase. *Neuron,* **32,** 123-140.

Patwardhan, S., Gashler, A., Siegel, M. G., Chang, L. C., Joseph, L. J., Shows, T. B., Le Beau, M. M. and Sukhatme, V. P. (1991) EGR3, a novel member of the Egr family of genes encoding immediate-early transcription factors. *Oncogene,* **6,** 917-928.

Peran M., Hicks B. W., Peterson N. L., Hooper H. and Salas R. (2001) Lateral mobility and anchoring of recombinant GABAA receptors depend on subunit composition. *Cell Motil Cytoskeleton* **50,** 89-100.

Petersohn D., Schoch S., Brinkmann D. R. and Thiel G. (1995) The human synapsin II gene promoter. Possible role for the transcription factor zif268/egr-1, polyoma enhancer activator 3, and AP2. *J Biol Chem* **270,** 24361-24369.

Petrini E. M., Marchionni I., Zacchi P., Sieghart W. and Cherubini E. (2004) Clustering of extrasynaptic GABA(A) receptors modulates tonic inhibition in cultured hippocampal neurons. *J Biol Chem* **279,** 45833-45843.

Pettit D. L., Perlman S. and Malinow R. (1994) Potentiated transmission and prevention of further LTP by increased CaMKII activity in postsynaptic hippocampal slice neurons. *Science* **266,** 1881-1885.

Pfeiffer F., Graham D. and Betz H. (1982) Purification by affinity chromatography of the glycine receptor of rat spinal cord. *J Biol Chem* **257,** 9389-9393.

Pignatelli M., Luna-Medina R., Perez-Rendon A., Santos A. and Perez-Castillo A. (2003) The transcription factor early growth response factor-1 (EGR-1) promotes apoptosis of neuroblastoma cells. *Biochem J* **373,** 739-746.

Polo, S., Sigismund, S., Faretta, M., Guidi, M., Capua, M. R., Bossi, G., Chen, H., De Camilli, P. and Di Fiore, P. P. (2002) A single motif responsible for ubiquitin recognition and monoubiquitination in endocytic proteins. *Nature,* **416,** 451-455.

Price D. L., Tanzi R. E., Borchelt D. R. and Sisodia S. S. (1998) Alzheimer's disease: genetic studies and transgenic models. *Annu Rev Genet* **32,** 461-493.

Prior P., Schmitt B., Grenningloh G., Pribilla I., Multhaup G., Beyreuther K., Maulet Y., Werner P., Langosch D., Kirsch J. and et al. (1992) Primary structure and alternative splice variants of gephyrin, a putative glycine receptor-tubulin linker protein. *Neuron* **8,** 1161-1170.

Quinones, A., Dobberstein, K. U. and Rainov, N. G. (2003) The egr-1 gene is induced by DNA-damaging agents and non-genotoxic drugs in both normal and neoplastic human cells. *Life Sci,* **72,** 2975-2992.

Qureshi S. A., Rim M., Bruder J., Kolch W., Rapp U., Sukhatme V. P. and Foster D. A. (1991) An inhibitory mutant of c-Raf-1 blocks v-Src-induced activation of the Egr-1 promoter. *J Biol Chem* **266,** 20594-20597.

Raasi S. and Pickart C. M. (2003) Rad23 ubiquitin-associated domains (UBA) inhibit 26 S proteasome-catalyzed proteolysis by sequestering lysine 48-linked polyubiquitin chains. *J Biol Chem* **278,** 8951-8959.

Racine R. J., Milgram N. W. and Hafner S. (1983) Long-term potentiation phenomena in the rat limbic forebrain. *Brain Res* **260,** 217-231.

Radimerski, T., Montagne, J., Rintelen, F., Stocker, H., van der Kaay, J., Downes, C. P., Hafen, E. and Thomas, G. (2002) dS6K-regulated cell growth is dPKB/dPI(3)K-independent, but requires dPDK1. *Nat Cell Biol,* **4,** 251-255.

Rakhit S., Clark C. J., O'Shaughnessy C T. and Morris B. J. (2005) N-methyl-D-aspartate and brain-derived neurotrophic factor induce distinct profiles of extracellular signal-regulated kinase, mitogen- and stress-activated kinase, and ribosomal s6 kinase phosphorylation in cortical neurons. *Mol Pharmacol* **67,** 1158-1165.

Ramakers G. M. and Storm J. F. (2002) A postsynaptic transient K(+) current modulated by arachidonic acid regulates synaptic integration and threshold for LTP induction in hippocampal pyramidal cells. *Proc Natl Acad Sci U S A* **99,** 10144-10149.

Ramirez S., Ait-Si-Ali S., Robin P., Trouche D. and Harel-Bellan A. (1997) The CREB-binding protein (CBP) cooperates with the serum response factor for transactivation of the c-fos serum response element. *J Biol Chem* **272,** 31016-31021.

Ramming M., Betz H. and Kirsch J. (1997) Analysis of the promoter region of the murine gephyrin gene. *FEBS Lett* **405,** 137-140.

Ramming, M., Kins, S., Werner, N., Hermann, A., Betz, H. and Kirsch, J. (2000) Diversity and phylogeny of gephyrin: tissue-specific splice variants, gene structure, and sequence similarities to molybdenum cofactor-synthesizing and cytoskeleton-associated proteins. *Proc Natl Acad Sci U S A,* **97,** 10266-10271.

Ratovitski T., Slunt H. H., Thinakaran G., Price D. L., Sisodia S. S. and Borchelt D. R. (1997) Endoproteolytic processing and stabilization of wild-type and mutant presenilin. *J Biol Chem* **272,** 24536-24541.

Raught B., Gingras A. C. and Sonenberg N. (2001) The target of rapamycin (TOR) proteins. *Proc Natl Acad Sci U S A* **98,** 7037-7044.

Rees, M. I., Andrew, M., Jawad, S. and Owen, M. J. (1994) Evidence for recessive as well as dominant forms of startle disease (hyperekplexia) caused by mutations in the alpha 1 subunit of the inhibitory glycine receptor. *Hum Mol Genet,* **3,** 2175-2179.

Rees, M. I., Harvey, K., Ward, H. et al. (2003) Isoform heterogeneity of the human gephyrin gene (GPHN), binding domains to the glycine receptor, and mutation analysis in hyperekplexia. *J Biol Chem,* **278,** 24688-24696.

Rees, M. I., Lewis, T. M., Kwok, J. B., Mortier, G. R., Govaert, P., Snell, R. G., Schofield, P. R. and Owen, M. J. (2002) Hyperekplexia associated with compound heterozygote mutations in the beta-subunit of the human inhibitory glycine receptor (GLRB). *Hum Mol Genet,* **11,** 853-860.

Regan-Klapisz, E., Sorokina, I., Voortman, J. et al. (2005) Ubiquilin recruits Eps15 into ubiquitin-rich cytoplasmic aggregates via a UIM-UBL interaction. *J Cell Sci,* **118,** 4437-4450.

Regehr W. G. and Tank D. W. (1990) Postsynaptic NMDA receptor-mediated calcium accumulation in hippocampal CA1 pyramidal cell dendrites. *Nature* **345,** 807-810.

Reinhard M., Halbrugge M., Scheer U., Wiegand C., Jockusch B. M. and Walter U. (1992) The 46/50 kDa phosphoprotein VASP purified from human platelets is a novel protein associated with actin filaments and focal contacts. *Embo J* **11,** 2063-2070.

Reinhard M., Giehl K., Abel K., Haffner C., Jarchau T., Hoppe V., Jockusch B. M. and Walter U. (1995) The proline-rich focal adhesion and microfilament protein VASP is a ligand for profilins. *Embo J* **14,** 1583-1589.

Reiss J., Gross-Hardt S., Christensen E., Schmidt P., Mendel R. R. and Schwarz G. (2001) A mutation in the gene for the neurotransmitter receptor-clustering protein gephyrin causes a novel form of molybdenum cofactor deficiency. *Am J Hum Genet* **68,** 208-213.

Rensink A. A., Gellekink H., Otte-Holler I., ten Donkelaar H. J., de Waal R. M., Verbeek M. M. and Kremer B. (2002) Expression of the cytokine leukemia inhibitory factor and pro-apoptotic insulin-like growth factor binding protein-3 in Alzheimer's disease. *Acta Neuropathol (Berl)* **104,** 525-533.

Ressler K. J., Paschall G., Zhou X. L. and Davis M. (2002) Regulation of synaptic plasticity genes during consolidation of fear conditioning. *J Neurosci* **22,** 7892-7902.

Reymann K. G., Schulzeck K., Kase H. and Matthies H. (1988) Phorbol ester-induced hippocampal long-term potentiation is counteracted by inhibitors of protein kinase C. *Exp Brain Res* **71,** 227-230.

Reynolds J. N., Hyland B. I. and Wickens J. R. (2001) A cellular mechanism of reward-related learning. *Nature* **413,** 67-70.

Reynolds J. N. and Wickens J. R. (2000) Substantia nigra dopamine regulates synaptic plasticity and membrane potential fluctuations in the rat neostriatum, in vivo. *Neuroscience* **99,** 199-203.

Rezvani K., Mee M., Dawson S., McIlhinney J., Fujita J. and Mayer R. J. (2003) Proteasomal interactors control activities as diverse as the cell cycle and glutaminergic neurotransmission. *Biochem Soc Trans* **31,** 470-473.

Richardson C. L., Tate W. P., Mason S. E., Lawlor P. A., Dragunow M. and Abraham W. C. (1992) Correlation between the induction of an immediate

early gene, zif/268, and long-term potentiation in the dentate gyrus. *Brain Res* **580,** 147-154.

Richly H., Rape M., Braun S., Rumpf S., Hoege C. and Jentsch S. (2005) A series of ubiquitin binding factors connects CDC48/p97 to substrate multiubiquitylation and proteasomal targeting. *Cell* **120,** 73-84.

Richter-Levin G. and Segal M. (1988) Serotonin releasers modulate reactivity of the rat hippocampus to afferent stimulation. *Neurosci Lett* **94,** 173-176.

Riezman H. (2002) Cell biology: the ubiquitin connection. *Nature* **416,** 381-383.

Rigby, M., Le Bourdelles, B., Heavens, R. P. et al. (1996) The messenger RNAs for the N-methyl-D-aspartate receptor subunits show region-specific expression of different subunit composition in the human brain. *Neuroscience,* **73,** 429-447.

Roberts L. A., Higgins M. J., O'Shaughnessy C. T., Stone T. W. and Morris B. J. (1996) Changes in hippocampal gene expression associated with the induction of long-term potentiation. *Brain Res Mol Brain Res* **42,** 123-127.

Rodriguez M. J., Robledo P., Andrade C. and Mahy N. (2005) In vivo co-ordinated interactions between inhibitory systems to control glutamate-mediated hippocampal excitability. *J Neurochem* **95,** 651-661.

Roehm N. W., Rodgers G. H., Hatfield S. M. and Glasebrook A. L. (1991) An improved colorimetric assay for cell proliferation and viability utilizing the tetrazolium salt XTT. *J. Immunol. Methods* **142,**257-265

Rogan M. T. and LeDoux J. E. (1996) Emotion: systems, cells, synaptic plasticity. *Cell* **85,** 469-475.

Rogan M. T., Staubli U. V. and LeDoux J. E. (1997) Fear conditioning induces associative long-term potentiation in the amygdala. *Nature* **390,** 604-607.

Rogozin I. B., Kochetov A. V., Kondrashov F. A., Koonin E. V. and Milanesi L. (2001) Presence of ATG triplets in 5' untranslated regions of eukaryotic cDNAs correlates with a 'weak' context of the start codon. *Bioinformatics* **17,** 890-900.

Rolls E. T., Baylis G. C., Hasselmo M. E. and Nalwa V. (1989) The effect of learning on the face selective responses of neurons in the cortex in the superior temporal sulcus of the monkey. *Exp Brain Res* **76,** 153-164.

Rosenberg M., Meier J., Triller A. and Vannier C. (2001) Dynamics of glycine receptor insertion in the neuronal plasma membrane. *J Neurosci* **21,** 5036-5044.

Rosenblum, K., Futter, M., Voss, K., Erent, M., Skehel, P. A., French, P., Obosi, L., Jones, M. W. and Bliss, T. V. (2002) The role of extracellular regulated kinases I/II in late-phase long-term potentiation. *J Neurosci,* **22,** 5432-5441.

Rosenmund C., Clements J. D. and Westbrook G. L. (1993) Nonuniform probability of glutamate release at a hippocampal synapse. *Science* **262,** 754-757.

Rusanescu, G., Qi, H., Thomas, S. M., Brugge, J. S. and Halegoua, S. (1995) Calcium influx induces neurite growth through a Src-Ras signaling cassette. *Neuron,* **15,** 1415-1425.

Russo M. W., Sevetson B. R. and Milbrandt J. (1995) Identification of NAB1, a repressor of NGFI-A- and Krox20-mediated transcription. *Proc Natl Acad Sci U S A* **92,** 6873-6877.

Sabatini B. L., Oertner T. G. and Svoboda K. (2002) The life cycle of Ca(2+) ions in dendritic spines. *Neuron* **33,** 439-452.

Sabatini D. M., Barrow R. K., Blackshaw S., Burnett P. E., Lai M. M., Field M. E., Bahr B. A., Kirsch J., Betz H. and Snyder S. H. (1999) Interaction of RAFT1 with gephyrin required for rapamycin-sensitive signaling. *Science* **284,** 1161-1164.

Sabatini, D. M., Erdjument-Bromage, H., Lui, M., Tempst, P. and Snyder, S. H. (1994) RAFT1: a mammalian protein that binds to FKBP12 in a rapamycin-dependent fashion and is homologous to yeast TORs. *Cell,* **78,** 35-43.

Sabers, C. J., Martin, M. M., Brunn, G. J., Williams, J. M., Dumont, F. J., Wiederrecht, G. and Abraham, R. T. (1995) Isolation of a protein target of the FKBP12-rapamycin complex in mammalian cells. *J Biol Chem,* **270,** 815-822.

Saeki Y., Sone T., Toh-e A. and Yokosawa H. (2002) Identification of ubiquitin-like protein-binding subunits of the 26S proteasome. *Biochem Biophys Res Commun* **296,** 813-819.

Sakamoto K. M., Bardeleben C., Yates K. E., Raines M. A., Golde D. W. and Gasson J. C. (1991) 5' upstream sequence and genomic structure of the human primary response gene, EGR-1/TIS8. *Oncogene* **6,** 867-871.

Salin P.A., Malenka R.C., Nicoll R.A. (1996) Cyclic AMP mediates a presynaptic form of LTP at cerebellar parallel fiber synapses. *Neuron*. **16**(4):797-803

Salin, H., Maurin, Y., Davis, S., Laroche, S., Mallet, J. and Dumas, S. (2002) Spatio-temporal heterogeneity and cell-specificity of long-term potentiation-induced mRNA expression in the dentate gyrus in vivo. *Neuroscience,* **110,** 227-236.

Salvador-Silva M., Ricard C. S., Agapova O. A., Yang P. and Hernandez M. R. (2001) Expression of small heat shock proteins and intermediate filaments in the human optic nerve head astrocytes exposed to elevated hydrostatic pressure in vitro. *J Neurosci Res* **66,** 59-73.

Sarker K. P. and Lee K. Y. (2004) L6 myoblast differentiation is modulated by Cdk5 via the PI3K-AKT-p70S6K signaling pathway. *Oncogene* **23,** 6064-6070.

Sassoe-Pognetto M. and Wassle H. (1997) Synaptogenesis in the rat retina: subcellular localization of glycine receptors, GABA(A) receptors, and the anchoring protein gephyrin. *J Comp Neurol* **381,** 158-174.

Sassoe-Pognetto M., Panzanelli P., Sieghart W. and Fritschy J. M. (2000) Colocalization of multiple GABA(A) receptor subtypes with gephyrin at postsynaptic sites. *J Comp Neurol* **420,** 481-498.

Sassoe-Pognetto M., Kirsch J., Grunert U., Greferath U., Fritschy J. M., Mohler H., Betz H. and Wassle H. (1995) Colocalization of gephyrin and GABAA-receptor subunits in the rat retina. *J Comp Neurol* **357,** 1-14.

Sassone-Corsi, P., Mizzen, C. A., Cheung, P., Crosio, C., Monaco, L., Jacquot, S., Hanauer, A. and Allis, C. D. (1999) Requirement of Rsk-2 for epidermal growth factor-activated phosphorylation of histone H3. *Science,* **285,** 886-891.

Scanziani M. (2000) GABA spillover activates postsynaptic GABA(B) receptors to control rhythmic hippocampal activity. *Neuron* **25,** 673-681.

Schafe G. E., Atkins C. M., Swank M. W., Bauer E. P., Sweatt J. D. and LeDoux J. E. (2000) Activation of ERK/MAP kinase in the amygdala is required for memory consolidation of pavlovian fear conditioning. *J Neurosci* **20,** 8177-8187.

Scherer S. W., Cheung J., MacDonald J. R., Osborne L. R., Nakabayashi K., Herbrick J. A., Carson A. R., Parker-Katiraee L., Skaug J., Khaja R., Zhang J., Hudek A. K., Li M., Haddad M., Duggan G. E., Fernandez B. A., Kanematsu E., Gentles S., Christopoulos C. C., Choufani S., Kwasnicka D., Zheng X. H., Lai Z., Nusskern D., Zhang Q., Gu Z., Lu F., Zeesman S., Nowaczyk M. J., Teshima I., Chitayat D., Shuman C., Weksberg R., Zackai E. H., Grebe T. A., Cox S. R., Kirkpatrick S. J., Rahman N., Friedman J. M., Heng H. H., Pelicci P. G., Lo-Coco F., Belloni E., Shaffer L. G., Pober B., Morton C. C., Gusella J. F., Bruns G. A., Korf B. R., Quade B. J., Ligon A.

H., Ferguson H., Higgins A. W., Leach N. T., Herrick S. R., Lemyre E., Farra C. G., Kim H. G., Summers A. M., Gripp K. W., Roberts W., Szatmari P., Winsor E. J., Grzeschik K. H., Teebi A., Minassian B. A., Kere J., Armengol L., Pujana M. A., Estivill X., Wilson M. D., Koop B. F., Tosi S., Moore G. E., Boright A. P., Zlotorynski E., Kerem B., Kroisel P. M., Petek E., Oscier D. G., Mould S. J., Dohner H., Dohner K., Rommens J. M., Vincent J. B., Venter J. C., Li P. W., Mural R. J., Adams M. D. and Tsui L. C. (2003) Human chromosome 7: DNA sequence and biology. *Science* **300,** 767-772.

Scherzinger, E., Lurz, R., Turmaine, M. et al. (1997) Huntingtin-encoded polyglutamine expansions form amyloid-like protein aggregates in vitro and in vivo. *Cell,* **90,** 549-558.

Schlingensiepen K. H., Luno K. and Brysch W. (1991) High basal expression of the zif/268 immediate early gene in cortical layers IV and VI, in CA1 and in the corpus striatum--an in situ hybridization study. *Neurosci Lett* **122,** 67-70.

Schmelzle T. and Hall M. N. (2000) TOR, a central controller of cell growth. *Cell* **103,** 253-262.

Schmitt B., Knaus P., Becker C. M. and Betz H. (1987) The Mr 93,000 polypeptide of the postsynaptic glycine receptor complex is a peripheral membrane protein. *Biochemistry* **26,** 805-811.

Schniepp, R., Kohler, K., Ladewig, T. et al. (2004) Retinal colocalization and in vitro interaction of the glutamate transporter EAAT3 and the serum- and glucocorticoid-inducible kinase SGK1 [correction]. *Invest Ophthalmol Vis Sci,* **45,** 1442-1449.

Schoenherr, C. J. and Anderson, D. J. (1995) The neuron-restrictive silencer factor (NRSF): a coordinate repressor of multiple neuron-specific genes. *Science,* **267,** 1360-1363.

Schoenherr, C. J., Paquette, A. J. and Anderson, D. J. (1996) Identification of potential target genes for the neuron-restrictive silencer factor. *Proc Natl Acad Sci U S A,* **93,** 9881-9886.

Schrader N., Kim E. Y., Winking J., Paulukat J., Schindelin H. and Schwarz G. (2004) Biochemical characterization of the high affinity binding between the glycine receptor and gephyrin. *J Biol Chem* **279,** 18733-18741.

Schultz W. (2002) Getting formal with dopamine and reward. *Neuron* **36,** 241-263.

Schuman E. M. (1997) Synapse specificity and long-term information storage. *Neuron* **18,** 339-342.

Schwab, M. S., Kim, S. H., Terada, N., Edfjall, C., Kozma, S. C., Thomas, G. and Maller, J. L. (1999) p70(S6K) controls selective mRNA translation during oocyte maturation and early embryogenesis in Xenopus laevis. *Mol Cell Biol,* **19,** 2485-2494.

Schwachtgen J. L., Campbell C. J. and Braddock M. (2000) Full promoter sequence of human early growth response factor-1 (Egr-1): demonstration of a fifth functional serum response element. *DNA Seq* **10,** 429-432.

Schwarz G., Schrader N., Mendel R. R., Hecht H. J. and Schindelin H. (2001) Crystal structures of human gephyrin and plant Cnx1 G domains: comparative analysis and functional implications. *J Mol Biol* **312,** 405-418.

Schweizer C., Balsiger S., Bluethmann H., Mansuy I. M., Fritschy J. M., Mohler H. and Luscher B. (2003) The gamma 2 subunit of GABA(A) receptors is required for maintenance of receptors at mature synapses. *Mol Cell Neurosci* **24,** 442-450.

Scotti A. L. and Reuter H. (2001) Synaptic and extrasynaptic gamma -aminobutyric acid type A receptor clusters in rat hippocampal cultures during development. *Proc Natl Acad Sci U S A* **98,** 3489-3494.

Seitanidou T., Nicola M. A., Triller A. and Korn H. (1992) Partial glycinergic denervation induces transient changes in the distribution of a glycine receptor-associated protein in a central neuron. *J Neurosci* **12,** 116-131.

Selcher, J. C., Atkins, C. M., Trzaskos, J. M., Paylor, R. and Sweatt, J. D. (1999) A necessity for MAP kinase activation in mammalian spatial learning. *Learn Mem,* **6,** 478-490.

Selcher, J. C., Weeber, E. J., Christian, J., Nekrasova, T., Landreth, G. E. and Sweatt, J. D. (2003) A role for ERK MAP kinase in physiologic temporal integration in hippocampal area CA1. *Learn Mem,* **10,** 26-39.

Semyanov A., Walker M. C., Kullmann D. M. and Silver R. A. (2004) Tonically active GABA A receptors: modulating gain and maintaining the tone. *Trends Neurosci* **27,** 262-269.

Sgambato, V., Pages, C., Rogard, M., Besson, M. J. and Caboche, J. (1998) Extracellular signal-regulated kinase (ERK) controls immediate early gene induction on corticostriatal stimulation. *J Neurosci,* **18,** 8814-8825.

Shen K. and Meyer T. (1999) Dynamic control of CaMKII translocation and localization in hippocampal neurons by NMDA receptor stimulation. *Science* **284,** 162-166.

Shen Y. and Linden D. J. (2005) Long-term potentiation of neuronal glutamate transporters. *Neuron* **46,** 715-722.

Shiang, R., Ryan, S. G., Zhu, Y. Z., Hahn, A. F., O'Connell, P. and Wasmuth, J. J. (1993) Mutations in the alpha 1 subunit of the inhibitory glycine receptor cause the dominant neurologic disorder, hyperekplexia. *Nat Genet,* **5,** 351-358.

Shimojo M. and Hersh L. B. (2006) Characterization of the REST/NRSF-interacting LIM domain protein (RILP): localization and interaction with REST/NRSF. *J Neurochem* **96,** 1130-1138.

Sidrauski C., Chapman R. and Walter P. (1998) The unfolded protein response: an intracellular signalling pathway with many surprising features. *Trends Cell Biol* **8,** 245-249.

Silva A. J., Paylor R., Wehner J. M. and Tonegawa S. (1992) Impaired spatial learning in alpha-calcium-calmodulin kinase II mutant mice. *Science* **257,** 206-211.

Simpson C. S. and Morris B. J. (1994) Haloperidol and fluphenazine induce junB gene expression in rat striatum and nucleus accumbens. *J Neurochem* **63,** 1955-1961.

Slifer M. A., Martin E. R., Bronson P. G., Browning-Large C., Doraiswamy P. M., Welsh-Bohmer K. A., Gilbert J. R., Haines J. L. and Pericak-Vance M. A. (2006) Lack of association between UBQLN1 and Alzheimer disease. *Am J Med Genet B Neuropsychiatr Genet* **141,** 208-213.

Smart T. G. (1997) Regulation of excitatory and inhibitory neurotransmitter-gated ion channels by protein phosphorylation. *Curr Opin Neurobiol* **7,** 358-367.

Smemo, S., Nowotny, P., Hinrichs, A. L. et al. (2006) Ubiquilin 1 polymorphisms are not associated with late-onset Alzheimer's disease. *Ann Neurol,* **59,** 21-26.

Sohn R. H. and Goldschmidt-Clermont P. J. (1994) Profilin: at the crossroads of signal transduction and the actin cytoskeleton. *Bioessays* **16,** 465-472.

Sola M., Kneussel M., Heck I. S., Betz H. and Weissenhorn W. (2001) X-ray crystal structure of the trimeric N-terminal domain of gephyrin. *J Biol Chem* **276,** 25294-25301.

Sola M., Bavro V. N., Timmins J., Franz T., Ricard-Blum S., Schoehn G., Ruigrok R. W., Paarmann I., Saiyed T., O'Sullivan G. A., Schmitt B., Betz H. and Weissenhorn W. (2004) Structural basis of dynamic glycine receptor clustering by gephyrin. *Embo J* **23,** 2510-2519.

Somogyi P., Tamas G., Lujan R. and Buhl E. H. (1998) Salient features of synaptic organisation in the cerebral cortex. *Brain Res Brain Res Rev* **26,** 113-135.

Sontag E., Fedorov S., Kamibayashi C., Robbins D., Cobb M. and Mumby M. (1993) The interaction of SV40 small tumor antigen with protein phosphatase 2A stimulates the map kinase pathway and induces cell proliferation. *Cell* **75,** 887-897.

Sossin W. S. (1996) Mechanisms for the generation of synapse specificity in long-term memory: the implications of a requirement for transcription. *Trends Neurosci* **19,** 215-218.

Spanakis, E. (1993) Problems related to the interpretation of autoradiographic data on gene expression using common constitutive transcripts as controls. *Nucleic Acids Res,* **21,** 3809-3819.

Spanakis, E. and Brouty-Boye, D. (1994) Evaluation of quantitative variation in gene expression. *Nucleic Acids Res,* **22,** 799-806.

Speese S. D., Trotta N., Rodesch C. K., Aravamudan B. and Broadie K. (2003) The ubiquitin proteasome system acutely regulates presynaptic protein turnover and synaptic efficacy. *Curr Biol* **13,** 899-910.

Squire L. R., Davis H. P. and Spanis C. W. (1980) Neurobiology of amnesia. *Science* **209,** 836-837.

Srivastava S., Weitzmann M. N., Kimble R. B., Rizzo M., Zahner M., Milbrandt J., Ross F. P. and Pacifici R. (1998) Estrogen blocks M-CSF gene expression and osteoclast formation by regulating phosphorylation of Egr-1 and its interaction with Sp-1. *J Clin Invest* **102,** 1850-1859.

Stallmeyer, B., Nerlich, A., Schiemann, J., Brinkmann, H. and Mendel, R. R. (1995) Molybdenum co-factor biosynthesis: the Arabidopsis thaliana cDNA cnx1 encodes a multifunctional two-domain protein homologous to a mammalian neuroprotein, the insect protein Cinnamon and three Escherichia coli proteins. *Plant J,* **8,** 751-762.

Stallmeyer B., Schwarz G., Schulze J., Nerlich A., Reiss J., Kirsch J. and Mendel R. R. (1999) The neurotransmitter receptor-anchoring protein gephyrin reconstitutes molybdenum cofactor biosynthesis in bacteria, plants, and mammalian cells. *Proc Natl Acad Sci U S A* **96,** 1333-1338.

Stanton P. K. and Sarvey J. M. (1984) Blockade of long-term potentiation in rat hippocampal CA1 region by inhibitors of protein synthesis. *J Neurosci* **4,** 3080-3088.

Strack S., Choi S., Lovinger D. M. and Colbran R. J. (1997) Translocation of autophosphorylated calcium/calmodulin-dependent protein kinase II to the postsynaptic density. *J Biol Chem* **272,** 13467-13470.

Strack S., McNeill R. B. and Colbran R. J. (2000) Mechanism and regulation of calcium/calmodulin-dependent protein kinase II targeting to the NR2B subunit of the N-methyl-D-aspartate receptor. *J Biol Chem* **275,** 23798-23806.

Strausberg R. L., Feingold E. A., Grouse L. H., Derge J. G., Klausner R. D., Collins F. S., Wagner L., Shenmen C. M., Schuler G. D., Altschul S. F., Zeeberg B., Buetow K. H., Schaefer C. F., Bhat N. K., Hopkins R. F., Jordan H., Moore T., Max S. I., Wang J., Hsieh F., Diatchenko L., Marusina K., Farmer A. A., Rubin G. M., Hong L., Stapleton M., Soares M. B., Bonaldo M. F., Casavant T. L., Scheetz T. E., Brownstein M. J., Usdin T. B., Toshiyuki S., Carninci P., Prange C., Raha S. S., Loquellano N. A., Peters G. J., Abramson R. D., Mullahy S. J., Bosak S. A., McEwan P. J., McKernan K. J., Malek J. A., Gunaratne P. H., Richards S., Worley K. C., Hale S., Garcia A. M., Gay L. J., Hulyk S. W., Villalon D. K., Muzny D. M., Sodergren E. J., Lu X., Gibbs R. A., Fahey J., Helton E., Ketteman M., Madan A., Rodrigues S., Sanchez A., Whiting M., Young A. C., Shevchenko

Y., Bouffard G. G., Blakesley R. W., Touchman J. W., Green E. D., Dickson M. C., Rodriguez A. C., Grimwood J., Schmutz J., Myers R. M., Butterfield Y. S., Krzywinski M. I., Skalska U., Smailus D. E., Schnerch A., Schein J. E., Jones S. J. and Marra M. A. (2002) Generation and initial analysis of more than 15,000 full-length human and mouse cDNA sequences. *Proc Natl Acad Sci U S A* **99,** 16899-16903.

Suggs S. V., Katzowitz J. L., Tsai-Morris C. and Sukhatme V. P. (1990) cDNA sequence of the human cellular early growth response gene Egr-1. *Nucleic Acids Res* **18,** 4283.

Sukhatme, V. P., Cao, X. M., Chang, L. C. et al. (1988) A zinc finger-encoding gene coregulated with c-fos during growth and differentiation, and after cellular depolarization. *Cell,* **53,** 37-43.

Surmeier D. J., Song W. J. and Yan Z. (1996) Coordinated expression of dopamine receptors in neostriatal medium spiny neurons. *J Neurosci* **16,** 6579-6591.

Suzuki K., Sato M., Morishima Y. and Nakanishi S. (2005) Neuronal depolarization controls brain-derived neurotrophic factor-induced upregulation of NR2C NMDA receptor via calcineurin signaling. *J Neurosci* **25,** 9535-9543.

Svaren, J., Sevetson, B. R., Apel, E. D., Zimonjic, D. B., Popescu, N. C. and Milbrandt, J. (1996) NAB2, a corepressor of NGFI-A (Egr-1) and Krox20, is induced by proliferative and differentiative stimuli. *Mol Cell Biol,* **16,** 3545-3553.

Swirnoff A. H. and Milbrandt J. (1995) DNA-binding specificity of NGFI-A and related zinc finger transcription factors. *Mol Cell Biol* **15,** 2275-2287.

Tachibana K., Scheuer P. J., Tsukitani Y., Kikuchi H., Van Engen D., Clardy J., Gopichand Y. and Schmitz F. J. (1981) Okadaic acid, a cytotoxic polyether from two marine sponges of the genus Halichondria. *J. Am. Chem. Soc.* **103,** 2469-2471.

Takagi M. and Yamamoto C. (1981) The long-lasting inhibition recorded in vitro from the lateral nucleus of the amygdala. *Brain Res* **206,** 474-478.

Takeuchi J., Fujimuro M., Yokosawa H., Tanaka K. and Toh-e A. (1999) Rpn9 is required for efficient assembly of the yeast 26S proteasome. *Mol Cell Biol* **19,** 6575-6584.

Tan, S. E., Wenthold, R. J. and Soderling, T. R. (1994) Phosphorylation of AMPA-type glutamate receptors by calcium/calmodulin-dependent protein kinase II and protein kinase C in cultured hippocampal neurons. *J Neurosci,* **14,** 1123-1129.

Tanaka, S., Uehara, T. and Nomura, Y. (2000) Up-regulation of protein-disulfide isomerase in response to hypoxia/brain ischemia and its protective effect against apoptotic cell death. *J Biol Chem,* **275,** 10388-10393.

Tang, S. J., Reis, G., Kang, H., Gingras, A. C., Sonenberg, N. and Schuman, E. M. (2002) A rapamycin-sensitive signaling pathway contributes to long-term synaptic plasticity in the hippocampus. *Proc Natl Acad Sci U S A,* **99,** 467-472.

Tang Y. P., Shimizu E., Dube G. R., Rampon C., Kerchner G. A., Zhuo M., Liu G. and Tsien J. Z. (1999) Genetic enhancement of learning and memory in mice. *Nature* **401,** 63-69.

Tapia-Ramirez J., Eggen B. J., Peral-Rubio M. J., Toledo-Aral J. J. and Mandel G. (1997) A single zinc finger motif in the silencing factor REST represses the neural-specific type II sodium channel promoter. *Proc Natl Acad Sci U S A* **94,** 1177-1182.

Tardin C., Cognet L., Bats C., Lounis B. and Choquet D. (2003) Direct imaging of lateral movements of AMPA receptors inside synapses. *Embo J* **22,** 4656-4665.

Tehrani M. H. and Barnes E. M., Jr. (1993) Identification of GABAA/benzodiazepine receptors on clathrin-coated vesicles from rat brain. *J Neurochem* **60,** 1755-1761.

Teyler T. J. (1987) Long-term potentiation and memory. *Int J Neurol* **21-22,** 163-171.

Thiel, G., Kaufmann, K., Magin, A., Lietz, M., Bach, K. and Cramer, M. (2000) The human transcriptional repressor protein NAB1: expression and biological activity. *Biochim Biophys Acta,* **1493,** 289-301.

Thiel G., Schoch S. and Petersohn D. (1994) Regulation of synapsin I gene expression by the zinc finger transcription factor zif268/egr-1. *J Biol Chem* **269,** 15294-15301.

Thinakaran G., Harris C. L., Ratovitski T., Davenport F., Slunt H. H., Price D. L., Borchelt D. R. and Sisodia S. S. (1997) Evidence that levels of presenilins (PS1 and PS2) are coordinately regulated by competition for limiting cellular factors. *J Biol Chem* **272,** 28415-28422.

Thinakaran G., Borchelt D. R., Lee M. K., Slunt H. H., Spitzer L., Kim G., Ratovitsky T., Davenport F., Nordstedt C., Seeger M., Hardy J., Levey A. I., Gandy S. E., Jenkins N. A., Copeland N. G., Price D. L. and Sisodia S. S. (1996) Endoproteolysis of presenilin 1 and accumulation of processed derivatives in vivo. *Neuron* **17,** 181-190.

Thomas A. V., Herl L., Spoelgen R., Hiltunen M., Jones P. B., Tanzi R. E., Hyman B. T. and Berezovska O. (2006) Interaction between presenilin 1 and ubiquilin 1 as detected by fluorescence lifetime imaging microscopy and a high-throughput fluorescent plate reader. *J Biol Chem* **281,** 26400-26407.

Thomas, K. L., Hall, J. and Everitt, B. J. (2002) Cellular imaging with zif268 expression in the rat nucleus accumbens and frontal cortex further dissociates the neural pathways activated following the retrieval of contextual and cued fear memory. *Eur J Neurosci,* **16,** 1789-1796.

Thomas P., Mortensen M., Hosie A. M. and Smart T. G. (2005) Dynamic mobility of functional GABAA receptors at inhibitory synapses. *Nat Neurosci* **8,** 889-897.

Thrower J. S., Hoffman L., Rechsteiner M. and Pickart C. M. (2000) Recognition of the polyubiquitin proteolytic signal. *Embo J* **19,** 94-102.

Thyss R., Virolle V., Imbert V., Peyron J. F., Aberdam D. and Virolle T. (2005) NF-kappaB/Egr-1/Gadd45 are sequentially activated upon UVB irradiation to mediate epidermal cell death. *Embo J* **24,** 128-137.

Todd A. J., Watt C., Spike R. C. and Sieghart W. (1996) Colocalization of GABA, glycine, and their receptors at synapses in the rat spinal cord. *J Neurosci* **16,** 974-982.

Tokuyama W., Okuno H., Hashimoto T., Li Y. X. and Miyashita Y. (2002) Selective zif268 mRNA induction in the perirhinal cortex of macaque monkeys during formation of visual pair-association memory. *J Neurochem* **81,** 60-70.

Topilko, P., Levi, G., Merlo, G., Mantero, S., Desmarquet, C., Mancardi, G. and Charnay, P. (1997) Differential regulation of the zinc finger genes Krox-20 and Krox-24 (Egr-1) suggests antagonistic roles in Schwann cells. *J Neurosci Res,* **50,** 702-712.

Toscano C. D., McGlothan J. L. and Guilarte T. R. (2006) Experience-dependent regulation of zif268 gene expression and spatial learning. *Exp Neurol* **200,** 209-215.

Tourtellotte W. G., Nagarajan R., Bartke A. and Milbrandt J. (2000) Functional compensation by Egr4 in Egr1-dependent luteinizing hormone regulation and Leydig cell steroidogenesis. *Mol Cell Biol* **20,** 5261-5268.

Tovar K. R. and Westbrook G. L. (2002) Mobile NMDA receptors at hippocampal synapses. *Neuron* **34,** 255-264.

Towbin H., Staehelin T. and Gordon J. (1979) Electrophoretic transfer of proteins from polyacrylamide gels to nitrocellulose sheets: procedure and some applications. *Proc Natl Acad Sci U S A* **76,** 4350-4354.

Treisman R. (1995) Journey to the surface of the cell: Fos regulation and the SRE. *Embo J* **14,** 4905-4913.

Tretter V., Ehya N., Fuchs K. and Sieghart W. (1997) Stoichiometry and assembly of a recombinant GABAA receptor subtype. *J Neurosci* **17,** 2728-2737.

Triller A., Cluzeaud F., Pfeiffer F., Betz H. and Korn H. (1985) Distribution of glycine receptors at central synapses: an immunoelectron microscopy study. *J Cell Biol* **101,** 683-688.

Tsai-Morris, C. H., Cao, X. M. and Sukhatme, V. P. (1988) 5' flanking sequence and genomic structure of Egr-1, a murine mitogen inducible zinc finger encoding gene. *Nucleic Acids Res,* **16,** 8835-8846.

Tullai, J. W., Schaffer, M. E., Mullenbrock, S., Kasif, S. and Cooper, G. M. (2004) Identification of transcription factor binding sites upstream of human genes regulated by the phosphatidylinositol 3-kinase and MEK/ERK signaling pathways. *J Biol Chem,* **279,** 20167-20177.

Turrigiano G. G., Leslie K. R., Desai N. S., Rutherford L. C. and Nelson S. B. (1998) Activity-dependent scaling of quantal amplitude in neocortical neurons. *Nature* **391,** 892-896.

Tusher V. G., Tibshirani R., Chu G. and Korzus E. (2001) Significance analysis of microarrays applied to the ionizing radiation response: The relation of transcription to memory formation. *Proc Natl Acad Sci U S A* **98,** 5116-5121.

Ule, J., Jensen, K. B., Ruggiu, M., Mele, A., Ule, A. and Darnell, R. B. (2003) CLIP identifies Nova-regulated RNA networks in the brain. *Science,* **302,** 1212-1215.

van Rijnsoever, C., Sidler, C. and Fritschy, J. M. (2005) Internalized GABA-receptor subunits are transferred to an intracellular pool associated with the postsynaptic density. *Eur J Neurosci,* **21,** 327-338.

van Zundert B., Alvarez F. J., Tapia J. C., Yeh H. H., Diaz E. and Aguayo L. G. (2004) Developmental-dependent action of microtubule depolymerization on the function and structure of synaptic glycine receptor clusters in spinal neurons. *J Neurophysiol* **91,** 1036-1049.

van Zundert, B., Alvarez, F. J., Yevenes, G. E., Carcamo, J. G., Vera, J. C. and Aguayo, L. G. (2002) Glycine receptors involved in synaptic transmission are selectively regulated by the cytoskeleton in mouse spinal neurons. *J Neurophysiol,* **87,** 640-644.

Vesque C. and Charnay P. (1992) Mapping functional regions of the segment-specific transcription factor Krox-20. *Nucleic Acids Res* **20,** 2485-2492.

Voges D., Zwickl P. and Baumeister W. (1999) The 26S proteasome: a molecular machine designed for controlled proteolysis. *Annu Rev Biochem* **68,** 1015-1068.

Vogt P. K. (2001) PI 3-kinase, mTOR, protein synthesis and cancer. *Trends Mol Med* **7,** 482-484.

Wadzinski, B. E., Wheat, W. H., Jaspers, S., Peruski, L. F., Jr., Lickteig, R. L., Johnson, G. L. and Klemm, D. J. (1993) Nuclear protein phosphatase 2A dephosphorylates protein kinase A-phosphorylated CREB and regulates CREB transcriptional stimulation. *Mol Cell Biol,* **13,** 2822-2834.

Walders-Harbeck B., Khaitlina S. Y., Hinssen H., Jockusch B. M. and Illenberger S. (2002) The vasodilator-stimulated phosphoprotein promotes actin polymerisation through direct binding to monomeric actin. *FEBS Lett* **529,** 275-280.

Waldvogel H. J., Baer K., Snell R. G., During M. J., Faull R. L. and Rees M. I. (2003) Distribution of gephyrin in the human brain: an immunohistochemical analysis. *Neuroscience* **116,** 145-156.

Walton M., Henderson C., Mason-Parker S., Lawlor P., Abraham W. C., Bilkey D. and Dragunow M. (1999) Immediate early gene transcription and synaptic modulation. *J Neurosci Res* **58,** 96-106.

Wan Q., Xiong Z. G., Man H. Y., Ackerley C. A., Braunton J., Lu W. Y., Becker L. E., MacDonald J. F. and Wang Y. T. (1997) Recruitment of functional GABA(A) receptors to postsynaptic domains by insulin. *Nature* **388,** 686-690.

Wang G., Sawai N., Kotliarova S., Kanazawa I. and Nukina N. (2000) Ataxin-3, the MJD1 gene product, interacts with the two human homologs of yeast DNA repair protein RAD23, HHR23A and HHR23B. *Hum Mol Genet* **9,** 1795-1803.

Wang H. and Olsen R. W. (2000) Binding of the GABA(A) receptor-associated protein (GABARAP) to microtubules and microfilaments suggests involvement of the cytoskeleton in GABARAPGABA(A) receptor interaction. *J Neurochem* **75,** 644-655.

Wang H., Bedford F. K., Brandon N. J., Moss S. J. and Olsen R. W. (1999) GABA(A)-receptor-associated protein links GABA(A) receptors and the cytoskeleton. *Nature* **397,** 69-72.

Wang H., Lim P. J., Yin C., Rieckher M., Vogel B. E. and Monteiro M. J. (2006) Suppression of polyglutamine-induced toxicity in cell and animal models of Huntington's disease by ubiquilin. *Hum Mol Genet* **15,** 1025-1041.

Wang J. H. and Feng D. P. (1992) Postsynaptic protein kinase C essential to induction and maintenance of long-term potentiation in the hippocampal CA1 region. *Proc Natl Acad Sci U S A* **89,** 2576-2580.

Washburn M. S. and Moises H. C. (1992a) Electrophysiological and morphological properties of rat basolateral amygdaloid neurons in vitro. *J Neurosci* **12,** 4066-4079.

Washburn M. S. and Moises H. C. (1992b) Inhibitory responses of rat basolateral amygdaloid neurons recorded in vitro. *Neuroscience* **50,** 811-830.

Wasylyk B., Hagman J. and Gutierrez-Hartmann A. (1998) Ets transcription factors: nuclear effectors of the Ras-MAP-kinase signaling pathway. *Trends Biochem Sci* **23,** 213-216.

Watson M. A. and Milbrandt J. (1990) Expression of the nerve growth factor-regulated NGFI-A and NGFI-B genes in the developing rat. *Development* **110,** 173-183.

Watt A. J., van Rossum M. C., MacLeod K. M., Nelson S. B. and Turrigiano G. G. (2000) Activity coregulates quantal AMPA and NMDA currents at neocortical synapses. *Neuron* **26,** 659-670.

Wehner J. M., Sleight S. and Upchurch M. (1990) Hippocampal protein kinase C activity is reduced in poor spatial learners. *Brain Res* **523,** 181-187.

Weiler, I. J., Irwin, S. A., Klintsova, A. Y. et al. (1997) Fragile X mental retardation protein is translated near synapses in response to neurotransmitter activation. *Proc Natl Acad Sci U S A,* **94,** 5395-5400.

Weinberger N. M. and Diamond D. M. (1987) Physiological plasticity in auditory cortex: rapid induction by learning. *Prog Neurobiol* **29,** 1-55.

Wenzel J., Desmond N. L. and Levy W. B. (1993) Somatic ribosomal changes induced by long-term potentiation of the perforant path-hippocampal CA1 synapses. *Brain Res* **619,** 331-333.

Wheat W. H., Roesler W. J. and Klemm D. J. (1994) Simian virus 40 small tumor antigen inhibits dephosphorylation of protein kinase A-phosphorylated

CREB and regulates CREB transcriptional stimulation. *Mol Cell Biol* **14,** 5881-5890.

Whiting P. J. (1999) The GABA-A receptor gene family: new targets for therapeutic intervention. *Neurochem Int* **34,** 387-390.

Whitmarsh A. J., Shore P., Sharrocks A. D. and Davis R. J. (1995) Integration of MAP kinase signal transduction pathways at the serum response element. *Science* **269,** 403-407.

Wiesel T. N. and Hubel D. H. (1963) Effects of Visual Deprivation on Morphology and Physiology of Cells in the Cats Lateral Geniculate Body. *J Neurophysiol* **26,** 978-993.

Wigstrom H. and Gustafsson B. (1986) Postsynaptic control of hippocampal long-term potentiation. *J Physiol (Paris)* **81,** 228-236.

Wilkinson C. R., Ferrell K., Penney M., Wallace M., Dubiel W. and Gordon C. (2000) Analysis of a gene encoding Rpn10 of the fission yeast proteasome reveals that the polyubiquitin-binding site of this subunit is essential when Rpn12/Mts3 activity is compromised. *J Biol Chem* **275,** 15182-15192.

Williams A. J., Khachigian L. M., Shows T. and Collins T. (1995) Isolation and characterization of a novel zinc-finger protein with transcription repressor activity. *J Biol Chem* **270,** 22143-22152.

Williams J. H., Errington M. L., Lynch M. A. and Bliss T. V. (1989) Arachidonic acid induces a long-term activity-dependent enhancement of synaptic transmission in the hippocampus. *Nature* **341,** 739-742.

Williams J. M., Beckmann A. M., Mason-Parker S. E., Abraham W. C., Wilce P. A. and Tate W. P. (2000) Sequential increase in Egr-1 and AP-1 DNA binding activity in the dentate gyrus following the induction of long-term potentiation. *Brain Res Mol Brain Res* **77,** 258-266.

Wilson M. A. and McNaughton B. L. (1993) Dynamics of the hippocampal ensemble code for space. *Science* **261,** 1055-1058.

Wisden W., Errington M. L., Williams S., Dunnett S. B., Waters C., Hitchcock D., Evan G., Bliss T. V. and Hunt S. P. (1990) Differential expression of immediate early genes in the hippocampus and spinal cord. *Neuron* **4,** 603-614.

Wonnacott S. (1990) The paradox of nicotinic acetylcholine receptor upregulation by nicotine. *Trends Pharmacol Sci* **11,** 216-219.

Worley, P. F., Bhat, R. V., Baraban, J. M., Erickson, C. A., McNaughton, B. L. and Barnes, C. A. (1993) Thresholds for synaptic activation of transcription factors in hippocampus: correlation with long-term enhancement. *J Neurosci,* **13,** 4776-4786.

Wu A. L., Wang J., Zheleznyak A. and Brown E. J. (1999) Ubiquitin-related proteins regulate interaction of vimentin intermediate filaments with the plasma membrane. *Mol Cell* **4,** 619-625.

Wu G. Y., Deisseroth K. and Tsien R. W. (2001) Activity-dependent CREB phosphorylation: convergence of a fast, sensitive calmodulin kinase pathway and a slow, less sensitive mitogen-activated protein kinase pathway. *Proc Natl Acad Sci U S A* **98,** 2808-2813.

Wu S., Mikhailov A., Kallo-Hosein H., Hara K., Yonezawa K. and Avruch J. (2002) Characterization of ubiquilin 1, an mTOR-interacting protein. *Biochim Biophys Acta* **1542,** 41-56.

Wu, Z. L., Thomas, S. A., Villacres, E. C., Xia, Z., Simmons, M. L., Chavkin, C., Palmiter, R. D. and Storm, D. R. (1995) Altered behavior and long-term potentiation in type I adenylyl cyclase mutant mice. *Proc Natl Acad Sci U S A,* **92,** 220-224.

Xia, Z., Dudek, H., Miranti, C. K. and Greenberg, M. E. (1996) Calcium influx via the NMDA receptor induces immediate early gene transcription by a MAP kinase/ERK-dependent mechanism. *J Neurosci,* **16,** 5425-5436.

Xie X., Lu J., Kulbokas E. J., Golub T. R., Mootha V., Lindblad-Toh K., Lander E. S. and Kellis M. (2005) Systematic discovery of regulatory motifs in human promoters and 3' UTRs by comparison of several mammals. *Nature* **434,** 338-345.

Yamagata K., Kaufmann W. E., Lanahan A., Papapavlou M., Barnes C. A., Andreasson K. I. and Worley P. F. (1994) Egr3/Pilot, a zinc finger transcription factor, is rapidly regulated by activity in brain neurons and colocalizes with Egr1/zif268. *Learn Mem* **1,** 140-152.

Yi J. J. and Ehlers M. D. (2005) Ubiquitin and protein turnover in synapse function. *Neuron* **47,** 629-632.

Yin, J. C. and Tully, T. (1996) CREB and the formation of long-term memory. *Curr Opin Neurobiol,* **6,** 264-268.

Yin J. C., Wallach J. S., Del Vecchio M., Wilder E. L., Zhou H., Quinn W. G. and Tully T. (1994) Induction of a dominant negative CREB transgene specifically blocks long-term memory in Drosophila. *Cell* **79,** 49-58.

Yin Y., Edelman G. M. and Vanderklish P. W. (2002) The brain-derived neurotrophic factor enhances synthesis of Arc in synaptoneurosomes. *Proc Natl Acad Sci U S A* **99,** 2368-2373.

Young R. S., Weaver D. D., Kukolich M. K., Heerema N. A., Palmer C. G., Kawira E. L. and Bender H. A. (1984) Terminal and interstitial deletions of the long arm of chromosome 7: a review with five new cases. *Am J Med Genet* **17,** 437-450.

Yu, J., de Belle, I., Liang, H. and Adamson, E. D. (2004) Coactivating factors p300 and CBP are transcriptionally crossregulated by Egr1 in prostate cells, leading to divergent responses. *Mol Cell,* **15,** 83-94.

Yuan, L. L., Adams, J. P., Swank, M., Sweatt, J. D. and Johnston, D. (2002) Protein kinase modulation of dendritic K+ channels in hippocampus involves a mitogen-activated protein kinase pathway. *J Neurosci,* **22,** 4860-4868.

Zamanillo, D., Sprengel, R., Hvalby, O. et al. (1999) Importance of AMPA receptors for hippocampal synaptic plasticity but not for spatial learning. *Science,* **284,** 1805-1811.

Zhang, F., Lin, M., Abidi, P., Thiel, G. and Liu, J. (2003) Specific interaction of Egr1 and c/EBPbeta leads to the transcriptional activation of the human low density lipoprotein receptor gene. *J Biol Chem,* **278,** 44246-44254.

Zhang W. and Benson D. L. (2001) Stages of synapse development defined by dependence on F-actin. *J Neurosci* **21,** 5169-5181.

Zhang X. and Liu Y. (2003) Suppression of HGF receptor gene expression by oxidative stress is mediated through the interplay between Sp1 and Egr-1. *Am J Physiol Renal Physiol* **284,** F1216-1225.

Zhao Y., Hegde A. N. and Martin K. C. (2003) The ubiquitin proteasome system functions as an inhibitory constraint on synaptic strengthening. *Curr Biol* **13,** 887-898.

Zhu J. J., Qin Y., Zhao M., Van Aelst L. and Malinow R. (2002) Ras and Rap control AMPA receptor trafficking during synaptic plasticity. *Cell* **110,** 443-455.